From the marrow to the tissue:

central and peripheral innate immune memory in cardiovascular diseases



Daniela Flores Gomez

RADBOUD UNIVERSITY PRESS

Radboud Dissertation Series

From the marrow to the tissue

central and peripheral innate immune memory in cardiovascular diseases

Daniela Flores Gomez

From the marrow to the tissue: central and peripheral innate immune memory in cardiovascular diseases

Daniela Flores Gomez

Radboud Dissertation Series

ISSN: 2950-2772 (Online); 2950-2780 (Print)

Published by RADBOUD UNIVERSITY PRESS Postbus 9100, 6500 HA Nijmegen, The Netherlands www.radbouduniversitypress.nl

Design: Proefschrift AIO | Annelies Lips

Cover: Generated in DALL:E by Daniela Flores Gomez

Printing: DPN Rikken/Pumbo

ISBN: 9789465150529

DOI: 10.54195/9789465150529

Free download at: https://doi.org/10.54195/9789465150529

© 2025 Daniela Flores Gomez

RADBOUD UNIVERSITY PRESS

This is an Open Access book published under the terms of Creative Commons Attribution-Noncommercial-NoDerivatives International license (CC BY-NC-ND 4.0). This license allows reusers to copy and distribute the material in any medium or format in unadapted form only, for noncommercial purposes only, and only so long as attribution is given to the creator, see http://creativecommons.org/licenses/by-nc-nd/4.0/.

From the marrow to the tissue

central and peripheral innate immune memory in cardiovascular diseases

Proefschrift ter verkrijging van de graad van doctor
aan de Radboud Universiteit Nijmegen
op gezag van de rector magnificus prof. dr. J.M. Sanders,
volgens besluit van het college voor promoties
in het openbaar te verdedigen op

maandag 2 juni 2025 om 12.30 uur precies

door

Daniela Flores Gomez geboren op 13 februari 1993

te Mexico-Stad (Mexico)

Promotoren:

Prof. dr. N.P. Riksen Prof. dr. M.G. Netea

Copromotor:

Dr. S. Bekkering

Manuscriptcommissie:

Prof. dr. N.M.A. Blijlevens Prof. dr. I. Bot (Universiteit Leiden) Dr. J. Kroon (Amsterdam UMC)

From the marrow to the tissue

central and peripheral innate immune memory in cardiovascular diseases

Dissertation to obtain the degree of doctor
from Radboud University Nijmegen
on the authority of the Rector Magnificus prof. dr. J.M. Sanders,
according to the decision of the Doctorate Board
to be defended in public on

Monday, June 2, 2025 at 12.30 pm

by

Daniela Flores Gomez born on February 13, 1993 in Mexico-City (Mexico)

Supervisors:

Prof. dr. N.P. Riksen Prof. dr. M.G. Netea

Co-supervisor:

Dr. S. Bekkering

Manuscript Committee:

Prof. dr. N.M.A. Blijlevens Prof. dr. I. Bot (Leiden University) Dr. J. Kroon (Amsterdam UMC) Para mis papás, To my dear parents,

Contents

Chapter 1	General introduction, aims and outline of the thesis		
Chapter 2	Trained Immunity in Atherosclerotic Cardiovascular Disease <i>ATVB 2020</i>	23	
Chapter 3	The Effect of Leptin on Trained Innate Immunity and on Systemic Inflammation in Subjects with Obesity. J Leukoc Biol. 2023	41	
Chapter 4	Interleukin-1ß induces trained innate immunity in human hematopoietic stem cells in vitro Stem Cell Reports 2024	81	
Chapter 5	Comparison of bone marrow and induced pluripotent stem cell-derived monocytes to human circulating monocytes for in vitro modeling To be submitted	115	
Chapter 6	Altered neutrophil phenotype and function in patients with calcific aortic valve disease To be submitted	145	
Chapter 7	Summary	175	
Chapter 8	General discussion and future perspective	181	
Chapter 9	Nederlandse Samenvatting	197	
Chapter 10	Resumen	203	
Appendices	Research Data Management PhD Portfolio List of publications Acknowledgements Curriculum Vitae	210 212 214 215 225	
	About the Author	227	



General introduction, aims and outline of the thesis

Cardiovascular disease

Cardiovascular diseases have existed for thousands of years (1). Nowadays, life expectancy has increased along with unhealthy habits and sedentary lifestyle, making CVD one of the leading causes of morbidity and mortality worldwide (2). The World Health Organization (WHO) reports that nearly 18 million people die as consequence of CVDs yearly (3). Most CVDs, including myocardial infarction, stroke, and peripheral arterial disease, are caused by atherosclerosis, which is a low-grade inflammatory disorder of the arterial wall (4).

Atherosclerotic CVD (ASCVD) is characterized by the progressive formation of plagues in the arterial wall, driven by endothelial dysfunction and a chronic inflammatory response. This increases vascular permeability promoting the accumulation of low-density lipoproteins (LDL) in the subendothelial space where they undergo oxidation (5, 6). OxLDL particles trigger an immune response, recruiting monocytes that then differentiate into macrophages. These engulf oxLDL becoming foam cells. Plague macrophages also further contribute to inflammation by the production of cytokines and chemokines. Accumulation of foam cells, and cells that have undergone necrosis and apoptosis, result in a growing necrotic core. Eventually, the lesion can erode or rupture leading to complete occlusion of the arterial lumen, which results in an acute cardiovascular event, such as myocardial infarction or stroke (5, 6). Calcific aortic valve disease (CAVD) is another CVD with increasing prevalence mainly due to the ageing of the population. CAVD is the most common type of valvular heart disease and causes progressive narrowing of the aortic valve with severe consequences. First, endothelial cells are activated by oxidative or mechanical stress changing the vascular permeability. This increases the oxidative environment and the infiltration of lipids and immune cells leading to the differentiation of osteoblast-like cells and fibrosis (7). These cells secrete remodeling proteins and deposit calcium resulting in calcification and stiffening of the valvular tissue. Over time, the valve becomes stenotic, which can impede blood flow and augment the cardiac workload (8). It is increasingly recognized that ASCVD and CAVD share common risk factors and common pathophysiological features. This latter includes chronic inflammation, and immune cell involvement (8).

Common risk factors for ASCVD and for CAVD include increased age, hypertension, smoking, dyslipoproteinemia, hyperglycemia and obesity (9-11). In addition to ageing, obesity and the associated insulin resistance, metabolic syndrome and diabetes mellitus are largely responsible for the projected increase in prevalence of these diseases in the next decades (12). Obesity can lead to metabolic dysregulation and low-grade inflammation favoring the development of metabolic syndrome and cardiovascular complications. Interestingly, the mechanisms of obesity-associated systemic inflammation are strongly sex-specific; e.g. it appeared that in a cohort of individuals with overweight or obesity, the presence of metabolic syndrome was associated with pro-inflammatory changes in men (increased circulating IL6 and leptin and higher monocyte cytokine production capacity), whereas in women this was associated with reduced anti-inflammatory proteins (decreased circulating adiponectin) (13). Leptin is a hormone produced predominantly by adipocytes with known pro-inflammatory effects on immune cells, but the exact mechanism how this contributes to obesity-associated cardiometabolic complications remains to be established (14).

Current treatment options for cardiovascular diseases

For many years, the majority of treatment options for ASCVD focused on treatment of the risk factors. These treatments included blood pressure lowering therapies, and statins to lower LDL cholesterol levels (15). Only recently, with better understanding of the role of chronic inflammation in atherogenesis, several randomized placebo-controlled trials have determined that anti-inflammatory therapies can further lower the risk of ASCVD.

The Canakinumab Anti-inflammatory Thrombosis Outcome Study (CANTOS) was the first trial to demonstrate a reduced incidence of cardiovascular events by targeting IL-1\(\beta\) with the monoclonal antibody canakinumab. In this trial, patients with a history of myocardial infarction treated with canakinumab showed a 15% lower risk of a major adverse cardiovascular event compared to placebo. However, this also led to higher number of fatal infections in the group receiving the treatment (16).

Colchicine, an old drug mainly used to treat gout, has been repurposed to prevent ASCVD due to its anti-inflammatory properties. The low-dose colchicine (LoDoCo) trial reported that low-dose colchicine combined with a standard secondary prevention therapy, reduced the risk of a cardiovascular event in patients with established coronary artery disease (17). Subsequently, colchicine lowered the risk of a major cardiovascular event by 30% in patients with chronic coronary disease (18) and reduced the risk by 25% of an ischemic cardiovascular event in patients with a recent myocardial infarction (19).

Contrary to ASCVD, there is no effective pharmacological treatment to date to prevent CAVD and aortic valve stenosis, which leaves surgical or endovascular valve replacement the only treatment options once severe symptoms have occurred (8, 20). Despite the optimal state-of-the-art treatment of risk factors, a significant residual risk for ASCVD remains in many patients. Broad anti-inflammatory therapies can further lower ASCVD risk, but this comes at a cost of more infections. Therefore, a better understanding of the inflammatory landscape and mechanisms of ASCVD and of CAVD is needed to identify novel, more selective, therapeutic targets. In this thesis, I explore the role of monocyte and neutrophil reprogramming in ASCVD and CAVD, with a particular focus on innate immune memory properties of these cells, a process also termed "trained immunity".

Immune cells as part of the pathophysiology of ASCVD and CAVD.

A key mechanism contributing to atherosclerotic plague formation is the accumulation of apolipoprotein B-containing lipoproteins in the subendothelial space. (21). In recent years, however, the perception of atherosclerosis changed from being a mere lipid storage disease into being a chronic inflammatory disorder of the vascular wall (22). Innate immune cells drive vascular wall inflammation, and formation and rupture of the atherosclerotic plaque (Figure 1) (23, 24). During atherosclerosis, endothelial cells are activated by local hemodynamic or systemic stimuli. This activation leads to increased expression of adhesion molecules, secretion of chemokines such as monocyte chemoattractant protein-1 (MCP-1) and changes in the permeability of the endothelial layer in the artery. Monocytes from the circulation are recruited to the lesion site to then transmigrate into the intima, where they differentiate into macrophages. These macrophages take up modified lipoproteins such as oxidized LDL (oxLDL) via scavenger receptors (e.g. CD36), becoming foam cells. As a result of the increased number of monocytes that differentiated into macrophages, become foam cells and are unable to leave the site, these cells die and form a growing necrotic core of the plague (25, 26). Ultimately, the plaque can erode or rupture, causing arterial occlusion which triggers a cardiovascular event to occur (27-29).

The role of neutrophils in vascular inflammation and ASCVD has recently gained attention. Neutrophils are the most abundant innate immune cell in the circulation and play a crucial role in the first-line of defense due to degranulation and neutrophil extracellular traps (NETs) formation (30). In the context of ASCVD, recent studies have described that neutrophils can adhere to endothelial cells and infiltrate the endothelium compromising the integrity of the vascular layer due to the secretion of pro-inflammatory mediators, degranulation and reactive oxygen species (ROS) production (31). The aforementioned processes also increase the recruitment of monocytes to the lesion site. The accumulation of ROS is proposed to be a crucial initiator of oxidation of LDL inducing NETs formation via TLR-PKC-IRAK-MAPK

pathway and NADPH-oxidase activation, causing neutrophil apoptosis. Additionally, NETs can also modulate macrophage phenotype and plaque instability (8, 30, 32). In large cohorts, circulating granulocyte numbers independently predict future ASCVD incidence and the causality has been proven by Mendelian Randomization studies (33).

Accumulating evidence also points to roles of monocyte-derived macrophages and neutrophils in the pathophysiology of CAVD, but data is more scarce then for ASCVD (8). Specifically, it has been reported that there is a higher neutrophilto-lymphocyte ratio and overall circulating neutrophil count in patients with the disease (34, 35). Moreover, it has been previously demonstrated the presence of NETs and neutrophil elastase (NE) in calcific aortic valves, possibly being an indicator of disease progression and enhancer of valve calcification (8, 36).

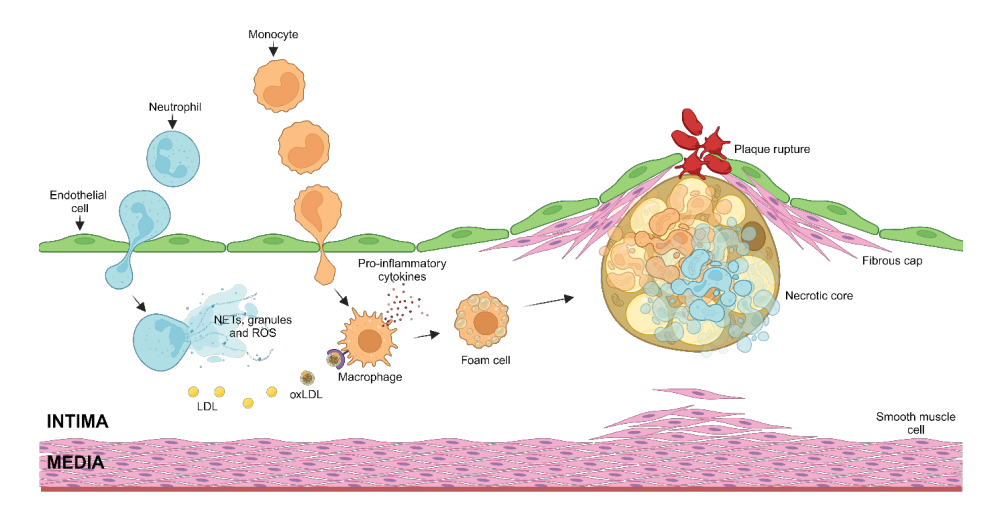


Figure 1. Pathogenesis of atherosclerosis. The role of neutrophils, monocytes and macrophages in the initiation, progression and rupture of the atherosclerotic plaque. Created with BioRender.

Interestingly, macrophages are not only activated in the inflammatory microenvironment of the growing plaque, but also circulating monocytes show a hyperresponsive phenotype in patients with ASCVD (37, 38). A few years ago, our group performed bone marrow aspirations of patients with established coronary artery disease and showed that also the hematopoietic progenitor cells in the bone marrow show functional and transcriptional reprogramming. Pathway analysis of differentially expressed genes pointed to an enrichment of pathways important in macrophage and neutrophil activation (39). It was recently proposed that a newly identified immunological mechanisms, called trained immunity, contributes to the innate immune reprogramming (24).

Trained immunity: the memory characteristics of innate immune cells

Over the past decade, it has been described that, in contrast to the traditional immunological paradigm, innate immune cells can also build immunological memory, and thereby develop a long-lasting pro-inflammatory phenotype (40). This long-lasting hyperresponsive state has been termed trained immunity. Accumulating evidence in the past years showed that trained immunity can contribute to the pathophysiology of ASCVD (24). Trained immunity was first identified in the context of recurrent infections, with monocytes undergoing metabolic and epigenetic rewiring after brief exposure to certain pathogens such as Bacille Calmette-Guérin, Candida albicans or its cell wall component β-glucan (40). Later it was shown that trained immunity could also be induced by endogenous atherogenic molecules such as oxLDL, lipoprotein (a), high glucose concentrations. and adrenal hormones (41, 42). Interestingly, innate immune memory is not restricted to monocytes/macrophages, but can also occur in other innate immune cells such as neutrophils and NK cells, and even in some non-immune cells (43, 44).

Trained immunity was first described in mature immune cells, specifically in circulating monocytes, tissue resident macrophages, and neutrophils (peripheral trained immunity). Given the short half-life of monocytes and neutrophils, this could not explain the observation that even three months (45) and one year (46) after BCG vaccination in healthy volunteers, monocytes and neutrophils (44) with a trained hyperresponsive phenotype were present in the circulation. Indeed, several studies have now shown that trained immunity is also induced in hematopoietic stem and progenitor cells at the bone marrow level (central trained immunity) (Figure 2) (24, 47), which can explain the long-term persistence of the trained phenotype in vivo. Central trained immunity was first observed in humans after BCG vaccination. It was described that monocytes in the circulation, despite of their short lifespan, had a pro-inflammatory phenotype up- to one year after the vaccination (46). Murine studies have shown that epigenetic reprogramming of hematopoietic progenitor cells (HPC) occurs via IL-1β signaling after brief exposure to β-glucan or after 4 weeks of a Western-type diet (WTD) (48, 49). Whether IL-1β can also induced trained immunity in human HPCs remains to the established. Research in the past few years has unequivocally shown in experimental murine models of atherosclerosis that trained immunity can accelerate atherosclerosis development in the context of hyperglycemia (50), intermittent high-fat diet (51), and following acute myocardial infarction (52) and stroke (53). Both for intermittent high-fat diet as well as for stroke, bone marrow IL-1β signaling was identified as key pathophysiological mechanism (51, 53) as triggers for trained immunity.

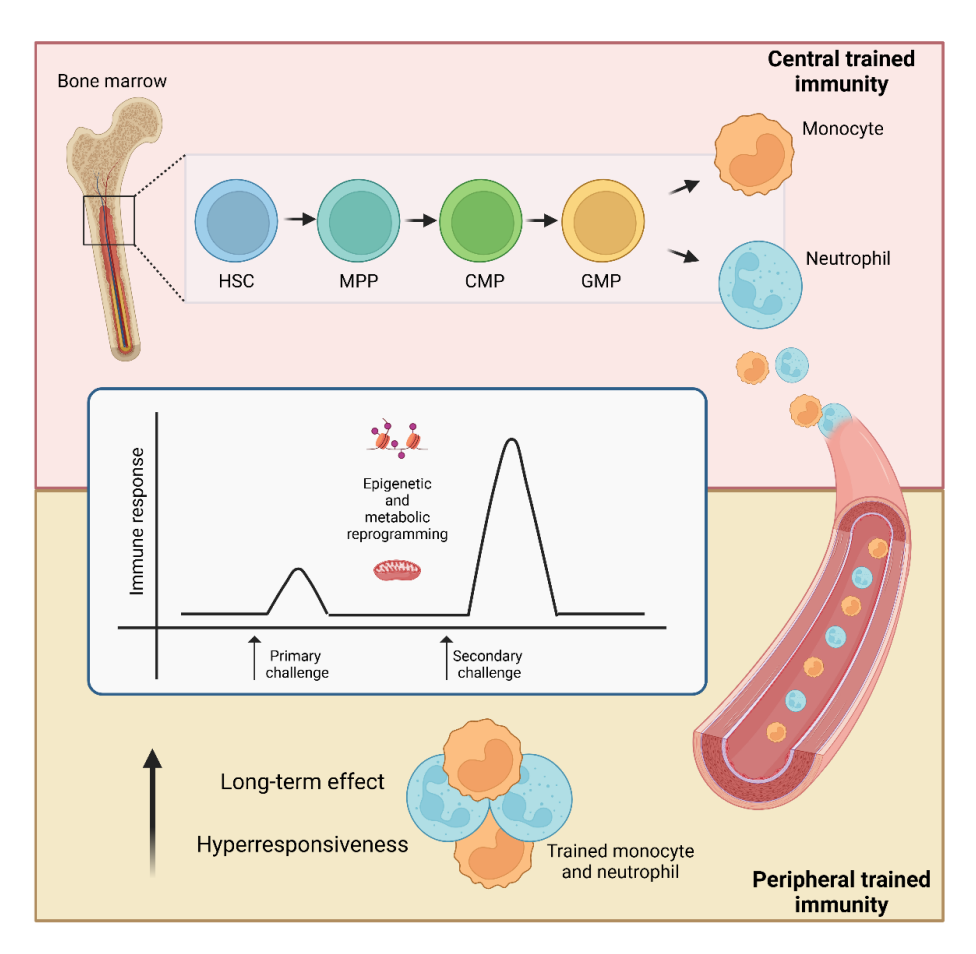


Figure 2. Schematic representation of central and peripheral trained immunity of monocytes. Abbreviations: hematopoietic stem cell (HSC), multipotent progenitor (MPP), common myeloid progenitor (CMP) and granulocyte/monocyte progenitor (GMP). Created with BioRender.

Aims and outline of the thesis

The aim of this thesis is to explore several aspects of innate immune reprogramming in the context of ASCVD and CAVD.

First, Chapter 2 provides a detailed overview of the triggers, mechanisms, and effects of trained immunity in atherosclerotic cardiovascular disease.

In Chapter 3 I study whether leptin can induce innate immune reprogramming in circulating monocytes using the standard in vitro trained immunity protocol. I also show the association between leptin and some key markers of inflammation in a cohort of obese subjects and explore sex-specific associations.

As described above, trained immunity can also occur in hematopoietic stem cells in the bone marrow niche, with experimental murine studies pointing to an important role of the IL-1β pathway. Based on these findings, we hypothesize in **Chapter 4** that IL-1ß induces trained immunity in human HPCs in vitro. For this, we expose BMderived HPCs to IL-1\(\text{\text{and}} \) and once they differentiate into macrophages, measure key immunological parameters to determine a trained phenotype including cytokine production and cell metabolism. Also, using RNA sequencing, we explore how this phenotype can contribute to atherogenesis.

Since I study trained immunity in primary human monocytes in chapter 3, and in HPC-derived monocytes in chapter 4, it is important to compare these monocyte phenotypes in order to be able to compare the results of the different models. Therefore, in **chapter 5** I systematically investigate the similarities and differences of human circulating monocytes, bone marrow-derived monocytes, and iPSC-derived monocytes (another source to obtain monocytes for in vitro studies) in vitro. We do a deep phenotypical, functional and transcriptomic characterization highlighting the similarities and differences of cells derived from these three different sources.

In the last chapter, I explore the role of immune cell reprogramming of neutrophils in patients with CAVD. In **Chapter 6**, we perform an exploratory study to investigate the phenotype of neutrophils from patients with severe CAVD and healthy controls.

The connection between the different chapters is illustrated in Figure 3.

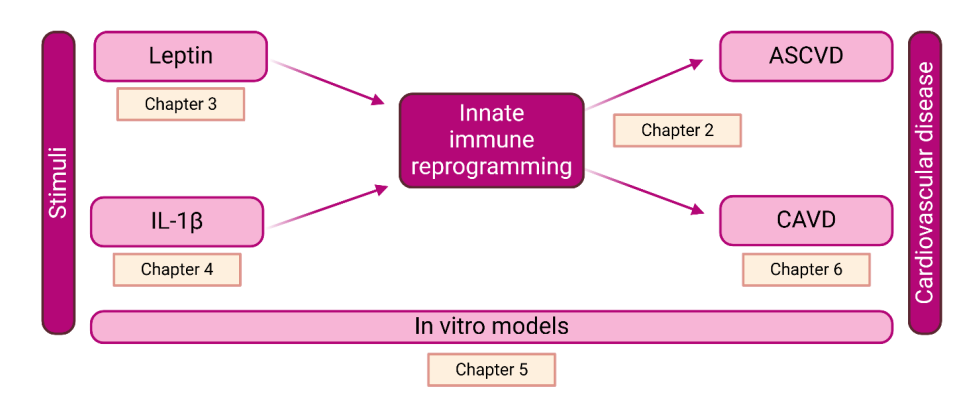


Figure 3. Schematic overview of the thesis. Created with BioRender.

References

- Thompson RC, Allam AH, Lombardi GP, Wann LS, Sutherland ML, Sutherland JD, et al. Atherosclerosis across 4000 years of human history: the Horus study of four ancient populations. The Lancet. 2013;381(9873):1211-22.
- Vaduganathan M, Mensah GA, Turco JV, Fuster V, Roth GA. The Global Burden of Cardiovascular Diseases and Risk. Journal of the American College of Cardiology. 2022;80(25):2361-71.
- WHO. Cardiovascular diseases (CVDs): World Health Organization (WHO); 2021 [updated 11 June 2021. Available from: https://www.who.int/news-room/fact-sheets/detail/cardiovasculardiseases-(cvds).
- Rout A, Duhan S, Umer M, Li M, Kalra D, Atherosclerotic cardiovascular disease risk prediction: current state-of-the-art. Heart. 2024;110(15):1005-14.
- Libby P, Ridker PM, Hansson GK. Inflammation in atherosclerosis: from pathophysiology to practice. J Am Coll Cardiol. 2009;54(23):2129-38.
- Libby P, Buring JE, Badimon L, Hansson GK, Deanfield J, Bittencourt MS, et al. Atherosclerosis. Nature Reviews Disease Primers. 2019;5(1):56.
- Moncla L-HM, Briend M, Bossé Y, Mathieu P. Calcific aortic valve disease: mechanisms, prevention 7. and treatment. Nature Reviews Cardiology. 2023;20(8):546-59.
- Broeders W, Bekkering S, El Messaoudi S, Joosten LAB, van Royen N, Riksen NP. Innate immune cells in the pathophysiology of calcific aortic valve disease: lessons to be learned from atherosclerotic cardiovascular disease? Basic Res Cardiol. 2022;117(1):28.
- Rhee EJ. The Influence of Obesity and Metabolic Health on Vascular Health. Endocrinol Metab (Seoul). 2022;37(1):1-8.
- 10. Powell-Wiley TM, Poirier P, Burke LE, Després J-P, Gordon-Larsen P, Lavie CJ, et al. Obesity and Cardiovascular Disease: A Scientific Statement From the American Heart Association. Circulation. 2021:143(21):e984-e1010.
- 11. Liu Y, Zhao A, Sun G, Wang R, Zhang J, Lip GYH, et al. Relationship between metabolic status, physical activity and cardiovascular disease in participants with obesity. International Journal of Obesity. 2024;48(6):788-95.
- 12. Joynt Maddox KE, Elkind MSV, Aparicio HJ, Commodore-Mensah Y, de Ferranti SD, Dowd WN, et al. Forecasting the Burden of Cardiovascular Disease and Stroke in the United States Through 2050—Prevalence of Risk Factors and Disease: A Presidential Advisory From the American Heart Association. Circulation. 2024;150(4):e65-e88.
- 13. Ter Horst R, van den Munckhof ICL, Schraa K, Aguirre-Gamboa R, Jaeger M, Smeekens SP, et al. Sex-Specific Regulation of Inflammation and Metabolic Syndrome in Obesity. Arterioscler Thromb Vasc Biol. 2020;40(7):1787-800.
- 14. Vilariño-García T, Polonio-González ML, Pérez-Pérez A, Ribalta J, Arrieta F, Aguilar M, et al. Role of Leptin in Obesity, Cardiovascular Disease, and Type 2 Diabetes. International Journal of Molecular Sciences. 2024;25(4):2338.
- 15. Marx N, Federici M, Schütt K, Müller-Wieland D, Ajjan RA, Antunes MJ, et al. 2023 ESC Guidelines for the management of cardiovascular disease in patients with diabetes: Developed by the task force on the management of cardiovascular disease in patients with diabetes of the European Society of Cardiology (ESC). European Heart Journal. 2023;44(39):4043-140.

- 16. Ridker PM, Everett BM, Thuren T, MacFadyen JG, Chang WH, Ballantyne C, et al. Antiinflammatory Therapy with Canakinumab for Atherosclerotic Disease. New England Journal of Medicine. 2017:377(12):1119-31.
- 17. Nidorf SM, Eikelboom JW, Budgeon CA, Thompson PL. Low-Dose Colchicine for Secondary Prevention of Cardiovascular Disease. Journal of the American College of Cardiology. 2013;61(4):404-10.
- 18. Nidorf SM, Fiolet ATL, Mosterd A, Eikelboom JW, Schut A, Opstal TSJ, et al. Colchicine in Patients with Chronic Coronary Disease. New England Journal of Medicine. 2020;383(19):1838-47.
- 19. Tardif J-C, Kouz S, Waters DD, Bertrand OF, Diaz R, Maggioni AP, et al. Efficacy and Safety of Low-Dose Colchicine after Myocardial Infarction. New England Journal of Medicine. 2019;381(26):2497-505.
- 20. Donato M, Ferri N, Lupo MG, Faggin E, Rattazzi M. Current Evidence and Future Perspectives on Pharmacological Treatment of Calcific Aortic Valve Stenosis. Int J Mol Sci. 2020;21(21).
- 21. Bekkering S, Quintin J, Joosten LA, van der Meer JW, Netea MG, Riksen NP. Oxidized low-density lipoprotein induces long-term proinflammatory cytokine production and foam cell formation via epigenetic reprogramming of monocytes. Arterioscler Thromb Vasc Biol. 2014;34(8):1731-8.
- 22. Libby P. Inflammation in atherosclerosis. Nature. 2002;420(6917):868-74.
- 23. Flores-Gomez D, Bekkering S, Netea MG, Riksen NP. Trained Immunity in Atherosclerotic Cardiovascular Disease. Arteriosclerosis, Thrombosis, and Vascular Biology. 2021;41(1):62-9.
- 24. Riksen NP, Bekkering S, Mulder WJM, Netea MG. Trained immunity in atherosclerotic cardiovascular disease. Nature Reviews Cardiology. 2023;20(12):799-811.
- 25. Jebari-Benslaiman S, Galicia-García U, Larrea-Sebal A, Olaetxea JR, Alloza I, Vandenbroeck K, et al. Pathophysiology of Atherosclerosis. Int J Mol Sci. 2022;23(6).
- 26. Roy P, Orecchioni M, Ley K. How the immune system shapes atherosclerosis: roles of innate and adaptive immunity. Nature Reviews Immunology. 2022;22(4):251-65.
- 27. De Meyer GRY, Zurek M. Puylaert P. Martinet W. Programmed death of macrophages in atherosclerosis: mechanisms and therapeutic targets. Nature Reviews Cardiology. 2024;21(5):312-25.
- 28. Swirski FK, Nahrendorf M. Leukocyte behavior in atherosclerosis, myocardial infarction, and heart failure. Science. 2013;339(6116):161-6.
- 29. Hou P, Fang J, Liu Z, Shi Y, Agostini M, Bernassola F, et al. Macrophage polarization and metabolism in atherosclerosis. Cell Death & Disease. 2023;14(10):691.
- 30. Zhang X, Kang Z, Yin D, Gao J. Role of neutrophils in different stages of atherosclerosis. Innate Immun. 2023;29(6):97-109.
- 31. Silvestre-Roig C, Braster Q, Ortega-Gomez A, Soehnlein O. Neutrophils as regulators of cardiovascular inflammation. Nat Rev Cardiol. 2020;17(6):327-40.
- 32. Soehnlein O. Multiple Roles for Neutrophils in Atherosclerosis. Circulation Research. 2012;110(6):875-88.
- 33. Luo J, Thomassen JQ, Nordestgaard BG, Tybjærg-Hansen A, Frikke-Schmidt R. Neutrophil counts and cardiovascular disease. European Heart Journal. 2023;44(47):4953-64.
- 34. Cho KI, Cho SH, Her AY, Singh GB, Shin ES. Prognostic Utility of Neutrophil-to-Lymphocyte Ratio on Adverse Clinical Outcomes in Patients with Severe Calcific Aortic Stenosis. PLoS One. 2016;11(8):e0161530.
- 35. Song J, Zheng Q, Ma X, Zhang Q, Xu Z, Zou C, et al. Predictive Roles of Neutrophil-to-Lymphocyte Ratio and C-Reactive Protein in Patients with Calcific Aortic Valve Disease. Int Heart J. 2019;60(2):345-51.

- 36. Liu Y, Jiang P, An L, Zhu M, Li J, Wang Y, et al. The role of neutrophil elastase in aortic valve calcification. J Transl Med. 2022;20(1):167.
- 37. Bekkering S, van den Munckhof I, Nielen T, Lamfers E, Dinarello C, Rutten J, et al. Innate immune cell activation and epigenetic remodeling in symptomatic and asymptomatic atherosclerosis in humans in vivo. Atherosclerosis. 2016;254:228-36.
- 38. Shirai T, Nazarewicz RR, Wallis BB, Yanes RE, Watanabe R, Hilhorst M, et al. The glycolytic enzyme PKM2 bridges metabolic and inflammatory dysfunction in coronary artery disease. J Exp Med. 2016;213(3):337-54.
- 39. Noz MP, Bekkering S, Groh L, Nielen TM, Lamfers EJ, Schlitzer A, et al. Reprogramming of bone marrow myeloid progenitor cells in patients with severe coronary artery disease. Elife. 2020;9.
- 40. Netea MG, Joosten LA, Latz E, Mills KH, Natoli G, Stunnenberg HG, et al. Trained immunity: A program of innate immune memory in health and disease. Science. 2016;352(6284):aaf1098.
- 41. Netea MG, Domínguez-Andrés J, Barreiro LB, Chavakis T, Divangahi M, Fuchs E, et al. Defining trained immunity and its role in health and disease. Nature Reviews Immunology. 2020;20(6):375-88.
- 42. Domínguez-Andrés J, Dos Santos JC, Bekkering S, Mulder WJM, van der Meer JWM, Riksen NP, et al. Trained immunity: adaptation within innate immune mechanisms. Physiol Rev. 2023;103(1):313-46.
- 43. Kleinnijenhuis J, Quintin J, Preijers F, Joosten LA, Jacobs C, Xavier RJ, et al. BCG-induced trained immunity in NK cells: Role for non-specific protection to infection. Clin Immunol. 2014;155(2):213-9.
- 44. Moorlag S, Rodriguez-Rosales YA, Gillard J, Fanucchi S, Theunissen K, Novakovic B, et al. BCG Vaccination Induces Long-Term Functional Reprogramming of Human Neutrophils. Cell Rep. 2020;33(7):108387.
- 45. Kleinnijenhuis J, Quintin J, Preijers F, Joosten LA, Ifrim DC, Saeed S, et al. Bacille Calmette-Guerin induces NOD2-dependent nonspecific protection from reinfection via epigenetic reprogramming of monocytes. Proc Natl Acad Sci U S A. 2012;109(43):17537-42.
- 46. Kleinnijenhuis J, Quintin J, Preijers F, Benn CS, Joosten LA, Jacobs C, et al. Long-lasting effects of BCG vaccination on both heterologous Th1/Th17 responses and innate trained immunity. J Innate Immun. 2014;6(2):152-8.
- 47. Vuscan P, Kischkel B, Joosten LAB, Netea MG. Trained immunity: General and emerging concepts. Immunological Reviews. 2024;323(1):164-85.
- 48. Mitroulis I, Ruppova K, Wang B, Chen LS, Grzybek M, Grinenko T, et al. Modulation of Myelopoiesis Progenitors Is an Integral Component of Trained Immunity. Cell. 2018;172(1-2):147-61.e12.
- 49. Christ A, Günther P, Lauterbach MAR, Duewell P, Biswas D, Pelka K, et al. Western Diet Triggers NLRP3-Dependent Innate Immune Reprogramming. Cell. 2018;172(1-2):162-75.e14.
- 50. Edgar L, Akbar N, Braithwaite AT, Krausgruber T, Gallart-Ayala H, Bailey J, et al. Hyperglycemia Induces Trained Immunity in Macrophages and Their Precursors and Promotes Atherosclerosis. Circulation. 2021;144(12):961-82.
- 51. Lavillegrand JR, Al-Rifai R, Thietart S, Guyon T, Vandestienne M, Cohen R, et al. Alternating highfat diet enhances atherosclerosis by neutrophil reprogramming. Nature. 2024;634(8033):447-56.
- 52. Dong Z, Hou L, Luo W, Pan LH, Li X, Tan HP, et al. Myocardial infarction drives trained immunity of monocytes, accelerating atherosclerosis. Eur Heart J. 2024;45(9):669-84.
- Simats A, Zhang S, Messerer D, Chong F, Beşkardeş S, Chivukula AS, et al. Innate immune memory after brain injury drives inflammatory cardiac dysfunction. Cell. 2024.



Chapter 2

Trained Immunity in Atherosclerotic Cardiovascular Disease

Daniela Flores-Gomez, Siroon Bekkering, Mihai G. Netea, and Niels P. Riksen

Arterioscler Thromb Vasc Biol. 2021 Jan;41(1):62-69

Abstract

Atherosclerosis is characterized by incessant inflammation in the arterial wall in which monocytes and macrophages play a crucial role. During the past few years, it has been reported that cells from the innate immune system can develop a longlasting proinflammatory phenotype after brief stimulation not only with microbial products but also endogenous atherogenic stimuli. This persistent hyperactivation of the innate immune system is termed trained immunity and can contribute to the pathophysiology of atherosclerosis. Trained immunity is mediated via epigenetic and metabolic reprogramming and occurs both in mature innate immune cells as well as their bone marrow progenitors. In addition to monocytes, other innate immune and nonimmune cells involved in different stages of atherosclerosis can develop comparable memory characteristics. This mechanism provides exciting novel pharmacological targets that can be used to prevent or treat cardiovascular diseases.

Highlights

- Trained immunity describes a state of persistent hyperresponsiveness of
- This is induced by several endogenous atherogenic stimuli via metabolic and
- memory characteristics.
- Trained immunity offers exciting novel pharmacological targets to prevent and treat atherosclerotic cardiovascular disease.

Keywords

Atherosclerosis, cardiovascular disease, inflammation, innate immunity, monocyte

Atherosclerosis is the principal cause of cardiovascular disease (CVD). In the process of atherosclerosis, monocytes play an important role in the formation, (de)stabilization, and rupture of the atherosclerotic plague (1). In spite of what was historically described, cells of the innate immune system can develop a phenotype resembling immunologic memory that is called trained immunity. This is characterized by a long-lasting proinflammatory phenotype with a stronger cytokine response to a subsequent stimulation (2). This persistent overactivation of the innate immune system could contribute to the incessant vascular wall inflammation that is characteristic of atherosclerosis (1).

In this review, we will discuss the different triggers and mechanisms of trained immunity in the context of atherosclerosis in vitro and in vivo and how the functional changes of trained cells (immune and nonimmune) could influence the pathophysiology of atherosclerosis.

Brief introduction to innate immune memory

Over the past decade, evidence indicated that innate immune cells, such as monocytes, macrophages, and natural killer cells (NK) can develop characteristics of immunologic memory after brief exposure to microorganisms. This innate immune memory, termed trained immunity, is characterized by an enhanced cytokine response to a secondary challenge through functional reprogramming of the cells (2). Short exposure of monocytes to pathogens, such as Bacille Calmette-Guérin, Candida albicans, or its cell wall component β-glucan can alter cell function via epigenetic and metabolic reprogramming, thereby provoking an increased production of proinflammatory cytokines and chemokines in response to a secondary insult, which can be different than the initial insult (3-5). The classical in vitro trained immunity model consists of the exposure of isolated human monocytes for 24 hours to diverse stimuli that could induce training, followed by a 6-day washout and resting phase where monocytes differentiate into macrophages. The monocyte-derived macrophages are then restimulated for another 24 hours with TLR (Toll-like receptor) agonists, mostly lipopolysaccharides (6). For a complete overview on trained immunity, its mechanisms, and effects, we refer to a future review article by Tercan et al in this series.

From an evolutionary perspective, trained immunity functions as a protective response of the host against recurrent infections, but it can also lead to a maladaptive state (7). This detrimental effect can be present in situations where immune cells contribute to the pathophysiology of chronic inflammatory disorders such as atherosclerosis. First, trained immunity could be one of the mechanisms that contribute to the known epidemiological association between the infectious burden and atherosclerotic CVD (8). Second, in addition to microbial products, trained immunity can also be induced by endogenous atherogenic stimuli, which is highlighted below.

Endogenous atherogenic stimuli that can induce trained immunity in vitro and in vivo

Nonmicrobial endogenous stimuli that can induce trained immunity include lipoproteins and adrenal hormones among other factors, which are known to contribute to the development of atherosclerotic CVD (ASCVD). In this section, we will discuss some atherogenic endogenous stimuli that trigger trained immunity in monocytes and macrophages in vitro and their associated clinical in vivo scenarios.

Lipoproteins

Lipoproteins are biochemical constructs that allow hydrophobic lipids to be transported in the blood and are of relevance in the development of CVD (9). oxLDL (oxidized low-density lipoprotein) is a modified lipoprotein and is one of the key atherogenic molecules within plagues that activates immune cells, by binding to membrane-bound receptors and triggering foam cell formation after uptake by macrophages (10). Monocyte-derived macrophages briefly exposed to a low concentration of oxLDL in vitro and restimulated with relevant TLR agonists 6 days later, such as Pam3CSK4 and lipopolysaccharides for TLR 2 and 4, respectively, produce more atherogenic cytokines and chemokines, such as TNF (tumor necrosis factor) α, IL (interleukin) 6, MCP1 (monocyte chemoattractant protein 1), and more matrix metalloproteinases than untrained controls. Furthermore, foam cell formation is enhanced 6 days after initial exposure to oxLDL, due to the overexpression of SR-A (scavenger receptor-A) and CD36 and downregulation of the cholesterol efflux transporters ABCA1 (ATP-binding cassette transporter A1) and ABCG1 (ATP-binding cassette transporter G1) (11). Mechanistically, oxLDL-induced training is dependent on TLR2 and 4 activation (11), and on interleukin-1 signaling, since it is prevented by concomitant incubation with IL-1 receptor antagonist (12).

Similar to Bacille Calmette-Guérin and β-glucan-induced training, these oxLDLtrained macrophages show profound metabolic and epigenetic rewiring. Glycolysis and oxidative phosphorylation are upregulated in oxLDL-induced cells, and this is dependent on the mTOR/HIF1a (mammalian target of rapamycin/hypoxia-inducible factor 1-α) signaling pathway (13). Pharmacological inhibition of the mTOR pathway and the signaling molecules involved, as well as inhibition of glycolysis with 2-deoxyglucose prevented the increase in glycolysis and the proinflammatory phenotype in macrophages (14). Further proof of an essential role for glycolysis in oxLDL-induced training stems from the observation that in a large cohort of healthy subjects, genetic variation in key glycolytic enzymes is associated with the induction of cytokine production following an ex vivo training protocol of isolated monocytes (13), oxLDL-trained macrophages are also characterized by epigenetic reprogramming: there is enrichment of the activating histone modification H3K4me3 (trimethylation of lysine 4 at histone 3), on promotors of genes encoding for proinflammatory and proatherogenic cytokines and chemokines such as IL6, TNFα, SR-A, and CD36 (11). Pharmacological blocking of histone methyltransferases completely prevented training by oxLDL, indicating that epigenetic changes underly trained immunity by oxLDL (11).

Patients with familial hypercholesterolemia who have strongly elevated levels of LDLc (low-density lipoprotein cholesterol) have an increased risk to develop ASCVD. Their monocytes have a trained phenotype in terms of elevated cytokine production, elevated monocyte activation markers, and upregulation of immune activation, metabolic and inflammatory pathways compared with healthy controls (15). This is associated with an enrichment of H3K4me3 and a lower presence of H3K9me3 in the promoter region of TNFa (15). In contrast to previous studies, where trained immunity was successfully prevented in vitro using statins (16), it was established that treatment with statins for three months does not revert trained immunity in vivo in familial hypercholesterolemia patients (15). Ex vivo analysis of monocytes from familial hypercholesterolemia patients showed that, despite the lowering in cholesterol levels after 3 months of treatment with statins, the proinflammatory phenotype in monocytes persisted, suggesting that statins can prevent training, but not revert it (15).

Another lipoprotein that can induce trained immunity is Lp(a) (lipoprotein[a]), the main circulating carrier of oxidized phospholipids, which plays an important role in atherogenesis (17). Monocytes from healthy donors incubated in vitro for 24 hours with Lp(a) isolated from patients with elevated Lp(a) levels show an increased proinflammatory cytokine production after TLR ligand challenge 6 days later compared to untrained controls. This monocyte-derived macrophage training was attenuated by anti-oxidized phospholipid antibodies, indicating that this process is mediated by oxidized phospholipids (18). Monocytes isolated from patients with elevated Lp(a) levels showed increased trans-endothelial migration capacity. In vivo, patients with elevated circulating Lp(a) levels had an increased binding of leukocytes to the arterial wall and increased arterial inflammation. After ex vivo stimulation with Pam3Cys and lipopolysaccharides, monocytes presented an enhanced capacity to produce proinflammatory cytokines, such as IL6 and TNF α (18). In a recent study, it was established that potent lowering of Lp(a) levels can reverse the proinflammatory activation of monocytes in patients with CVD, showing that at least part of this proinflammatory effect is reversible (19).

A recent study in mice investigated hypercholesterolemia-induced innate immune memory by exposing atherosclerosis prone Ldlr-/- mouse to western-type diet. It has been shown that a 4-week period of western-type diet-induced long-term proinflammatory reprogramming of circulating innate immune cells and their myeloid progenitor cells in the bone marrow that persisted after reversing to a normal chow diet for another 4 weeks. These trained hematopoietic stem and progenitor cells were characterized by an augmented proliferation and inclination towards myelopoiesis and a subsequent heightened inflammatory response towards following subsequent challenges (12), Interestingly, in this model, trained immunity also appeared to be dependent on inflammatory pathways, such as IL1β and NLRP3 (NLR family pyrin domain-containing 3) activation (12). The finding that trained immunity occurs at the level of myeloid progenitors explains the observation in humans in vivo that trained immunity (in this case by Bacille Calmette-Guérin vaccination) persists at least a few months despite the short halflife of circulating monocytes (3, 20). To read more about trained immunity in the bone marrow, the reader is referred to a future article by Chavakis et al in this series.

Adrenal Hormones

Acute stress, for example, in the setting of a myocardial infarction, or chronic psychosocial stress is associated with an increased risk of ASCVD and in animal models with a temporary acceleration of atherosclerosis (21). An acute myocardial infarction is known to accelerate atherosclerosis and to increase future risk of ASCVD by activation of the sympathetic nervous system and subsequent bone marrow release of inflammatory immune cells (22). To understand the link between catecholamines, inflammation, and CVD, it was recently proposed that catecholamines induce trained immunity (23). Indeed, monocyte-derived macrophages exposed to a relevant concentration of epinephrine/norepinephrine showed increased levels of TNFα and IL6 upon lipopolysaccharides restimulation 6 days later. Similar to oxLDL, this trained immunity phenotype was associated with an increased glycolytic capacity and oxidative phosphorylation. Pharmacological

inhibition studies showed that the β-adrenergic receptor 1 and 2 and the cAMPprotein kinase A pathway were essential for catecholamine-induced training (23). This proinflammatory monocyte phenotype was also observed in patients with pheochromocytoma, a rare neuroendocrine tumor in the adrenal glands causing overproduction of catecholamines, who are exposed daily to transient bouts of catecholamine release (24). These patients showed signs of systemic inflammation and a more elevated ex vivo cytokine response in stimulated monocytes. Interestingly, the increased TNFa production did not significantly reduce one month after the surgical removal of the tumor. Epigenetic analysis showed that H3K4me3 was enriched in promoter regions of proinflammatory genes, although this did not reach significance because of the low patient number (23).

Aldosterone is another adrenal hormone that is associated with CVD. Elevated autonomous adrenal production of aldosterone, also denominated primary hyperaldosteronism, is a common cause of hypertension, which is linked to a higher risk of ASCVD (25). To explore whether innate immune activation is involved in mediating this higher risk, human monocytes were briefly exposed to aldosterone using the classical trained immunity model. Indeed, their production of proinflammatory cytokines upon lipopolysaccharides and Pam3Cys restimulation by monocyte-derived macrophages 6 days later was augmented, which was regulated via the MR (mineralocorticoid receptor). Mechanistically, aldosterone did not induce any changes in glycolysis and oxidative phosphorylation as seen in oxLDL training, but it did affect the intracellular metabolism by inducing fatty acid synthesis (26). Furthermore, aldosterone-induced training was associated with enrichment of H3K4me3 at the promoters of proinflammatory cytokines, such as TNFα and IL6, indicating that aldosterone causes training of monocyte-derived macrophages in vitro. In patients with primary hyperaldosteronism, however, circulating monocytes were not characterized by an enhanced cytokine production capacity. Only after ex vivo differentiation into macrophages in autologous serum, the macrophages of primary hyperaldosteronism patients showed a higher TNFα expression (27). Importantly, patients with primary hyperaldosteronism appeared to have arterial wall inflammation, as assessed by uptake of radiolabeled fluorodeoxyglucose (27). These findings suggest that aldosterone is different from the well-established trained immunity mechanisms induced by other stimuli and further research should be done to investigate what mechanisms underly the vascular wall inflammation and increased CVD risk in these patients.

Trained Immunity in Patients With Established CVD

In addition to patients with risk factors for atherosclerosis, trained immunity characteristics have also been reported in patients with established ASCVD. Freshly isolated monocytes from patients with symptomatic coronary artery disease showed an enhanced cytokine production capacity compared to healthy controls which persisted after ex vivo differentiation to macrophages for 5 days. This active state of inflammation leads to the generation of reactive oxygen species in the mitochondria regulated by the glycolytic enzyme PKM2 (pyruvate kinase M2) boosting the production of IL6 and IL1B via STAT3 (signal transducer and activator of transcription 3) (28). In an independent study, the enhanced cytokine production capacity of circulating monocytes was associated with metabolic and epigenetic characteristics of trained immunity: an upregulation of key glycolytic enzymes and epigenetic rewiring in histone marks of key proinflammatory genes related to atherosclerosis (29).

This inflammatory phenotype was recently shown to be reversed by lifestyle intervention in a small proof of principle study in patients at risk of CVD. In a group of patients with obesity with or without hypertension, an intervention to reduce sedentary behavior for 16 weeks showed favorable results. This intervention resulted in a significant reduction in cytokine production capacity of isolated monocytes upon ex vivo TLR stimulation. This came along with decreased glycolysis and oxidative phosphorylation rate suggesting that trained immunity is involved. This study, however, did not explore the epigenetic level; thus, it remains to be established whether lifestyle indeed targets trained immunity (30). Altogether, reducing sedentary behavior could represent an important approach in the prevention or reduction of inflammation in atherosclerosis.

In addition, a recent study suggests that trained immunity might also contribute to cerebral small vessel disease. This is the most important vascular cause for cognitive decline and dementia, which is characterized by arteriolosclerosis and share important risk factors with atherosclerosis. Within a cohort of patients with cerebral small vessel disease, cytokine production after ex vivo stimulation of isolated monocytes was associated with the rate of progression of the disease on MRI imaging (31). Further analysis of possible underlying epigenetic changes is warranted.

Trained immunity beyond the monocyte

Recent evidence indicates that trained immunity occurs not only in monocytes but also in other innate immune and nonimmune cells that play key roles in atherosclerosis, including NK, endothelial cells, and vascular smooth muscle cells (vSMC).

NK cells are innate immune granular cells that provide the host antitumoral and antiviral protection (32). There is abundant documentation of the presence of NK cells in the atherosclerotic plaque. Chemokines, such as MCP1 and fractalkine (CX3CL1 [chemokine (C-X3-C motif) ligand 1]), can recruit NK cells to the arterial wall and consecutive activation leads to the production of proatherogenic cytokines like IFN (interferon) v. Interestingly, the infiltration with NK cells is higher in symptomatic carotid plagues than in asymptomatic plagues (33). In the arterial wall in presence of oxLDL, NK cells interact with dendritic cells leading to enhanced activation of NK cells and maturation of dendritic cells, subsequently promoting the inflammatory potential of both cell populations and worsening the atherosclerotic lesion (34). Interestingly, similar to other innate immune cells, NK cells have the potential to develop immunologic memory. Bacille Calmette-Guérin vaccination of healthy volunteers increased the production of proinflammatory cytokines in NK cells upon unrelated microbial restimulation via epigenetic reprogramming 3 months after vaccination (35). Similarly, infection with cytomegalovirus confers NK cell memory, independent of T and B cells immunologic memory (36, 37). Given that oxLDL has a role in activation of NK cells and inflammation, it is tempting to speculate about the effect of trained immunity in NK cells and their role in atherogenesis. It is possible that (non)infectious or endogenous stimuli could also induce trained immunity in NK cells contributing to plaque inflammation but further investigation is warranted.

Nonimmune cells have also been shown to exhibit memory phenotypes (38), and it is likely that this mechanism could also contribute to atherogenesis. Endothelial cell and vSMC, both contributing to plaque formation, have been acknowledged to have immune characteristics with their ability to secrete cytokines, recognize molecular patterns, and present antigens. In endothelial cell cultures, a brief period of high-glucose exposure induces a long-lasting proinflammatory phenotype with increased cytokine production. This hyperglycemic memory is mediated by epigenetic modifications written by methyltransferase Set7 (39), regulating the expression of key atherogenic proteins such as MCP1 (40). To read more about the potential role of glucose in trained immunity, we refer to the future article by Choudhury et al in this series. More recently, Lp(a) and specifically its oxidized phospholipids were also shown to be able to reprogram endothelial cells into a more proinflammatory and proatherogenic phenotype via upregulation of glycolysis, similar to training of monocytes (41). In vSMCs, a series of receptors including LOX-1 (lectin-like oxidized low-density lipoprotein receptor) and TLRs, are of importance in the initiation and progression of atherosclerosis (42). The overexpression of these genes, sometimes driven by the epigenetic modification H3K9me3, result in the activation of proinflammatory pathways and signals that do not only affect the cellular metabolism but also induce the production of cytokines and chemokines related to atherosclerosis (43). A similar phenotype was observed after short stimulation of vSMC with oxLDL, indicating a training potential of vascular nonimmune cells (44). Additionally, other nonimmune cells such as fibroblasts, can undergo epigenetic reprogramming and present an increased inflammatory response upon restimulation in arthritis, strengthening the theory of immunologic memory in nonimmune cells (45, 46). Although the role of endothelial cell and vSMC in atherosclerosis has been widely established, recent studies suggest that trained immunity can contribute to the long-term functional effects, triggered by atherogenic stimuli.

Clinical Applications and remaining questions

Although in the last few years anti-inflammatory therapies, such as canakinumab (47) and colchicine (48), have been shown to reduce CVD, there are important adverse effects and a large residual risk remains. Therefore, novel therapies are urgently needed and trained immunity might provide exciting novel pharmacological targets that can be used in this regard.

Central mechanisms regulating the inflammatory landscape in trained immunity are metabolic and epigenetic reprogramming of the myeloid cells, which are described in detail by Lutgens et al in this series and previous reviews (2). Theoretically, these processes are amenable for pharmacological modulation, as have been described in detail by Mulder et al (49). Specific epigenetic enzymes that regulate trained immunity are KDM5 (lysine demethyltransferase 5) and Set7 (SET domain containing 7, histone lysine methyltransferase). In trained immunity specifically, the accumulation of fumarate can induce epigenetic reprogramming by inhibiting the KDM5 histone demethylases (50). Furthermore, the methyltransferase Set7 was found to have an important role in β-glucan-induced trained immunity, regulating H3K4me1-mediated changes in oxidative phosphorylation. Set7 also regulates gene expression previously associated with the induction of myelopoiesis of bone

marrow progenitors (51). In addition to histone methylation and histone acetylation (mainly H3K27ac [histone 3 lysine 27 acetylation]), other epigenetic mechanisms are involved in trained immunity, including DNA methylation and long noncoding RNAs, which are described in detail elsewhere (2, 4).

In addition to epigenetic remodeling, the metabolic adaptations that occur during training offer potential therapeutic targets. Important metabolic pathways that have been identified are the glycolysis pathway, glutaminolysis, and the mevalonate pathway (2). In isolated human monocytes inhibition of the inducible glycolytic enzyme PFKFB3 (6-phosphofructo-2-kinase/fructose-2,6-bisphosphatase 3) with the small-molecule 3PO (3-[3-pyridinyl]-1-[4-pyridinyl]-2-propen-1-one) prevents oxLDL-induced trained immunity in vitro (13). Interestingly, 3PO only partially inhibits glycolysis, and it has recently been reported that systemic administration of 3PO to atherosclerosis prone mice indeed significantly reduces atherosclerotic lesion development, although the focus of this paper was on endothelial cell glycolytic metabolism (52). Statins can prevent trained immunity induced by β -glucan and oxLDL in vitro (16). It is important to realize, however, that statins were not able to revert the trained immune phenotype in patients with hypercholesterolemia, in whom the epigenetic marks were already written (15).

The most important drawback of interfering pharmacologically in epigenetic and metabolic processes is that these processes occur in every single cell in the human body with diverse functions. Therefore, it is critical to combine drugs that specifically target enzymes involved in trained immunity with delivery methods that allow specific targeting of cell types. Nanoparticles have been used in the treatment of inflammatory diseases due to their potential to target specific cells (49). For example, in murine atherosclerosis models, statin loaded rHDL (reconstituted high-density lipoprotein) nanoparticles were able to block plaque formation by specifically targeting plaque macrophages (53). Similarly, carbon nanotubes loaded with antiphagocytic pathway inhibitors reactivated phagocytosis and decreased the expression of proinflammatory cytokines in lesional macrophages in Ldlr deficient mice (54). Given the versatility of nanoparticles, it is possible to develop diverse immunotherapies that are able to provide specificity and target only the regions and cell types of interest.

Conclusions

Evidence indicates that low-grade inflammation is part of the pathogenesis of atherosclerosis and is largely mediated by the immune system. In this review, we highlighted the mechanisms that could associate trained immunity to the development and progression of ASCVD based on current clinical and in vitro data (Figure). Better understanding of molecular and systemic consequences of trained immunity and its effect on atherosclerosis will allow the development of novel targeted treatments to prevent and regulate ASCVD.

Acknowledgments

The Figure was created with BioRender.com.

Nonstandard Abbreviations and Acronyms

3PO 3-[3-pyridinyl]-1-[4-pyridinyl]-2-propen-1-one

ASCVD atherosclerotic cardiovascular disease

cardiovascular disease CVD

chemokine (C-X3-C motif) ligand 1 CX3CI1

IFN interferon Ш interleukin

I DI c low-density lipoprotein cholesterol Ldlr low-density lipoprotein receptor

Lp(a) lipoprotein(a)

MCP1 monocyte chemoattractant protein 1

mTOR/HIF1a mammalian target of rapamycin/hypoxia-inducible factor 1-α

NK natural killer cell

oxLDL oxidized low-density lipoprotein

PFKFB3 6- phosphofructo-2-kinase/fructose-2,6-bisphosphatase

PKM2 pyruvate kinase M2

rHDI reconstituted high-density lipoprotein

SR-A scavenger receptor-A TLR Toll-like receptor TNF tumor necrosis factor

vascular smooth muscle cell vSMC

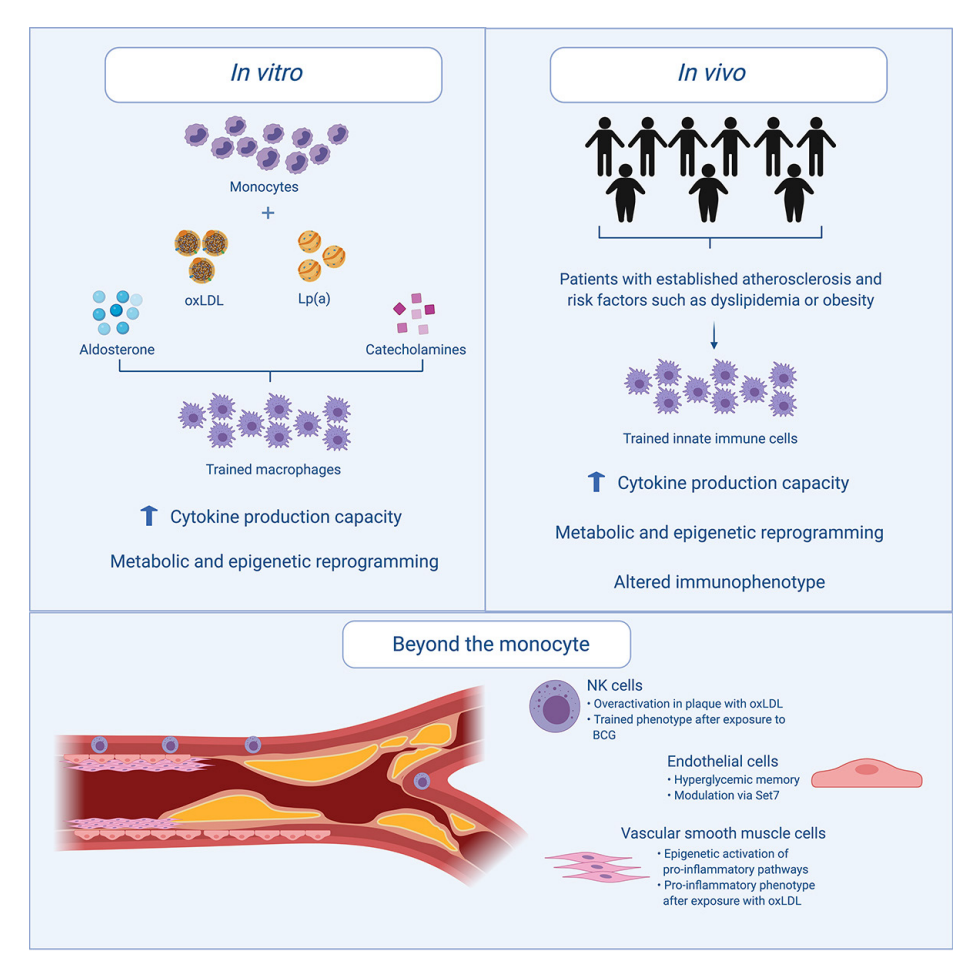


Figure: Schematic summary of trained immunity in atherosclerosis in humans. Several endogenous atherogenic stimuli have been found to induce trained immunity in human monocytes in vitro. This phenotype is characterized by an increased cytokine production capacity and metabolic and epigenetic reprogramming. These aspects can also be present in isolated monocytes from patients with established atherosclerosis or risk factors for cardiovascular disease. Likewise, trained immunity appears to affect other innate immune and nonimmune cells related to atherosclerosis. Lp(a) indicates lipoprotein(a); NK, natural killer cell; and oxLDL, oxidized low-density lipoprotein.

References

- 1 Moore KJ, Sheedy FJ, Fisher EA. Macrophages in atherosclerosis: a dynamic balance. Nat Rev Immunol. 2013:13(10):709-21.
- Netea MG, Domínguez-Andrés J, Barreiro LB, Chavakis T, Divangahi M, Fuchs E, et al. Defining 2. trained immunity and its role in health and disease. Nat Rev Immunol. 2020;20(6):375-88.
- 3. Kleinnijenhuis J, Quintin J, Preijers F, Joosten LA, Ifrim DC, Saeed S, et al. Bacille Calmette-Guerin induces NOD2-dependent nonspecific protection from reinfection via epigenetic reprogramming of monocytes. Proc Natl Acad Sci U S A. 2012;109(43):17537-42.
- Saeed S, Quintin J, Kerstens HH, Rao NA, Aghajanirefah A, Matarese F, et al. Epigenetic programming of monocyte-to-macrophage differentiation and trained innate immunity. Science. 2014;345(6204):1251086.
- Cheng SC, Quintin J, Cramer RA, Shepardson KM, Saeed S, Kumar V, et al. mTOR- and HIF-1α-mediated aerobic glycolysis as metabolic basis for trained immunity. Science. 2014;345(6204):1250684.
- Quintin J, Saeed S, Martens JHA, Giamarellos-Bourboulis EJ, Ifrim DC, Logie C, et al. Candida albicans infection affords protection against reinfection via functional reprogramming of monocytes. Cell Host Microbe. 2012;12(2):223-32.
- Netea MG, Joosten LA, Latz E, Mills KH, Natoli G, Stunnenberg HG, et al. Trained immunity: A program of innate immune memory in health and disease. Science. 2016;352(6284):aaf1098.
- Leentjens J, Bekkering S, Joosten LAB, Netea MG, Burgner DP, Riksen NP. Trained Innate Immunity as a Novel Mechanism Linking Infection and the Development of Atherosclerosis. Circ Res. 2018;122(5):664-9.
- Burnett JR. Lipids, lipoproteins, atherosclerosis and cardiovascular disease. Clin Biochem Rev. 2004:25(1):2.
- 10. Moore KJ, Tabas I. Macrophages in the pathogenesis of atherosclerosis. Cell. 2011;145(3):341-55.
- 11. Bekkering S, Quintin J, Joosten LA, van der Meer JW, Netea MG, Riksen NP. Oxidized low-density lipoprotein induces long-term proinflammatory cytokine production and foam cell formation via epigenetic reprogramming of monocytes. Arterioscler Thromb Vasc Biol. 2014;34(8):1731-8.
- 12. Christ A, Günther P, Lauterbach MAR, Duewell P, Biswas D, Pelka K, et al. Western Diet Triggers NLRP3-Dependent Innate Immune Reprogramming. Cell. 2018;172(1-2):162-75.e14.
- 13. Keating ST, Groh L, Thiem K, Bekkering S, Li Y, Matzaraki V, et al. Rewiring of glucose metabolism defines trained immunity induced by oxidized low-density lipoprotein. J Mol Med (Berl). 2020;98(6):819-31.
- 14. Sohrabi Y, Lagache SMM, Schnack L, Godfrey R, Kahles F, Bruemmer D, et al. mTOR-Dependent Oxidative Stress Regulates oxLDL-Induced Trained Innate Immunity in Human Monocytes. Front Immunol. 2018;9:3155.
- 15. Bekkering S, Stiekema LCA, Bernelot Moens S, Verweij SL, Novakovic B, Prange K, et al. Treatment with Statins Does Not Revert Trained Immunity in Patients with Familial Hypercholesterolemia. Cell Metab. 2019;30(1):1-2.
- 16. Bekkering S, Arts RJW, Novakovic B, Kourtzelis I, van der Heijden C, Li Y, et al. Metabolic Induction of Trained Immunity through the Mevalonate Pathway. Cell. 2018;172(1-2):135-46.e9.
- 17. Boffa MB, Koschinsky ML. Oxidized phospholipids as a unifying theory for lipoprotein(a) and cardiovascular disease. Nat Rev Cardiol. 2019;16(5):305-18.

- 18. van der Valk FM, Bekkering S, Kroon J, Yeang C, Van den Bossche J, van Buul JD, et al. Oxidized Phospholipids on Lipoprotein(a) Elicit Arterial Wall Inflammation and an Inflammatory Monocyte Response in Humans. Circulation. 2016;134(8):611-24.
- 19. Stiekema LCA, Prange KHM, Hoogeveen RM, Verweij SL, Kroon J, Schnitzler JG, et al. Potent lipoprotein(a) lowering following apolipoprotein(a) antisense treatment reduces the proinflammatory activation of circulating monocytes in patients with elevated lipoprotein(a). Eur Heart J. 2020;41(24):2262-71.
- 20. Cirovic B, de Bree LCJ, Groh L, Blok BA, Chan J, van der Velden W, et al. BCG Vaccination in Humans Elicits Trained Immunity via the Hematopoietic Progenitor Compartment. Cell Host Microbe. 2020;28(2):322-34.e5.
- 21. Song H, Fang F, Arnberg FK, Mataix-Cols D, Fernández de la Cruz L, Almqvist C, et al. Stress related disorders and risk of cardiovascular disease: population based, sibling controlled cohort study. Bmj. 2019;365:l1255.
- 22. Dutta P, Courties G, Wei Y, Leuschner F, Gorbatov R, Robbins CS, et al. Myocardial infarction accelerates atherosclerosis. Nature. 2012;487(7407):325-9.
- 23. van der Heijden C, Groh L, Keating ST, Kaffa C, Noz MP, Kersten S, et al. Catecholamines Induce Trained Immunity in Monocytes In Vitro and In Vivo. Circ Res. 2020;127(2):269-83.
- 24. Pacak K, Wimalawansa SJ. Pheochromocytoma and paraganglioma. Endocrine Practice. 2015;21(4):406-12.
- 25. Monticone S, D'Ascenzo F, Moretti C, Williams TA, Veglio F, Gaita F, et al. Cardiovascular events and target organ damage in primary aldosteronism compared with essential hypertension: a systematic review and meta-analysis. Lancet Diabetes Endocrinol. 2018;6(1):41-50.
- 26. van der Heijden C, Keating ST, Groh L, Joosten LAB, Netea MG, Riksen NP. Aldosterone induces trained immunity: the role of fatty acid synthesis. Cardiovasc Res. 2020;116(2):317-28.
- 27. van der Heijden C, Smeets EMM, Aarntzen E, Noz MP, Monajemi H, Kersten S, et al. Arterial Wall Inflammation and Increased Hematopoietic Activity in Patients With Primary Aldosteronism. J Clin Endocrinol Metab. 2020;105(5):e1967-80.
- 28. Shirai T, Nazarewicz RR, Wallis BB, Yanes RE, Watanabe R, Hilhorst M, et al. The glycolytic enzyme PKM2 bridges metabolic and inflammatory dysfunction in coronary artery disease. J Exp Med. 2016;213(3):337-54.
- 29. Bekkering S, van den Munckhof I, Nielen T, Lamfers E, Dinarello C, Rutten J, et al. Innate immune cell activation and epigenetic remodeling in symptomatic and asymptomatic atherosclerosis in humans in vivo. Atherosclerosis. 2016;254:228-36.
- 30. Noz MP, Hartman YAW, Hopman MTE, Willems P, Tack CJ, Joosten LAB, et al. Sixteen-Week Physical Activity Intervention in Subjects With Increased Cardiometabolic Risk Shifts Innate Immune Function Towards a Less Proinflammatory State. J Am Heart Assoc. 2019;8(21):e013764.
- 31. Noz MP, Ter Telgte A, Wiegertjes K, Joosten LAB, Netea MG, de Leeuw FE, et al. Trained Immunity Characteristics Are Associated With Progressive Cerebral Small Vessel Disease. Stroke. 2018;49(12):2910-7.
- 32. Abel AM, Yang C, Thakar MS, Malarkannan S. Natural Killer Cells: Development, Maturation, and Clinical Utilization. Front Immunol. 2018;9:1869.

- 33. Bonaccorsi I, Spinelli D, Cantoni C, Barillà C, Pipitò N, De Pasquale C, et al. Symptomatic Carotid Atherosclerotic Plagues Are Associated With Increased Infiltration of Natural Killer (NK) Cells and Higher Serum Levels of NK Activating Receptor Ligands. Front Immunol. 2019;10:1503.
- 34. Bonaccorsi I, De Pasquale C, Campana S, Barberi C, Cavaliere R, Benedetto F, et al. Natural killer cells in the innate immunity network of atherosclerosis. Immunol Lett. 2015;168(1):51-7.
- Kleinnijenhuis J, Quintin J, Preijers F, Joosten LA, Jacobs C, Xavier RJ, et al. BCG-induced trained immunity in NK cells: Role for non-specific protection to infection. Clin Immunol. 2014;155(2):213-9.
- 36. Schlums H, Cichocki F, Tesi B, Theorell J, Beziat V, Holmes TD, et al. Cytomegalovirus infection drives adaptive epigenetic diversification of NK cells with altered signaling and effector function. Immunity. 2015;42(3):443-56.
- 37. Sun JC, Madera S, Bezman NA, Beilke JN, Kaplan MH, Lanier LL. Proinflammatory cytokine signaling required for the generation of natural killer cell memory. J Exp Med. 2012;209(5):947-54.
- 38. Hamada A, Torre C, Drancourt M, Ghigo E. Trained Immunity Carried by Non-immune Cells. Front Microbiol, 2018:9:3225.
- 39. Okabe J, Orlowski C, Balcerczyk A, Tikellis C, Thomas MC, Cooper ME, et al. Distinguishing hyperglycemic changes by Set7 in vascular endothelial cells. Circ Res. 2012;110(8):1067-76.
- 40. Siebel AL, Fernandez AZ, El-Osta A. Glycemic memory associated epigenetic changes. Biochem Pharmacol. 2010;80(12):1853-9.
- 41. Schnitzler JG, Hoogeveen RM, Ali L, Prange KHM, Waissi F, van Weeghel M, et al. Atherogenic Lipoprotein(a) Increases Vascular Glycolysis, Thereby Facilitating Inflammation and Leukocyte Extravasation. Circ Res. 2020;126(10):1346-59.
- 42. Lim S, Park S. Role of vascular smooth muscle cell in the inflammation of atherosclerosis. BMB Rep. 2014;47(1):1-7.
- 43. Harman JL, Dobnikar L, Chappell J, Stokell BG, Dalby A, Foote K, et al. Epigenetic Regulation of Vascular Smooth Muscle Cells by Histone H3 Lysine 9 Dimethylation Attenuates Target Gene-Induction by Inflammatory Signaling. Arterioscler Thromb Vasc Biol. 2019;39(11):2289-302.
- 44. Schnack L, Sohrabi Y, Lagache SMM, Kahles F, Bruemmer D, Waltenberger J, et al. Mechanisms of Trained Innate Immunity in oxLDL Primed Human Coronary Smooth Muscle Cells. Front Immunol. 2019;10:13.
- 45. Huber LC, Brock M, Hemmatazad H, Giger OT, Moritz F, Trenkmann M, et al. Histone deacetylase/ acetylase activity in total synovial tissue derived from rheumatoid arthritis and osteoarthritis patients. Arthritis Rheum. 2007;56(4):1087-93.
- 46. Kawabata T, Nishida K, Takasugi K, Ogawa H, Sada K, Kadota Y, et al. Increased activity and expression of histone deacetylase 1 in relation to tumor necrosis factor-alpha in synovial tissue of rheumatoid arthritis. Arthritis Res Ther. 2010;12(4):R133.
- 47. Ridker PM, Everett BM, Thuren T, MacFadyen JG, Chang WH, Ballantyne C, et al. Antiinflammatory Therapy with Canakinumab for Atherosclerotic Disease. N Engl J Med. 2017;377(12):1119-31.
- 48. Tardif JC, Kouz S, Waters DD, Bertrand OF, Diaz R, Maggioni AP, et al. Efficacy and Safety of Low-Dose Colchicine after Myocardial Infarction. N Engl J Med. 2019;381(26):2497-505.
- 49. Mulder WJM, Ochando J, Joosten LAB, Fayad ZA, Netea MG. Therapeutic targeting of trained immunity. Nat Rev Drug Discov. 2019;18(7):553-66.
- 50. Arts RJ, Novakovic B, Ter Horst R, Carvalho A, Bekkering S, Lachmandas E, et al. Glutaminolysis and Fumarate Accumulation Integrate Immunometabolic and Epigenetic Programs in Trained Immunity. Cell Metab. 2016;24(6):807-19.

- 51. Keating ST, Groh L, van der Heijden C, Rodriguez H, Dos Santos JC, Fanucchi S, et al. The Set7 Lysine Methyltransferase Regulates Plasticity in Oxidative Phosphorylation Necessary for Trained Immunity Induced by β-Glucan. Cell Rep. 2020;31(3):107548.
- 52. Perrotta P, Van der Veken B, Van Der Veken P, Pintelon I, Roosens L, Adriaenssens E, et al. Partial Inhibition of Glycolysis Reduces Atherogenesis Independent of Intraplaque Neovascularization in Mice. Arterioscler Thromb Vasc Biol. 2020;40(5):1168-81.
- 53. Duivenvoorden R, Tang J, Cormode DP, Mieszawska AJ, Izquierdo-Garcia D, Ozcan C, et al. A statin-loaded reconstituted high-density lipoprotein nanoparticle inhibits atherosclerotic plaque inflammation. Nat Commun. 2014;5:3065.
- 54. Flores AM, Hosseini-Nassab N, Jarr KU, Ye J, Zhu X, Wirka R, et al. Pro-efferocytic nanoparticles are specifically taken up by lesional macrophages and prevent atherosclerosis. Nat Nanotechnol. 2020;15(2):154-61.



Chapter 3

The effect of leptin on trained innate immunity and on systemic inflammation in subjects with obesity

Daniela Flores Gomez, Siroon Bekkering, Rob ter Horst, Benjamin Cossins, Inge C L van den Munckhof, Joost H W Rutten, Leo A B Joosten, Mihai G Netea and Niels P Riksen

J Leukoc Biol. 2024 Jan 19;115(2):374-384

Abstract

Leptin is associated with cardiometabolic complications of obesity, such as metabolic syndrome and atherosclerosis. In obese men, the presence of metabolic syndrome is associated with higher circulating leptin and interleukin (IL)-6 concentrations and increased monocyte cytokine production capacity. Here, we investigated the effects of leptin on monocyte function and systemic inflammatory markers in obese individuals. We specifically explored whether leptin can induce long-term changes in innate immune function by inducing innate immune memory (also called trained immunity). We exposed human primary monocytes for 24 h to relevant leptin concentrations in vitro and measured cytokine production. In addition, after removing leptin, we incubated monocytes for 5 d in culture medium, and we restimulated them on day 6 to assess cytokine production capacity, phagocytosis, and foam cell formation. Direct stimulation with leptin did not induce cytokine production, but exposure to 50 ng/mL leptin augmented lipopolysaccharide- and R848-induced tumor necrosis factor α (TNF-α) production after 1 wk. In a separate in vivo study in a cohort of 302 obese subjects (body mass index [BMI] >27 kg/m2, 55 to 81 vr), we measured circulating leptin, inflammatory markers, and cytokine production upon ex vivo stimulation of isolated peripheral blood mononuclear cells. Circulating leptin concentrations positively correlated with circulating IL-1β and IL-6, which was more pronounced in men than in women. Four single nucleotide polymorphisms in the leptin gene influenced circulating IL-6 concentrations in men, suggesting a direct effect of leptin on IL-6. In conclusion, in vitro, leptin does not directly stimulate monocytes to produce cytokines, yet induces long-term monocyte hyperresponsiveness, i.e. trained immunity. In obese subjects, leptin is associated with circulating IL-6 in a sex-dependent manner. The underlying mechanisms of the sex-specific effect of leptin on innate immune cells remain to be further investigated.

Keywords

Introduction

During the last decades, a large proportion of the world's population became overweight or obese leading to an increase in related cardiometabolic complications (1). Obesity is associated with low-grade systemic inflammation, and this contributes to its metabolic and atherosclerotic consequences (1, 2). However, the mechanisms driving this association have not yet been fully elucidated (3).

Atherosclerotic cardiovascular disease is a chronic, low-grade inflammatory disorder of the vascular wall, and its pathophysiology is strongly mediated by innate immune cells such as monocytes (4). Circulating monocytes are recruited to the vascular wall, where they differentiate into macrophages playing an important role in the formation and destabilization of atherosclerotic plaques (5). Obesity is associated with the activation of innate immune cells such as monocytes and macrophages (6). It has recently been described that monocytes can build a longterm hyperresponsive phenotype after brief exposure to endogenous atherogenic stimuli, including oxidized low-density lipoprotein (oxLDL) (7), lipoprotein(a) (8), and adrenal hormones (9, 10). This de facto innate immune memory has been termed trained immunity and probably contributes to atherosclerotic cardiovascular disease development (11). Importantly, recent experimental studies have shown that obesity can also induce trained immunity, which persists after weight loss (12-14).

Obesity is associated with an increased production of adipose tissue-related proinflammatory molecules, such as the adipokine leptin (15). While its main function is to regulate appetite, leptin is also involved in other physiological processes such as energy homeostasis, and metabolic and immune regulation (16, 17).

The concentrations of circulating leptin in the blood are directly proportional to the amount of adipose tissue and, generally, women have higher levels of circulating leptin than men (18). We recently explored the association between circulating leptin and the presence of metabolic syndrome (MetS) in individuals with overweight or obesity (19). We observed that in men, circulating leptin and interleukin (IL)-6 concentrations are higher in the presence of MetS, whereas in women, the presence of MetS is associated with lower anti-inflammatory adiponectin levels (19). Additionally, the production capacity of isolated peripheral blood mononuclear cells (PBMCs) for IL-6 and IL-1β was higher in men with MetS compared to overweight men without MetS (19).

Based on these observations, we hypothesized that leptin contributes to the adverse metabolic and cardiovascular complications of obesity by inducing trained immunity in circulating innate immune cells.

In the present study, we performed a series of *in vitro* studies in isolated primary human monocytes using physiologically relevant concentrations of leptin. We subsequently explored the association between circulating leptin concentrations and markers of inflammation and cytokine production capacity of PBMCs in a cohort of obese individuals. These results help to understand the role of leptin in the regulation of inflammation in obesity.

Methods

Reagents

Human recombinant leptin was dissolved in 20 mM of Tris-HCl pH 8, according to the instructions of the manufacturer (R&D Systems). Toll-like receptor (TLR) agonists include lipopolysaccharide (LPS) for TLR4 (Sigma-Aldrich: Escherichia coli serotype 055:B5, further purified as described)(20) and Pam3Cys for TLR2 (EMC micro-collections; L2000). Cells were cultured in RPMI 1640 Dutch modified culture medium supplemented with 50 µg/mL gentamycin (Centrafarm), 1 mM pyruvate (Invitrogen), 2 mM glutamine (Invitrogen), and 10% human pooled serum.

Preparation of oxidized low-density lipoprotein

oxLDL was prepared from LDL, which was previously isolated by density-grade ultra-centrifugation from EDTA blood from healthy volunteers. LDL was dialyzed in a Slide-A-Lyzer Dialysis Cassette, 10 K MWCO, 3 mL (Thermo Fisher Scientific) for 7 h in phosphate-buffered saline (PBS), refreshing the buffer after 1 and 3 h. LDL was then oxidized by incubation with 20 µM CuSO4, for 16 h in a heat block at 37 °C, 600 rpm followed by 1 h of dialysis in PBS as previously described (21). The protein concentration was measured with BCA Protein Assay Kit (Thermo Fisher Scientific).

Cell isolation

Human PBMCs and monocytes were isolated from the blood of healthy volunteers after written informed consent (Sanguin Bloodbank) as described previously (22). Briefly, PBMCs were isolated by density gradient centrifugation with Ficoll-Plague PLUS (GE Healthcare Biosciences) followed by 3 washes with cold PBS. Monocytes were isolated from PBMCs by differential centrifugation using hyperosmotic Percoll solution (Sigma-Aldrich) and washed with cold PBS 1 time as described previously (22). Cells were resuspended in supplemented RPMI 1640 and counted using a Sysmex Hematoanalyzer XE5000.

Direct stimulation and in vitro training experiments

PBMCs were diluted to a concentration of $5 \times 10^6/\text{mL}$ in supplemented RPMI. A total of 5 × 10⁵ cells were plated per well in round-bottom 96-well plates and were stimulated for 24 h with RPMI only as the negative control, and 1, 50, and 100 ng/mL of human recombinant leptin. After 24 h, the plates were centrifuged and supernatants were collected and stored at −20 °C until further assessment.

Trained immunity was assessed using the well-established training protocol as described before (23, 24). In brief, monocytes were diluted to a concentration of $1 \times$ 106/mL in supplemented RPMI medium. Cells were plated on flat-bottom 96- or 6-well culture plates for 1 h, followed by a warm PBS wash to remove the nonadherent cells. This step allows Percoll-isolated monocytes to reach a purity of >95%, as previously reported (24). The monocytes were incubated with 10% human pooled serum and oxLDL (10 µg/mL), human recombinant leptin (1, 5, and 50 ng/mL), or both for 24 h, after which the cells were washed with warm PBS. The cells were then incubated for 6 d in medium containing RPMI + 10% human pooled serum. After this period, they were restimulated for 24 h with RPMI only, LPS (10 ng/mL), R848 (5 µg/mL), or Pam3Cys (10 μg/mL) to assess IL-6 and TNF-α; and LPS + Nigericin (10 ng/mL and 1 μM, respectively) to assess intra- and extracellular IL-1β. Following this incubation period, the plate was centrifuged and supernatants were collected. Additionally, 100 µL of 0.5% Triton X (Sigma-Aldrich) were added to the cells for intracellular measurements. All the material was stored at -20 °C until further assessment.

Cytokine measurements

IL-6 (DY201), TNF- α (DY210), and IL-1 β (DY206) were measured in supernatants by enzyme-linked immunosorbent assay following the manufacturer's instructions (R&D Systems).

Flow cytometry

Monocytes were isolated using magnetic-activated cell sorting using a pan-monocyte isolation kit according to the manufacturer's instructions (purity >95%, data not shown) (Miltenyi Biotec). A total of 1×10^6 cells were plated per well in a 6-well culture plate following the trained immunity protocol described previously. Cells were stimulated with RPMI only, oxLDL (10 µg/mL), leptin (1 or 50 ng/mL), or both. After 6 d the cells were detached using Accutase solution (400 to 600 units/mL; Sigma-Aldrich), counted in a CASY cell counter (Omni Life Science), and used for flow cytometry analysis.

TLR2 and TLR4 expression was determined by flow cytometry. Trained macrophages were stained with monoclonal antibodies CD45, CD284, CD282 (TLR2), and live/dead stain FVS620 (Table 1) in buffer containing 1% bovine serum albumin (Sigma-Aldrich) and PBS for 30 min. After the incubation time, the cells were washed and resuspended in the same buffer to be measured with a CytoFlex flow cytometer (Beckman Coulter; RRID: SCR_017217) that underwent daily quality control. The gating strategy is shown in Supplementary Figure 1, and gates were determined by fluorescence minus one method (25). In short, macrophages were gated based on CD45+ and sidescatter properties, then the selection continued based on TLR2+ or TLR4+. Median fluorescence intensity was assessed on TLR2- or TLR4-positive cells. Data were analyzed with Kaluza 2.1 software (Beckman Coulter; RRID:SCR 016182).

Table 1: Flow cytometry panel used to measure the expression of TLR2 and 4 in trained macrophages at day 6.

Marker	Fluorochrome	Clone	Manufacturer	Cat#	RRID#
CD45	BV510	30-F11	BioLegend	103137	AB_2561392
CD284 (TLR4)	PE	HTA125	BioLegend	312806	AB_2205002
CD282 (TLR2)	APC	W15145C	BioLegend	392304	AB_2721443
FVS620 (live/dead)	ECD	_	BD	564996	AB_2869636

Abbreviations: APC = allophycocyanin; BV = brilliant violet; ECD = phycoerythrin-Texas Red conjugate/ electron coupled dye.

Phagocytosis assay

To assess changes in macrophage phagocytosis capacity, we used the trained immunity model and exposed monocytes to leptin (1 and 50 ng/mL) and oxLDL 10 μg/mL for 24 h. Monocytes were differentiated into macrophages for 6 d and subsequently, a phagocytosis assay was performed according to the instructions of the manufacturer (Cayman Chemical; 500209). In short, latex beads (rabbit IgC FITC) were added to the macrophages for 3 h. The cell nucleus was then stained with Hoechst blue and dead cells were stained with 4 uM ethidium homodimer and wheat germ agglutinin. The phagocytosis rate was quantified using R version 4.2.2 (R Foundation for Statistical Computing). Cell clusters were separated from the background in a greyscale image by blurring and brightening and adaptive thresholding. Cluster size was then measured in number of pixels allowing filtering of clusters to identify single cells. Identified clusters were converted to masks in the blue, green, and red channels to then measure median fluorescence intensity. The phagocytic rate in the macrophages trained with leptin or oxLDL was expressed as the fold increase compared to the uptake by the untrained RPMI control cells.

Foam cell formation

To determine the effect of leptin training on macrophage lipoprotein uptake, a foam cell formation assay was performed as described previously (7). Monocytes were trained for 24 h with leptin (1 and 50 ng/mL) and oxLDL 10 µg/mL and differentiated into macrophages. To induce foam cell formation, at day 6, macrophages were incubated with serum-free RPMI medium for 4 h. Then, cells were incubated with medium containing RPMI only or oxLDL 50 µg/mL for 24 h. The accumulation of lipids was then visualized by Oil Red O staining. We quantified the intracellular lipid droplets using the R package EBImage. In brief, cells were identified and isolated from the images, before re-analysis to identify droplets within the cells. Cell identification was performed by inverting the bright-field image, converting it to grayscale, brightening and blurring, and applying an adaptive threshold to identify foreground components. To maximize the area of the cells covered, and account for gaps, the foreground area was dilated, and all enclosed areas were filled to make a continuous cell. Each cell was then reprocessed in turn to identify droplets within, starting by reverting to bright field, brightening, adaptive thresholding, and finally quantification. To differentiate oil droplets from the bright halo (resulting from dilation of the cells) and nonstained areas in the cells, light transmittance was reduced to a 93% to identify the droplets with red stain in them. A schematic representation of the quantification can be found in Supplementary Figure 2.

300-Obesity cohort description

To validate our in vitro data, we used data from the 300-Obesity (300-OB) cohort. This cohort consists of 302 obese individuals with BMI ≥27 kg/m² between 55 and 82 yr of age, mostly of Western European background, and has been reported previously (19). Circulating leptin (R&D Systems), IL-6 (Sanguin; M9316), and IL-1β (R&D Systems; DY201) were measured in EDTA plasma using enzyme-linked immunosorbent assay according to the manufacturer's instructions. PBMCs were isolated from EDTA blood with density gradient centrifugation with Ficoll-Plague PLUS (GE Healthcare Biosciences). A total of 5×10^5 PBMCs were stimulated for 24 h in 96-well round-bottom plates at 37 °C and 5% CO2 with RPMI as negative control and LPS in a low dose (1 ng/mL) and a high dose (100 ng/mL) as well as Pam3Cys (1 µg/mL). After the 24 h incubation period, supernatants were collected and stored at -20 °C until cytokine assessment. TNF-α (R&D Systems; DY210), IL-6 (Sanquin; M9316), and IL-1β (R&D Systems; DY201) cytokine production after stimulation was measured according to the instructions of the manufacturer.

300-OB cohort correlation analysis

Spearman correlation was calculated between leptin plasma concentration, circulatory cytokines, and cytokine production capacity of PMBCs in all the participants, and in groups stratified according to sex and MetS.

We corrected for age as a cofactor and for multiple testing using the Benjamini-Hochberg false discovery rate method. Adjusted P values ≤0.05 were considered statistically significant.

300-OB cohort single nucleotide polymorphism analysis

Genotypina

About half of the samples (n = 134) were genotyped using the Illumina HumanCoreExome-24 BeadChip Kit (later renamed to Infinium CoreExome-24 Kit). The other half of the samples (n = 168) were previously genotyped using the Illumina Infinium Omni-express chip because the volunteers had participated in another study (26), and the genotype data from this study were used. The 2 sets were merged, keeping only single nucleotide polymorphisms (SNPs) in common between the 2 datasets. After imputation (described below), principal component analysis was used to verify that there were no differences between the 2 batches. As an additional precaution, in all genetic analyses "chip origin" was used as a covariate. Out of the 302 total participants, 24 had to be excluded from genetic analyses due to data quality, familial relationships, or ethnicity. To prevent false positives, the final data were filtered for minor allele frequency (MAF) > 0.10, and all genotypes that are present should have at least 3 samples.

Data processing

The genotypes from the Illumina HumanCoreExome-24 BeadChip Kit were called using optiCall (27). A sex check was performed using the software package plink (28). Using plink, for both sets the minimum MAF was set to 0.001, and we excluded markers that failed the Hardy-Weinberg equilibrium test at a specified significance threshold of P value <1×10⁻⁴. Only SNPs with a 99% genotyping rate were included. The data from the Illumina Infinium Omni-express were then lifted from GrCh38 to GrCh37 using a variation of liftOver (https://github.com/sritchie73/liftOverPlink), the original liftOver being provided by University of California, Santa Cruz (29). The data were then aligned to the 1000 Genomes dataset (phase3 shapeit2 mvncall integrated v5a.20130502) using Genotype Harmonizer (30), set to consider 500 flanking variants. Finally, the 2 sets of genotypes were combined keeping only SNPs present in both sets and imputed using the Michigan Imputation Server selecting

the Haplotype Reference Consortium reference panel hrc.r1.1.2016 (31) and phasing using Eagle (32). The data were filtered for having a minimum MAF of 0.1, a minimum imputation R2 score of 0.3, and minimum output empirical R2 of 0.3 (as provided in the imputation results). Data were annotated using beftools. By overlapping the data with the 1000 Genomes dataset and applying multidimensional scaling, we identified 5 participants that had non-Western European ancestry, and they were removed from further genetic analyses. Additionally, we checked for family relationships. If 2 or more individuals were related (PI HAT threshold >0.6), we excluded all but 1 of these. In total, 9 people were excluded on this basis. We seguenced several genes for all 302 participants using an independent method. For 10 participants, all from the 168 volunteers that were sequenced in a previous study, their genetic data did not match between the SNP chip data and the second sequencing run. Therefore, these individuals were excluded from genetic analyses. This means that out of the 302 total participants, 24 had to be excluded from genetic analyses. To prevent false positives, the final data were filtered for MAF > 0.10 and all genotypes that are present should have at least 3 samples.

OTL analysis

All QTL analyses were performed using the MatrixEQTL package in the R programming language. This package constructs linear regression models for each combination of SNP (independent variable) and quantitative variable (dependent variable) separately. The quantitative variables (cytokine production capacity and plasma markers) were log transformed, and MetS, National Cholesterol Education Program criteria, chip origin, and sex were used as covariates. The National Cholesterol Education Program criteria define MetS as the presence of 3 or more of the following criteria: abdominal obesity, high blood pressure, high glucose levels, high triglyceride levels, and low high-density lipoprotein cholesterol (33). QTL results were filtered for correlated SNPs. For all SNPs with an $R^2 \ge 0.8$, only the most significant result was kept. Specifically, R² values were calculated based on the SNP dosage values, and filtering always kept the most significant SNP out of any correlated set. Samples with missing values were excluded from each analysis independently.

Statistics

The Shapiro-Wilk test was performed to assess the normality of the data. Data did not follow a normal distribution, therefore only nonparametric tests were executed. For the QTL in vivo data, values were log-transformed for normalization and reduction of variability as described previously. In vitro data are presented as mean ± SEM and experiments were performed with at least 6 donors. Statistical significance was determined with Wilcoxon signed rank test using GraphPad Prism 9 (GraphPad Software). The 300-OB cohort data analysis was performed with IBM SPSS Statistics 25 and RStudio version 4.0.2. Two-sided P values below 0.05 were considered to be statistically significant. For the phagocytosis and foam cell formation experiments, we did not perform any statistical testing, as this was only done in monocytes from 3 donors.

Results

Short and long-term effects of leptin on monocytes

To study the direct stimulatory effect of leptin on monocytes, we exposed PBMCs to physiologically relevant leptin concentrations (1, 50, and 100 ng/mL) and measured the IL-6 and TNF- α concentrations in the supernatant. None of the leptin concentrations induced any cytokine production in PBMCs (data not shown).

Next, using the well-established trained immunity protocol (24), we explored whether a brief exposure of monocytes to leptin induces trained immunity (Figure 1A). Therefore, we exposed monocytes for 24 h to leptin and assessed cytokine production capacity in response to other stimuli in the monocytederived macrophages 6 d later. Twenty-four-hour exposure to leptin dosedependently augmented TNF-α production following LPS exposure on day 6, which was statistically significant for 50 ng/mL of leptin (Figure 1C). There was no effect of leptin pre-exposure on LPS-induced IL-6 production (Figure 1B), nor on Pam3Cys-induced cytokine production. In addition, we restimulated the cells with the TLR7/8 agonist R848. We found that 24 h exposure to leptin 50 ng/mL significantly augmented R848-induced TNF- α production (Figure 1E). Finally, we also investigated whether leptin-trained macrophages produced more IL-1β by restimulating the cells with nigericin and LPS. Figure 1F-H shows that total IL-1β production tends to increase after training with leptin (1 and 50 ng/mL) and upon restimulation with LPS + Nigericin; however, this increase was not statistically significant because of the large interindividual variability.

We subsequently determined whether the increased TNF-α production upon restimulation was due to an upregulation of TLR4/2 in the leptin-exposed macrophages. Flow cytometry analysis of monocyte-derived macrophages on day 6 after training showed no significant changes in the percentage of cells positive for TLR2 or TLR4, and the level of expression of the receptors on TLR4/2-positive cells did not change either (Supplementary Figure 3), ruling out TLR upregulation as an explanation for the enhanced cytokine response.

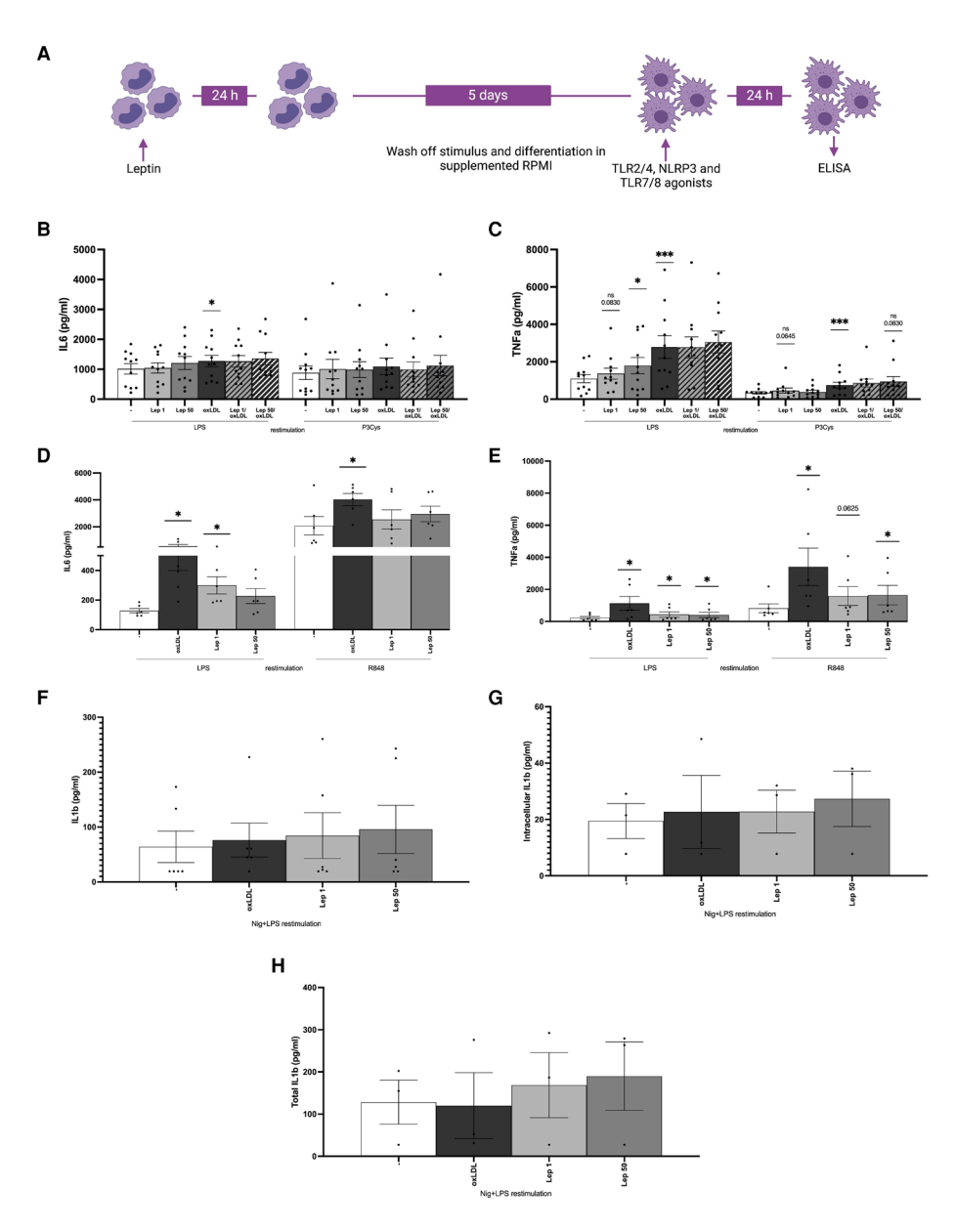


Figure 1: Exposure of human primary monocytes during 24 h to human recombinant leptin and oxLDL induces trained immunity. (A) Schematic representation of the experimental setup. Human primary monocytes from healthy volunteers were exposed for 24 h to medium alone, human recombinant leptin (1 and 50 ng/mL), oxLDL (10 µg/mL), or leptin + oxLDL. After 6 d of resting, cells were restimulated with LPS, Pam3Cys, and R848, and we measured (B, D) IL-6 and (C, E) TNF- α (n = 11 [A, B], n = 6 [C, D]; *P < 0.05, ***P < 0.001). To induce the secretion of IL-1 β , at day 6 cells were also restimulated with LPS + Nigericin. (F) Extracellular, (G) intracellular, and (H) total IL-1β were measured (n = 3). Created with BioRender.com.

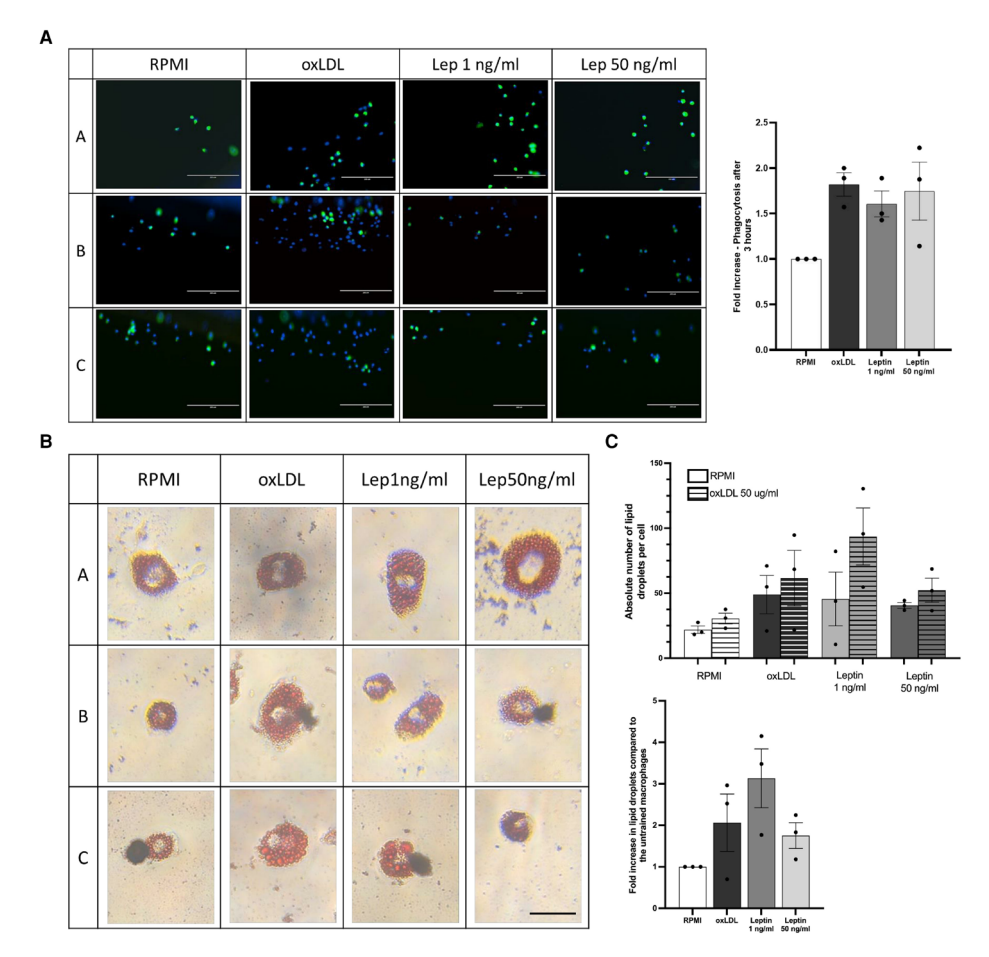


Figure 2: Training human primary monocytes with human recombinant leptin and oxLDL augments phagocytosis and foam cell formation. Human primary monocytes were exposed during 24 h to human recombinant leptin (1 and 50 ng/mL) or oxLDL 10 μ g/mL. (A) After 6 d, the macrophages were exposed to fluorescent latex beads for 3 h and after washing images with the EVOS microscope were made to measure fluorescent beads uptake (10× magnification, scale bar = 200 μ m). The uptake of beads in oxLDL and leptin-trained cells is expressed as fold change compared to the untrained control cells (n = 3). (B) Foam cell formation was induced by incubating the trained macrophages for 24 h with RPMI only or oxLDL 50 μ g/mL followed by Oil Red O staining. (C) Foam cell morphology and lipid uptake quantification of trained macrophages was compared with untrained control (n = 3; scale bar = 25 μ m).

Leptin exposure augments phagocytosis and foam cell formation in macrophages

To assess whether brief leptin exposure also affects other macrophage functions, we performed phagocytosis and foam cell formation assay in the macrophages. We observed that both oxLDL- and leptin-trained monocyte-derived macrophages

showed a higher uptake of latex-beads after 3 hours, compared with the untrained control (Figure 2A). To determine if there was higher lipoprotein uptake in leptintrained macrophages, we incubated the cells for 24 h with 50 µg/mL of oxLDL or RPMI without oxLDL and performed an Oil Red O staining to identify the intracellular lipid droplets. Morphologically, the cells exposed to oxLDL and leptin are bigger with more lipid droplets compared to the untrained control (Figure 2B, representative pictures). Automated quantification of the lipid droplets in each cell showed that for all 3 donors, the average number of lipid droplets per cell were higher in the leptin-trained cells than in the untrained macrophages (Figure 2C).

Leptin does not modulate oxLDL-induced training in monocytes

It has been shown previously that brief exposure of monocytes to oxLDL induces a trained macrophage phenotype characterized by increased cytokine production capacity (7). Some endogenous stimuli such as glucose can enhance this effect (34), indicating a synergistic effects of specific metabolic stimuli. We studied whether coexposure of cells to leptin also modulates oxLDL-induced trained immunity. We stimulated human primary monocytes for 24 h with oxLDL (10 µg/mL) with or without co-incubation with leptin (1 and 50 ng/mL) (Figure 1A). We confirmed that 24-hour oxLDL-exposure augments LPS-induced TNF-α and IL-6 production, and Pam3Cys-induced TNF-α production at day 6 compared to RPMI-exposed cells, but co-incubation with leptin did not potentiate this effect (Figure 1B and C).

Circulating IL-6 and IL-1β are correlated to circulating leptin in obese patients in vivo

We subsequently aimed to explore whether the immunomodulatory effects of leptin we observed in vitro translate into differences in immune cell function in vivo. Therefore, we assessed the correlation between the leptin concentration and circulating proinflammatory cytokine and PBMC cytokine production after 24 h stimulation with TLR2/4 agonists in a cohort of 300 obese individuals (300-OB) (age and false discovery rate corrected) (Figure 3).

In this analysis, we also explored whether associations were influenced by sex and by the absence or presence of MetS. In our cohort, there was a significant correlation between the leptin concentration and circulating IL-1B concentrations in men but not in women and IL-6 in men and women. Moreover, correlations were only observed in individuals without MetS. There was no significant correlation between circulating leptin concentrations and cytokine production of isolated PBMCs.

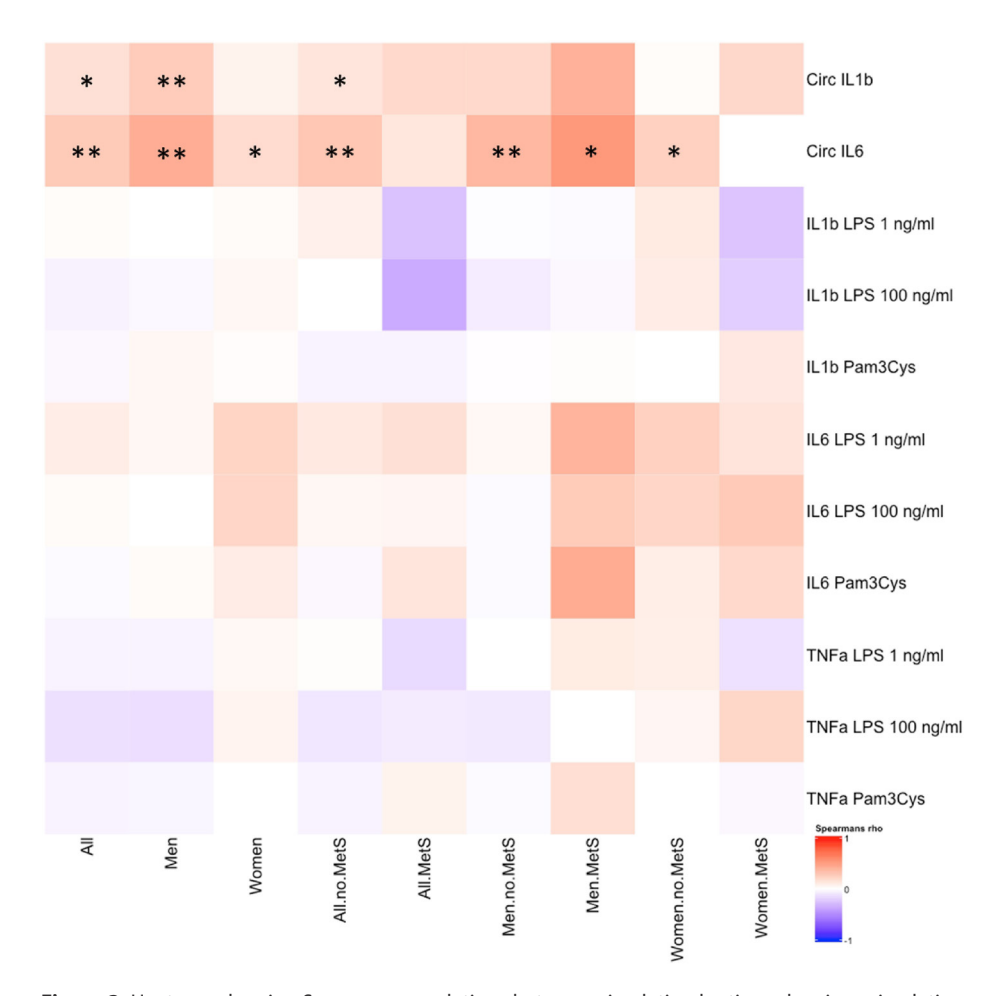


Figure 3: Heatmap showing Spearman correlations between circulating leptin and various circulating cytokines and cytokines produced by ex vivo stimulation of PBMCs in 302 obese individuals, either in the entire cohort or in subgroups, indicated on the horizontal axis. Spearman correlation was performed, and data are presented divided in columns for all individuals, men, and women with and without MetS. Cells colored in red indicate a positive correlation and in blue indicate a negative correlation. Age- and false discovery rate-corrected data, *P < 0.05, **P < 0.01.

Genetic variants in the leptin gene modulate circulating IL-6 levels in men

The strong association between leptin and IL-6 in the male participants of the 300-OB cohort could be driven by a direct effect of leptin and leptin receptor stimulation on IL-6 production, by an effect of IL-6 on leptin production, or by an independent factor that influences both leptin and IL-6 concentrations. To explore the causality of this association, we made use of genetic variants in the genes encoding for leptin (LEP), the leptin receptor (LEPR), and IL-6. We proposed

that if leptin receptor stimulation directly affects the IL-6 concentration, functional SNPs in the leptin gene or its receptor gene would also affect the circulating IL-6 concentration. Similarly, we explored the effect of SNPs in the IL-6 gene on the circulating leptin concentration. Given the fact that the correlation between circulating leptin and IL-6 is restricted to males (Figure 3), we performed the analysis in males and females separately.

We tested for associations between SNPs in the leptin gene (170 SNPs) and leptin receptor gene (182 SNPs) and the circulatory IL-6 concentration. We also tested for associations between SNPs in the IL-6 gene (153 SNPs) and circulatory leptin in obese males and females or both. The complete list of SNPs can be found in Supplementary Table 1. We identified 4 SNPs in the leptin gene that were associated at a suggestive threshold with circulating IL-6: variants rs896183 (located in LEP [P = 0.0041, b = -0.1117], rs11772985 (located in LEP [P = 0.0086, b = -0.1048]), rs13237683 (located in LEP [P = 0.0138, b = -0.0974]) and rs12706830 (located in LEP [P = 0.0457, b = 0.1106]) (Figure 4A). Interestingly, these associations were only present in men, echoing the male-specific associations between the circulating concentrations of leptin and IL-6 (Figure 3). All variants were located in exonic regions of the gene as shown in Figure 4B and C. Genotyped SNPs in the leptin receptor were not associated with circulating IL-6, and SNPs in IL-6 were not associated with circulating leptin.

Discussion

In this study, we aimed to assess the effects of leptin on innate immune cell function and systemic inflammation in the context of obesity. We observed that, in vitro, relevant concentrations of leptin do not have a direct stimulatory effect on cytokine production of human primary PBMCs and monocytes. However, 24-hour exposure to leptin did augment TNF-α and IL-1β production after 6-day differentiation of monocytes into macrophages, which point to trained innate immunity. In addition, leptin-trained macrophages showed increased foam cell formation and increased phagocytic capacity. In vivo, in a cohort of 300 overweight and obese individuals, there was no association between circulating leptin and cytokine production of isolated PBMCs. Nonetheless, there was a strong positive association between circulating leptin and IL-6 and IL-1β concentrations. Genetic analyses suggest that the direction of this association is from leptin to IL-6. Importantly, this effect was mainly seen in men and not in women.

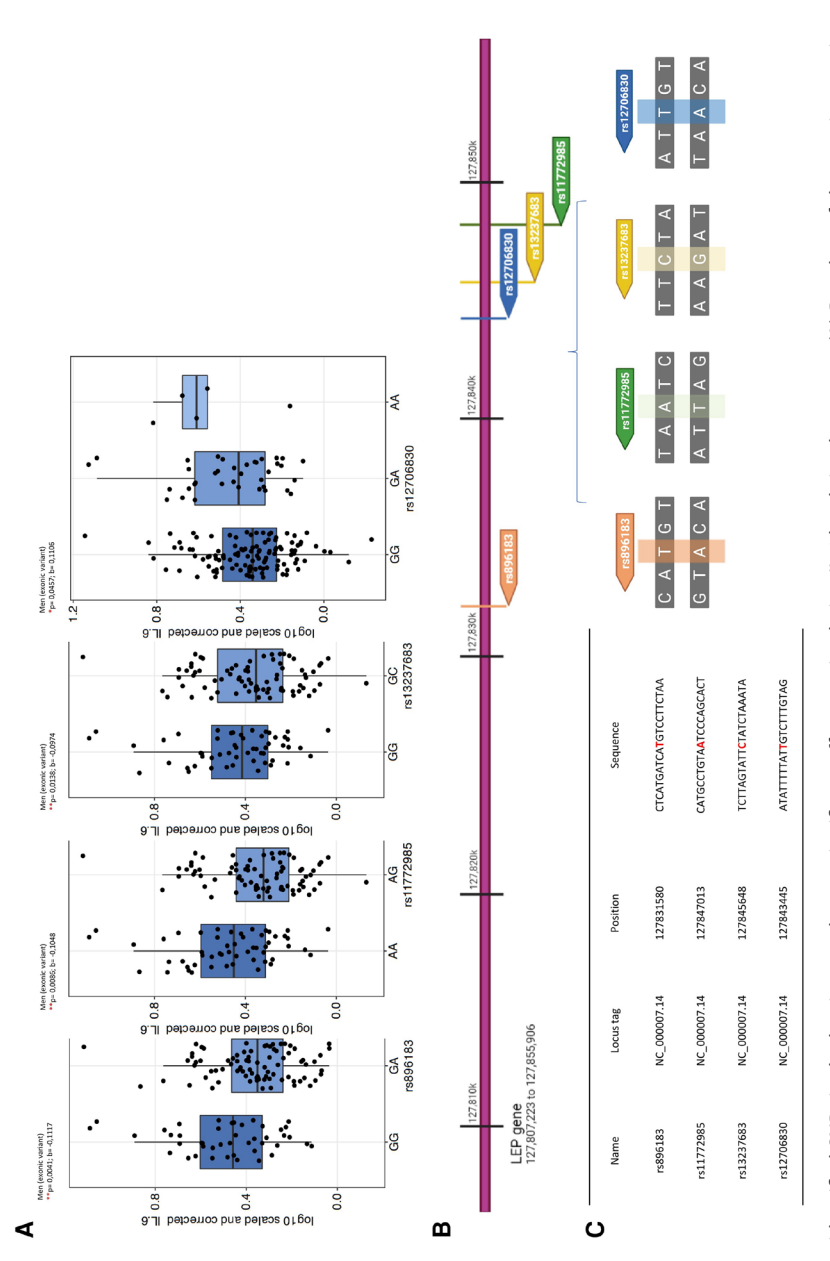


Figure 4: Four identified SNPs in the leptin gene have a significant effect on circulating IL-6 levels in obese men. (A) Boxplots of the exonic genetic variants in the leptin loci rs896183, rs11772985, rs13237683, and rs12706830 indicating the circulating IL-6 levels per genotype (300-OB cohort, n = 302). (B) Position and location of the SNPs in the leptin gene as well as (C) identification of affected nucleotide in the sequence. False discovery rate-corrected data, *P < 0.05, **P < 0.01. For the full list of identified SNPs, see Supplementary Table 1. GeneCards—the human gene database (35, 36). Created with BioRender.com.

Leptin is an adipokine mainly produced in the adipose tissue and normal leptin levels in the circulation range from 1 to 100 ng/mL in obese individuals (37, 38). Leptin has been suggested to contribute to the low-grade inflammation that accompanies obesity (17). Additionally, the proinflammatory effects of leptin have been proposed to contribute to the increased risk of autoimmune diseases in patients with obesity, including type 1 diabetes mellitus, multiple sclerosis, and rheumatoid arthritis (39, 40). We recently reported profound sex differences in the association between leptin and metabolic dysregulation in obesity (19). In men, the presence of MetS was associated with higher circulating leptin and IL-6 concentrations and with higher PBMC cytokine production capacity, whereas in women, MetS was associated with lower adiponectin concentrations (19, 41).

Our in vitro studies showed that leptin, in physiological concentrations, does not directly activate PBMCs. This is in contrast to previous studies that reported that a brief exposure of PBMCs to high concentrations of leptin (1,000 ng/mL) can induce a higher expression of TNF-α and IL-6 (42-44), although these concentrations are not in the physiological range. Our findings were corroborated in vivo, as there was no association between circulating leptin concentrations and PBMC cytokine production capacity. This suggests that a direct effect of leptin on monocytes cannot explain the previous observation that men with MetS have higher circulating leptin and increased PBMC cytokine production capacity.

In contrast, 24-h exposure of monocytes to leptin induced long-term changes in the function of monocyte-derived macrophages (also termed trained immunity). We have previously reported that various atherogenic endogenous molecules can induce trained immunity, including oxLDL and lipoprotein(a), glucose, and the adrenal hormones aldosterone and catecholamines (7-10, 45). The hallmark of trained immunity is an augmented cytokine production capacity that persists even when the stimulus has long been removed (46). Indeed, we observed that 24 h exposure of monocytes to 50 ng/mL augmented the production of TNF-α in the monocyte-derived macrophages after restimulation with TLR4 and TLR7/8 agonists. We previously reported that oxLDL-trained macrophages showed increased foam cell formation (7), and we could now confirm that also for leptintrained macrophages. It has previously been reported that exposure to leptin during the 7 days of monocyte-to-macrophage differentiation increased foam cell formation (47, 48), and our study now demonstrates that this also holds true when only the monocytes are briefly exposed to leptin. Finally, we assessed phagocytosis capacity in the trained macrophages, since this is a crucial process involved in the development of atherosclerotic plaques (49). We observed that leptin exposure appeared to increase the uptake of latex beads, as a measure for phagocytosis. In summary, we found that leptin-trained macrophages have an atherogenic phenotype, with increased cytokine production capacity, foam cell formation, and phagocytosis. In murine models of atherosclerosis, trained immunity can contribute to the development of atherosclerosis in the context of hyperglycemia (50) and hyperlipidemia (51). This remains to be established for leptin-induced trained immunity. Interestingly, in mice, a limited period of obesity also induces trained immunity by reprogramming of hematopoietic myeloid progenitor cells, which results in persistent immune cell hyperresponsiveness also after returning to normal body weight (14). Stearic acid was identified as a possible factor triggering this trained immunity. Our results suggest that leptin could also contribute to this obesity-induced innate immune memory, although its effects are relatively small.

In our cohort of overweight and obese individuals, although there was no correlation between circulating leptin and PBMC cytokine production capacity, we did identify a strong correlation between circulating leptin concentrations and circulating IL-6 and IL-1\u00ed. A potential explanation is that leptin-trained monocytederived macrophages play a role in heightened production of IL-1B and IL-6 in vivo because these cytokines are mainly derived from tissue-resident macrophages, such as Kupffer cells (52, 53). In addition, direct effects of leptin on macrophages have been previously described. Leptin can augment the phagocytic function of macrophages and their cytokine production capacity (54). More recently, Monteiro et al. (55) reported that leptin augments LPS-induced proinflammatory cytokine production in murine macrophages.

The interrelation between leptin and inflammatory cytokines is complex, with leptin affecting cytokine production of immune cells and adipocytes, which can subsequently modulate leptin production by adipocytes (17). To gain insight into the causal directionality of the association between circulating leptin and IL-6, we performed a detailed analysis of SNPs in the genes encoding leptin and the leptin receptor, and IL-6. We identified 4 SNPs in the leptin gene that were significantly associated with IL-6 concentrations exclusively in men. This suggests that, in men, the association between leptin and IL-6 is driven by a direct effect of leptin on IL-6 production. More research is needed to elucidate the strong sex differences in the relation between leptin and inflammatory cytokines.

There are some limitations in our study. First, all our in vitro experiments were performed with PBMCs and monocytes from healthy volunteers, but we are not informed about the sex, weight, circulating leptin levels, or BMI of these individuals.

Second, while we showed that leptin induced trained immunity in terms of augmented cytokine production capacity, we did not investigate the underlying epigenetic and metabolic processes that characterize trained immunity. Also, we did not investigate other time points than the 6 days after removal of the leptin. Third, the stratification of the cohort according to sex and MetS reduced the power of the cohort study This could have caused the lack of association in the subgroup of obese individuals with MetS. Finally, we have not confirmed that leptin-induced trained immunity occurs in vivo; this would allow a prospective follow-up of our cohort to compare subjects who lost weight to subjects with persistent obesity. Therefore, more research is needed to investigate the relevance and importance of leptin-induced trained immunity in mediating the obesogenic memory recently described.

In conclusion, these results increase our understanding of the inflammatory effects of leptin and highlight a crucial sex-specific mechanism; however, more research is needed to be able to understand how leptin mediates the inflammatory response in the tissue. Additionally, it is essential to study the intracellular mechanisms involved in this response.

Acknowledgments

The figures were created with BioRender.com.

Author contributions

D.F.G., S.B., J.H.W.R., L.A.B.J., M.G.N., and N.P.R. were responsible for conceptualization of the study. D.F.G., S.B., and I.C.L.M. performed the investigation (experiments). Data curation and analysis was performed by D.F.G., S.B., R.H., and B.C. Project oversight was done by S.B. and N.R. D.F.G. and S.B. wrote the draft manuscript, which was afterward reviewed and edited by all coauthors.

Funding

J.H.W.R., L.A.B.J., M.G.N., and N.P.R were supported by a CVON grant from the Dutch Heart Foundation and Dutch Cardiovascular Alliance (DCVA; CVON2018-27), N.P.R. was further supported by a grant of the ERA-CVD Joint Transnational Call 2018, which is supported by the Dutch Heart Foundation in the Hague (JTC2018, project MEMORY; 2018T093). S.B. was supported by the Dutch Heart Foundation in the Haque (Dekker grant 2018-T028). M.G.N. was further supported by a European Research Council Advanced Grant (FP/2007-2013/ERC grant 2012-322698) and a Spinoza Prize by NWO (NWO SPI 92-266).

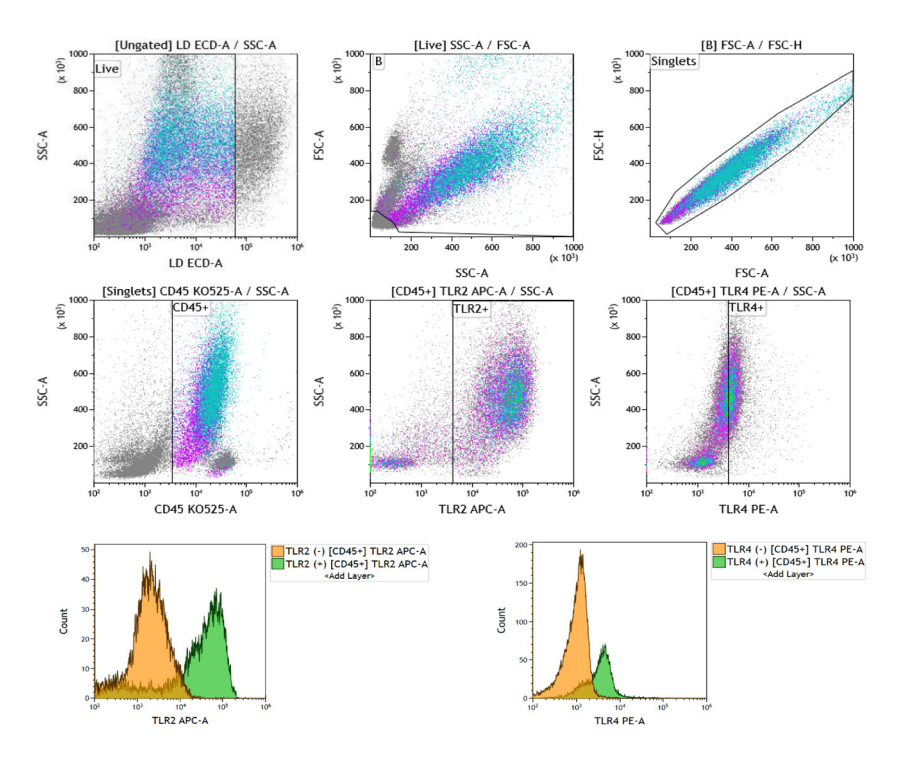
References

- 1 Rosengren A. Obesity and cardiovascular health: the size of the problem. Eur Heart J. 2021:42(34):3404-6.
- Liu Y, Douglas PS, Lip GYH, Thabane L, Li L, Ye Z, et al. Relationship between obesity severity, 2. metabolic status and cardiovascular disease in obese adults. Eur J Clin Invest. 2023;53(3):e13912.
- 3. Powell-Wiley TM, Poirier P, Burke LE, Després JP, Gordon-Larsen P, Lavie CJ, et al. Obesity and Cardiovascular Disease: A Scientific Statement From the American Heart Association. Circulation. 2021:143(21):e984-e1010.
- Gupta RM, Lee-Kim VS, Libby P. The March of Monocytes in Atherosclerosis: One Cell at a Time. Circ Res. 2020:126(10):1324-6.
- Libby P, Ridker PM, Hansson GK. Progress and challenges in translating the biology of atherosclerosis. Nature. 2011;473(7347):317-25.
- 6. Rohm TV, Meier DT, Olefsky JM, Donath MY. Inflammation in obesity, diabetes, and related disorders. Immunity. 2022;55(1):31-55.
- 7. Bekkering S, Quintin J, Joosten LA, van der Meer JW, Netea MG, Riksen NP. Oxidized low-density lipoprotein induces long-term proinflammatory cytokine production and foam cell formation via epigenetic reprogramming of monocytes. Arterioscler Thromb Vasc Biol. 2014;34(8):1731-8.
- 8. van der Valk FM, Bekkering S, Kroon J, Yeang C, Van den Bossche J, van Buul JD, et al. Oxidized Phospholipids on Lipoprotein(a) Elicit Arterial Wall Inflammation and an Inflammatory Monocyte Response in Humans. Circulation. 2016;134(8):611-24.
- 9. van der Heijden C, Groh L, Keating ST, Kaffa C, Noz MP, Kersten S, et al. Catecholamines Induce Trained Immunity in Monocytes In Vitro and In Vivo. Circ Res. 2020;127(2):269-83.
- 10. van der Heijden C, Keating ST, Groh L, Joosten LAB, Netea MG, Riksen NP. Aldosterone induces trained immunity: the role of fatty acid synthesis. Cardiovasc Res. 2020;116(2):317-28.
- 11. Domínguez-Andrés J, Dos Santos JC, Bekkering S, Mulder WJM, van der Meer JWM, Riksen NP, et al. Trained immunity: adaptation within innate immune mechanisms. Physiol Rev. 2023;103(1):313-46.
- 12. Blaszczak AM, Bernier M, Wright VP, Gebhardt G, Anandani K, Liu J, et al. Obesogenic Memory Maintains Adipose Tissue Inflammation and Insulin Resistance. Immunometabolism. 2020;2(3).
- 13. Cottam MA, Caslin HL, Winn NC, Hasty AH. Multiomics reveals persistence of obesity-associated immune cell phenotypes in adipose tissue during weight loss and weight regain in mice. Nat Commun. 2022;13(1):2950.
- 14. Hata M, Andriessen E, Hata M, Diaz-Marin R, Fournier F, Crespo-Garcia S, et al. Past history of obesity triggers persistent epigenetic changes in innate immunity and exacerbates neuroinflammation. Science. 2023;379(6627):45-62.
- 15. Kiernan K, MacIver NJ. The Role of the Adipokine Leptin in Immune Cell Function in Health and Disease. Front Immunol. 2020;11:622468.
- 16. Kelesidis T, Kelesidis I, Chou S, Mantzoros CS. Narrative review: the role of leptin in human physiology: emerging clinical applications. Ann Intern Med. 2010;152(2):93-100.
- 17. likuni N, Lam QL, Lu L, Matarese G, La Cava A. Leptin and Inflammation. Curr Immunol Rev. 2008;4(2):70-9.
- 18. Couillard C, Mauriège P, Prud'homme D, Nadeau A, Tremblay A, Bouchard C, et al. Plasma leptin concentrations: gender differences and associations with metabolic risk factors for cardiovascular disease. Diabetologia. 1997;40(10):1178-84.

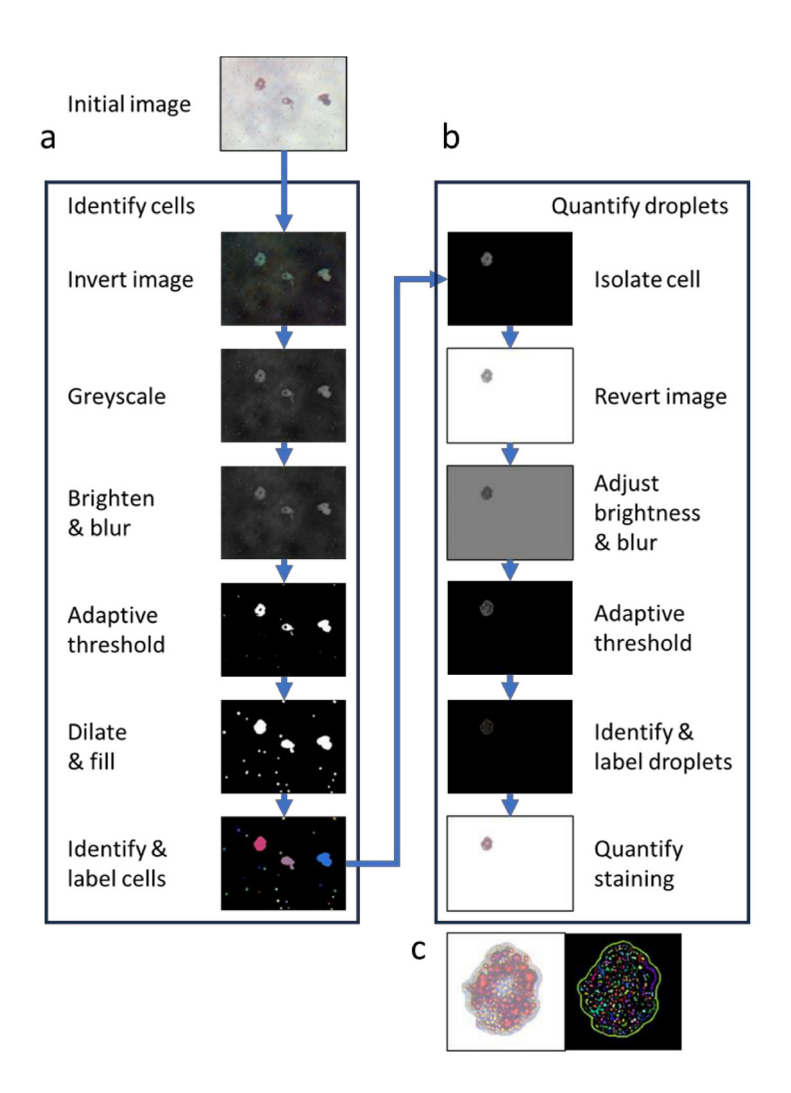
- 19. Ter Horst R. van den Munckhof ICL, Schraa K. Aguirre-Gamboa R. Jaeger M. Smeekens SP, et al. Sex-Specific Regulation of Inflammation and Metabolic Syndrome in Obesity. Arterioscler Thromb Vasc Biol. 2020;40(7):1787-800.
- 20. Hirschfeld M, Ma Y, Weis JH, Vogel SN, Weis JJ. Cutting edge: repurification of lipopolysaccharide eliminates signaling through both human and murine toll-like receptor 2. J Immunol. 2000:165(2):618-22.
- 21. van Tits LJ, Stienstra R, van Lent PL, Netea MG, Joosten LA, Stalenhoef AF. Oxidized LDL enhances pro-inflammatory responses of alternatively activated M2 macrophages: a crucial role for Krüppel-like factor 2. Atherosclerosis. 2011;214(2):345-9.
- 22. Repnik U, Knezevic M, Jeras M. Simple and cost-effective isolation of monocytes from buffy coats. J Immunol Methods. 2003;278(1-2);283-92.
- 23. Domínguez-Andrés J, Arts RJW, Bekkering S, Bahrar H, Blok BA, de Bree LCJ, et al. In vitro induction of trained immunity in adherent human monocytes. STAR Protoc. 2021;2(1):100365.
- 24. Bekkering S, Blok BA, Joosten LA, Riksen NP, van Crevel R, Netea MG. In Vitro Experimental Model of Trained Innate Immunity in Human Primary Monocytes. Clin Vaccine Immunol. 2016:23(12):926-33.
- 25. Feher K, Kirsch J, Radbruch A, Chang HD, Kaiser T. Cell population identification using fluorescence-minus-one controls with a one-class classifying algorithm. Bioinformatics. 2014;30(23):3372-8.
- 26. Galesloot TE, Vermeulen SH, Swinkels DW, de Vegt F, Franke B, den Heijer M, et al. Cohort Profile: The Nijmegen Biomedical Study (NBS). Int J Epidemiol. 2017;46(4):1099-100j.
- 27. Shah TS, Liu JZ, Floyd JA, Morris JA, Wirth N, Barrett JC, et al. optiCall: a robust genotype-calling algorithm for rare, low-frequency and common variants. Bioinformatics. 2012;28(12):1598-603.
- 28. Purcell S, Neale B, Todd-Brown K, Thomas L, Ferreira MA, Bender D, et al. PLINK: a tool set for whole-genome association and population-based linkage analyses. Am J Hum Genet. 2007;81(3):559-75.
- 29. Kent WJ, Sugnet CW, Furey TS, Roskin KM, Pringle TH, Zahler AM, et al. The human genome browser at UCSC. Genome Res. 2002;12(6):996-1006.
- 30. Deelen P, Bonder MJ, van der Velde KJ, Westra HJ, Winder E, Hendriksen D, et al. Genotype harmonizer: automatic strand alignment and format conversion for genotype data integration. BMC Res Notes. 2014;7:901.
- 31. McCarthy S, Das S, Kretzschmar W, Delaneau O, Wood AR, Teumer A, et al. A reference panel of 64,976 haplotypes for genotype imputation. Nat Genet. 2016;48(10):1279-83.
- 32. Loh PR, Danecek P, Palamara PF, Fuchsberger C, Y AR, H KF, et al. Reference-based phasing using the Haplotype Reference Consortium panel. Nat Genet. 2016;48(11):1443-8.
- 33. Third Report of the National Cholesterol Education Program (NCEP) Expert Panel on Detection, Evaluation, and Treatment of High Blood Cholesterol in Adults (Adult Treatment Panel III) final report. Circulation. 2002;106(25):3143-421.
- 34. Thiem K, Keating ST, Netea MG, Riksen NP, Tack CJ, van Diepen J, et al. Hyperglycemic Memory of Innate Immune Cells Promotes In Vitro Proinflammatory Responses of Human Monocytes and Murine Macrophages. J Immunol. 2021;206(4):807-13.
- 35. Safran M, Rosen N, Twik M, BarShir R, Stein TI, Dahary D, et al. Practical guide to life science databases. Singapore: The GeneCards Suite. Springer Nature Singapore; 2021.

- 36. Stelzer G, Rosen N, Plaschkes I, Zimmerman S, Twik M, Fishilevich S, et al. The GeneCards Suite: From Gene Data Mining to Disease Genome Sequence Analyses. Curr Protoc Bioinformatics. 2016:54:1.30.1-1..3.
- 37. Pérez-Pérez A, Sánchez-Jiménez F, Vilariño-García T, Sánchez-Margalet V. Role of Leptin in Inflammation and Vice Versa. Int J Mol Sci. 2020;21(16).
- 38. Kumar R, Mal K, Razaq MK, Magsi M, Memon MK, Memon S, et al. Association of Leptin With Obesity and Insulin Resistance. Cureus. 2020;12(12):e12178.
- 39. Kwiat VR, Reis G, Valera IC, Parvatiyar K, Parvatiyar MS. Autoimmunity as a seguela to obesity and systemic inflammation. Front Physiol. 2022;13:887702.
- 40. Matarese G. The link between obesity and autoimmunity. Science. 2023;379(6639):1298-300.
- 41. Eglit T, Lember M, Ringmets I, Rajasalu T. Gender differences in serum high-molecular-weight adiponectin levels in metabolic syndrome. Eur J Endocrinol. 2013;168(3):385-91.
- 42. Zarkesh-Esfahani H, Pockley G, Metcalfe RA, Bidlingmaier M, Wu Z, Ajami A, et al. High-dose leptin activates human leukocytes via receptor expression on monocytes. J Immunol. 2001;167(8):4593-9.
- 43. Santos-Alvarez J, Goberna R, Sánchez-Margalet V. Human leptin stimulates proliferation and activation of human circulating monocytes. Cell Immunol. 1999;194(1):6-11.
- 44. Frisullo G, Angelucci F, Mirabella M, Caggiula M, Patanella K, Nociti V, et al. Leptin enhances the release of cytokines by peripheral blood mononuclear cells from relapsing multiple sclerosis patients. J Clin Immunol. 2004;24(3):287-93.
- 45. El-Osta A, Brasacchio D, Yao D, Pocai A, Jones PL, Roeder RG, et al. Transient high glucose causes persistent epigenetic changes and altered gene expression during subsequent normoglycemia. J Exp Med. 2008;205(10):2409-17.
- 46. Riksen NP, Bekkering S, Mulder WJ, Netea MG. Trained immunity in atherosclerotic cardiovascular disease. Nature Reviews Cardiology. 2023;20(12):799-811.
- 47. Miyazaki A, Imawari M. New Frontiers in Lifestyle-Related Diseases: Springer; 2008.
- 48. Hongo S, Watanabe T, Arita S, Kanome T, Kageyama H, Shioda S, et al. Leptin modulates ACAT1 expression and cholesterol efflux from human macrophages. Am J Physiol Endocrinol Metab. 2009;297(2):E474-82.
- 49. Schrijvers DM, De Meyer GR, Herman AG, Martinet W. Phagocytosis in atherosclerosis: Molecular mechanisms and implications for plaque progression and stability. Cardiovasc Res. 2007;73(3):470-80.
- 50. Edgar L, Akbar N, Braithwaite AT, Krausgruber T, Gallart-Ayala H, Bailey J, et al. Hyperglycemia Induces Trained Immunity in Macrophages and Their Precursors and Promotes Atherosclerosis. Circulation. 2021;144(12):961-82.
- 51. Christ A, Günther P, Lauterbach MAR, Duewell P, Biswas D, Pelka K, et al. Western Diet Triggers NLRP3-Dependent Innate Immune Reprogramming. Cell. 2018;172(1-2):162-75.e14.
- 52. Elchaninov AV, Fatkhudinov TK, Vishnyakova PA, Lokhonina AV, Sukhikh GT. Phenotypical and Functional Polymorphism of Liver Resident Macrophages. Cells. 2019;8(9).
- 53. Oishi Y, Manabe I. Macrophages in inflammation, repair and regeneration. Int Immunol. 2018;30(11):511-28.
- 54. Loffreda S, Yang SQ, Lin HZ, Karp CL, Brengman ML, Wang DJ, et al. Leptin regulates proinflammatory immune responses. Faseb j. 1998;12(1):57-65.
- 55. Monteiro LB, Prodonoff JS, Favero de Aguiar C, Correa-da-Silva F, Castoldi A, Bakker NVT, et al. Leptin Signaling Suppression in Macrophages Improves Immunometabolic Outcomes in Obesity. Diabetes. 2022;71(7):1546-61.

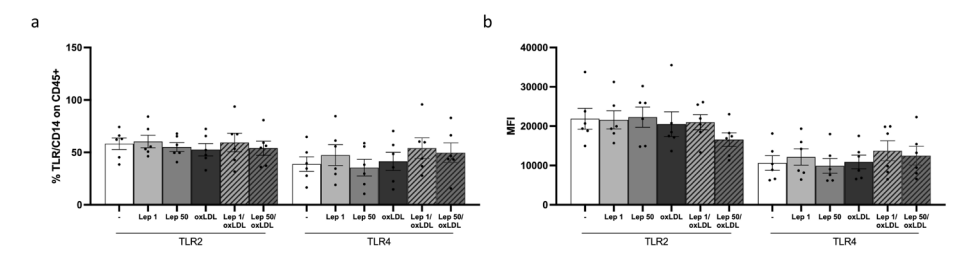
Supplementary Material



Supplementary Figure 1: Gating strategy to identify TLR2 and TLR4 in human primary monocytes. Before running the samples, monocytes were isolated using pan monocyte MACS, with a purity of 95%+. Monocytes were defined as CD45+ cells after previous exclusion of dead cells, debris and doublets. Next, the TLR2 and 4+ cells were selected using the fluorescence minus one method (FMO) and side scatter properties. Additionally, these two markers were quantified using a histogram. TLR2/4 percentages and median fluorescence intensity were calculated.



Supplementary Figure 2: Foam cell oil droplet quantification. Images were assessed in two steps, (a) identifying cells on the slide, and (b) identifying droplets within those cells. (a) The initial image was inverted and converted to greyscale, before brightening and blurring, this was then subjected to adaptive thresholding to identify foreground and background. To minimize gaps in the cells, this threshold was then dilated and filled to complete the clusters. (b) For each identified "cell", the cluster was isolated, reinverted, and darkened to increase contrast, before applying adaptive thresholding. Droplets identified were then screened to identify the halo surrounding the cells and non-stained sections of the cell by requiring less than 93% light transmittance in each droplet. (c) A magnified look at the identified cell.



Supplementary Figure 3: Percentage (a) and median florescence intensity (b, MFI) of TLR2 and 4 in monocytes were measured after exposure for 24 hours to medium alone, human recombinant leptin, oxLDL or both. After 6 days resting period cells were detached and surface markers were measured with flow cytometry (n=6).

Supplementary Table 1a: Table of genetic variants identified in the 300OB cohort. Identified SNPs in the (a) leptin gene (LEP) and the (b) leptin receptor gene (LEPR) and its effect in circulating IL-6. (c) Identified SNPs in the IL-6 gene and its effect in circulating leptin.

Group	SNP	Consequence	Corrected	Beta	Gene
		gene	p-value		
all	rs10244329	IL.6	0.198793588	0.060561831	LEP
all	rs11772985	IL.6	0.198793588	-0.059955993	LEP
all	rs28954091	IL.6	0.198793588	-0.052129475	LEP
all	rs13237683	IL.6	0.198793588	-0.055173301	LEP
all	rs896183	IL.6	0.198793588	-0.053034343	LEP
all	rs1376268	IL.6	0.236055948	0.04757834	LEP
all	rs4731435	IL.6	0.236055948	0.045644796	LEP
all	rs4731429	IL.6	0.25965217	-0.042265087	LEP
all	rs4731420	IL.6	0.293074352	0.054904161	LEP
all	rs791595	IL.6	0.293074352	-0.054855815	LEP
all	rs10487505	IL.6	0.293074352	-0.037957173	LEP
all	rs6976221	IL.6	0.293074352	0.051044216	LEP
all	rs62666460	IL.6	0.293074352	0.058290673	LEP
all	rs4731419	IL.6	0.293074352	-0.040722787	LEP
all	rs35589574	IL.6	0.293074352	0.047665328	LEP
all	rs13233734	IL.6	0.293074352	-0.038565206	LEP
all	rs4731422	IL.6	0.298864992	0.036369885	LEP
all	rs11763618	IL.6	0.298864992	-0.03388289	LEP
all	rs791601	IL.6	0.312563137	-0.032272872	LEP
all	rs3750035	IL.6	0.312563137	0.034455027	LEP
all	rs36102951	IL.6	0.312563137	-0.034142302	LEP
all	rs10264361	IL.6	0.312563137	-0.046172011	LEP
all	rs10954176	IL.6	0.317559295	-0.036221377	LEP

Supplementary Table 1a: Continued

Group	SNP	Consequence gene	Corrected p-value	Beta	Gene
all	rs6966236	IL.6	0.321709094	0.042111288	LEP
all	rs12706830	IL.6	0.321709094	0.046914691	LEP
all	rs4731434	IL.6	0.321709094	-0.032268486	LEP
all	rs12537998	IL.6	0.333265753	-0.031009405	LEP
all	rs10231132	IL.6	0.333265753	0.040394159	LEP
all	rs791597	IL.6	0.35614132	-0.03181664	LEP
all	rs28954369	IL.6	0.35614132	-0.05613384	LEP
all	rs6979784	IL.6	0.373443277	-0.036346459	LEP
all	rs1116656	IL.6	0.379235881	-0.026077658	LEP
all	rs11981584	IL.6	0.379235881	-0.034342623	LEP
all	rs34579650	IL.6	0.402629962	0.03172857	LEP
all	rs77106988	IL.6	0.405089785	0.040946311	LEP
all	rs74942683	IL.6	0.405089785	-0.04119365	LEP
all	rs13308439	IL.6	0.405089785	-0.024459454	LEP
all	rs4731437	IL.6	0.405089785	0.039570543	LEP
all	rs7779866	IL.6	0.405089785	0.026115895	LEP
all	rs73456868	IL.6	0.424379845	0.021221435	LEP
all	rs6467165	IL.6	0.486908993	-0.034229031	LEP
all	rs2402885	IL.6	0.548071014	0.022108457	LEP
all	rs4731412	IL.6	0.552138629	0.029554792	LEP
all	rs1451006	IL.6	0.56070921	0.027339403	LEP
all	rs2071045	IL.6	0.562413266	-0.019869896	LEP
all	rs4731418	IL.6	0.622017355	-0.015403328	LEP
all	rs13221116	IL.6	0.65242498	-0.022219921	LEP
all	rs1116655	IL.6	0.65242498	-0.01502963	LEP
all	rs7794771	IL.6	0.667472617	-0.012888963	LEP
all	rs56095188	IL.6	0.667472617	0.012061585	LEP
all	rs6947095	IL.6	0.741657628	-0.011408479	LEP
all	rs62481070	IL.6	0.829157178	-0.0108794	LEP
all	rs791602	IL.6	0.829157178	-0.006610029	LEP
all	rs41457646	IL.6	0.858505769	-0.007482078	LEP
all	rs111983802	IL.6	0.868372048	0.006637995	LEP
all	rs11766170	IL.6	0.878146874	-0.005662004	LEP
all	rs6956123	IL.6	0.918453491	-0.003633709	LEP
men	rs896183	IL.6	0.004124131	-0.111691674	LEP
men	rs11772985	IL.6	0.008593592	-0.104781409	LEP
men	rs13237683	IL.6	0.013782427	-0.097366597	LEP

Supplementary Table 1a: Continued

Group	SNP	Consequence gene	Corrected p-value	Beta	Gene
men	rs12706830	IL.6	0.04565642	0.110640741	LEP
men	rs6966236	IL.6	0.108283638	0.093684074	LEP
men	rs6976221	IL.6	0.110797331	0.088818311	LEP
men	rs4728096	IL.6	0.110797331	0.064383104	LEP
men	rs35589574	IL.6	0.110797331	0.081977576	LEP
men	rs34579650	IL.6	0.110797331	0.080767124	LEP
men	rs10487505	IL.6	0.116283734	-0.060235087	LEP
men	rs13245201	IL.6	0.116283734	-0.060562261	LEP
men	rs13233734	IL.6	0.118420966	-0.062536748	LEP
men	rs4731419	IL.6	0.118420966	-0.065148899	LEP
men	rs791601	IL.6	0.144246404	-0.057008806	LEP
men	rs111983802	IL.6	0.144246404	0.087405844	LEP
men	rs4731412	IL.6	0.217201238	0.087898149	LEP
men	rs12538332	IL.6	0.217201238	0.05911257	LEP
men	rs1451006	IL.6	0.232900515	0.073194957	LEP
men	rs1376268	IL.6	0.297650858	0.045161374	LEP
men	rs56095188	IL.6	0.30547142	0.045096339	LEP
men	rs10264361	IL.6	0.361743175	-0.055009166	LEP
men	rs28954369	IL.6	0.399530819	-0.072069063	LEP
men	rs4731429	IL.6	0.399947072	-0.037217437	LEP
men	rs791602	IL.6	0.409250793	-0.040205404	LEP
men	rs4731422	IL.6	0.507342341	0.033569769	LEP
men	rs4731418	IL.6	0.507342341	-0.0328541	LEP
men	rs41457646	IL.6	0.507342341	0.045524501	LEP
men	rs4731435	IL.6	0.507342341	0.02903257	LEP
men	rs11763618	IL.6	0.507342341	-0.030069906	LEP
men	rs4731420	IL.6	0.507342341	0.039649597	LEP
men	rs791595	IL.6	0.507342341	-0.039488178	LEP
men	rs62481070	IL.6	0.528460171	-0.047665237	LEP
men	rs3750035	IL.6	0.528460171	0.027920126	LEP
men	rs10231132	IL.6	0.596022637	0.032332173	LEP
men	rs62666460	IL.6	0.623243959	0.03504311	LEP
men	rs13221116	IL.6	0.623243959	0.040157138	LEP
men	rs36102951	IL.6	0.623243959	-0.022029102	LEP
men	rs77106988	IL.6	0.623243959	0.035628492	LEP
men	rs4731436	IL.6	0.623243959	0.033156729	LEP
men	rs74942683	IL.6	0.623243959	-0.032275656	LEP

Supplementary Table 1a: Continued

Group	SNP	Consequence	Corrected	Beta	Gene
		gene	p-value		
men	rs7794771	IL.6	0.623243959	-0.020774653	LEP
men	rs4731434	IL.6	0.623243959	-0.020579137	LEP
men	rs10954176	IL.6	0.623243959	-0.022400323	LEP
men	rs11981584	IL.6	0.623695648	-0.025493008	LEP
men	rs6979784	IL.6	0.637000479	-0.022658325	LEP
men	rs6467165	IL.6	0.637000479	-0.032218832	LEP
men	rs12537998	IL.6	0.652833514	-0.016491339	LEP
men	rs791597	IL.6	0.652833514	-0.018517649	LEP
men	rs13308439	IL.6	0.68506069	-0.014735918	LEP
men	rs2402885	IL.6	0.713718846	0.015433011	LEP
men	rs1116656	IL.6	0.713718846	-0.012067621	LEP
men	rs2071045	IL.6	0.713718846	-0.014856351	LEP
men	rs1116655	IL.6	0.713718846	0.013205112	LEP
men	rs73456868	IL.6	0.713718846	0.010418121	LEP
men	rs6947095	IL.6	0.848978714	-0.007671274	LEP
men	rs6956123	IL.6	0.851732302	-0.00946608	LEP
men	rs11766170	IL.6	0.865289097	-0.007234294	LEP
women	rs13221116	IL.6	0.588865782	-0.125964115	LEP
women	rs34821625	IL.6	0.588865782	-0.060536427	LEP
women	rs1376348	IL.6	0.588865782	-0.093400152	LEP
women	rs10954176	IL.6	0.588865782	-0.065581509	LEP
women	rs10244329	IL.6	0.588865782	0.062225682	LEP
women	rs3828942	IL.6	0.588865782	-0.060615054	LEP
women	rs111574076	IL.6	0.604789717	0.056040655	LEP
women	rs1376268	IL.6	0.659631684	0.051991789	LEP
women	rs36093592	IL.6	0.659631684	-0.088202948	LEP
women	rs791595	IL.6	0.715003807	-0.062243421	LEP
women	rs4731420	IL.6	0.715003807	0.062209551	LEP
women	rs11763618	IL.6	0.715003807	-0.040438784	LEP
women	rs12538332	IL.6	0.761744411	-0.048842796	LEP
women	rs4731422	IL.6	0.761744411	0.039544761	LEP
women	rs12532999	IL.6	0.761744411	-0.040657231	LEP
women	rs12537998	IL.6	0.761744411	-0.041567259	LEP
women	rs791597	IL.6	0.761744411	-0.041750149	LEP
women	rs4731434	IL.6	0.762158365	-0.038582839	LEP
women	rs1116655	IL.6	0.762158365	-0.043483712	LEP
women	rs3750035	IL.6	0.762158365	0.037326981	LEP

Supplementary Table 1a: Continued

Group	SNP	Consequence gene	Corrected p-value	Beta	Gene
women	rs791602	IL.6	0.769598956	0.032003512	LEP
women	rs62666460	IL.6	0.769598956	0.046992498	LEP
women	rs34579650	IL.6	0.769598956	-0.038716503	LEP
women	rs28954369	IL.6	0.769598956	-0.066397938	LEP
women	rs12671256	IL.6	0.769598956	0.030266729	LEP
women	rs11764840	IL.6	0.769598956	-0.0299476	LEP
women	rs77106988	IL.6	0.769598956	0.047057738	LEP
women	rs56091545	IL.6	0.769598956	-0.038885077	LEP
women	rs12538722	IL.6	0.769598956	-0.029126024	LEP
women	rs1451006	IL.6	0.832577683	-0.043643512	LEP
women	rs1116656	IL.6	0.832577683	-0.023483989	LEP
women	rs896183	IL.6	0.832577683	0.022097179	LEP
women	rs10231132	IL.6	0.832577683	0.031873806	LEP
women	rs11981584	IL.6	0.832577683	-0.027642898	LEP
women	rs62481064	IL.6	0.939627946	-0.021645475	LEP
women	rs12532565	IL.6	0.939627946	-0.030170848	LEP
women	rs6947095	IL.6	0.939627946	-0.019166434	LEP
women	rs6976221	IL.6	0.939627946	0.017217194	LEP
women	rs4731412	IL.6	0.939627946	-0.022139456	LEP
women	rs2402885	IL.6	0.939627946	0.016645197	LEP
women	rs4731418	IL.6	0.939627946	0.011795308	LEP
women	rs10264361	IL.6	0.939627946	-0.015934796	LEP
women	rs7779866	IL.6	0.939627946	-0.011716496	LEP
women	rs6954653	IL.6	0.939627946	0.012286457	LEP
women	rs13233734	IL.6	0.939627946	-0.008608857	LEP
women	rs11772985	IL.6	0.939627946	-0.00831246	LEP
women	rs2060736	IL.6	0.939627946	0.011506671	LEP
women	rs7778167	IL.6	0.939627946	0.008069646	LEP
women	rs10487505	IL.6	0.939627946	-0.006007384	LEP
women	rs4731437	IL.6	0.939627946	0.012168111	LEP
women	rs6467165	IL.6	0.939627946	-0.008981622	LEP
women	rs4731419	IL.6	0.939627946	-0.004800531	LEP
women	rs4728092	IL.6	0.939627946	-0.005420252	LEP
women	rs2071045	IL.6	0.940178381	-0.00448299	LEP
women	rs62481070	IL.6	0.987751122	0.001100843	LEP
women	rs6956123	IL.6	0.987751122	0.000811179	LEP

Supplementary Table 1b

Group	SNP	Consequence	Corrected	Beta	Gene
		gene	p-value		
all	rs10158579	IL.6	0.819865499	-0.048718994	LEPR
all	rs12062820	IL.6	0.819865499	-0.043743164	LEPR
all	rs7546924	IL.6	0.819865499	-0.03425292	LEPR
all	rs9436741	IL.6	0.819865499	-0.036383008	LEPR
all	rs3806318	IL.6	0.819865499	-0.039263255	LEPR
all	rs6689005	IL.6	0.819865499	-0.047257735	LEPR
all	rs6671498	IL.6	0.819865499	0.032668012	LEPR
all	rs4655517	IL.6	0.819865499	0.028491609	LEPR
all	rs7418057	IL.6	0.819865499	-0.028257749	LEPR
all	rs17127618	IL.6	0.819865499	-0.038564755	LEPR
all	rs1751485	IL.6	0.819865499	-0.025592966	LEPR
all	rs1751490	IL.6	0.819865499	0.02539569	LEPR
all	rs7534511	IL.6	0.819865499	-0.025454307	LEPR
all	rs60807413	IL.6	0.819865499	-0.044951068	LEPR
all	rs1046011	IL.6	0.819865499	0.024942819	LEPR
all	rs4655584	IL.6	0.819865499	0.024573624	LEPR
all	rs1171279	IL.6	0.819865499	-0.026242728	LEPR
all	rs4655781	IL.6	0.819865499	0.02772336	LEPR
all	rs9436302	IL.6	0.819865499	-0.028017344	LEPR
all	rs7413823	IL.6	0.819865499	-0.023415026	LEPR
all	rs2148683	IL.6	0.819865499	-0.022170272	LEPR
all	rs12033452	IL.6	0.819865499	0.023256878	LEPR
all	rs1475398	IL.6	0.82611134	-0.021967914	LEPR
all	rs9436740	IL.6	0.82611134	-0.028291409	LEPR
all	rs7553258	IL.6	0.82611134	0.02105511	LEPR
all	rs55953331	IL.6	0.82611134	0.029481265	LEPR
all	rs12409877	IL.6	0.82611134	-0.018573558	LEPR
all	rs55966874	IL.6	0.833175123	-0.038532258	LEPR
all	rs55730790	IL.6	0.835351961	-0.026005234	LEPR
all	rs10749754	IL.6	0.835351961	0.016166518	LEPR
all	rs77980027	IL.6	0.835351961	-0.025063405	LEPR
all	rs4655598	IL.6	0.861232593	-0.015789023	LEPR
all	rs4655537	IL.6	0.861232593	0.016484637	LEPR
all	rs12022410	IL.6	0.865187207	0.015049231	LEPR
all	rs4554758	IL.6	0.87620839	-0.014232223	LEPR
all	rs4655802	IL.6	0.903612497	-0.013488507	LEPR
all	rs3762274	IL.6	0.903612497	0.012544118	LEPR

Supplementary Table 1b: Continued

Group	SNP	Consequence gene	Corrected p-value	Beta	Gene
all	rs11208680	IL.6	0.903612497	0.014652229	LEPR
all	rs61781408	IL.6	0.903612497	-0.016905566	LEPR
all	rs3790434	IL.6	0.903612497	-0.012240328	LEPR
all	rs4916047	IL.6	0.903612497	-0.010374783	LEPR
all	rs3828037	IL.6	0.903612497	0.010012836	LEPR
all	rs913200	IL.6	0.903612497	-0.009860941	LEPR
all	rs58372192	IL.6	0.91383979	0.017019927	LEPR
all	rs61779725	IL.6	0.91383979	0.010784543	LEPR
all	rs6658922	IL.6	0.926215546	0.007830062	LEPR
all	rs61779782	IL.6	0.926215546	-0.00758806	LEPR
all	rs6700201	IL.6	0.926215546	-0.009399294	LEPR
all	rs2025805	IL.6	0.926215546	0.006571489	LEPR
all	rs36072366	IL.6	0.926215546	-0.007946713	LEPR
all	rs74081641	IL.6	0.926215546	-0.008622	LEPR
all	rs111313184	IL.6	0.926215546	-0.006864284	LEPR
all	rs3790436	IL.6	0.926215546	-0.005244913	LEPR
all	rs10493380	IL.6	0.926215546	-0.006157104	LEPR
all	rs6656451	IL.6	0.950464109	0.003798005	LEPR
all	rs4655762	IL.6	0.950464109	-0.003904265	LEPR
all	rs12082008	IL.6	0.97960259	0.002493583	LEPR
all	rs6672992	IL.6	0.993772452	-0.001351658	LEPR
all	rs6662904	IL.6	0.993772452	0.000889544	LEPR
all	rs114403972	IL.6	0.993772452	0.000889163	LEPR
all	rs11585329	IL.6	0.994552974	0.00021246	LEPR
men	rs9436741	IL.6	0.374148471	-0.056004596	LEPR
men	rs4655518	IL.6	0.374148471	0.059061194	LEPR
men	rs7413823	IL.6	0.374148471	-0.0591001	LEPR
men	rs1751485	IL.6	0.374148471	-0.053329923	LEPR
men	rs1751490	IL.6	0.374148471	0.05264898	LEPR
men	rs1046011	IL.6	0.374148471	0.054261129	LEPR
men	rs9436300	IL.6	0.374148471	-0.05193799	LEPR
men	rs11804091	IL.6	0.374148471	-0.065776343	LEPR
men	rs10158579	IL.6	0.374148471	-0.063602445	LEPR
men	rs1171280	IL.6	0.374148471	-0.05010479	LEPR
men	rs72921454	IL.6	0.374148471	-0.068265914	LEPR
men	rs4655781	IL.6	0.374148471	0.057022846	LEPR
men	rs4655517	IL.6	0.374148471	0.042794849	LEPR

Supplementary Table 1b: Continued

Group	SNP	Consequence	Corrected	Beta	Gene
		gene	p-value		
men	rs7418057	IL.6	0.374148471	-0.042342518	LEPR
men	rs7553258	IL.6	0.374148471	0.050482735	LEPR
men	rs7529650	IL.6	0.374148471	-0.044809207	LEPR
men	rs4655598	IL.6	0.374148471	-0.046658976	LEPR
men	rs9436299	IL.6	0.374148471	-0.046381472	LEPR
men	rs58372192	IL.6	0.456797374	0.071843211	LEPR
men	rs12062820	IL.6	0.544638853	-0.044290373	LEPR
men	rs9436746	IL.6	0.544638853	-0.039743003	LEPR
men	rs9436302	IL.6	0.544638853	-0.041253203	LEPR
men	rs3806318	IL.6	0.593609948	-0.040030874	LEPR
men	rs9662547	IL.6	0.593609948	-0.036036346	LEPR
men	rs3790429	IL.6	0.593609948	-0.044440781	LEPR
men	rs6671498	IL.6	0.707107219	0.030699632	LEPR
men	rs4655584	IL.6	0.739745387	0.028208134	LEPR
men	rs6662244	IL.6	0.743743771	0.02417857	LEPR
men	rs55964802	IL.6	0.783110119	-0.028614707	LEPR
men	rs1475397	IL.6	0.783110119	-0.025863717	LEPR
men	rs6656451	IL.6	0.783110119	-0.024047142	LEPR
men	rs60807413	IL.6	0.783110119	-0.040885547	LEPR
men	rs6700201	IL.6	0.783110119	-0.028555662	LEPR
men	rs3828034	IL.6	0.792411042	-0.025490092	LEPR
men	rs17127601	IL.6	0.792411042	-0.031161969	LEPR
men	rs9436738	IL.6	0.792411042	0.031700507	LEPR
men	rs61779772	IL.6	0.792411042	0.019128969	LEPR
men	rs3828037	IL.6	0.792411042	0.018603129	LEPR
men	rs55953331	IL.6	0.792411042	0.026533557	LEPR
men	rs3762274	IL.6	0.792411042	0.017463194	LEPR
men	rs6588143	IL.6	0.792411042	-0.016159064	LEPR
men	rs2148683	IL.6	0.792411042	-0.014407547	LEPR
men	rs3790436	IL.6	0.792411042	0.015950567	LEPR
men	rs12022410	IL.6	0.792411042	0.015188145	LEPR
men	rs114403972	IL.6	0.792411042	0.021710963	LEPR
men	rs4655802	IL.6	0.792411042	0.014102803	LEPR
men	rs111313184	IL.6	0.792411042	-0.018994567	LEPR
men	rs11208646	IL.6	0.792411042	0.01463483	LEPR
men	rs6704167	IL.6	0.792411042	-0.013946146	LEPR
men	rs55966874	IL.6	0.792411042	-0.023951249	LEPR

Supplementary Table 1b: Continued

Group	SNP	Consequence gene	Corrected p-value	Beta	Gene
men	rs9436740	IL.6	0.792411042	-0.016666996	LEPR
men	rs7546924	IL.6	0.792411042	-0.010818813	LEPR
men	rs4655537	IL.6	0.792411042	0.011916924	LEPR
men	rs4916047	IL.6	0.792411042	0.010548951	LEPR
men	rs7537093	IL.6	0.804415486	-0.01119055	LEPR
men	rs11585329	IL.6	0.881827121	0.010609372	LEPR
men	rs6660481	IL.6	0.907432229	0.005703231	LEPR
men	rs6689005	IL.6	0.907432229	0.008639234	LEPR
men	rs10493377	IL.6	0.907432229	0.00557342	LEPR
men	rs36072366	IL.6	0.93483312	0.005100144	LEPR
men	rs55730790	IL.6	0.934895102	0.004748797	LEPR
men	rs6672992	IL.6	0.969467643	-0.001990299	LEPR
men	rs11208680	IL.6	0.98104831	-0.000779329	LEPR
women	rs7546924	IL.6	0.589143684	-0.085082178	LEPR
women	rs6689005	IL.6	0.589143684	-0.109411087	LEPR
women	rs60807413	IL.6	0.987457251	-0.103039793	LEPR
women	rs4916047	IL.6	0.987457251	-0.058964575	LEPR
women	rs4655802	IL.6	0.987457251	-0.05830358	LEPR
women	rs2148683	IL.6	0.987457251	-0.049079003	LEPR
women	rs72921454	IL.6	0.987457251	0.069805311	LEPR
women	rs7515643	IL.6	0.987457251	-0.046010034	LEPR
women	rs55730790	IL.6	0.987457251	-0.061536447	LEPR
women	rs9436729	IL.6	0.987457251	-0.044975232	LEPR
women	rs58372192	IL.6	0.987457251	-0.08500906	LEPR
women	rs3790433	IL.6	0.987457251	0.046099172	LEPR
women	rs9436745	IL.6	0.987457251	0.047700841	LEPR
women	rs61781408	IL.6	0.987457251	-0.049521208	LEPR
women	rs36072366	IL.6	0.987457251	-0.047009826	LEPR
women	rs7537733	IL.6	0.987457251	-0.032003302	LEPR
women	rs11804091	IL.6	0.987457251	0.047860583	LEPR
women	rs17127905	IL.6	0.987457251	-0.029736326	LEPR
women	rs17407229	IL.6	0.987457251	0.032184986	LEPR
women	rs10493377	IL.6	0.987457251	-0.02833943	LEPR
women	rs6588147	IL.6	0.987457251	0.025994655	LEPR
women	rs55966874	IL.6	0.987457251	-0.054577877	LEPR
women	rs11208646	IL.6	0.987457251	-0.027680313	LEPR
women	rs6672992	IL.6	0.987457251	-0.030635841	LEPR

Supplementary Table 1b: Continued

Group	SNP	Consequence	Corrected	Beta	Gene
		gene	p-value		
women	rs6688776	IL.6	0.987457251	-0.020403835	LEPR
women	rs3790436	IL.6	0.987457251	-0.021579918	LEPR
women	rs9436740	IL.6	0.987457251	-0.025669077	LEPR
women	rs6696658	IL.6	0.987457251	-0.017825128	LEPR
women	rs4370791	IL.6	0.987457251	-0.01624253	LEPR
women	rs2104563	IL.6	0.987457251	0.016298934	LEPR
women	rs4655598	IL.6	0.987457251	0.013866262	LEPR
women	rs61779772	IL.6	0.987457251	-0.013571158	LEPR
women	rs61781283	IL.6	0.987457251	0.017014777	LEPR
women	rs1046011	IL.6	0.987457251	-0.013269685	LEPR
women	rs11808888	IL.6	0.987457251	0.019642458	LEPR
women	rs2025805	IL.6	0.987457251	0.01072186	LEPR
women	rs72683129	IL.6	0.987457251	0.017947615	LEPR
women	rs3806318	IL.6	0.987457251	-0.01538273	LEPR
women	rs6700896	IL.6	0.987457251	-0.010827718	LEPR
women	rs6656451	IL.6	0.987457251	0.009914197	LEPR
women	rs7418057	IL.6	0.987457251	0.009973162	LEPR
women	rs4655517	IL.6	0.987457251	-0.009933196	LEPR
women	rs10749753	IL.6	0.987457251	0.007325713	LEPR
women	rs6660481	IL.6	0.987457251	-0.007888748	LEPR
women	rs1475397	IL.6	0.987457251	0.008170835	LEPR
women	rs4655772	IL.6	0.987457251	-0.006558142	LEPR
women	rs72683113	IL.6	0.987457251	-0.007654549	LEPR
women	rs6700201	IL.6	0.987457251	-0.006784277	LEPR
women	rs1751485	IL.6	0.987457251	0.004583524	LEPR
women	rs6671498	IL.6	0.987457251	-0.005416867	LEPR
women	rs12062820	IL.6	0.987457251	0.006237986	LEPR
women	rs11208680	IL.6	0.987457251	0.005434883	LEPR
women	rs11585329	IL.6	0.987457251	0.005333826	LEPR
women	rs10789188	IL.6	0.987457251	0.003783974	LEPR
women	rs6696954	IL.6	0.99564261	0.0020001	LEPR
women	rs3828037	IL.6	0.99564261	-0.001036535	LEPR
women	rs55964802	IL.6	0.99564261	-0.000892542	LEPR
women	rs114403972	IL.6	0.997803373	-0.000126856	LEPR

Supplementary Table 1c

Group	SNP	Consequence gene	Corrected p-value	Beta	Gene
all	rs12055945	Leptin	0.862362386	0.051620676	IL6
all	rs1916819	Leptin	0.862362386	0.04781873	IL6
all	rs58062407	Leptin	0.862362386	0.043509951	IL6
all	rs62449525	Leptin	0.862362386	0.043624688	IL6
all	rs12537965	Leptin	0.862362386	0.024553092	IL6
all	rs10950917	Leptin	0.862362386	-0.026296039	IL6
all	rs7787688	Leptin	0.862362386	-0.024064393	IL6
all	rs1608554	Leptin	0.862362386	-0.023802943	IL6
all	rs59084784	Leptin	0.862362386	0.02374164	IL6
all	rs13242809	Leptin	0.862362386	0.025812143	IL6
all	rs2905333	Leptin	0.862362386	-0.021720717	IL6
all	rs34788132	Leptin	0.862362386	0.025496734	IL6
all	rs35116860	Leptin	0.862362386	0.022474987	IL6
all	rs13243243	Leptin	0.862362386	0.026068415	IL6
all	rs17147267	Leptin	0.862362386	0.030166859	IL6
all	rs73683966	Leptin	0.862362386	-0.023699831	IL6
all	rs12531874	Leptin	0.862362386	-0.027583607	IL6
all	rs2091114	Leptin	0.862362386	0.019715512	IL6
all	rs4621699	Leptin	0.862362386	-0.021759836	IL6
all	rs62449486	Leptin	0.862362386	0.023735875	IL6
all	rs2905340	Leptin	0.862362386	-0.019838983	IL6
all	rs6969502	Leptin	0.862362386	0.023268457	IL6
all	rs62449495	Leptin	0.862362386	0.023107648	IL6
all	rs10265548	Leptin	0.862362386	0.023188941	IL6
all	rs35263987	Leptin	0.862362386	0.019807816	IL6
all	rs115622312	Leptin	0.862362386	-0.021719382	IL6
all	rs10260111	Leptin	0.905364881	0.017273079	IL6
all	rs10156056	Leptin	0.907442879	0.02279653	IL6
all	rs1524099	Leptin	0.907442879	0.014435081	IL6
all	rs11981240	Leptin	0.907442879	0.015040967	IL6
all	rs1800797	Leptin	0.907442879	0.012791632	IL6
all	rs7776857	Leptin	0.907442879	0.012732577	IL6
all	rs1524101	Leptin	0.907442879	-0.013725615	IL6
all	rs28572733	Leptin	0.907442879	0.012023832	IL6
all	rs1524102	Leptin	0.907442879	0.01164816	IL6

Supplementary Table 1c: Continued

Group	SNP	Consequence gene	Corrected p-value	Beta	Gene
all	rs56260469	Leptin	0.907442879	0.010656103	IL6
all	rs4722172	Leptin	0.907442879	0.011361838	IL6
all	rs10229457	Leptin	0.907442879	0.009187234	IL6
all	rs4719711	Leptin	0.907442879	-0.008024011	IL6
all	rs10259425	Leptin	0.907442879	0.00961389	IL6
all	rs13236645	Leptin	0.907442879	-0.007819259	IL6
all	rs6954667	Leptin	0.907442879	-0.007653983	IL6
all	rs13246138	Leptin	0.946983322	-0.006531131	IL6
all	rs34075886	Leptin	0.956686748	0.003868264	IL6
all	rs2069840	Leptin	0.956686748	0.00356784	IL6
all	rs77529569	Leptin	0.956686748	0.006066818	IL6
all	rs2056576	Leptin	0.956686748	0.003133857	IL6
all	rs4722166	Leptin	0.956686748	0.002402404	IL6
all	rs6954897	Leptin	0.956686748	-0.002245569	IL6
all	rs7804146	Leptin	0.956686748	0.002057166	IL6
all	rs62449490	Leptin	0.956686748	-0.001515949	IL6
all	rs1818879	Leptin	0.956686748	0.001200121	IL6
men	rs7801503	Leptin	0.85586096	0.075352851	IL6
men	rs13242809	Leptin	0.85586096	0.05453141	IL6
men	rs10950917	Leptin	0.85586096	-0.050340922	IL6
men	rs17147267	Leptin	0.85586096	0.062598951	IL6
men	rs12055945	Leptin	0.85586096	0.051716504	IL6
men	rs62449525	Leptin	0.85586096	0.064559563	IL6
men	rs10260111	Leptin	0.85586096	0.040283284	IL6
men	rs62449495	Leptin	0.85586096	0.04688957	IL6
men	rs2091114	Leptin	0.85586096	0.036494678	IL6
men	rs1524099	Leptin	0.85586096	0.033848423	IL6
men	rs59084784	Leptin	0.85586096	0.034327327	IL6
men	rs28572733	Leptin	0.85586096	0.032432639	IL6
men	rs4386870	Leptin	0.85586096	0.040142434	IL6
men	rs34075886	Leptin	0.85586096	0.028966534	IL6
men	rs10270171	Leptin	0.85586096	0.036323156	IL6
men	rs4722172	Leptin	0.85586096	0.037412316	IL6
men	rs7787532	Leptin	0.85586096	-0.027268023	IL6
men	rs2961311	Leptin	0.85586096	-0.027458163	IL6

Supplementary Table 1c: Continued

Group	SNP	Consequence gene	Corrected p-value	Beta	Gene
men	rs7783020	Leptin	0.85586096	0.027690928	IL6
men	rs7802277	Leptin	0.85586096	-0.035598548	IL6
men	rs2905333	Leptin	0.85586096	-0.022741611	IL6
men	rs6969502	Leptin	0.85586096	0.026325063	IL6
men	rs4722166	Leptin	0.85586096	0.022644589	IL6
men	rs7776857	Leptin	0.85586096	0.021317498	IL6
men	rs4719711	Leptin	0.85586096	-0.01883384	IL6
men	rs1800797	Leptin	0.85586096	0.0200928	IL6
men	rs6461665	Leptin	0.85586096	0.019316307	IL6
men	rs34788132	Leptin	0.85586096	0.021807205	IL6
men	rs2056577	Leptin	0.85586096	-0.017155845	IL6
men	rs7787688	Leptin	0.85586096	-0.017030931	IL6
men	rs115622312	Leptin	0.85586096	-0.01859883	IL6
men	rs11981240	Leptin	0.85586096	0.016190763	IL6
men	rs7383869	Leptin	0.85586096	0.012179829	IL6
men	rs77529569	Leptin	0.85586096	0.022549172	IL6
men	rs4270847	Leptin	0.85586096	-0.014086984	IL6
men	rs6954667	Leptin	0.85586096	-0.011633054	IL6
men	rs10259425	Leptin	0.85586096	0.013414111	IL6
men	rs35924322	Leptin	0.85586096	0.011101476	IL6
men	rs7804146	Leptin	0.85586096	0.010145419	IL6
men	rs13243243	Leptin	0.85586096	0.012828502	IL6
men	rs2069840	Leptin	0.85586096	0.009340841	IL6
men	rs2097677	Leptin	0.85586096	0.010362791	IL6
men	rs1818879	Leptin	0.862487186	0.008265886	IL6
men	rs4552807	Leptin	0.862487186	0.00854896	IL6
men	rs35116860	Leptin	0.875185101	0.007397326	IL6
men	rs56260469	Leptin	0.917992229	0.005189018	IL6
men	rs150971244	Leptin	0.963789137	0.002736488	IL6
men	rs10156056	Leptin	0.96475234	0.002544371	IL6
men	rs1524102	Leptin	0.96475234	0.001313572	IL6
women	rs1524101	Leptin	0.936263528	-0.089977285	IL6
women	rs12537965	Leptin	0.936263528	0.048532245	IL6
women	rs34884022	Leptin	0.936263528	0.043512607	IL6
women	rs10265548	Leptin	0.936263528	0.048963444	IL6

Supplementary Table 1c: Continued

Group	SNP	Consequence gene	Corrected p-value	Beta	Gene
women	rs11763992	Leptin	0.936263528	0.045851286	IL6
women	rs2056577	Leptin	0.936263528	0.044446039	IL6
women	rs12055945	Leptin	0.936263528	0.043576804	IL6
women	rs1880241	Leptin	0.936263528	-0.034796823	IL6
women	rs73683966	Leptin	0.936263528	-0.040203935	IL6
women	rs58062407	Leptin	0.936263528	0.046398013	IL6
women	rs13243243	Leptin	0.936263528	0.038322749	IL6
women	rs10156056	Leptin	0.936263528	0.052231505	IL6
women	rs1524102	Leptin	0.936263528	0.034548292	IL6
women	rs10260111	Leptin	0.936263528	-0.03237675	IL6
women	rs4722172	Leptin	0.936263528	-0.038069359	IL6
women	rs17302823	Leptin	0.936263528	0.033164826	IL6
women	rs7787688	Leptin	0.936263528	-0.028293559	IL6
women	rs4722166	Leptin	0.936263528	-0.029468582	IL6
women	rs35779989	Leptin	0.936263528	-0.026823216	IL6
women	rs6954897	Leptin	0.936263528	-0.024012728	IL6
women	rs55986907	Leptin	0.936263528	0.027735476	IL6
women	rs4722167	Leptin	0.936263528	0.025919908	IL6
women	rs1818879	Leptin	0.936263528	-0.022668005	IL6
women	rs4621699	Leptin	0.936263528	-0.02503768	IL6
women	rs6963866	Leptin	0.936263528	0.021577608	IL6
women	rs6461665	Leptin	0.936263528	-0.023006122	IL6
women	rs68072554	Leptin	0.936263528	-0.021599252	IL6
women	rs2091114	Leptin	0.936263528	-0.018913647	IL6
women	rs1880243	Leptin	0.936263528	0.019371595	IL6
women	rs13242809	Leptin	0.936263528	-0.017366859	IL6
women	rs1524099	Leptin	0.936263528	-0.015150775	IL6
women	rs35828931	Leptin	0.936263528	-0.014765116	IL6
women	rs77529569	Leptin	0.936263528	-0.021697327	IL6
women	rs115622312	Leptin	0.936263528	-0.017749519	IL6
women	rs12531874	Leptin	0.936263528	-0.016932907	IL6
women	rs7802442	Leptin	0.936263528	-0.012336669	IL6
women	rs7805828	Leptin	0.936263528	-0.010777639	IL6
women	rs2905342	Leptin	0.936263528	0.011666986	IL6
women	rs7793526	Leptin	0.936263528	-0.011166608	IL6

Supplementary Table 1c: Continued

Group	SNP	Consequence gene	Corrected p-value	Beta	Gene
women	rs2069840	Leptin	0.936263528	-0.010588387	IL6
women	rs17147267	Leptin	0.936263528	-0.01532888	IL6
women	rs62449526	Leptin	0.936263528	-0.01218042	IL6
women	rs62449525	Leptin	0.936263528	0.011250373	IL6
women	rs1800797	Leptin	0.936263528	0.006981726	IL6
women	rs10950917	Leptin	0.936263528	0.007216499	IL6
women	rs11981240	Leptin	0.936263528	0.007039067	IL6
women	rs10259425	Leptin	0.936263528	0.007664401	IL6
women	rs7804146	Leptin	0.936263528	-0.006041461	IL6
women	rs6954681	Leptin	0.936263528	-0.006950989	IL6
women	rs73684321	Leptin	0.96656725	0.004600799	IL6
women	rs2905333	Leptin	0.976319563	-0.001525015	IL6
women	rs7776857	Leptin	0.976319563	-0.001163392	IL6



Chapter 4

Interleukin-1ß induces trained innate immunity in human hematopoietic progenitor cells *in vitro*

Daniela Flores Gomez, Willemijn Hobo, Diede van Ens, Elise L. Kessler, Boris Novakovic, Nicolaas P.M. Schaap, Wim H.C. Rijnen, Leo A.B. Joosten, Mihai G. Netea, Niels P. Riksen* and Siroon Bekkering*

*Shared senior authorship

Stem Cell Reports. 2024 Dec 10;19(12):1651-1664

Abstract

Innate immune cells can develop a long-lasting hyperresponsive phenotype, termed trained immunity, mediated by epigenetic and metabolic reprogramming. In mice, exposure to Bacille Calmette-Guérin (BCG), β-glucan, or Western diet induces trained immunity by reprogramming hematopoietic progenitor cells (HPCs), through interleukin-1ß (IL-1ß) signaling in the bone marrow (BM). We investigated whether IL-1\(\beta\) induces trained immunity in primary human BM-derived HPCs in vitro. We exposed human BM-derived HPCs to IL-1 β for 4 h. HPCs were expanded and differentiated into monocytes followed by functional and transcriptomic characterization. IL-1B -exposed HPCs showed higher granulocyte-macrophage colony-forming units. The monocyte offspring produced more tumor necrosis factor (TNF) and IL-1ß after restimulation with lipopolysaccharide (LPS) and Pam3Cys and is metabolically more active. Transcriptomic analysis showed upregulation of key atherogenic and inflammatory pathways. In conclusion, brief exposure of human BM-derived HPCs to IL-1β in vitro induces a trained immunity phenotype.

Highlights

- Exposure of HPCs to IL-1β leads to production of inflammatory monocytes
- HPC-derived trained monocytes have increased cytokine production
- This is associated with increased glycolysis and oxidative phosphorylation
- IL-1β induces innate immune memory in human bone marrow HPCs in vitro

Keywords

trained immunity

Introduction

The innate immune system can develop a long-lasting pro-inflammatory phenotype after brief exposure to microorganisms or endogenous substances, such as modified lipoproteins, glucose, urate, or danger-associated molecular patterns (1). This phenomenon is called trained immunity, is mediated by epigenetic and metabolic reprogramming, and is characterized by an increased cytokine production capacity (2).

In addition to mature immune cells, such as monocytes, trained immunity can also occur in the bone marrow progenitor cells, which is called "central trained immunity" (3). This explains the observation that, after subcutaneous administration of Bacille Calmette-Guérin (BCG), a potent inducer of trained immunity, trained monocytes are present in the human circulation up to one year, despite the short half-life of circulating monocytes (4). In mice, short-term exposure to BCG, β-glucan, or Western-type diet induces trained immunity by epigenetic reprogramming of hematopoietic progenitor cells (HPCs). Murine studies demonstrated that BCG promotes proliferation of HPCs and confers protection against other infections (5). This has also been shown in studies in humans, in whom bone marrow HPCs showed functional and transcriptional reprogramming 3 months after BCG vaccination (6). Mitroulis et al. demonstrated that β-glucan induced HPC reprogramming via interleukin-1β (IL-1β) signaling in the bone marrow (7). The trained HPCs were characterized by increased proliferation, and myeloid skewing. In addition to infectious stimuli, 4 weeks of a Western-type diet in Ldlr-/- mice induced a similar effect resulting in enhanced stem cell proliferation and immune response, which was dependent on NLRP3 inflammasome activation and IL-1ß signaling (8). Bone marrow myeloid reprogramming has also been studied in humans in the context of atherosclerotic cardiovascular diseases. Patients with established coronary artery disease have transcriptionally reprogrammed HPCs and increased cytokine production capacity (9). Similar findings were reported for patients with familial hypercholesterolemia (10). A key role for IL-1 β in cardiovascular diseases has been shown by the observation that the anti-IL-1β antibody canakinumab lowers future cardiovascular disease risk (11).

Based on these published data, we hypothesize that also in humans, IL-1ß induces HPC-trained immunity. To test this, we designed an in vitro model to study trained immunity in human bone-marrow-derived HPCs and studied the effects of brief exposure to IL-1\u00ed. We assessed the functional and transcriptional parameters of trained HPC-derived monocytes and macrophages. Additionally, we performed a colony formation unit to investigate the proliferation and differentiation capacity of trained cells. Our results will help to understand how IL-1ß signaling can have prolonged pro-inflammatory effects on the innate immune system.

Results

IL-1\(\beta \) induces a shift toward myeloid cell proliferation

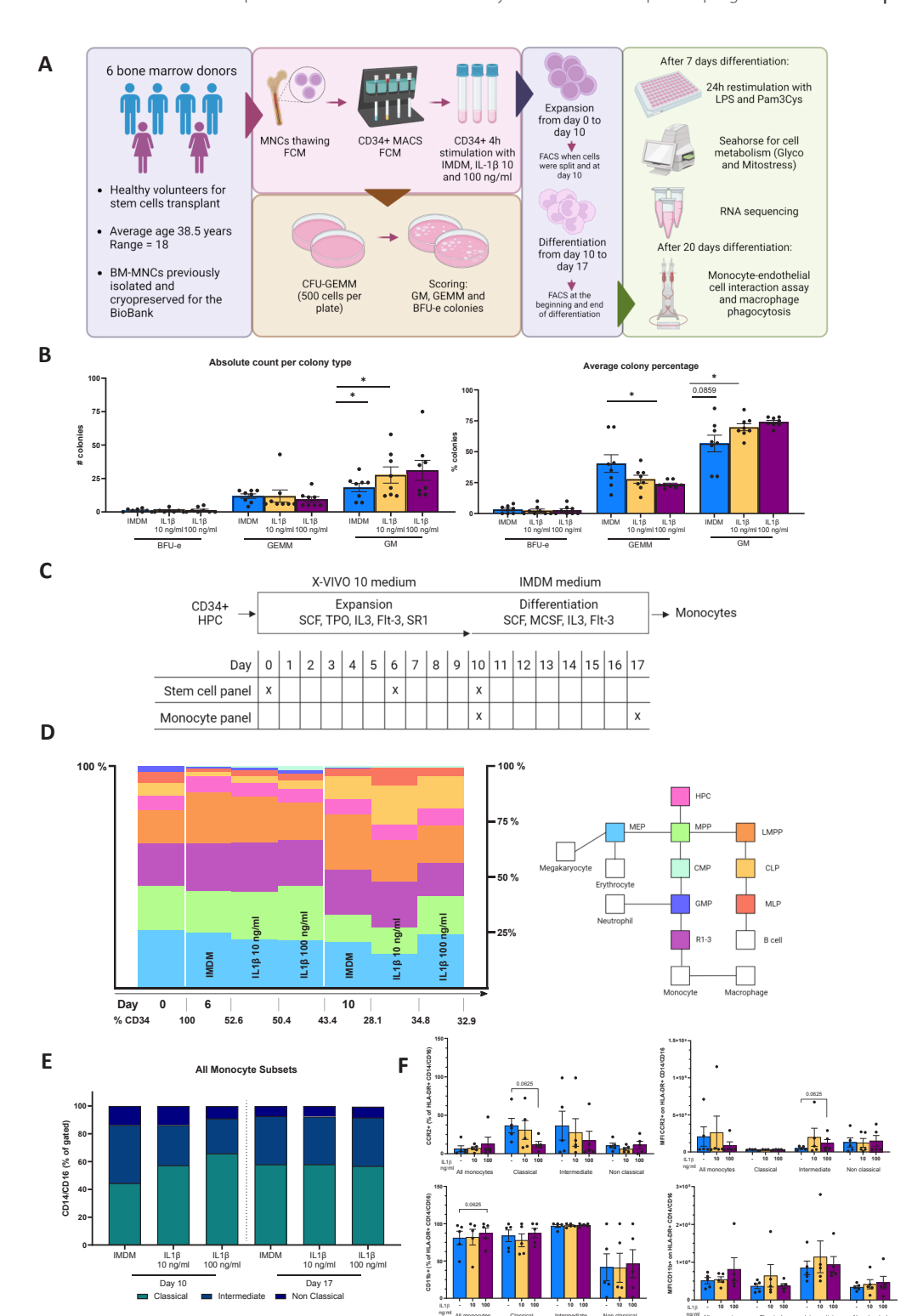
To study the effect of IL-1\beta on HPC proliferation, we exposed isolated CD34+ cells to IL-1β for 4 h and subsequently performed a colony-forming unit (CFU) assay (Figure 1A).

Exposure of HPCs to IL-1B increased myeloid cell production in CFU assay in a dosedependent manner. Both the absolute colony count and the colony percentage of the granulocyte-macrophage (GM) population (Figure 1B) were significantly higher in the IL-1β-exposed conditions compared to the Iscove's modified Dulbecco's medium (IMDM) control cells.

No effect of IL-1B on monocyte differentiation

After 4-h stimulation of HPCs with IL-1β, cells were expanded for 10 days and differentiated into monocytes for another 7 days. During the culture time, the cells had similar morphology and expansion and differentiation rates (Figure S1). During the expansion and differentiation time, flow cytometry was performed to understand the effect of IL-1β on the lineage of differentiation of HPC (Figure 1C). As shown in Figure 1D, progenitor populations changed over the course of expansion, but did not significantly differ between trained and untrained conditions. We

> Figure 1: Schematic overview, proliferation and differentiation during expansion and differentiation of HPCs. (A) Schematic overview of the experimental design. (B) Proliferation and differentiation capacity of human bone marrow hematopoietic progenitor cells (HPCs). Number and percentages of colonies counted after 14 days of incubation of control (IMDM) and IL-1 β -exposed HPCs (IL-1 β 10 and 100 ng/mL). 500 HPCs were initially seeded per condition in duplicate (n = 4 independent HPCs donors, Wilcoxon matched-pairs signed-rank test, *p < 0,05 compared to IMDM control). (C) Schematic overview of the flow cytometry panels to identify stem cell progenitor populations during expansion and mature cells during differentiation. (D) Progenitor populations in controls and IL-1β-exposed cells (10 and 100 ng/mL) at day 0, day 6, and day 10 of expansion (n = 4 independent HPC donors, Wilcoxon matched-pairs signed-rank test, differences were not significant). (E) Monocyte subsets identified at the beginning and end of differentiation of HPCs with M-CSF in control and cells exposed to IL-1β (10 and 100 ng/mL). IL-1β induces an increase of classical monocytes at the beginning of the differentiation (n = 5 independent HPC donors, Wilcoxon matched-pairs signed-rank test, differences were not significant). (F) CD11b and CCR2 activation markers expression and median fluorescence intensity (MFI) in the different bone-marrow-derived monocyte subsets after 7 days of differentiation. (n = 5 independent HPC donors, Wilcoxon matched-pairs signed-rank test). See also Figures S1–S3.



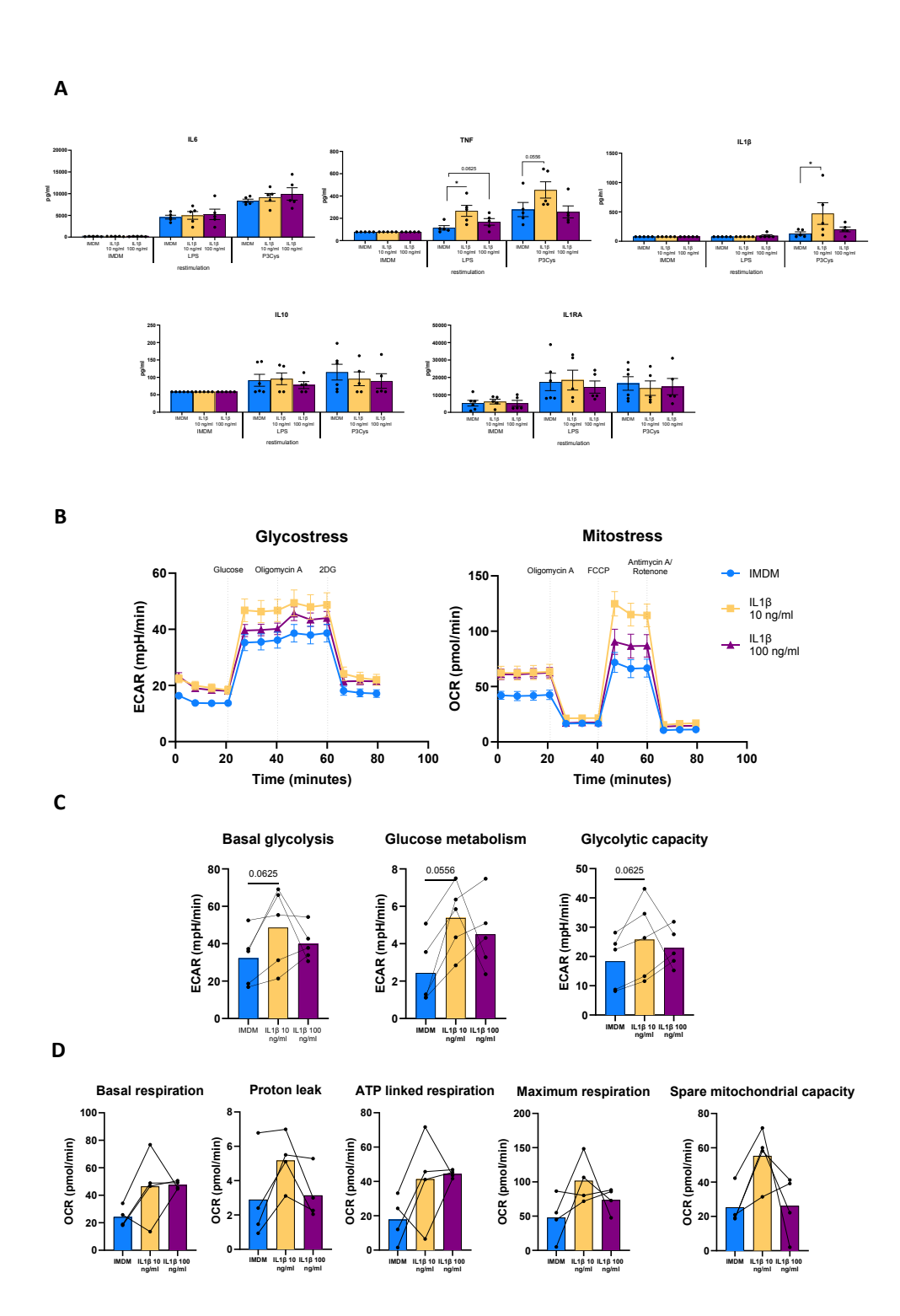
subsequently defined the three monocyte subsets with flow cytometry during the 7 days of differentiation. A sequential ontogeny scenario describes that classical monocytes can differentiate into intermediate monocytes and, finally, non-classical monocytes (12). Although there was a trend toward more classical monocytes after IL-1β (100 ng/mL) exposure at day 10, there were no differences on day 17 (Figure 1E). Neither were there any significant differences in the surface expression of CD11b and CCR2 (Figure 1F).

IL-18 increases HPC-derived monocyte cytokine production and cellular metabolism

The classical functional hallmark of trained immunity is an increased cytokine production capacity upon restimulation (1, 13). After short exposure of CD34+ cells to IL-1\(\beta\), cells were expanded for 10 days and differentiated into monocytes for 7 days. Then, HPC-derived monocytes were restimulated with TLR2 and 4 agonists to assess cytokine response. Tumor necrosis factor (TNF) production after lipopolysaccharide (LPS) stimulation and IL-1ß production after Pam3Cys stimulation were significantly increased in the monocytes derived from HPCs after IL-1β exposure (10 ng/mL). The anti-inflammatory cytokines IL-10 and IL-1Ra did not show any increase in the IL-1 β situation (Figure 2A).

The functional hyperresponsiveness of trained cells is accompanied by an increase in glycolysis and oxidative phosphorylation (2, 3). To explore the effects of IL-1β on these metabolic processes, we performed Seahorse analysis of HPCs-derived monocytes. This revealed that glycolysis (extracellular acidification rate), as well as mitochondrial respiration (oxygen consumption rate [OCR]), displays a trend to be higher in IL-1β-trained HPC-derived monocytes compared to untrained controls (Figure 2B). This upregulation was also observed in various individual parameters

> Figure 2: Short exposure of HPCs to IL-1 β augments cytokine production capacity and affects cellular metabolism of bone-marrow-derived monocytes. HPCs were exposed to IL-1β (10 and 100 ng/mL) for 4 h. After 10 days of expansion and 7 days of differentiation. (A) Cells were restimulated with LPS and Pam3Cys for 24 h and IL-6, TNF, IL-10, and IL-1RA production were measured (n = 5 independent HPC donors, *p < 0.05, Wilcoxon matched-pairs signed-rank test). (B) Extracellular acidification rate (ECAR) over time during subsequent injection of glucose, oligomycin A, and 2DG. Oxygen consumption rate over time during subsequent injection of oligomycin A, FCCP, and antimycin A/rotenone (n = 5 independent HPC donors for glycol stress test and n = 4 independent HPC donors for mito stress test, Wilcoxon matched-pairs signed-rank test). (C) Bar graphs with individual points of basal glycolysis, glucose metabolism, and glycolytic capacity of IL-1\(\beta\)-trained cells compared to control (n = 5 independent HPC donors, Wilcoxon matched-pairs signed-rank test). (D) Bar graphs with individual points of basal respiration, proton leak, ATP-linked respiration, maximum respiration, and spare mitochondrial capacity of IL-1 β -trained cells compared to control (n = 4 independent HPC donors, Wilcoxon matched-pairs signed-rank test).



of glycolysis and mitochondrial respiration such as basal glycolysis, maximum glycolytic capacity, basal respiration, and maximum mitochondrial respiration (Figures 2C and 2D). It is remarkable that the changes appeared more pronounced after exposure to 10 ng/mL IL-1β than after exposure to 100 ng/mL, which aligns well with the cytokine production capacity in both conditions (Figures 2A and 2B).

Table 1: Dynamic epigenetic modifier genes. Seventeen genes from the EpiFactors database of 773 epigenetic modifiers were in the list of 371 dynamic genes (p < 0.05, FC > 1.2) in response to IL-1 β at rest or after LPS exposure, relative to IMDM macrophages.

HGNC_symbol	UniProt_AC	Function	Row.names	log2FoldChange
RB1	P06400	Chromatin_remodeling_ Histone_modification_write	ENSG00000139687	0.4255035
EPC1	Q9H2F5	Polycomb_group_ (PcG)_protein	ENSG00000120616	0.5183384
PADI2	Q9Y2J8	Histone_modification	ENSG00000117115	-0.5777374
ATXN7	O15265	Histone_modification_ write_cofactor	ENSG00000163635	0.4969222
CBLL1	Q75N03	RNA_modification	ENSG00000105879	-0.3146693
LEO1	Q8WVC0	Histone_modification_ write_cofactor	ENSG00000166477	-0.6266516
SUV39H1	O43463	Histone_modification_write_ Histone_modification_write	ENSG00000101945	-0.389872459
ZNF687	Q8N1G0	Histone_modification_ erase_cofactor	ENSG00000143373	-0.7940353
PELP1	Q8IZL8	Histone_modification_read_ Histone_modification_ write_cofactor	ENSG00000141456	0.9922168
TLK1	Q9UKI8	Histone_modification_write	ENSG00000198586	-0.7335763
TET2	Q6N021	DNA_modification	ENSG00000168769	-0.4899147
GSG2	Q8TF76	Histone_modification_write	ENSG00000177602	-1.098119
DZIP3	Q86Y13	Histone_modification_write	ENSG00000198919	0.8927027
SMARCAL1	Q9NZC9	Chromatin_remodeling	ENSG00000138375	-0.657767344
USP49	Q70CQ1	Histone_modification_erase	ENSG00000164663	-0.79180809
TAF6	P49848	Histone_chaperone	ENSG00000106290	-0.869155484
APOBEC3A	P31941	DNA_modification_ RNA_modification	ENSG00000128383	-2.046492087

Effects of IL-1\(\beta \) on HPC-derived monocyte RNA transcription

To investigate the effects of IL-1ß exposure on transcriptional changes in HPCderived monocytes, we performed RNA sequencing on isolated HPC-derived monocytes exposed to IL-1\beta 10 ng/mL (4 h), followed by expansion (10 days), differentiation (7 days), and stimulation with LPS for 4 h (Figure 3A). Following expansion and differentiation, IMDM and IL-1B monocytes display limited differences in gene expression profile before restimulation (Figure 3B). Some of these genes are involved in relevant biological processes as seen in Figure 3C, such as myeloid leukocyte migration, inflammatory response, and granulocyte chemotaxis.

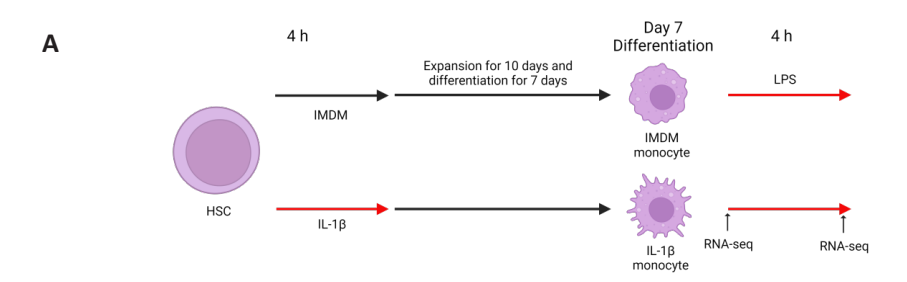
p value	uns_IMDM_ CPM_mean	uns_IL1_CPM_ mean	LPS_IMDM_ CPM_mean	LPS_IL1_CPM_ mean
0.02512911	30.10721	35.07385	17.32411	23.93343
0.03820138	17.91373	19.09535	16.88228	24.48446
0.01846565	27.86381	28.84332	22.57345	14.95674
0.02535242	21.01068	21.27799	16.05089	22.54999
0.03907087	63.81039	63.00588	61.67063	49.84006
0.03412533	59.58235	54.63181	45.91457	30.6547
0.048444966	22.41103926	20.22470767	19.85635302	15.28346169
0.03142792	10.3149	9.052185	11.01229	6.06947
0.03417424	1.905422	1.664677	1.383398	2.641318
0.0185721	169.5784	144.4192	118.6951	68.78121
0.003111455	182.861	151.5804	137.961	98.30065
 0.005134638	5.759229	4.306792	4.360039	2.105806
0.01575299	6.091953	4.536273	3.760852	6.784402
0.042628458	9.609686796	6.122826505	5.696649864	5.011683018
0.01000105	8.15194296	4.521924333	6.678193826	7.186339536
0.042491593	6.090293369	3.246512457	3.758781191	2.431951576
0.008185171	4.947446991	1.683743614	3.208114535	2.842598104

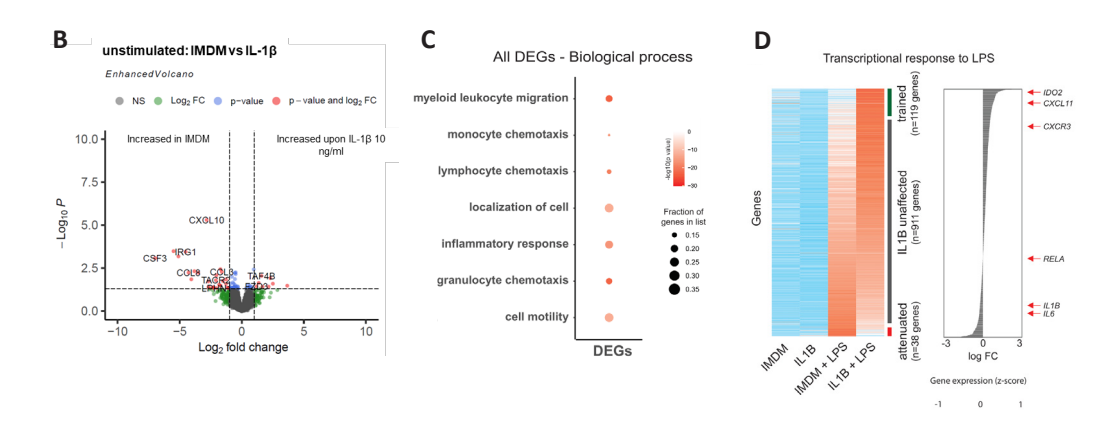
Next, we analyzed gene expression following LPS exposure, to determine how IL-1B exposure influenced the monocyte response to secondary stimulation (Figure 3D). The heatmap was ranked by the effect of IL-1\beta on LPS response, with "trained" (119 genes), "unaffected" (911 genes) and "attenuated" (38 genes) responses by IL-1β exposure of HPCs, based on both conditions before and after LPS restimulation. Interestingly, IL1B and IL-6 genes were clustered as IL-1β-unaffected genes, contrary to what we observed in the cytokine production capacity of these trained HPC-derived monocytes. Similarly, pathways like TNF signaling, Jak-STAT, and chemokine signaling were more represented in the attenuated or unaffected genes (higher fractions of differentially expressed genes present), while the "trained" gene group was enriched for apoptosis and ferroptosis (Figure 3E).

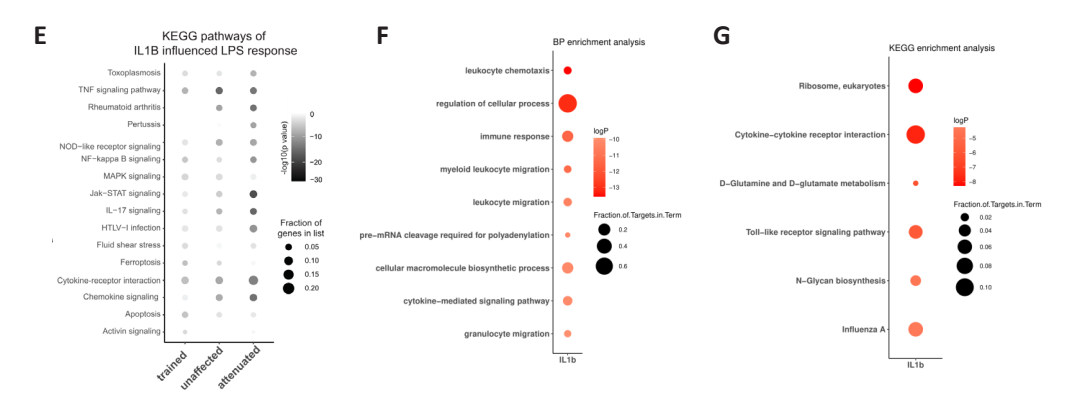
We further looked at the effect of IL-1 β exposure on the expression of epigenetic regulators, by downloading the list of 773 epigenetic modifiers from the FANTOM Consortium EpiFactors database (14). We found that, of these 773 epigenetic factors, 17 were in the list of 371 dynamic genes (p < 0.05, FC > 1.2) in response to IL-1β at rest or after LPS exposure, relative to IMDM macrophages (see Table 1). In general, epigenetic factors were slightly more likely to be dynamic (2.2% vs. 1.8%) compared to all genes. This includes TET2, which is less expressed in IL-1β-exposed cells, both at rest and after LPS exposure.

Finally, we also performed pathway analysis on the 371 dynamic genes in response to at rest or after LPS exposure, relative to IMDM macrophages (see Figures 3F and 3G). Gene Ontology Biological Process analysis revealed an enrichment in "regulation of cellular processes" and "cellular macromolecule biosynthetic process," suggesting involvement in metabolic processes. Moreover, enrichment in "leukocyte chemotaxis," "immune response," and "leukocyte migration" fits with our functional results suggestive of increased adherence to endothelial cells (ECs).

> Figure 3: Short exposure to IL-1β 10 ng/mL and restimulation with LPS induce transcriptional changes in HPC-derived monocytes. (A) Schematic overview of the protocol used to collect RNA samples of IL-1β-trained cells. Magnetically sorted monocytes were stimulated with 10 ng/mL LPS for 4 h. Samples were collected before and after LPS restimulation for RNA-seq. (B) Volcano plot showing up and down-regulated genes between IMDM and IL-1β-exposed monocytes before LPS exposure. p values were adjusted for multiple comparisons. (C) Top biological pathways enriched in the differentially expressed gene (DEG) list, according to p value and fraction of DEG present. (D) Transcriptional response to LPS restimulation. Genes were clustered in 3 groups: IL-1β trained (119 genes), IL-1β attenuated (911 genes), and unaffected (38 genes). (E) KEGG pathway analysis showing the influence of IL-1β upon LPS restimulation in the trained, IL-1β-attenuated, and unaffected clusters according to p value and fraction of DEG present. For all the analysis, n = 3 independent HPC donors was used. (F) Biological Process (BP) enrichment and (G) KEGG pathway enrichment analysis on the 371 dynamic genes (p < 0.05, FC > 1.2), in response to at rest or after LPS exposure, relative to IMDM macrophages.







Kyoto Encyclopedia of Genes and Genomes (KEGG) pathway analysis showed enrichment in "cytokine-cytokine receptor interaction" and "Toll-like receptor signaling pathway," which again align with the functional hyperresponsive cytokine production after Toll-like receptor stimulation.

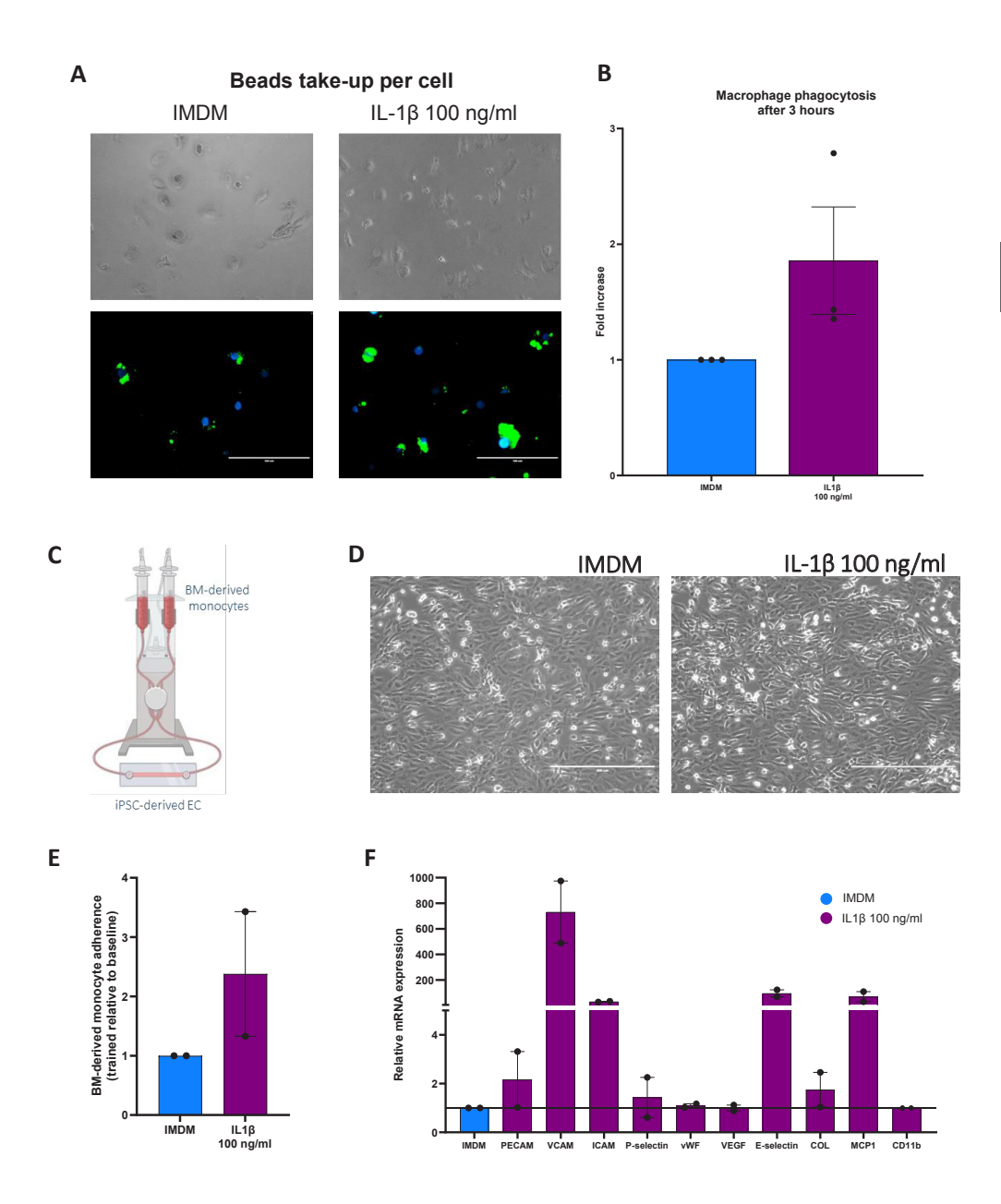
Exploratory studies of IL-1\beta on macrophage phagocytosis and **EC** interactions

To further characterize and determine the change in functionality of IL-1β-trained cells, we differentiated HPC-derived monocytes into macrophages and measured their phagocytic capacity after 3 h. As seen in Figure 4A, IL-1ß (100 ng/mL)-trained HPC-derived monocyte-derived macrophages have higher phagocytic capacity compared to untrained control. Phagocytosis was quantified by measuring the beads intake (green) overlayed with the presence of an existing cell (blue) (Figure 4B).

We subsequently assessed the interaction and adherence of HPC-derivedmonocytes to induced pluripotent stem cell (iPSC)-derived ECs in a continuous flow system (Figure 4C). After 3 h of flow, IL-1β-trained HPC-derived monocytes showed a higher adherence to ECs compared to untrained controls (Figures 4D and 4E). Subsequently, we measured the gene expression of various markers of endothelial and vascular dysfunction in the cells (iPSC-EC and attached HPC-derived monocytes) used in the system, and we observed that key genes such as vascular cell adhesion molecule, intercellular cell adhesion molecule, and E-selectin are upregulated after interaction with IL-1β-trained HPC-derived monocytes (Figure 4F).

As these experiments were only performed in two donors, we did not perform any statistical testing.

> Figure 4: IL-1β induces increased phagocytosis and a suggestively higher endothelial cell interaction with HPC-derived monocytes. (A) After 4 h of HPC exposure to IL-1β 100 ng/mL or untrained control, HPC-derived monocytes were differentiated into macrophages. After that, we added fluorescent Latex beads for 3 h and after washing made images with the EVOS microscope to measure phagocytosis capacity. Macrophages are visualized with 10× magnification, scale bar, 200 μm. (B) Phagocytosis rate quantification of IL-1 β -trained macrophages compared to untrained control (n = 3 independent HPC donors, Wilcoxon matched-pairs signed-rank test). (C) General overview of the IBIDI system to measure endothelial cell (EC)-monocyte interaction. (D) Visualization of HPC-derived monocytes attached to EC of IL-1 β -trained cells compared to the control (10× magnification, scale bar, 400 μ m). (E) Relative adherence of IL-1 β 100 ng/mL trained monocytes to EC relative to baseline (n = 2 independent HPC donors). (F) Relative mRNA expression of cell adhesion molecules and endothelial activation markers indicating various stages of leukocyte extravasation (n = 2 independent HPC donors).



Discussion

In this study, we aimed to test our hypothesis that brief exposure of human HPCs to IL-1β would lead to long-term pro-inflammatory effects by trained immunity, characterized by myeloid skewing and production of monocytes and macrophages with persistent pro-inflammatory characteristics. Indeed, after brief exposure of HPCs to IL-1β for only 4 h, there was an increased colony formation of GM colonies after 14 days. On a functional level, exposure to IL-1\beta augmented TNF and IL-1\beta secretion by HPC-derived monocytes upon restimulation with LPS and Pam3Cvs 17 days later, respectively, whereas the production of the anti-inflammatory cytokines IL-10 and IL-1Ra remains unaffected. This hyperresponsiveness was accompanied by a trend of increased glycolysis and oxidative phosphorylation.

Accumulating experimental evidence points to a central role of trained immunity in the pathophysiology of several diseases, including atherosclerosis (3). Mechanistically, IL-1ß signaling has been identified in experimental murine models as a key mechanism in the bone marrow niche, responsible for trained immunity triggered by β -glucan (7) as well as by Western diet (8). In human cells in vitro, Arts et al. previously described that 24 h exposure of human monocytes to 1 and 10 ng/mL of IL-1β induces trained immunity (15).

In patients with an acute myocardial infarction, plasma and bone marrow IL-1B concentrations rapidly increase (16, 17), which could be a trigger for the trained immunity that develops after myocardial infarction (18).

Based on these earlier studies, we hypothesized that also in human HPCs, brief exposure to IL-1β triggers trained immunity. Indeed, we observed that proinflammatory cytokine production, which is the major functional hallmark of trained immunity, is increased in HPC-derived monocytes after brief IL-1β exposure. RNA sequencing analysis of LPS-restimulated monocytes showed an enrichment in ferroptosis and apoptosis pathways, indicating processes which are critical in the development and progression of atherosclerotic plagues (19). For some parameters, including cytokine production, but not proliferation, the effect of IL-1β was stronger in 10 ng/mL than in 100 ng/mL. Interestingly, this dose dependency with lower concentration, giving rise to a stronger trained-immunity response, is not new. We have previously reported for both LPS and Pam3Cys (TLR2 agonist) that the trained immunity effect was stronger with lowering of the concentrations from 100 ng/mL to 0.1 pg/mL for LPS and from 100 µg/mL to 100 pg/mL for Pam3Cys (20).

We did not fully elucidate the mechanisms through which IL-1ß induced memory effects. In general, trained immunity is dependent on profound metabolic and epigenetic reprogramming (21). We previously showed that oxLDL- and β-glucan-trained cells are characterized by increased glycolysis and oxidative phosphorylation (2, 13). This fits with our current finding that monocytes derived from IL-1β-exposed HPCs present increased cell metabolism (glycolysis and oxidative phosphorylation), although this did not reach statistical significance due to limited sample size. Pathway analyses of differentially expressed genes in the IL-18-trained cells also showed enrichment in metabolism-related pathways, but these need further evaluation in future studies. Although we did not perform any epigenomic assays, we explored epigenetic genes among the list of IL-1β-induced dynamic genes and observed a slightly higher percentage of dynamic genes compared to all genes. Among these dynamic genes was TET2, which is involved in DNA demethylation. It is known that BCG-induced trained immunity is associated with changes in DNA methylation (22). In addition, it is known in experimental models that myeloid TET2 deficiency is associated with increased IL-1β production, and with enhanced atherosclerosis development (23). How exactly lower TET2 expression leads to the hyperresponsive trained phenotype needs further investigation. Lavillegrand et al. recently showed that high-fat diet-induced trained immunity developed in the bone marrow niche due to increased IL-1ß production by bone marrow granulocytes, which further stimulated myeloid skewing (24). It would be interesting to further investigate IL-1 β production by progenitor cells and their offspring cells in the bone marrow.

An unexpected finding was that in the trained cells, the protein concentrations on TNF and IL-1\(\beta\) in the supernatants after LPS stimulation were higher, in contrast to the mRNA of these proteins in the sequencing analysis. Interestingly, we had the same observation for training with β-glucan (25, 26). Specifically, despite observing increased TNF secretion in β-glucan and heme-trained macrophages, we did not find a difference in H3K27ac levels at the TNF promoter or increased TNF expression following restimulation in beta-glucan and heme-trained macrophages. One explanation is that the innate immune training signature in the trained macrophages involves the up-regulation of mechanisms resulting in cytokine release (e.g., lysosome maturation, Warburg effect) but not cytokine gene priming. This is in contrast to LPS-induced tolerance, which indeed attenuates both TNF secretion and RNA expression.

The main parameters in our study are proliferation and cytokine production capacity. In addition to that, we performed some exploratory studies on phagocytosis and on adhesion to iPSC-derived ECs, which are both key aspects of atherosclerosis pathophysiology We observed that training with IL-1β tends to increase monocyte attachment to iPSC-derived ECs. In addition, relative mRNA expression of key cell adhesion molecules was suggestively higher in the iPSC-derived ECs that encountered IL-1β-trained HPC-derived monocytes. These findings suggest that the monocytes that derive from trained HPCs can accelerate atherosclerosis formation by augmented attachment to ECs. These findings, however, are preliminary and need future validation, since we only performed these complex experiments for two donors, and therefore could not perform statistical testing.

After differentiation into macrophages within the arterial wall, phagocytosis is an important mechanism modulating further plaque growth, by foam cell formation and by engulfing necrotic neighboring cells in a process called efferocytosis (27). It appeared that macrophages derived from IL-1β-trained HPCs have more phagocytic capacity compared to untrained controls.

The strength of our study is that we performed a very extensive panel of functional, flow cytometric, and transcriptional parameters to characterize the monocytes and macrophages that derive from the HPCs. We show long-lasting and biologically relevant changes even after only 4 h of HPC exposure to IL-1\(\text{L}\). This strongly underscores the relevance of previous preclinical studies on IL-1β-induced trained immunity for the human situation. There are also some limitations to our study. First, all the experiments were performed in vitro in isolated HPCs. Even though we made use of cytokines and growth factor mimicking the bone marrow niche, there are some local niche factors that could alter cell function in vitro. Second, for some of the atherosclerosis-related functional characterization, we only performed experiments in two donors and only for one IL-1ß concentration, which precluded us from formal statistical testing. This makes the results obtained exploratory and would need additional experiments and higher donor number in future studies.

In conclusion, our results convincingly demonstrate that a brief exposure of human HPCs to IL-1 β induces trained immunity, which results in the formation of monocytes and macrophages with pro-inflammatory functions. These results strongly underscore the relevance of previous preclinical studies on IL-1β-induced trained immunity for the human situation and allow for the further use of this model to study trained immunity at the level of the bone marrow and to unravel mechanisms and potential therapeutics.

Experimental procedures

Human subjects

Bone marrow was aspirated from otherwise healthy patients undergoing orthopedic surgery and from healthy stem cell donors, which were between 30 and 48 years old. Exclusion criteria were use of immunosuppressants, recurrent infections, bone marrow malignancies/diseases, mental incapacitation, or previous radiation treatment. All donors provided written informed consent. The use of this material was approved by the Ethics Committee (Ethical Approval CMO Arnhem-Nijmegen, 2013/064) and all the experiments were performed according to the principles in the declaration of Helsinki.

Human bone-marrow-derived mononuclear cell isolation and cryopreservation

Bone marrow mononuclear cells (BM-MNCs) were isolated by density centrifugation using Ficoll-Plague PLUS (GE Healthcare Biosciences), followed by 3 washes with cold phosphate-buffered saline (PBS, Gibco). Mononuclear cells (MNCs) were cryopreserved in a freezing solution containing IMDM (Gibco), 1% penicillin/ streptomycin (p/s, Gibco), 250 IU/mL of sodium heparin (6006501), and 7% dimethyl sulfoxide for cell culture (DMSO, AppliChem, A3672-0250) and were stored in liquid nitrogen until further use.

Thawing of MNCs

Thawing of bone-marrow-derived MNCs was performed using DNase from bovine pancreas (Sigma) and magnesium chloride (MgCl., Sigma-Aldrich, M2393-100g). See supplementary methods for details.

CD34+ magnetic-activated cell sorting

BM-MNCs were centrifuged at 300G, 4°C for 10 min and the pellet was resuspended in 300 µL of magnetic-activated cell sorting (MACS) buffer containing PBS, pH 7.2, 0.5% sterile bovine serum albumin solution (BSA 30%, Merck, A9576-50ML), and 2 mM UltraPure EDTA (0.5 M, pH 8, Life Technologies). CD34+ HPCs were isolated from BM-MNC with MACS using a CD34 Microbead Kit according to the manufacturer's instructions (purity >95%, data not shown) (MACS, 130-046-702, Miltenyi Biotec). After separation, cells were resuspended in supplemented IMDM and viable cells were manually counted using the trypan blue exclusion method.

CD34+ cell stimulation with IL-1B

As shown in Figure 1A, HPCs were stimulated in a round-bottom 5 mL polystyrene Falcon tube (Corning, 352058) for 4 h with IMDM only as negative control and 10 and 100 ng/mL of IL-1β (R&D). After 4 h, the cells were spun down at 500 g for 10 min at room temperature, the supernatant containing the stimulus was removed, and the cells were resuspended in X-VIVO 10 serum-free hematopoietic cell medium (Lonza, BE04-380Q). Then, viable cells were manually counted using the trypan blue method.

Proliferation and differentiation assay CFU-GEMM

CFU assay for granulocyte, erythrocyte, monocyte, and megakaryocyte (CFU-GEMM) was performed by culturing 500 cells of previously stimulated HPCs or controls in methylcellulose medium (STEMCELL Technologies, GF H84435) in 35 mm polystyrene Petri dishes (Corning, 430165). The plates were seeded in duplicate and incubated for 14 days at 37°C and 5% CO₂. A CFU assay can derive colonies including blast forming unit erythrocyte (BFU-e), GM, and granulocyte/ erythrocyte/monocyte/megakaryocyte (GEMM). After 14 days, BFU-e, GM, and GEMM colonies were scored and counted using a gridded scoring plate in an inverted microscope using high-power focus (Leica DMi1) according to the manufacturer.

CD34+ cell expansion

A total of 5×10^4 previously stimulated or unstimulated HPCs were seeded per well in a flat-bottom 24-well plate (Sarstedt) and were expanded in X-VIVO 10 medium supplemented with 4% FCS, 1% p/s, human stem cell factor 50 ng/mL (SCF, 130-093-991, Miltenyi Biotec), human thrombopoietin 15 ng/mL (130-094-745, Miltenyi Biotec), human IL-3, 30 ng/mL (130-093-909, Miltenyi Biotec), human FMS-like tyrosine kinase 3 ligand 30 ng/mL (Flt-3L, 130-096-474, Miltenyi Biotec), and StemRegenin-1 aryl hydrocarbon receptor agonist 2 μM (#72342, Stem Cell Technologies). Medium was changed on day 3 and day 6 of proliferation. Cells were split at ~75%-80% confluence and re-seeded in a concentration of 5×10^4 cells per well, allowing them to be in culture for at least 2 days before ending the proliferation phase.

Cells were detached using warm Versene (Life Technologies) for 5 min and cold PBS + 2 mM EDTA washes. Cells were then centrifuged at 300G, 10 min at 4°C, and resuspended in IMDM + 1% p/s. Viable cells were counted using the trypan blue exclusion method.

CD34+ cell differentiation into monocytes

After 10 days of expansion, cells were differentiated into monocytes for 7 days using IMDM medium supplemented with 10% FCS, 1% p/s, SCF 25 ng/mL, human macrophage colony stimulating factor 30 ng/mL (M-CSF, 130-096-491, Miltenyi Biotec), IL-3 30 ng/mL, and Flt-3L 30 ng/mL. Medium was changed on day 3 of differentiation. Cells were detached using warm Versene for 5 min and cold PBS + 2 mM EDTA washes. Cells were then centrifuged at 300G, 10 min at 4°C, and resuspended in IMDM + 1% p/s. Viable cells were counted using the trypan blue exclusion method.

Differentiation was continued for part of the cells for 13 more days to increase the number of cells, using supplemented IMDM as mentioned before. After 20 days of differentiation in total, cells were detached and used for IBIDI flow experiments, macrophage differentiation, macrophage polarization, and phagocytosis.

Flow cytometry

Flow cytometry was performed at several time points (Figure 1C): during expansion of HPCs and their differentiation into monocytes. During expansion, stem cell markers relevant to progenitor populations were measured at day 0, 6, and 10. Cells were stained with monoclonal antibodies cluster of differentiation (CD)117, CD19, CD38, CD10, CD45RA, CD34, CD123, CD45, CD90, and live/dead stain FVS700 (Table S1). After staining, markers were measured on a CytoFlex cytometer (Beckman Coulter, Brea, USA, RRID: SCR 017217). Gating strategy is shown in Figure S2 and described in supplementary methods, where gates were determined by fluorescence minus one (FMO) method (28).

During differentiation, flow cytometry was performed at day 10 and 17 of culture (day 0 and 7 of differentiation, Figure 1B), Differentiated cells were stained with monoclonal antibodies CD16, HLA-DR, CD10, CD14, CCR2, CD45, CD11b, CD66b, CD15, and live/dead stain FVS620 (Table S2). Gating strategy is shown in Figure S3 and described in supplementary methods, where gates were determined by FMO method as previously mentioned. Samples were analyzed with FlowJo v10.8 Software (BD Life Sciences).

HPC-derived monocyte restimulation

After 7 days of differentiation, HPC-derived monocytes were diluted to a concentration of 500,000 cells/mL. A total of 50,000 cells were plated in flat-bottom 96-well plates (Sarstedt) and were stimulated in duplo with LPS 10 ng/mL (Sigma-Aldrich, Dt. Louis, MO; E. coli serotype 055:B5) further purified as described (29), and Pam3Cys 10 µg/mL (EMC microcollections, Tübingen, Germany; L2000) for 24 h at 37°C with 5% CO₃. After 24 h, the plate was centrifuged, and supernatant was collected and stored at -20°C until further use. Cytokine assessment of stimulated cells was done using commercial ELISA kits for TNF (DY210), IL-6 (DY201), IL-1B (DY201-05), IL-10 (DY217B), and IL-1RA (DY280) according to the manufacturer (R&D Systems).

Metabolic analysis (Seahorse)

In a previously hydrated and calibrated cartridge, 100,000 HPC-derived monocytes were plated in quintuplets in Seahorse assay medium (Dulbecco's modified Eagle's medium [Sigma] supplemented with 200 mM L-glutamine [Sigma] and 100 mM pyruvate [Sigma]) and incubated for 1 h at 37°C in a non-CO₃ incubator.

OCR was measured in a XFp Analyzer (Seahorse, Bioscience) in Seahorse medium supplemented with sodium pyruvate 1 mM (Life Technologies), L-glutamine 2 mM (Sigma), and D-glucose 11 mM (Sigma), using a Cell Mito Stress Test Kit (see supplementary methods).

Pan monocyte MACS isolation

HPC-derived monocytes were isolated after 7 days of differentiation using MACS using a pan monocyte kit according to the manufacturer (MACS, Miltenyi Biotec). After separation, cells were resuspended in IMDM medium + 1% p/s and counted in a CASY Counter.

RNA isolation for RNA sequencing

After pan monocyte magnetic separation, a total of 5×10^5 cells were transferred to a round-bottom 5 mL polystyrene Falcon tube and were stimulated for 4 h at 37°C, 5% CO₃ with IMDM only as negative control or LPS 10 ng/mL. After incubation, the cell suspension was centrifuged at 3,420 g, 4°C for 5 min. Pellet was resuspended in RLT buffer, snap-frozen in liquid nitrogen, and stored at -80°C. RNA was isolated using the RNeasy Micro Kit (QIAGEN) according to the manufacturer's instructions.

RNA sequencing analysis

RNA quality control was performed using the Bioanalyzer Agilent 2100. Isolated RNA was sent for next-generation sequencing on the DNBSeq 400 platform (BGI Solutions, Hong Kong). Libraries were prepared using the Illumina TruSeg Stranded mRNA kit with a starting input of 100 ng (where available) and sequenced, with the generation of approximately 20 million 100-bp paired-end reads per sample. To infer gene expression levels, RNA sequencing reads were aligned to hg19 human transcriptome using Bowtie2 (30). Quantification of gene expression, as reads per transcript, was performed using Htseq (31), and counts per million (CPM) were calculated. Statistical analysis was performed using DESeg2, with pairwise comparisons performed between IMDM and IL-1\u00ed groups. Differentially expressed genes were identified as those showing p value < 0.05, FC > 1.5, and CPM >1. Differential gene lists from all comparisons were then merged, and the combined list of differential genes was used for plotting.

IBIDI flow experiments

IBIDI flow experiments were performed to study EC-monocyte interaction. See supplementary methods for detailed protocol.

RNA isolation, cDNA synthesis, and qPCR for IBIDI flow experiments

RNA purification of iPSC-derived ECs that encountered HPC-derived monocytes was performed using TriPure (Roche, 11667157001) according to the manufacturer. cDNA was obtained by synthesis using gScript cDNA synthesis kit (QuantaBio 95047-100). Quantitative PCR was done using SYBR green and relevant primers as seen in Table S3 (Integrated DNA Technologies, IDT) in a CFX96 Touch Real-Time PCR (Bio-Rad). For a detailed protocol, see supplementary methods.

Macrophage differentiation and polarization

At day 20, differentiation and polarization of HPC-derived monocyte-derived macrophages was performed in Roswell Park Memorial Institute 1640 medium (RPMI) supplemented with M-CSF 50 ng/mL (PeproTech, 300-25) for 4 days followed by 3 more days RPMI supplemented with interferon-y (PeproTech, P01579.1), 50 ng/mL and LPS 10 ng/mL (PeproTech, 297-473-0) for M1 macrophages, and IL-4 10 ng/mL (PeproTech, 130-093-924) for M2 macrophages. Cells were incubated at 37°C, CO₂ 5%.

Phagocytosis and quantification

After macrophage differentiation and polarization, a phagocytosis assay was performed according to the manufacturer (Cayman Chemical, 500209), where latex beads (rabbit IgG FITC complexes, green) were added to the macrophage culture for 3 h. Cell nuclei were stained with Hoechst 33342 (1:10,000 in PBS, blue) and dead cells were stained using 4 µM ethidium homodimer-1 (Invitrogen L3224B, red). Phagocytosis rate was quantified as described in supplementary methods.

Statistical analysis

The experiments present in this article were done using 4 to 6 independent HPC donors (n = 4-6). The exact n used is mentioned in detail in the figure legends. Each experiment was performed in duplicate for each independent donor and all the data present in this article are shown as mean \pm standard error of the mean. A two-sided value of p \leq 0.05 was considered statistically significant. Statistical analysis was performed using GraphPad Prism version 10.0 (La Jolla, CA, USA). Normality was assessed using Shapiro-Wilk test. Data did not follow a normal distribution; hence, all tests performed were non-parametric unless indicated otherwise per section. For the functional assays of phagocytosis and endothelial cell interactions, we did not perform statistical analysis as this was done only in 2 independent donors.

Resource availability

Lead contact

Further information and requests for resources and reagents should be directed to and will be fulfilled by the lead contact, Niels P. Riksen (niels.riksen@radboudumc.nl).

Materials availability

No new reagents were generated for this article.

Data and code availability

The accession number for the RNA-seq data reported in this paper is GEO: GSE253764.

Acknowledgements

We would like to thank Daniek Kapteijn for helping with IBIDI experiments and Benjamin Cossins for helping with the quantification of the phagocytosis assay. L.A.B.J., M.G.N., and N.P.R. were supported by a CVON grant from the Dutch Heart Foundation and Dutch Cardiovascular Alliance (CVON2018-27). N.P.R. was further supported by a grant of the ERA-CVD Joint Transnational Call 2018, which is supported by the Dutch Heart Foundation in the Hague (JTC2018, project MEMORY; 2018T093). N.P.R. and M.G.N. were supported by a Project Program Grant of the NHLBI (Project 15-0893 and NIH/NHLBI P01HL131478). S.B. was supported by the Dutch Heart Foundation in the Hague (Dekker grant 2018-T028). M.G.N. was supported by a European Research Council (ERC) Advanced Grant (FP/2007-2013/ERC grant 2012-322698) and a Spinoza Prize (NWO SPI 92-266). E.L.K. was supported by the Netherlands Heart Institute (Fellowship #282) and E.L.K. and N.P.R. by the Netherlands Heart Institute (IMPRESS). B.N. is supported by an NHMRC (Australia) Investigator Grant (GNT1173314). The figures were created with BioRender.com.

Author contributions

D.F.-G., S.B., W.H., D.v.E., and N.P.R. were responsible for conceptualization of the study. W.H., D.v.E., N.P.M.S., and W.H.C.R. collected and resourced the bone marrow material. D.F.-G., S.B., and E.L.K. performed the investigation (experiments). Data curation and formal analysis was performed by D.F.-G., S.B., E.L.K., and B.N. Project oversight and supervision was done by S.B., N.P.R., M.G.N., and L.A.B.J. D.F.-G. and S.B. wrote the original draft manuscript, which was afterward reviewed and edited by all the co-authors.

Declaration of interests

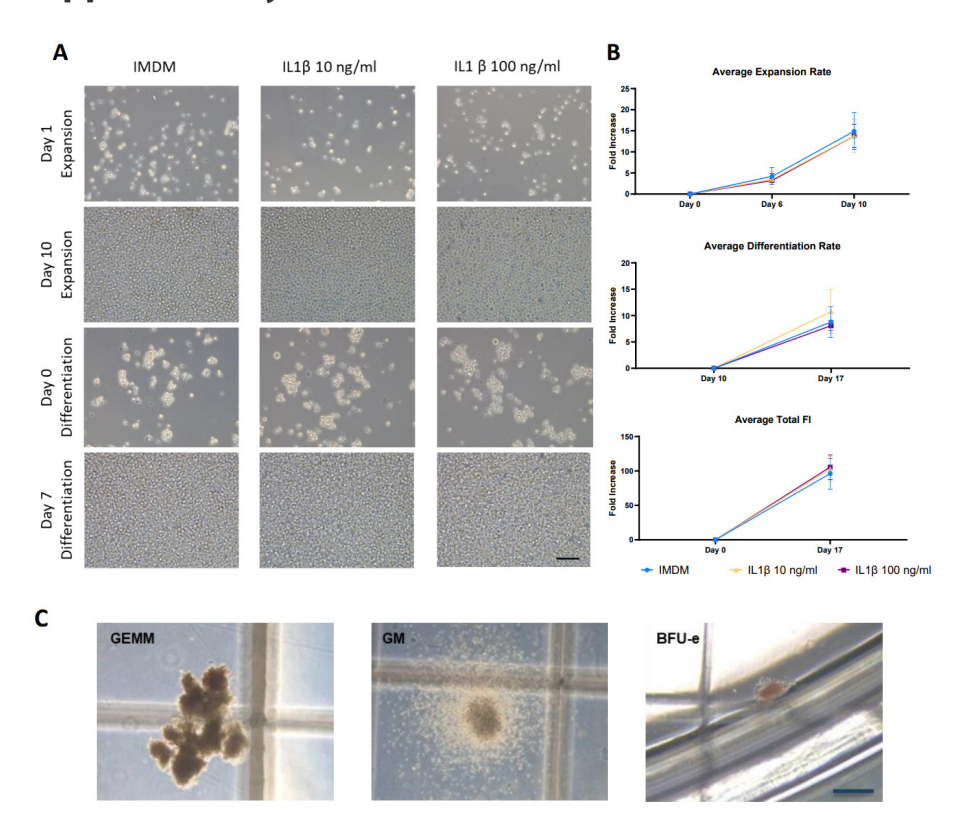
M.G.N. and L.A.B.J. are scientific founders of TTxD and Lemba TX. M.G.N. is scientific founder of Biotrip. W.H.C.R. is a consultant for Stryker for educational purposes only.

References

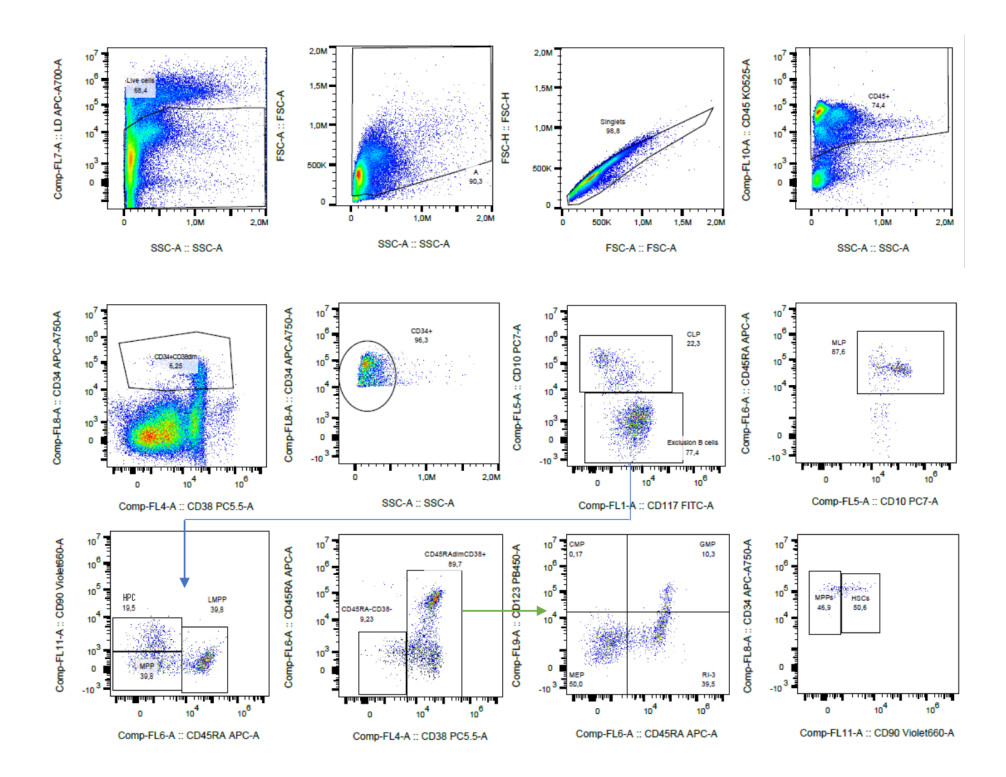
- 1. Bekkering S, Domínguez-Andrés J, Joosten LAB, Riksen NP, Netea MG. Trained Immunity: Reprogramming Innate Immunity in Health and Disease. Annu Rev Immunol. 2021;39:667-93.
- Domínguez-Andrés J, Dos Santos JC, Bekkering S, Mulder WJM, van der Meer JWM, Riksen NP, et al. Trained immunity: adaptation within innate immune mechanisms. Physiol Rev. 2023;103(1):313-46.
- 3. Riksen NP, Bekkering S, Mulder WJM, Netea MG. Trained immunity in atherosclerotic cardiovascular disease. Nature Reviews Cardiology. 2023;20(12):799-811.
- 4. Kleinnijenhuis J, Quintin J, Preijers F, Benn CS, Joosten LA, Jacobs C, et al. Long-lasting effects of BCG vaccination on both heterologous Th1/Th17 responses and innate trained immunity. J Innate Immun. 2014;6(2):152-8.
- 5. Kaufmann E, Sanz J, Dunn JL, Khan N, Mendonça LE, Pacis A, et al. BCG Educates Hematopoietic Stem Cells to Generate Protective Innate Immunity against Tuberculosis. Cell. 2018;172(1-2):176-90.e19.
- 6. Cirovic B, de Bree LCJ, Groh L, Blok BA, Chan J, van der Velden W, et al. BCG Vaccination in Humans Elicits Trained Immunity via the Hematopoietic Progenitor Compartment. Cell Host Microbe. 2020;28(2):322-34.e5.
- 7. Mitroulis I, Ruppova K, Wang B, Chen LS, Grzybek M, Grinenko T, et al. Modulation of Myelopoiesis Progenitors Is an Integral Component of Trained Immunity. Cell. 2018;172(1-2):147-61.e12.
- 8. Christ A, Günther P, Lauterbach MAR, Duewell P, Biswas D, Pelka K, et al. Western Diet Triggers NLRP3-Dependent Innate Immune Reprogramming. Cell. 2018;172(1-2):162-75.e14.
- Noz MP, Bekkering S, Groh L, Nielen TM, Lamfers EJ, Schlitzer A, et al. Reprogramming of bone marrow myeloid progenitor cells in patients with severe coronary artery disease. Elife. 2020;9.
- 10. Stiekema LCA, Willemsen L, Kaiser Y, Prange KHM, Wareham NJ, Boekholdt SM, et al. Impact of cholesterol on proinflammatory monocyte production by the bone marrow. Eur Heart J. 2021;42(42):4309-20.
- 11. Ridker PM, Everett BM, Thuren T, MacFadyen JG, Chang WH, Ballantyne C, et al. Antiinflammatory Therapy with Canakinumab for Atherosclerotic Disease. N Engl J Med. 2017;377(12):1119-31.
- 12. Ruder AV, Wetzels SMW, Temmerman L, Biessen EAL, Goossens P. Monocyte heterogeneity in cardiovascular disease. Cardiovasc Res. 2023;119(11):2033-45.
- 13. Tercan H, Riksen NP, Joosten LAB, Netea MG, Bekkering S. Trained Immunity. Arteriosclerosis, Thrombosis, and Vascular Biology. 2021;41(1):55-61.
- 14. Medvedeva YA, Lennartsson A, Ehsani R, Kulakovskiy IV, Vorontsov IE, Panahandeh P, et al. EpiFactors: a comprehensive database of human epigenetic factors and complexes. Database (Oxford). 2015;2015:bav067.
- 15. Arts RJW, Moorlag S, Novakovic B, Li Y, Wang SY, Oosting M, et al. BCG Vaccination Protects against Experimental Viral Infection in Humans through the Induction of Cytokines Associated with Trained Immunity. Cell Host Microbe. 2018;23(1):89-100.e5.
- 16. Guillén I, Blanes M, Gómez-Lechón MJ, Castell JV. Cytokine signaling during myocardial infarction: sequential appearance of IL-1 beta and IL-6. Am J Physiol. 1995;269(2 Pt 2):R229-35.
- 17. Sreejit G, Nooti SK, Jaggers RM, Athmanathan B, Ho Park K, Al-Sharea A, et al. Retention of the NLRP3 Inflammasome-Primed Neutrophils in the Bone Marrow Is Essential for Myocardial Infarction-Induced Granulopoiesis. Circulation. 2022;145(1):31-44.
- 18. Dong Z, Hou L, Luo W, Pan L-H, Li X, Tan H-P, et al. Myocardial infarction drives trained immunity of monocytes, accelerating atherosclerosis. European Heart Journal. 2024;45(9):669-84.

- 19. Ouyang S, You J, Zhi C, Li P, Lin X, Tan X, et al. Ferroptosis: the potential value target in atherosclerosis. Cell Death Dis. 2021;12(8):782.
- 20. Ifrim DC, Quintin J, Joosten LA, Jacobs C, Jansen T, Jacobs L, et al. Trained immunity or tolerance: opposing functional programs induced in human monocytes after engagement of various pattern recognition receptors. Clin Vaccine Immunol. 2014;21(4):534-45.
- 21. Fanucchi S, Domínguez-Andrés J, Joosten LAB, Netea MG, Mhlanga MM. The Intersection of Epigenetics and Metabolism in Trained Immunity. Immunity. 2021;54(1):32-43.
- 22. Bannister S, Kim B, Domínguez-Andrés J, Kilic G, Ansell BRE, Neeland MR, et al. Neonatal BCG vaccination is associated with a long-term DNA methylation signature in circulating monocytes. Sci Adv. 2022;8(31):eabn4002.
- 23. Fuster JJ, MacLauchlan S, Zuriaga MA, Polackal MN, Ostriker AC, Chakraborty R, et al. Clonal hematopoiesis associated with TET2 deficiency accelerates atherosclerosis development in mice. Science. 2017;355(6327):842-7.
- 24. Lavillegrand J-R, Al-Rifai R, Thietart S, Guyon T, Vandestienne M, Cohen R, et al. Alternating highfat diet enhances atherosclerosis by neutrophil reprogramming. Nature. 2024;634(8033):447-56.
- 25. Jentho E, Ruiz-Moreno C, Novakovic B, Kourtzelis I, Megchelenbrink WL, Martins R, et al. Trained innate immunity, long-lasting epigenetic modulation, and skewed myelopoiesis by heme. Proc Natl Acad Sci U S A. 2021;118(42).
- 26. Novakovic B, Habibi E, Wang SY, Arts RJW, Davar R, Megchelenbrink W, et al. β-Glucan Reverses the Epigenetic State of LPS-Induced Immunological Tolerance. Cell. 2016;167(5):1354-68.e14.
- 27. Kojima Y, Weissman IL, Leeper NJ. The Role of Efferocytosis in Atherosclerosis. Circulation. 2017;135(5):476-89.
- 28. Feher K, Kirsch J, Radbruch A, Chang HD, Kaiser T. Cell population identification using fluorescence-minus-one controls with a one-class classifying algorithm. Bioinformatics. 2014:30(23):3372-8.
- 29. Hirschfeld M, Ma Y, Weis JH, Vogel SN, Weis JJ. Cutting edge: repurification of lipopolysaccharide eliminates signaling through both human and murine toll-like receptor 2. J Immunol. 2000:165(2):618-22.
- 30. Langmead B, Salzberg SL. Fast gapped-read alignment with Bowtie 2. Nat Methods. 2012;9(4):357-9.
- 31. Anders S, Pyl PT, Huber W. HTSeq--a Python framework to work with high-throughput sequencing data. Bioinformatics. 2015;31(2):166-9.
- 32. Thomas GD, Hamers AAJ, Nakao C, Marcovecchio P, Taylor AM, McSkimming C, et al. Human Blood Monocyte Subsets: A New Gating Strategy Defined Using Cell Surface Markers Identified by Mass Cytometry. Arterioscler Thromb Vasc Biol. 2017;37(8):1548-58.

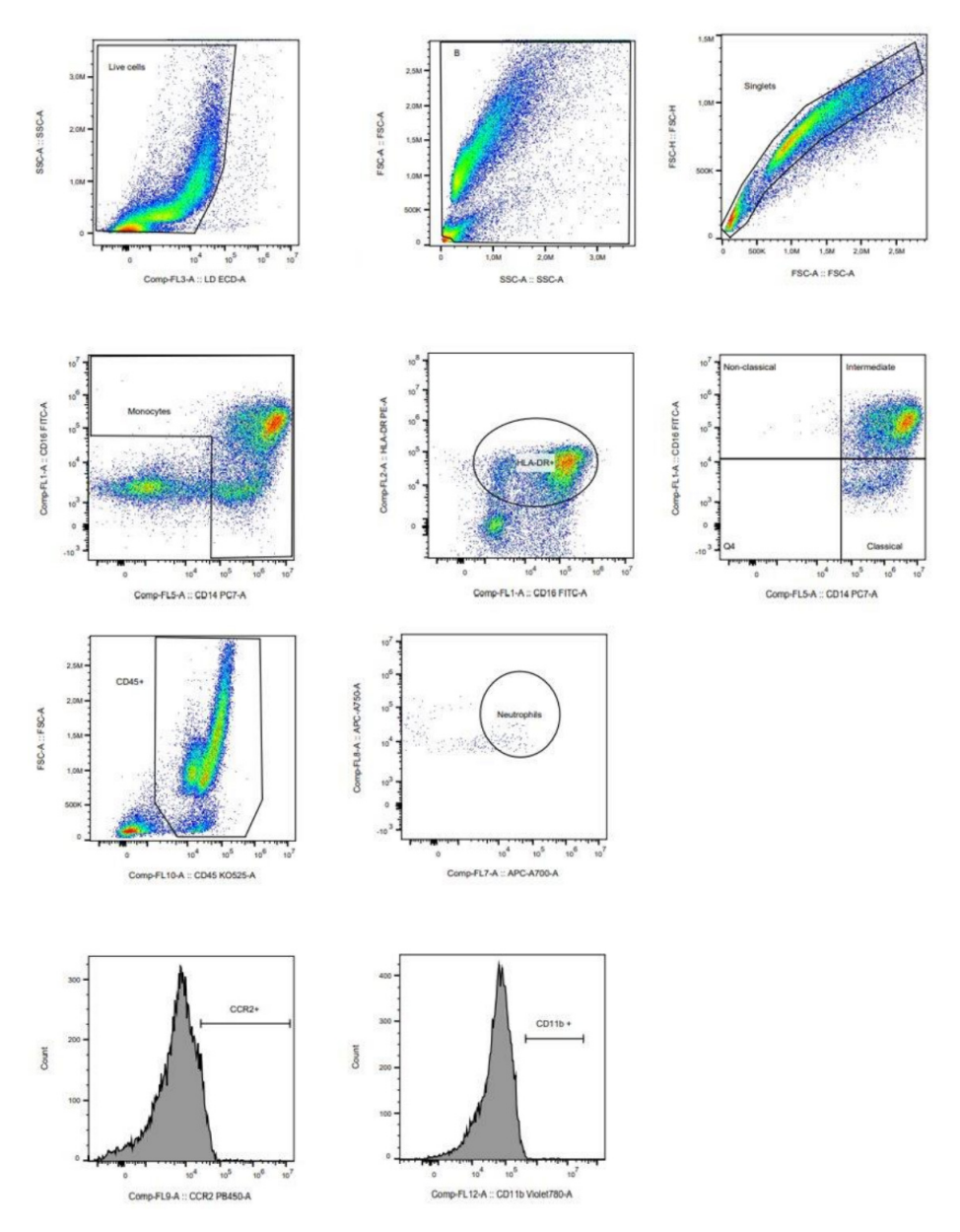
Supplementary Material



Supplementary Figure 1: A) Morphology of HPCs-derived hematopoietic progenitor cells during expansion from day 1 to day 10. At day 10 of expansion, cells were differentiated into monocytes for 7 days with M-CSF (20x magnification, scale bar = 2000 μ m). B) Average expansion, differentiation and total fold increase during the cell culture time (17 days in total, n=6 independent HPCs donors). C) Morphology of HPCs-derived hematopoietic progenitor cells during expansion from day 1 to day 10. At day 10 of expansion, cells were differentiated into monocytes for 7 days with M-CSF (20x magnification, scale bar = 2000 μ m).



Supplementary Figure 2: Gating strategy of stem cell progenitor populations from human bone marrow. Leukocytes were defined as CD45+ cells, after previous exclusion of dead cells, debris and doublets. Stem cells were defined as CD34+CD38dim. Then, the lymphoid line was identified using CD117+CD10+. Next, the non-lymphoid cells were identified using CD117+CD10- where LMPP, MPP and HPC were identified using CD90 and CD45RA. Lastly, in CD45RAdimCD38+ cells, CMP, GMP, R1-3 and MEP were identified using CD45RA and CD123. See table in Figure 3 for additional details. Populations were selected using the fluorescence minus one method (FMO) and side scatter properties.



Supplementary Figure 3: Gating strategy to identify HPCs-derived monocytes. Leukocytes were defined as CD45+ cells, after previous exclusion of dead cells, debris and doublets. Neutrophils were identified from CD45+ cells using CD66b and CD15. To identify monocytes, CD14 and CD16 markers were used from CD45+, where only HLA-DR+ cells were selected for identification of monocytes subsets. Subsets were defined with CD14 and CD16 as follows: classical (CD14++CD16-), intermediate CD14++CD16+) and non-classical (CD14+CD16++). CCR2 and CD11b markers were also identified from monocytes and its subsets. Populations were selected using the fluorescence minus one method (FMO) and side scatter properties.

Supplementary Table 1. Flow cytometry panel used to identify stem cell progenitor populations. Abbreviations: Cluster of differentiation (CD, fluorescein isothiocyanate (FITC), phycoerythrin-Texas Red conjugate/electron coupled dye (ECD), peridin chlorophyll protein complex (PerCP), phycoerythrin (PE), allophycocyanin (APC).

Marker	Fluorochrome	Clone	Manufacturer	Cat #	RRID#
CD117	FITC	104D2	Biolegend	313231	AB_2566218
CD19	ECD	J3-119	Beckman Coulter	A07770	AB_2940901
CD38	PerCP/Cyanine 5.5 (PC5.5)	HIT2	Biolegend	356613	AB_2562182
CD10	PE/Cyanine 7 (PC7)	HI10A	Biolegend	312213	AB_2146549
CD45RA	APC	HI100	Biolegend	304112	AB_314416
CD34	APC/Fire 750 (APC-A750)	581	Biolegend	343536	AB_2650736
CD123	Brilliant violet 421 (BV421)	6H6	Biolegend	306017	AB_10900244
CD45	Brilliant violet 510 (BV510)	HI30	Biolegend	304036	AB_2561383
CD90	Brilliant violet 650 (BV650)	5E10	Biolegend	328143	AB_2734319

Supplementary Table 2. Flowcytometry panel used to identify neutrophils, monocyte subsets and monocyte activation markers.

Marker Fluorochrome		Clone	Manufacturer	Cat #	RRID#
CD16	FITC	3g8	Biolegend	302006	AB_314206
HLA-DR	PE	immu-357	Beckman Coulter	IM1639	AB_131284
CD10	PC5.5	HI10	Biolegend	312215	AB_ 10643591
CD14	PC7	61D3	LifeTechnologies	25-0149-42	AB_1582276
CC192 (CCR2)	BV421	48607	BD Biosciences	564067	AB_2738573
CD45	BV510	HI30	Biolegend	304036	AB_2561940
CD11b	BV785	ICRF44	Biolegend	301346	AB_2563794
CD66b	APC-700	G10F5	Biolegend	305114	AB_2566038
CD15	APC-Cy7	W6D3	Biolegend	323047	AB_2750189

Abbreviations: Cluster of differentiation (CD), fluorescein isothiocyanate (FITC), phycoerythrin (PE), peridin chlorophyll protein complex (PerCP), allophycocyanin (APC).

Supplementary Table 3. Overview of the primers used. All the primers were ordered from IDT.

Gene	Protein	Primer name	Primer sequence '5 \rightarrow 3'
GAPDH	GAPDH	GAPDH Forward	ACACTCACTCTTCTACCTTTG
		GAPDH Reverse	CAAATTCATTGTCGTACCAG
βactin	β actin	β actin Forward	GATCGGCHHCTCCATCCTG
		β actin Reverse	GACTCGTCATACTCCTGCTTGC
CD31	PECAM	CD31 Forward	CATGCAATGAAACCAATAAATGAT
		CD31 Reverse	GAGCCTTCCGTTCTAGAGTATCTG
VCAM1	CD106	VCAM Forward	CATGCAATGAAACCAATAAATGAT
		VCAM Reverse	GAGCCTTCCGTTCTAGAGTATCTG
ICAM1	CD54	ICAM Forward	TTGAACCCCACAGTCACCTAT
		ICAM Reverse	CCTCTGGCTTCGTCAGAATCA
SELP	P-selectin	P-selectin Forward	TGAGCACTGCTTGAAGAAAAAGC
		P-selectin Reverse	CACGTATTCACATTCTGGCCC
SELE	E-selectin	E-selectin Forward	GGCAGTGGACACAGCAAATC
		E-selectin Reverse	TGGACAGCATCGCATCTCA
VEGFA	VEGFA	VEGF Forward	TGCTGTCTTGGGTGCATTGG
		VEGF Reverse	GCATAATCTGCATGGTGATGTTGG
COL1A1	Collagen 1	Collagen Forward	ATCAACCGGAGGAATTTCCGT
		Collagen Reverse	CACCAGGACGACCAGGTTTTC
vWF	vWF	vWF Forward	AGCCTTGTGAAACTGAAGCAT
		vWF Reverse	GCCCTGGTTGCCATTGTAATTC
CCL2	MCP1	MCP1 Forward	GATCGGAACCAAATGAGATCAG
		MCP1 Reverse	GTGGAAAAGGTAGTGGATGC
CD11b	ITGAM	CD11b Forward	ACTTGCAGTGAGAACACGTATG
		CD11b Reverse	TCATCCGCCGAAAGTCATGTG

Abbreviations: Glyceraldehyde 3-phosphate dehydrogenase (GAPDH), cluster of differentiation (CD), vascular cell adhesion protein-1 (VCAM1), intercellular cell adhesion protein-1 (ICAM1), vascular endothelial growth factor A (VEGFA), von Willebrand factor (vWF) and chemokine ligand 2 (CCL2).

Supplementary Experimental Procedures

Thawing of MNCs

Per cryovial of cells, a mix of thawing medium containing 1.4 ml heat-inactivated fetal calf serum (FCS, Hyclone Cytiva), 25mM MgCl₃ and 66 µg/ml of DNAse (10 mg/ml or 2000 U/mg) was prepared. Cells were taken from liquid nitrogen storage and put in a water bath at 37°C until a small clump of ice was still visible. Cells were transferred to the tube with thawing medium, mixed gently, and incubated for 10 minutes at room temperature. Cells were washed with room temperature PBS and centrifuged for 5 minutes at 500G. Cells were resuspended in IMDM medium and counted in a CASY cell counter (Omni Life Science, OLS).

Flow cytometry

To identify progenitor population, HPCs were selected based on CD45+-CD34+CD38dim after filtering for live cells and singlets. Then, cells from the lymphoid lineage (progenitor B cells) were excluded using CD10-CD117+. Next, CMP, GMP, R1-3 (pre-monocytes), and MEP were identified after gating for CD45RAdimCD38+ using the CD123 and CD45RA markers. Lastly, HPC, LMPP, and MPP were identified from the B cell exclusion using CD90 and CD45RA markers.

To identify bone marrow-derived monocytes, neutrophils were identified based on CD45+CD66b+CD15+ after filtering for live cells and singlets. Next, monocytes were identified based on CD45+HLA-DR+ and side scatter properties. Monocyte subsets were determined using CD14/CD16 as percentage of gated (HLA-DR/ CD16). CD11b and C-C chemokine receptor type 2 (CCR2) activation markers were identified in the total monocytes and their subsets by counting the positive signal of the marker based on the FMO. Monocyte subsets were identified according to current recommendations (32).

Metabolic analysis (Seahorse)

First, oligomycin A 1 µM (Sigma) was injected following the basal measurements to inhibit ATP synthase and induce a decrease in electron flow and respiration (ATPlinked respiration and proton leak). Then, carbonyl cyanide-4 (trifluoromethoxy) phenylhydrazone 1 µM (FCCP, Sigma) was injected to cause a collapse in the proton gradient and alter the mitochondrial membrane potential causing respiration to reach its maximum level (maximal respirator capacity). Lastly, an injection containing antimycin A 2.5 µM (Sigma) and rotenone 1.25 µM (Sigma) is done to shut down mitochondrial respiration and measure respiratory activity outside the mitochondria (reserve capacity).

Extracellular acidification rate (ECAR) was measured in a XFp Analyzer in Seahorse medium supplemented with L-Glutamine 1 mM (Sigma), using a Glyco Stress Test Kit. First, D-Glucose 11 mM is injected to induce the glycolytic pathway under basal conditions (basal glycolysis). Then, oligomycin A 1 μ M inhibitor is injected as an ATP synthase inhibitor to switch cellular respiration to glycolysis and measure the cell maximum glycolytic capacity. Lastly, a final injection with 2-deoxy-D-glucose (2-DG, Sigma) 22 mM is performed to inhibit glycolysis resulting.

Interpretation and analysis of Seahorse results was performed for ECAR and OCR measurements according to the guide of Glycolysis and MitoStress Test Kit from the manufacturer (Agilent Seahorse XF).

IBIDI Flow Experiments

A monolayer of iPSC-derived endothelial cells (ECs) was seeded in 0.4 μ m IBIDI u-slide (IBIDI 80186) for 2 hours. Then the slide was attached to a pump system (9.3 mbar of pressure, 3 dyn of shear stress, 4.99 ml/min of flow rate, 300/1s of shear rate, 20 s unidirectional and 0.5 s oscillation) for perfusion during 2 hours at 37°C, 5% CO_2 . After these 4h, medium was changed to starvation medium containing iPSC-EC medium (Promocell C22110), 0.5% FBS, p/s, and SP431542 (Selleckchem S1067). 20-day differentiated control or 100 ng/ml IL-1 β -trained HPC-derived monocytes were added to the perfusion system and flowed through the slide for 2 hours. At the end of the assay, pictures of the slide were taken with an EVOS microscope and adhered monocytes were manually counted by 2 different people. Before the counting, a consensus was reached between the two researchers on the considerations to determine a cell an adhered monocyte or not. The counting was done blinded in at least 3 pictures of the slide. Lastly, iPSCs-derived ECs in the slide were collected and stored in TriZol at -80°C until further use.

RNA isolation, cDNA synthesis, and gPCR for IBIDI flow experiments

RNA purification of iPSCs-derived ECs that encountered HPCs-derived monocytes was performed using TriPure (Roche, 11667157001) and chloroform (Sigma Aldrich 32211-1L-1M) followed by precipitation of RNA with isopropanol (Sigma Aldrich 33539-2.51-M). Isolated RNA was then dissolved in nuclease-free water (Integrated DNA Technologies (IDT) 11-05-01-14) and concentration was measured in Xpose (Trinean, Belgium).

cDNA was obtained by synthesis using qScript cDNA synthesis kit (QuantaBio 95047-100). Quantitative PCR (qPCR) was done using SYBR green and relevant primers as seen in Supplementary Table 3 (Integrated DNA Technologies, IDT) in a CFX96 Touch

Real-Time PCR (BioRad). The protocol used consisted of incubation for 3 minutes at 95C, followed by 40 cycles of 10 seconds at 95°C, then 30 seconds at 60°C and lastly 10 seconds at 95°C. Single-product amplification was confirmed using a melting curve analysis. Expression of mRNA was normalized for the geometric mean of the expression of the housekeeping genes human β-actin (ACT2) and glyceraldehyde 3-phosphate dehydrogenase (GAPDH) (Δ CT). Then, relative differences (Δ Δ CT) were calculated, and data was used as normalized fold induction ($2^{\Delta}\Delta CT$).

Phagocytosis and quantification

Phagocytosis rate was quantified using R 4.2.2 (EBImage package 4.40.0). In short, green, blue, and red channels were brought to a grey scale which was brightened. Then, clusters were separated from the background with adaptive thresholding which were then measure in number of pixels identifying single cells, multiple cells, or debris. The thresholds to calculate single and multiple cells were based on equivalent pixel size of monocytes and macrophages (8 and 10 µm). Clusters were then used to identify green, blue, and red regions and its mean fluorescence. Bead uptake was then calculated based in the overlay of blue and green color.



Chapter 5

Phenotypic and functional comparison between bone marrow-derived and induced pluripotent stem cell-derived monocytes and primary circulating human monocytes

Daniela Flores Gomez,* Elise L. Kessler,* Siroon Bekkering, Laszlo Groh, Ben Cossins, Daniek Kapteijn, Emile van Vliet, Willemijn Hobo, Nicolaas Schaap, Wim H.C. Rijnen, Boris Novakovic, Joost P.G. Sluijter, Mihai G. Netea, Saskia C.A. de Jager, Niels P. Riksen

In preparation

^{*} These authors contributed equally to this work

Abstract

In vitro studies on monocyte or macrophage-associated diseases often use human circulating monocytes, which exhibit variability due to genetic differences and experimental methods, and have limited lifespan. Induced pluripotent stem cell (iPSC)-derived monocytes offer prolonged availability and less heterogeneity. Bone marrow (BM)-derived monocytes are used to investigate how manipulation of bone marrow progenitors affect monocyte phenotype. However, to date, similarities and differences between BM- and iPSC-derived monocytes and primary circulating monocytes have not been investigated in detail. This study compares human circulating monocytes and macrophages to iPSC- and BM-derived monocytes and macrophages. We isolated human circulating monocytes from healthy donors, generated iPSC-derived monocytes from iPSCs, and differentiated monocytes derived from BM mononuclear cells. We studied morphology, monocyte subsets, functionality, metabolic pathways, gene expression, gene accessibility, and polarization towards macrophages.

We found that the general morphology of all monocytes is comparable (round/ granulated cells). iPSCs- and BM-derived monocytes have a higher percentage of intermediate monocytes and a lower percentage of non-classical and classical monocytes, compared to circulating monocytes. All respond to TLR ligands by producing cytokines, including IL-6, TNFα, and IL-1Ra, with slight differences in effect size. Circulating and BM-derived monocytes have higher glycolytic capacity than iPSC-derived monocytes. Epigenetic and transcriptomic analysis showed that BM- and iPSC-derived monocytes appear to be further differentiated into the monocyte-to-macrophage lineage than blood-derived human circulating monocytes. All macrophages display phagocytic capacity and in an exporatory setup, we showed that upon TNFα stimulation, all monocytes adhere to iPSC-derived endothelial cells under flow.

These findings indicate that iPSC- and BM-derived monocytes/macrophages can serve as alternatives for *in vitro* disease modeling, but exhibit developmental and functional differences.

Keywords

Bone marrow-derived monocytes, human circulating monocytes, induced pluripotent stem cell (iPSC)-derived monocytes, macrophages

Introduction

Monocytes and macrophages serve crucial roles in numerous processes throughout life, contributing to tissue homeostasis, repair processes, initiation and mediation of immune responses, and pathogen clearance. Additionally, these cells are involved in the pathophysiology of many different immune related diseases such as infections, cancer, autoimmune and cardiovascular disease (CVD) (1, 2). It is therefore essential to understand how monocyte/macrophage function is changed in pathophysiological conditions, and how to rebalance monocyte/ macrophage function during disease. An important recent discovery is that infections or brief disturbances in endogenous metabolites, such as hyperglycemia or hypercholesterolemia, can induce long-term functional hyperresponsiveness of circulating monocytes and tissue macrophages. This phenomenon of epigenetic reprogramming of innate immune cells and myeloid progenitor cells in the bone marrow (3, 4) has been termed 'trained immunity' (5, 6).

Until now, most in vitro studies on (modulation of) monocyte function have been conducted in human primary monocytes isolated from the peripheral circulation (referred from now in this paper as human circulating monocytes) obtained from Peripheral Blood Mononuclear Cells (PBMCs). However, availability of these primary monocytes is often limited for non-clinical laboratories, and they are characterized by a large interindividual functional heterogeneity, depending on genetic and environmental factors (7). Furthermore, they have very limited lifespan in culture. To investigate the effect of modulation of monocyte progenitor cells on monocyte/macrophage function, researchers have used human Bone Marrow (BM)-derived monocytes/macrophages (8, 9). Recent years, an alternative source for monocytes/macrophages has been established using induced Pluripotent Stem Cells (iPSC) (2). While all these monocyte sources are available, there is a lack of understanding whether these monocyte types are equivalent and can be used interchangably. Therefore, there is a strong need of comprehensive characterization. of the differences and similarities between iPSC-derived, BM-derived, and human circulating monocytes/macrophages.

In this study we aim to compare iPSC-derived, BM-derived, and human circulatingmonocytes and macrophages to highlight their similarities and differences with regard to morphology, gene and surface marker expression, epigenetic make-up, metabolism, ability to polarize, and function.

Material & Methods

For this study, human blood was obtained from healthy volunteers after informed written consent (Sanquin blood bank Nijmegen, The Netherlands; and the UMC Utrecht (code: F1P150)). iPSC lines were deposited in the European Bank for induced pluripotent Stem Cells (EBiSC, https://ebisc.org/) and registered in the online registry for human iPSC lines (hPSCreg). Human bone marrow was collected from healthy stem cell donors and patients who underwent orthopedic surgery. Exclusion criteria included bone marrow diseases/malignancies, use of immune suppressants, previous treatment with hip radiation, and physical or mental incapacitation. Donors were also excluded if they did not have a full understanding of the Dutch language. The use of these donors was approved by the local Ethics Committee (Ethical Approval CMO Arnhem-Nijmegen 2013/064). All donors provided written informed consent. All the experiments were conducted according to the Declaration of Helsinki.

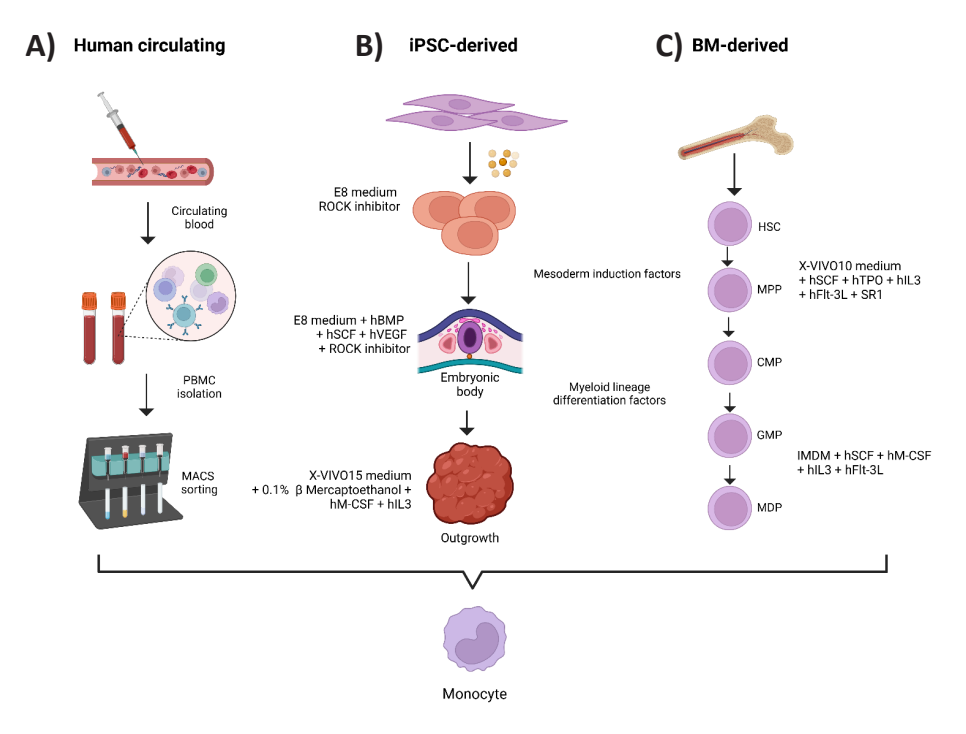


Figure 1: Schematic overview of iPSC and BM culture and differentiation towards monocytes. Left: induced pluripotent stem cell (iPSC)-derived monocyte differentiation protocol. IPSCs are differentiated via de mesoderm towards the myeloid lineage and form monocytes in outgrowths. Right: bone marrow (BM)-derived monocyte differentiation. In short, hematopoietic progenitor cells (HPC) undergo differentiation through the multipotent progenitor (MPP), common myeloid progenitor (CMP), and granulocyte/monocyte progenitor (GMP), which results in fully differentiated monocytes.

Figure 1 presents an overview of the isolation and preparation of human circulating monocytes, iPSC-derived, and BM-derived monocytes, which is consecutively described below.

Human circulating monocytes

PBMCs were isolated from EDTA blood by density-centrifugation using Ficoll-Plague PLUS (GE Healthcare Biosciences, 17144003) at 620g with no acceleration or brake, followed by 3 washes with cold PBS. Cluster of differentiation (CD)14+CD16+ monocytes were isolated with immunomagnetic negative selection, where unwanted cells are targeted for removal with Tetrameric Antibody Complexes recognizing specific non-monocyte cell markers conjugated to magnetic particles (STEMCELL Technologies, 19058) as depicted in Figure 1A. Cells were cultured in RMPI 1640 Medium (ThermoFisher Scientific, 21875034) with 1% penicillin/streptomycin (p/s Thermofisher Scientific, 15140122) and 10% heatinactivated fetal bovine serum (FBS; Corning, BV 35-079-CV).

Induced pluripotent stem cell culture and differentiation towards monocytes

iPSCs from four healthy human donors were used in this study and differentiated towards monocytes (Figure 1B): NP0144-41 (male), and NP0115-4H, NP0143-18, and NP0141-31B (all female). iPSCs were cultured in Essential 8™ Basal medium (Gibco, A15169-01) with supplement (Gibco, A28584-01) and 10 µM Rock inhibitor (S-27632, BD Biosciences 562822) under normal culture conditions (5% CO2 at 37°C) and passaged using 0.5 mM EDTA (ThermoFisher, 15575020EDTA) in phosphate-buffered saline (PBS).

As shown in Figure 1B, iPSC-derived monocytes were differentiated as described before (10) with minor adaptations. In short, iPSCs were cultured towards primitive mesoderm in embryoid bodies (EBs) in E8 containing 50 ng/mL human bone morphogenetic protein-4 (hBMP4, Peprotech 120-05ET-250), 20 ng/mL human stem cell factor (hSCF, Peprotech, 300-07), 50 ng/mL human vascular endothelial growth factor (hVEGF, Prepotech, AF-100-20), and 10 µM Rock Inhibitor. EBs were then subjected to myeloid differentiation into monocytes into monocytes by 100 ng/mL human macrophage colony-stimulating factor (hM-CSF, Peprotech, 300-25-100 μg) and 25 ng/mL human interleukin-3 (hIL-3, Peprotech 200-03-100) in X-VIVO 15 medium (Lonza BE02-060R) supplemented with 1% p/s, 1% GlutaMAX (ThermoFischer Scientific, 31980030), and 0.1% ß-Mercapto Ethanol (Gibco, 31350-010). Medium was changed every 5-7 days to harvest the iPSC-derived monocytes in suspension until the EBs stopped producing (maximum of 6 weeks).

Human bone marrow-derived mononuclear cells (MNCs) were isolated from bone marrow as shown in Figure 1C. In short, MNCs were isolated by densitycentrifugation using Ficoll-Plaque PLUS (GE Healthcare Biosciences), followed by 3 washes with cold PBS. Hematopoietic progenitor cells (HPCs - CD34+) were isolated using a MACS CD34 Microbead Kit (MACS, Miltenyi Biotec, 130-046-702) according to the manufacturer's instructions (purity > 95%). CD34+ cells were expanded for 10 days (5% CO2 at 37°C) using X-VIVO 10 serum-free Hematopoietic Cell Medium (Lonza, BE04-380Q), supplemented with 4% heat inactivated fetal calf serum (FCS, Hyclone Cytiva), 1% p/s, human stem cell factor 50 ng/mL (SCF, Miltenyi Biotec, 130-093-991), human thrombopoietin 15 ng/mL (TPO, Miltenvi Biotec, 130-094-745), human interleukin-3 30 ng/mL (IL-3 Miltenyi Biotec, 130-093-909), human FMS-like tyrosine kinase 3 ligand 30 ng/mL (Flt-3L, Miltenyi Biotec, 130-096-47) and StemRegenin-1 Aryl hydrocarbon receptor (AHR) agonist 2 µM (SR1, Stem Cell Technologies, 72342). After 10 days, cells were differentiated into monocytes for 20 days (5% CO2 at 37°C) using Iscove's Modified Dulbecco's Medium (IMDM) supplemented with 10% FCS, 1% p/s, SCF 50 ng/mL, human M-CSF 30 ng/mL (130-096-491, Miltenyi Biotec), IL-3 30 ng/mL, and Flt-3L 30 ng/mL.

Fluorescent immunohistochemistry labeling of monocytes

Fixated monocytes (4% paraformaldehyde (Klinipath, 4186)) were stained at day 0 with CD14 and CD16 (ThermoFisher MA133348 and BS-6028R). Secondary labeling was achieved by appropriate goat anti-mouse Alexa fluor-488 (Thermo Fisher Scientific A-11029, 1:400), and goat anti-rabbit Alexa fluor-568 antibodies (Thermo Fisher Scientific A11036, 1:500) for 1.5 hours at room temperature. Nuclear staining was achieved by and 1 μ g/mL Hoechst (Thermo Fisher Scientific 62249) incubated for 2 minutes afterwards. All cells were imaged with a fluorescent microscope (EVOS).

Induced pluripotent stem cell culture and differentiation towards endothelial cells

iPSC-ECs were differentiated as described before (11) and filtered using FcR Block (Miltenyi Biotec, 130-059-901) and CD144 beads (Miltenyi Biotec, 130-097-857). Cells were then purified in the MACS MultiStand separator column (Miltenyi Biotec) and resuspended in iPSC-EC medium ((Promocell, C22110) supplemented with FBS, p/s, and transforming growth factor-1 (TGF-1, SP431542 (Selleckchem, S1067)), and transferred to fibronectin (Promocell, C-43060) coated T75 flasks.

Macrophage differentiation and polarization

Macrophage differentiation and polarization of the monocytes obtained from the three different methods described above was performed using appropriate medium (mentioned in the section for each type of monocyte). First, the cells were differentiated in to macrophages using 50 ng/mL human M-CSF (Peprotech, 300-25) for 4 days followed by polarization with 50 ng/mL human interferon-y (IFN-y, Peprotech P01579.1) and 10 ng/mL LPS (Peprotech, 297-473-0) for M1; and 10 ng/ mL human IL-4 (Peprotech 130-093-924) for M2. To visually confirm whether the monocytes successfully differentiated into M1 and M2 phenotypes, macrophages were stained with CD80 and CD206 (ThermoFisher 14-0869-82 and 25-2069-42). All cells were imaged with a fluorescent microscope (EVOS).

Phagocytosis assay

A phagocytosis assay was performed according to the manufacturer's protocol (Cayman chemical, 500290) to investigate if macrophages take up fluorescent latex beads. Macrophages (6x104/well) were polarized in a 96-wells plate and incubated for 3 hours with the fluorescent latex beads (rabbit IgG FITC complexes, 0.1 micron mean particle size) with a final dilution of 1:100. Cells were washed with trypan blue quenching solution (1:10) for 2 minutes, followed by a wash with assay buffer. Then, Hoechst 33342 (1:10,000 in PBS) and dead staining (4 µM ethidium homodimer-1 (EhtD-1, Invitrogen L3224B) were incubated for 45 minutes in the dark to detect nuclei and dead cells. For Z-stack pictures, cells were also stained with wheat germ agglutinin (WGA, Alexa Fluor 680 conjugated, 1:400) incubated for 10 minutes in the dark to show cell outline. After washing with PBS, all cells were imaged with a fluorescent microscope (EVOS).

Flow cytometry

Flow cytometry was performed to distinguish the number and marker expression of classical, intermediate, and non-classical monocyte subsets in human circulating, iPSC, and BM-derived monocytes. Human circulating and BM-derived monocytes were stained fresh and iPSCs were fixated before staining (4% paraformaldehyde (Klinipath, 4186)). Antibodies used for staining are shown in Supplementary Table S1. Cells were measured with a Cytoflex flow cytometer (Beckman Coulter RRID: SCR 017217.) The gating strategy (Supplementary Figure S1) was determined using the fluorescence minus one method (12). In short, we identified monocytes filtering by side scatter and CD45+ properties. Then, monocyte subset size (discriminated by CD14/CD16 expression patterns) was determined as a percentage of gated HLA-DR+/CD16. All data was analyzed with FlowJo™ v10.8 Software (BD Life Sciences).

Assay of Transposase-Accessible Chromatin sequencing (ATAC) and analysis

Human circulating, iPSC-derived, or BM-derived monocytes and macrophages were used for ATAC sequencing analysis and as previously reported (13) according to the manufacturer's instructions (Illumina, US). In short, lysis and transposition of 50,000 cells were done using TDE1 Tagment DNA Enzyme, TD buffer (Illumina Tagment DNA TDE1 Enzyme Buffer), and 1% Digitonin (Promega, G9441) and incubation for 30 minutes at 37°C. Then, DNA was isolated and purified using QIAGEN MinElute PCR purification kit (OIAGEN, 28004), and samples were stored at -20°C until processed for sequencing, After sequencing, ATAC reads were first aligned with the human genome assembly hg19 using Burrow's Wheeler alignment (bwa) (14). Binary Alignment Map (BAM) files were screened and duplicate reads and reads with poor quality were removed using SAMtools (15). MACS2 tool was then used to identify the ATAC peaks using default settings (16), to then use deepTools and bigwig files to visualize the quality of the sequencing data (17). Peaks were then normalized using DESeg2 R package (18), and pairwise comparisons were done. An adjusted p-value of <0.05, fold change >2, and reads/peak>20 was used to identify differential peaks. Adjacent peaks were subsequently merged, and principal component analysis (PCA) plots were made. All ATACseq data generated for this article are available in the NCBI Gene Expression Omnibus under accession number GSE261697.

RNA isolation and RNA sequencing

Total RNA was isolated from the monocytes obtained from the three different sources (circulating, iPSC- and BM-derived) using a TriPure kit according to the manufacturer's instructions (Roche 11667157001). For RNA sequencing, isolated RNA was sent to Single Cell Discoveries (Utrecht, The Netherlands), where RNA extraction and library preparation followed the CEL-seq2 protocol (sequencing depth 10 million reads/sample). RNA-seq fastq files were mapped to the genome using bowtie2 and HTSeq was used to count reads per transcript. Data analysis and visualization was performed with R version 4.2.3. Bulk RNA sequencing counts were normalized, and differential gene expression was analyzed using DESeq2_1.36.0 method (18). Significant differentially expressed genes between experimental groups were filtered according to their fold change threshold of > 1.2 adjusted p-value <0.05 and counts per million (CPM) >5. All RNAseq data generated for this article are available in the NCBI Gene Expression Omnibus under accession number GSE261696.

Cytokine production capacity

To measure cytokine production, 1x10⁵ monocytes/well were cultured in flatbottom 96-well plates (Corning) in either culture medium as negative control or culture medium containing 10 ng/mL LPS (serotype O55:B5; Sigma-Aldrich; further purified as described previously (19)) for stimulation. After 24 hours, supernatants were collected and stored at -20°C. Cytokine levels in supernatants of stimulated cells was determined using commercial enzyme-linked immunosorbent assay (ELISA) kits for IL-6 (R&D Systems, DY201), TNFα (R&D Systems, DY210), and IL-1Ra (R&D Systems, DY280) according to the manufacturer's instructions.

Metabolic analysis by Seahorse assay

To assess the rates of oxidative phosphorylation (OXPHOS) and glycolysis, an optimized monocyte amount per source (100,000 human circulating monocytes, 100,000 BM-derived monocytes and 300,000 iPSC-derived monocytes) was plated onto calibrated cartridges in Seahorse assay medium (Dulbecco's Modified Eagle Medium (DMEM, Sigma, 5030) with 2 mM L-glutamine (Sigma, G3126)). Mitochondrial respiration was assessed by the Oxygen consumption rate (OCR) using a Cell Mito Stress Test Kit containing 1 µM Oligomycin A (Sigma, O4876), an optimized amount of carbonyl cyanide-p- trifluoromethoxyphenyl-hydrazon (FCCP, Sigma, C2920, 2 µM for human circulating and iPSC-derived; 1 μM for BM-derived), and 1.25 μM rotenone (Sigma, R8875)/2.5 µM antimycin A (Sigma, A8674). Extracellular acidification rate (ECAR), a surrogate measure for lactate production by glycolysis, was measured using unbuffered DMEM medium supplemented with L-Glutamine 1 mM with a Glyco Stress Test Kit containing D-glucose (Sigma, G8644) 11 mM, Oligomycin A 1 μM, and 2-deoxy-D-glucose (2-DG, Sigma, D6134) 22 mM. Assays were measured in an XFe96 Analyzer (Seahorse, Bioscience). To interpret the results of this analysis, we followed the guide of Glycolysis and MitoStress Test Kit from the manufacturer (Agilent Seahorse XF). For OCR, maximum respiration was calculated by subtracting the average of measurements after FCCP injection minus the average of the reserve capacity (after Rotenone/Antimycin A). For ECAR, glycolysis was calculated by subtracting the average measurement after glucose injecting minus basal; maximum glycolytic capacity was calculated as the average of measurements after oligomycin A injection minus basal and glycolytic reserve was the result of the average after oligomycin A injection minus the average of measurements after glucose injection.

Exploratory endothelial flow experiments (IBIDI)

To investigate the ability of monocytes to attach to the vasculature, IBIDI flow experiments were performed in an exploratory setting with monocytes, that were either treated with human TNFα (Miltenyi Biotech,130-094-020) for stimulation, or were kept unstimulated. The experiment was performed as follows: primary circulating monocytes, iPSC-derived monocytes, and BM-derived monocytes were isolated/ harvested and exposed for 4 hours to TNFa. During this time, a monolayer of iPSC- derived endothelial cells was cultured in 0.4 μ m μ -slides (IBIDI 80186) for 2 hours and subsequently attached to the pump system and perfused for another 2 hours (pressure 9.3 mbar, shear stress 3.00 dyn, flow rate 4.99 mL/min, shear rate 300 1/s, unidirectional 20 s and oscillating 0.5 s). Next, the medium was changed to starvation medium (iPSC-EC medium with 0.5% FBS), monocytes were added to the slides, and the system was perfused for 2 hours. After 2 hours, four random, non-overlapping images were taken per slide with an EVOS microscope for manually counting monocyte adherence.

Statistics

All data in this study are shown as mean \pm standard errors of the mean and a two-sided p-value smaller than 0.05 was considered statistically significant. Data were analyzed using GraphPad Prism version 10.0 (La Jolla, CA, USA) using the appropriate (non)parametric tests after normality of residuals was assessed using D'Agostino-Pearson omnibus test.

Results

Morphology, surface markers, and subsets of monocytes

To compare the morphology of human circulating, iPSC-derived, and BM-derived monocytes, we used brightfield imaging and fluorescently labeled the cells for surface markers CD14 and CD16. iPSC- and BM-derived monocytes appear larger than human circulating monocytes (Figure 2A), yet expression of specific surface markers was similar (Figure 2B). We subsequently explored the monocyte subset composition by flow cytometry, based on FMO and CD14 and CD16 expression in the iPSCderived, BM-derived, and human circulating monocytes (representative density plots in Figure 2C). There were robust differences in the distribution of the three monocyte subsets according to the monocyte source, with means of 6.6% non-classical, 7.6% intermediate, and 85.9% being classical monocytes for the human primary circulating monocytes, versus 0.2%, 21.1% and 78.7% for the iPSC-derived and 0.4%, 59.4% and 40.2% for the BM-derived monocytes respectively (Figure 2D). The individual data from all individual donors can be found in Supplementary Figure S2. In conclusion, human circulating monocytes are mainly composed of classical monocytes compared to iPSC- and BM-derived monocytes, which contain a much higher percentage of intermediate monocytes. In all conditions, the percentage of non-classical monocytes is the lowest (0.4-6.6%) compared to the other two subsets.

Epigenomic and transcriptomic characteristics of monocytes and macrophages

To compare the epigenomic landscape of the different monocytes, we assessed chromatic accessibility by ATAC analysis. Dynamic open chromatin regions during monocyte-to-macrophage differentiation were identified and an average of log2 fold change was calculated for each cell type relative to human circulating monocytes (Figure 3A). BM- and iPSC-derived monocytes fell between human circulating monocytes and macrophages (M0, M1 and M2 polarized) on this 'differentiation axis', indicating that their chromatin accesibility profile is an intermediate between human circulating monocytes and macrophages (Figure 3A). In addition, PCA plots based on dynamic ATAC-peaks between monocytes and each macrophage subset show that BM- and iPSC-derived monocytes clustered most closely with M0 and M1 macrophages (PC2) and then with M2 macrophages (PC3) (Figure 3B). By plotting the ATAC-seg signal at peaks that are enriched (up) or depleted (down) in different comparisons (e.g., Monocyte vs. M0, M0 vs. M1), BMand iPSC-derived monocytes showed an intermediate profile between monocytes and macrophages and were most similar to the M0 macrophage subset (Figure 3C).

To subsequently evaluate the transcriptional similarities and differences between the various monocytes and macrophages, we performed RNAseg analysis. In line with the chromatin accessibility, gene expression of iPSC-derived monocytes falls in between human circulating monocytes and macrophages based on differentiation-associated genes, while BM-derived monocytes are more similar to macrophages (Figure 4A). This finding is also reflected in the PCA plots in Figure 4B, where BM-derived monocytes cluster closer to human ex vivodifferentiated macrophages. iPSC-derived monocytes cluster closer to human ex vivo-differentiated macrophages than to human circulating monocytes. When comparing the upregulated gene expression of the different monocytes and macrophages (Figure 4C), we observe a similar trend. BM- and iPSC-derived monocyte upregulated gene expression is higher than in human circulating monocytes and comparable to macrophages of all subtypes. We also observed this for gene expressions that were downregulated (Figure 4C).

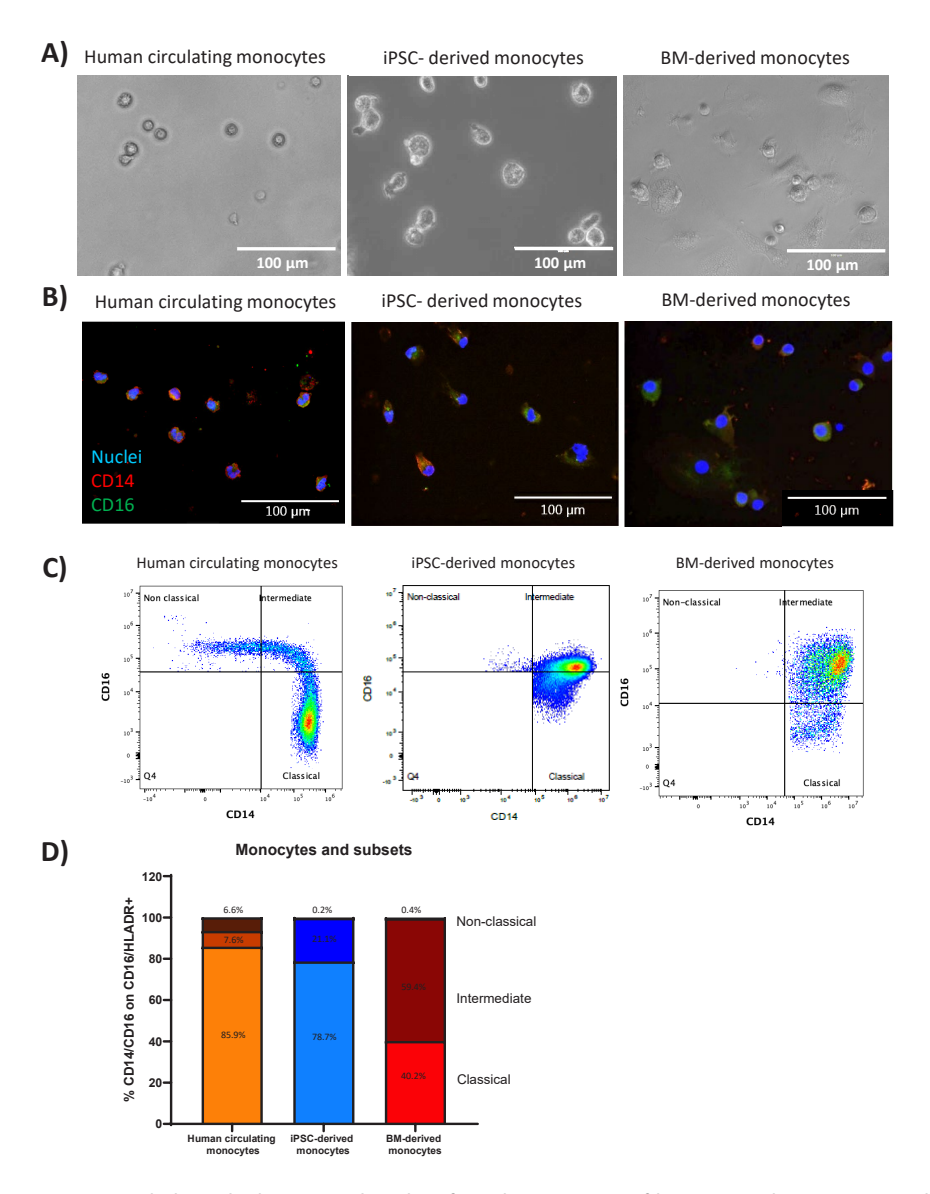


Figure 2: Morphological, phenotypical, and surface characteristics of human circulating, iPSC-, and BM-derived monocytes. A) iPSC- and BM-derived monocytes are similar in morphology compared to human circulating monocytes: round and granular, but slightly larger in size. B) Fluorescent staining of monocytic surface markers (CD14 in red, CD16 in green, and Hoechst nuclear labeling in blue) in human circulating, iPSC-, and BM-derived monocytes. C) Representative density plots of the monocyte subsets present in human circulating (orange), iPSC (blue), and BM-derived (red) monocytes (classical CD14++CD16-, intermediate CD14++CD16+ and non-classical CD14+CD16++). Individual data can be found in Supplementary Figure S2. D) Histogram of average (n=3) monocyte subsets present in human circulating (orange), iPSC (blue), and BM-derived (red) monocytes. Overall, iPSC and BM monocytes have a higher percentage of intermediate monocytes and a lower percentage of non-classical and classical monocytes, compared to circulating monocytes.

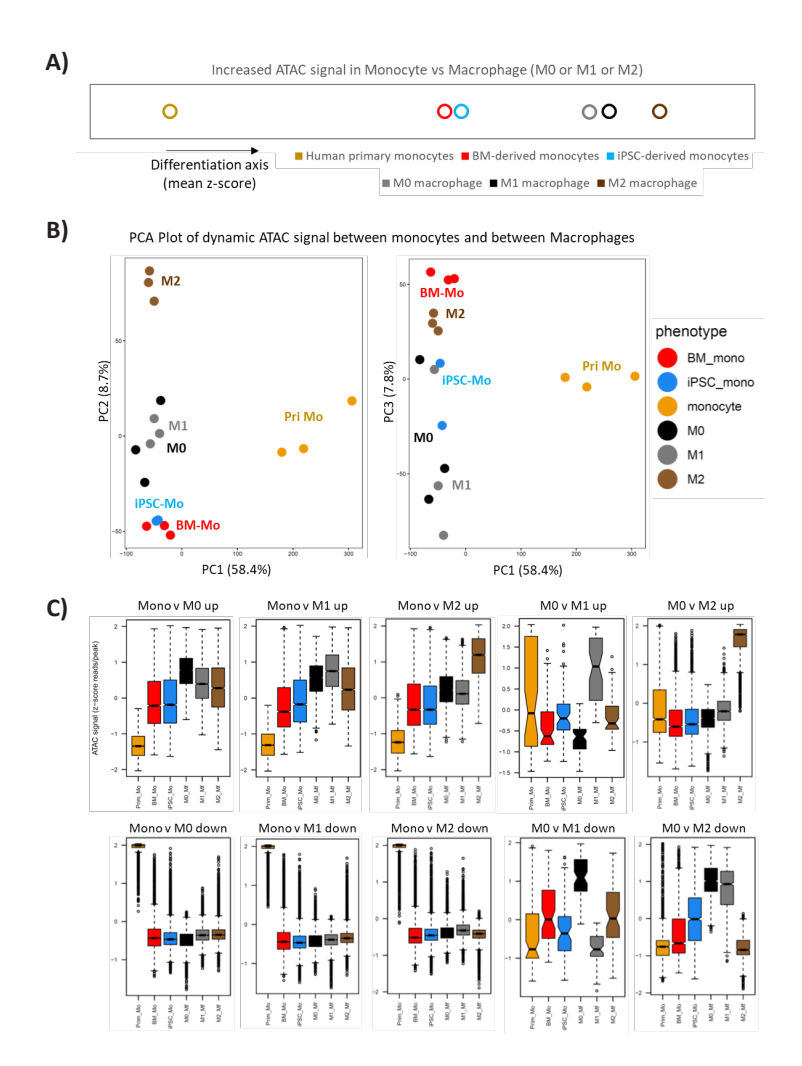


Figure 3: Comparison of chromatin availability between monocytes and macrophages. To compare chromatin availability, we performed ATAC sequencing for BM-derived, iPSC-derived, and human circulating cells monocytes and M0, M1, and M2 macrophages. A) Schematic overview of the monocyte-to-macrophage-axis show that chromatin accessibility of BM- and iPSC-derived monocytes clusters between human circulating monocytes and macrophages. B) PCA plots of dynamic ATAC signal between monocytes and macrophages (PC1 versus PC2 and PC1 versus PC3) confirm that BMand iPSC-derived monocytes fall more into the region of human circulating macrophages, especially close to M0. All cells cluster within monocyte and macrophage types. C) Up- (upper row) and down-(lower row) regulated chromatin accessibility confirms that BM- and iPSC-derived monocytes align more with human circulating macrophages than monocytes epigenetically.

Overall, these data indicate that BM- and iPSC-derived monocytes display an open chromatin and transcriptional landscape that is an intermediate between primary monocytes and in vitro differentiated macrophages.

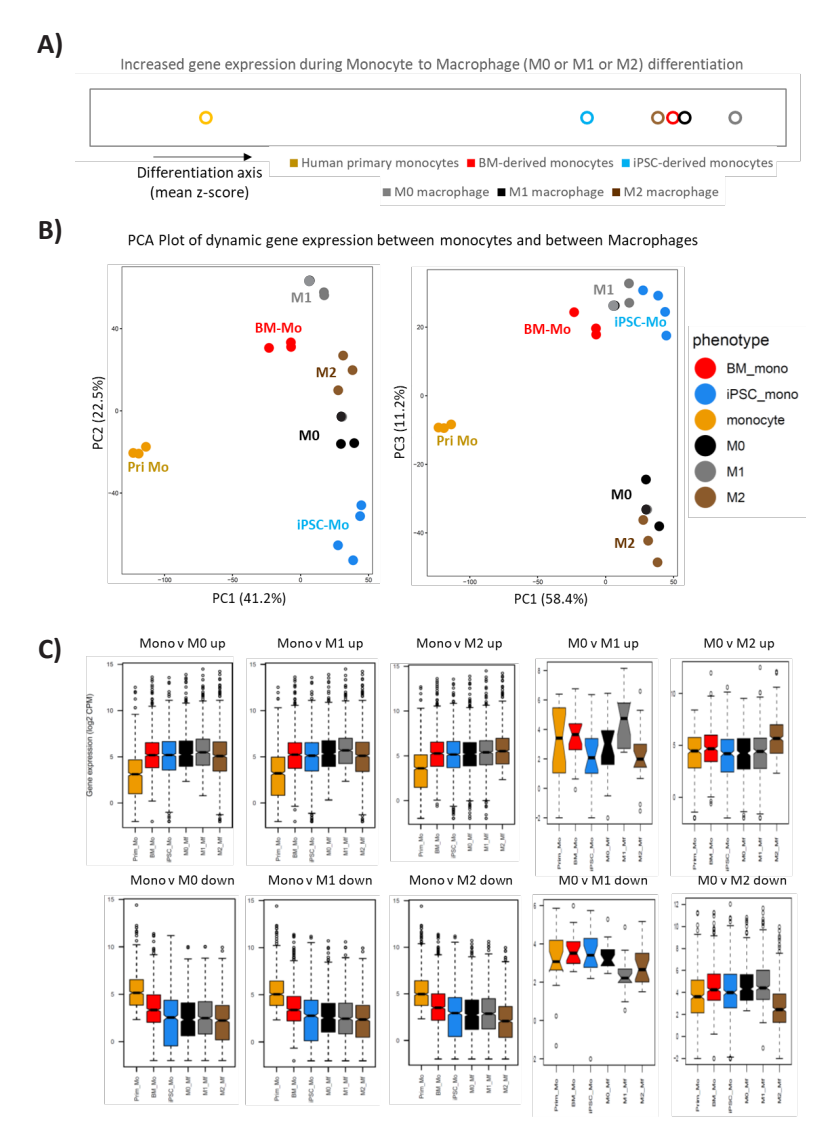


Figure 4: Comparison of gene expression between monocytes and macrophages. To compare gene expression, we performed RNA sequencing for BM-derived, iPSC-derived, and human circulating cells monocytes and M0, M1, and M2 macrophages. A) Dot plot of mean log2 fold change relative to day 0 monocytes, based on primary monocyte-to-macrophage differentiation associated gene expression (p.adj <0.05, FC >2, CPM >5). This schematic overview of the monocyte-to-macrophage-axis shows that the open chromatin landscape, BM- and iPSC-derived monocytes is between human circulating monocytes and macrophages. B) PCA plots of dynamic gene expression between monocytes and macrophages (PC1 versus PC2 and PC1 versus PC3) confirm that BM- and iPSC-derived monocytes fall more into the region of human circulating macrophages. All cells cluster within monocyte and macrophage types. C) Up- (upper row) and down- (lower row) regulated gene expression confirms that BM- and iPSC-derived monocytes align more with human circulating macrophages than monocytes epigenetically.

Cytokine production and metabolic characteristics of primary and induced monocytes

To compare the functional characteristics of the monocytes, we stimulated 100,000 human circulating, BM-derived and iPSC-derived monocytes with 10 ng/ml LPS for 24 hours and measured IL-6, TNFα and IL-1Ra cytokine production in the three monocyte sources (Figure 5A). Overall, all three monocyte types responded to TLR stimulation by increased cytokine production for IL-6, TNFα, and IL-1Ra. IL-6 production was higher in the BM-derived monocytes compared to iPSC-derived and human circulating monocytes. TNFa was higher in the primary circulating cells (Figure 5A) compared to BM-derived monocytes. IL-1Ra secretion did not differ between monocyte types.

To investigate the metabolic characteristics between the three cell sources, we performed Seahorse assays on cultured monocytes. Overall, all monocytes are metabolically active regarding mitochondrial respiration (OCR) and glycolysis/ extracellular acidification rate (ECAR) (Figure 5B). While assessing the maximum respiration, maximum glycolytic capacity, basal respiration and basal glycolytic rate of the cells, we observed that iPSC-derived monocytes rely more on mitochondrial respiration. Human circulating and BM-derived monocytes have significantly higher maximum glycolytic capacity compared to iPSC-derived monocytes. Additionally, human circulating monocytes have significantly higher maximum respiration capacity compared to iPSC and BM-derived monocytes (Figure 5C). Whereas BMderived monocytes showed higher basal glycolytic rate, primary monocytes have a much greater glycolytic reserve, hinting to an increased metabolic flexibility. The individual data for all the donors can be found in Supplementary Figure S3.

Monocyte adherence to endothelial cells

We subsequently investigated the adherence capacity of the monocytes to nonstimulated endothelial cells under flow in an exploratory setting. After exposure of monocytes to TNFa for 4 hours, human circulating and iPSC-derived monocytes respectively showed a 1.6 and 3.5 fold increased adherence to endothelial cells, compared to non-stimulated controls under flow, while BM-derived monocyte adherence was not different. Statistical analysis was not performed due to the low number of experiments (Figure 6A).

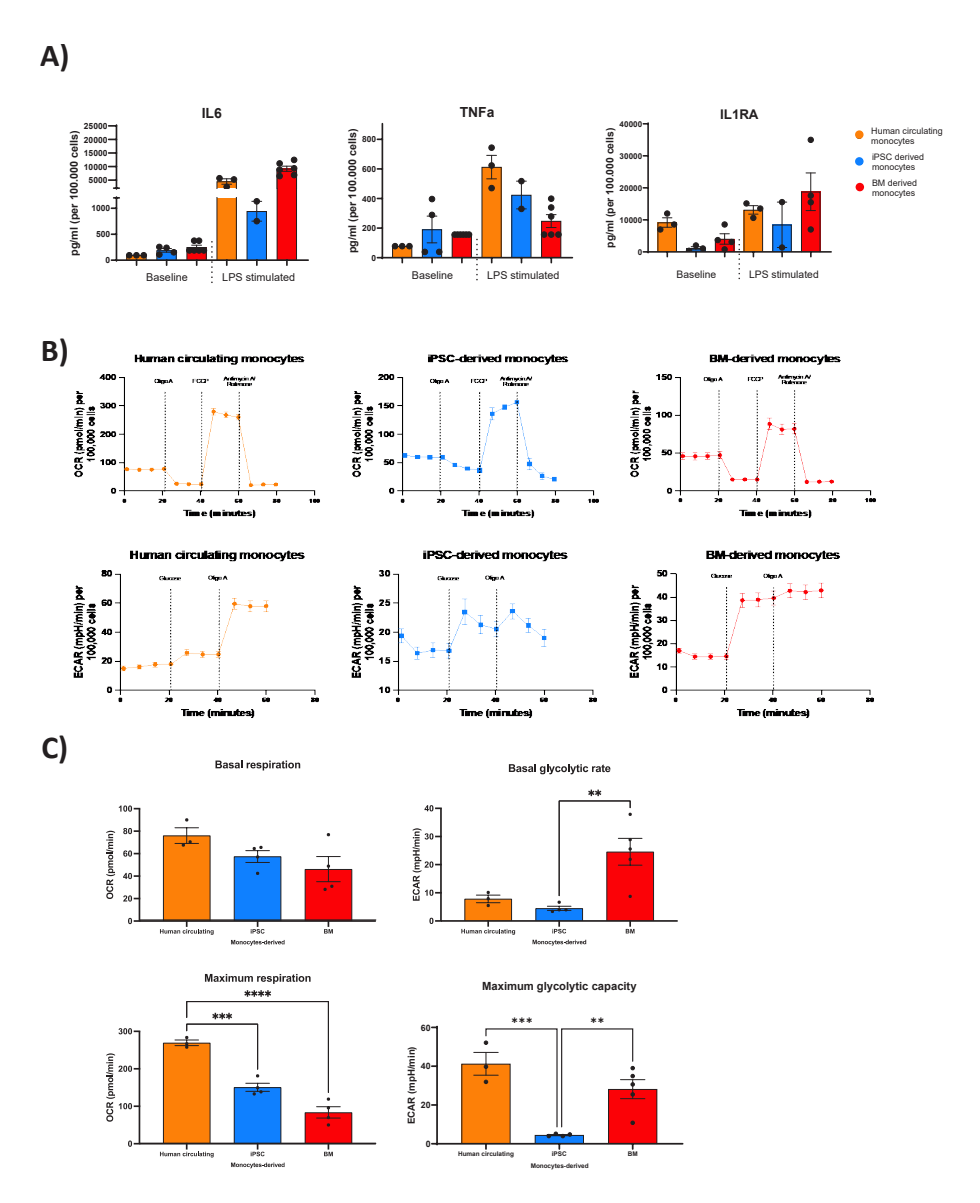


Figure 5: Assessment of monocyte subsets, cytokine production capacity, and cell metabolism of human circulating in iPSC-, and BM-derived monocytes per 100,000 cells. A) IL-6, TNF α , and IL-1Ra cytokine production capacity after stimulation with LPS of the different types of monocytes. B) Cell metabolism was measured as oxygen consumption (OCR) and extracellular acidification rate (ECAR) over time using glucose, oligomycin A, FCCP, rotenone/antimycin A as inhibitors of different stages of cell respiration. C) Basal respiration and maximum respiration capacity (OCR) during mitochondrial respiration and basal glucolytic rate and maximum glycolytic capacity (ECAR) during glycolysis of human circulating, iPSC-, and BM-derived monocytes. A one-way-ANOVA (parametric) and Mann-Whitney test (non-parametric) were performed with *p<0.05, **p<0.01, and ***p<0.001.

Differentiation towards macrophages and phagocytosis

One hallmark of monocytes is their ability to differentiate into functional macrophages. Figure 6B depicts a schematic presentation of the polarization of human circulating, iPSC-, and BM- monocytes into macrophages using M-CSF and subsequent polarization into M1 (IFN-y + LPS) and M2 (IL-4) (Supplementary Figure S4).

Finally, we assessed the phagocytosis capacity of the monocyte-derived M1-type macrophages with latex-beads (Figure 6D). We observed that all macrophages could perform phagocytosis and encapsulate latex beads.

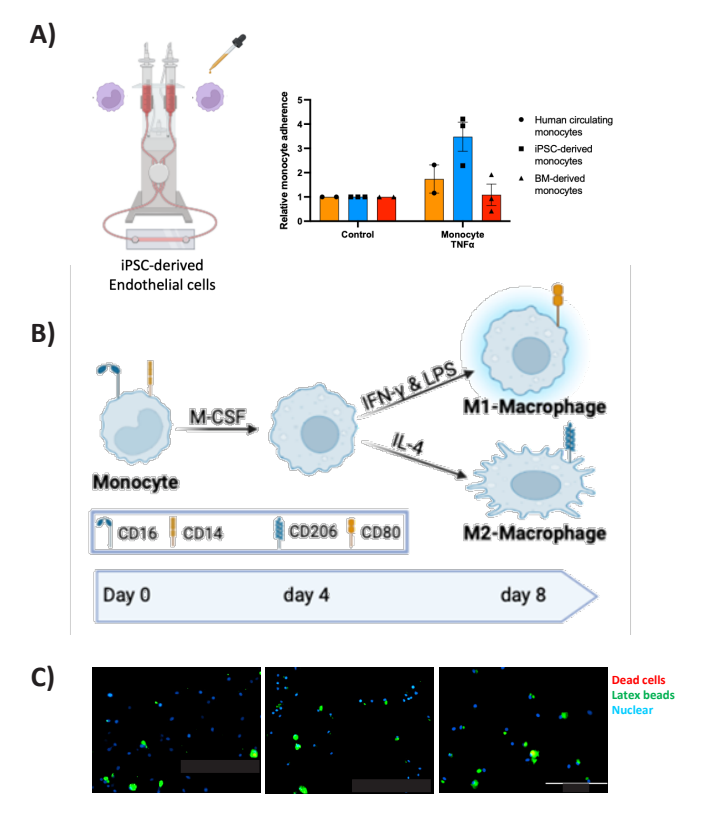
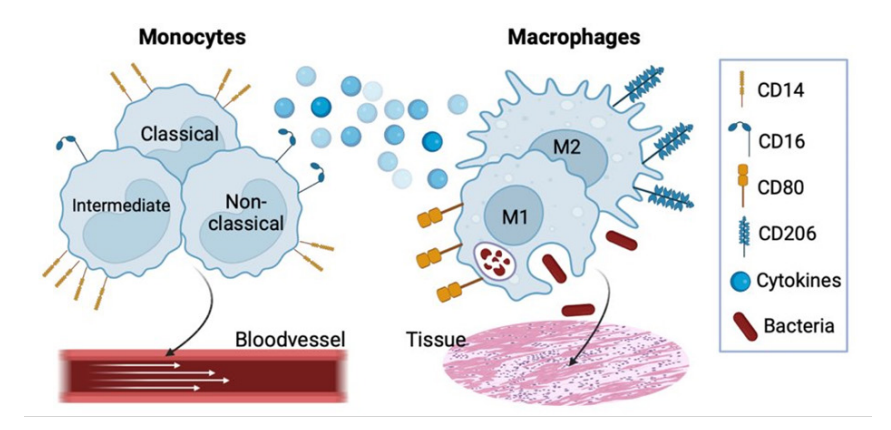


Figure 6: Exploratory assessment of monocyte adherence to iPSC-derived endothelial cells (EC) under flow and differentiation, polarization, and characterization of monocyte-derived macrophages. A) Left: schematic depiction of the IBIDI flow system containing a pump with (un)treated monocytes and a tissue slide with iPSC-ECs used for this exploratory experiment. Right: Relative adherence of human circulating, iPSC-, and BM-derived monocytes to iPSC-derived ECs under flow conditions of this exploratory experiment. iPSC monocytes have a tendency towards higher relative adherence than BM monocytes compared to human circulating monocytes. B) Schematic presentation of differentiation of human circulating, iPSC-, and BM- monocytes into macrophages using M-CSF and polarization into M1 (IFN-γ + LPS) and M2 (IL-4) macrophages. C) Polarized human circulating, iPSC- and BM-monocytederived macrophages phagocytosis capability after 3 hours.

iPSC-derived and BM-derived monocytes and macrophages are relevant alternatives for human primary circulating monocytes and macrophages to perform *in vitro* characterization and use in experiments. A comprehensive comparison between the monocytes derived from these sources, however, is lacking. Therefore, we set out to compare various functional and phenotypic parameters that characterize monocytes and macrophages, which are summarized in Figure 7 and Table 1.



	Monocytes	Macrophages			
Morphology	Round, granulated	Round (M1) or elongated (M2), granulated			
Location	Circulating	Tissue (non-circulating)			
Subtypes	Classical, intermediate, non-classical	M1, M2			
Expression	CD14 and CD16	CD80 (M1) and CD206 (M2)			
Metabolism	Glycolysis and mitochondrial respiration				
Secretion	Cytokines and chemokines				
Function	Interact with vasculature, differentiate into phagocytotic cells	Phagocytosis			

Figure 7: Definition of monocytes and macrophages used in this study. Upper part: Schematic overview of the definition of monocytes and macrophages. Lower part: Tabular summary of the main characteristics between monocytes and macrophages. Abbreviations: CD Cluster of differentiation.

Table 1: Summary of similarities and differences between human circulating and iPSC- and BMderived monocytes and macrophages. Comparison of monocytes and macrophages was performed on phenotypical, functional, and transcriptomic read-outs and the results are summarized here.

			Human circulating monocytes	iPSC- derived monocytes	BM-derived monocytes	
		Morphology	Round and granulated			
	Phenotype	Subsets	Classicals, intermediates, non-classicals to intermediates			
			Comparable bas	Comparable baseline secretion		
		Cytokine/ chemokine secretion	TNFa (LI	Higher IL6, lower TNFa (LPS stimulation)		
			Comparable basal respiration (OCR)			
Monocytes	Function	Metabolism	Higher maximum glycolytic capacity (ECAR)	Lower maximum glycolytic capacity (ECAR)	Higher maximum glycolytic capacity (ECAR)	
			Higher maximum respiration capacity	Lower maximum respiration capacity		
		Adherence	after stimulation with TNE		Unchanged EC adherence	
	Transcriptome	Gene expression (RNA)		Closer to prim human macro than monocyt	phages	
	iranscriptome	Chromatin accessibility (ATAC)	Closer to primary human macrophages than monocytes		phages	

Magraphagas	Phenotype	Types	Successful differentiation into macrophages		
Macrophages	Function	Phagocytosis	Phagocytosis		

We observed clear differences in the CD14/CD16 expression, which is used to categorize monocyte subsets with CD14++ CD16- denoting classical monocytes, CD14+ CD16++ representing non-classical monocytes, and CD14++ CD16+ corresponding to intermediate monocytes (20). We observed that circulating monocytes mainly consist of classical monocytes, while BM- and iPSC-derived monocytes have a higher percentage of intermediate monocytes. This observations could have been the result of the prolonged culture time of iPSCs and BM-derived monocytes. For the future, as many diseases are associated with specific monocyte subsets (e.g., non-classical monocytes), it is important to be able to switch BM- and iPSC-derived monocytes toward non-classical subsets. For this, it could be interesting to either prolong monocyte culture, to age classical monocytes towards non-classical monocytes (21), or develop a selective induction protocol, e.g., using IL-8 and TNFa, both associated with non-classical monocyte development in elderly humans (22).

We further used ATACseq to assess chromatin accessibility and RNA expression to assess gene transcription for the comparison between the different monocytes and monocyte-derived macrophages. We showed that from an epigenetic and transcriptional point of view, BM- and iPSC-derived monocytes are more closely resembling primary human macrophages than human circulating monocytes, indicating that they are further differentiated in the monocyte-to-macrophage lineage. Importantly, these differences could have been induced by the use of M-CSF during the differentiation of BM- and iPSC-derived monocytes or by the timing of the differentiation, e.g. shorter differentiation might lead to less mature cells. M-CSF is known to drive macrophage differentiation programs (23). In vitro. the cells are in differentiation for at least 7 days with this cytokine, which might explain why these cells have a more macrophage-like phenotype compared to human circulating monocytes. In the future, different differentiation protocols could be tested and established to minimize the use or concentration of M-CSF in vitro and/or the duration of the differentiation (24). In summary, the iPSC-derived and BM-derived monocytes appear to be further differentiated in the monocyte-tomacrophage lineage.

An important immunological function of monocytes is the production of cytokines after stimulation with inflammatory stimuli, such as LPS. Monocytes from all three sources showed the capacity to produce IL-6, TNFa, and IL1-Ra after stimulation with LPS, but this was highest for human circulating monocytes and for BM derived monocytes. The energy that is necessary for the increase in cytokine production after LPS stimulation is derived from a rapid increase in glycolytic rate. Indeed, similar to the cytokine production capacity, the maximum glycolytic capacity was higher in human circulating monocytes and BM-derived monocytes, compared to the iPSC-derived monocytes.

The findings of our study offer important novel information to take into account when deciding which model to use for *in vitro* monocyte experiments, in addition to the known advantages and disadvantages of each cellular source. iPSC-

derived monocytes and macrophages offer a potentially limitless supply and genetic customization, but face challenges related to differentiation efficiency and variability in protocols (25, 26). BM-derived monocytes and macrophages originate from hematopoietic stem cells in the bone marrow, are more difficult to obtain, but can be differentiated into various cell types, thereby representing a natural physiological source with heterogeneity based on the bone marrow microenvironment (27). PBMC-derived monocytes are isolated from peripheral blood, and although easily accessible, may exhibit functional alterations due to isolation procedures and genetic and environmental factors (7, 28). In addition, they have very short lifespan in vitro. When comparing their applications, iPSC-derived monocytes offer personalized disease modeling, drug screening, and potential cell-based therapies in various fields, such as cardiovascular, but also cancer and immune diseases, such as HIV (26, 29). BM-derived monocytes are crucial to investigate how manipulation of progenitor cells affect monocyte offspring (30-32). PBMC-derived monocytes and macrophages are commonly used to study immune responses and infectious disease due to their representation of circulating immune cells and easy accessibility (33, 34). In conclusion, iPSC technology offers customization and potential for disease modeling, while BM- and PBMC-derived cells at this moment still provide more physiological relevance. Other research groups have compared the various monocyte sources, but most of the time only cell sub-populations derived from two sources were compared (1, 24). Moreover, these studies were limited in the parameters that were characterized. To our knowledge, this paper is the first to perform in-depth comparisons between these three cell sources to ensure proper use in future studies.

Limitations and future perspectives

Some of the differences between cells may not only be explained by source, but also by donor and technical variations, and age/maturation of cells in culture. Differences in metabolism might arise from the fact that cells that have been in culture longer often show exhaustion, which has already been reported for other leukocytes (35, 36). Given the potential effect of the duration of protocols and the specific stimuli used (e.g. M-CSF), it needs to be emphasized that the findings of our study cannot be extrapolated to all iPSC- and BM-derived monocytes, and are specific for the conditions that we used in the process of monocyte isolation and differentiation. Another limitation is that for the monocyte adherence assay, one experiment failed leaving us with a limited number of measurements for some conditions. This prevented us for formal statistical testing and these results should be considered as hypothesis-generating or explorative.

It is important to understand the similarities and differences between monocyte sources when using them for *in vitro* disease modeling. Besides that, for iPSC-and BM-derived monocytes and macrophages, it is essential to know that they resemble their human circulating counterparts morphologically and functionally well enough and can differentiate into functional macrophages. In this study, we compared human circulating, iPSC- and BM-derived monocytes, and monocytederived macrophages. Although all monocytes and macrophages were able to produce cytokines upon stimulation and to perform phagocytosis, respectively, there were profound differences. Most interesting was the finding that on a transcriptional and chromatin accessibility level, iPSC- and BM-derived monocytes are more similar to human macrophages than monocytes. This means that they are suitable for research, but differences should be considered when performing experiments and careful selection of the source should be performed together with monitoring their phenotype.

Acknowledgements and Funding

We would like to thank Dr. K. Neef from the Regenerative Medicine Center Utrecht and T. Saric from the University of Cologne, Center for Physiology and Pathophysiology, Institute for Neurophysiology, Germany for providing us with the iPS cell lines. Furthermore, ELK was supported by the Netherlands Heart Institute (Fellowship #282) and ELK, SdJ, and NPR by the Netherlands Heart Institute (IMPRESS). MGN, and NPR were supported by a CVON grant from the Dutch Heart Foundation and Dutch Cardiovascular Alliance (CVON2018-27). NPR was further supported by a grant of the ERA-CVD Joint Transnational Call 2018, which is supported by the Dutch Heart Foundation in the Hague (JTC2018, project MEMORY; 2018T093). SB is supported by the Dutch Heart Foundation in the Hague (Dekker grant 2018-T028). MGN is further supported by a European Research Council (ERC) Advanced Grant (FP/2007-2013/ERC grant 2012-322698), and a Spinoza Prize (NWO SPI 92-266). JPGS European Research Council, Grant/Award Number: Project EVICARE [No. 725229]. BN is supported by an NHMRC (Australia) Investigator Grant (GNT1173314). The figures were created with BioRender.com.

Contributions

DFG, ELK, SB, JPGS, and NPR were responsible for conceptualization of the study. WH, MS and WHCR collected and provided all the bone marrow material. DFG, ELK, DK, LG, and EvV performed the investigation (experiments). Data curation and

analysis was performed by DFG, ELK, BC, and BN. Project oversight was done by SB, SdJ, JPGS, MGN, and NPR. DFG and ELK wrote the draft manuscript, which was afterward reviewed and edited by all co-authors.

Declaration of interest

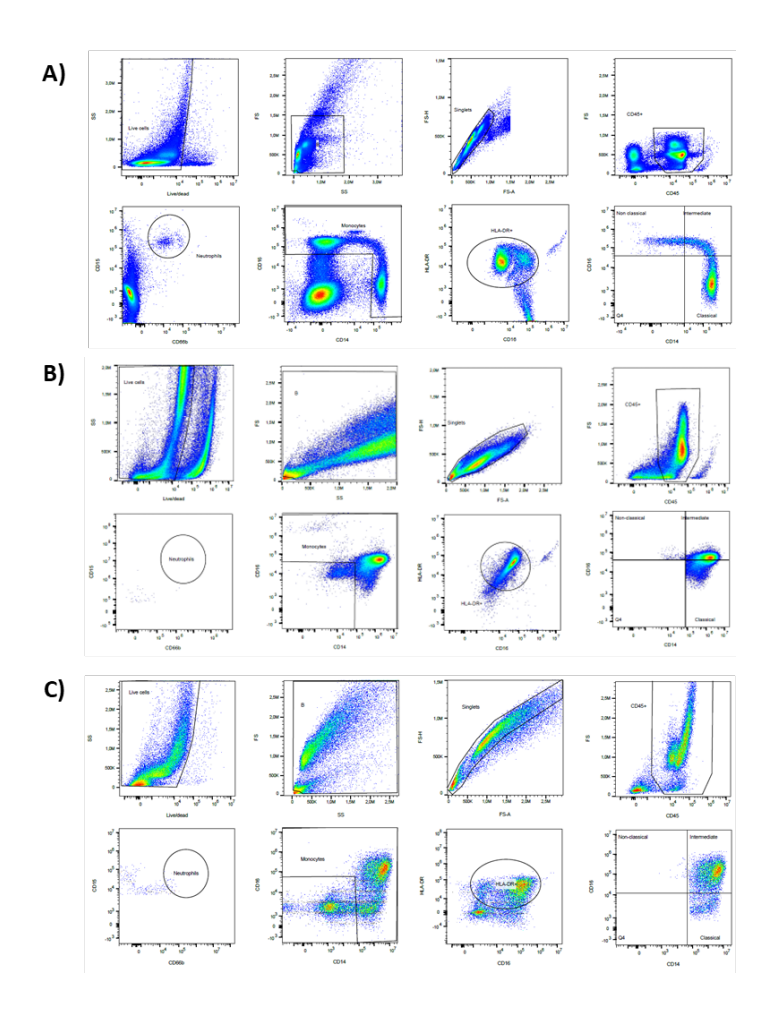
MGN is scientific founder of TTxD, Lemba and Biotrip. WHCR is consultant for Stryker for educational purposes only.

References

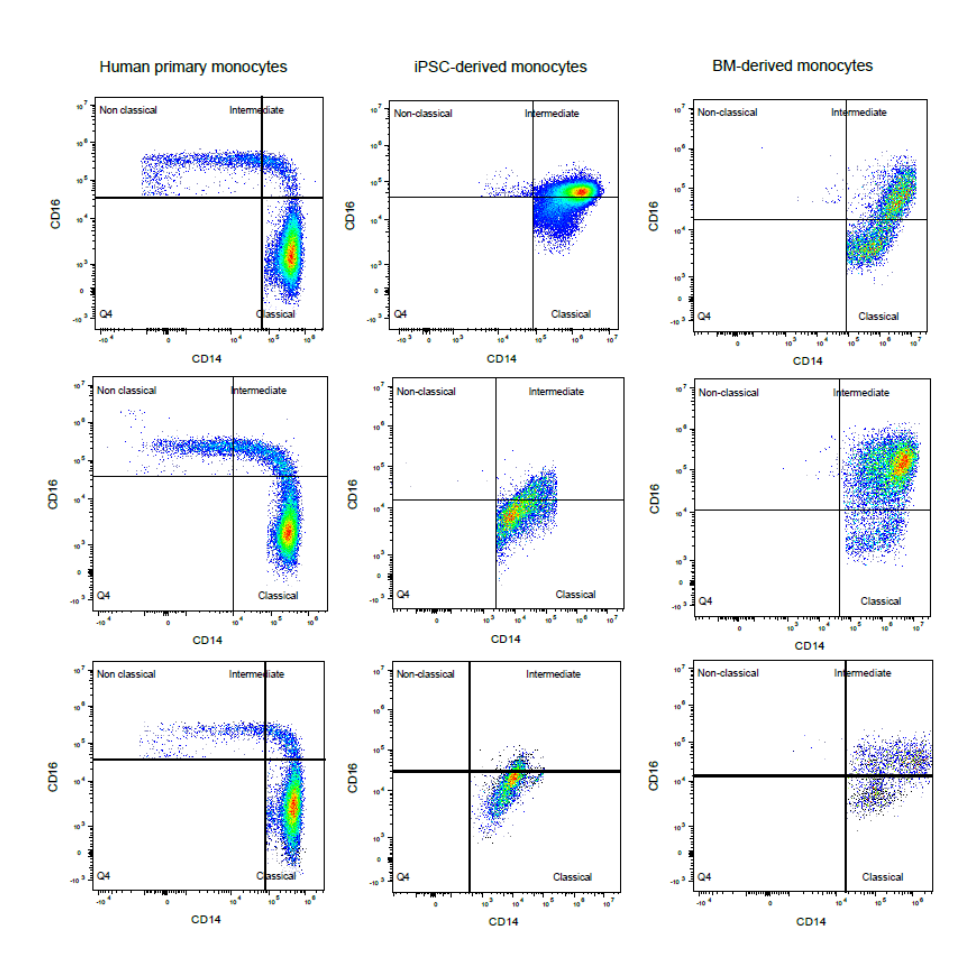
- Monkley S, Krishnaswamy JK, Göransson M, Clausen M, Meuller J, Thörn K, et al. Optimised generation of iPSC-derived macrophages and dendritic cells that are functionally and transcriptionally similar to their primary counterparts. PLoS One. 2020;15(12):e0243807.
- Williams H, Mack CD, Li SCH, Fletcher JP, Medbury HJ. Nature versus Number: Monocytes in Cardiovascular Disease. Int J Mol Sci. 2021;22(17).
- 3. Riksen NP, Bekkering S, Mulder WJM, Netea MG. Trained immunity in atherosclerotic cardiovascular disease. Nat Rev Cardiol. 2023;20(12):799-811.
- Domínguez-Andrés J, Dos Santos JC, Bekkering S, Mulder WJM, van der Meer JWM, Riksen NP, et al. Trained immunity: adaptation within innate immune mechanisms. Physiol Rev. 2023;103(1):313-46.
- Netea MG, Domínguez-Andrés J, Barreiro LB, Chavakis T, Divangahi M, Fuchs E, et al. Defining trained 5. immunity and its role in health and disease. Nature Reviews Immunology, 2020;20(6):375-88.
- 6. Ochando J, Mulder WJM, Madsen JC, Netea MG, Duivenvoorden R. Trained immunity — basic concepts and contributions to immunopathology. Nature Reviews Nephrology. 2023;19(1):23-37.
- Ter Horst R, Jaeger M, Smeekens SP, Oosting M, Swertz MA, Li Y, et al. Host and Environmental 7. Factors Influencing Individual Human Cytokine Responses. Cell. 2016;167(4):1111-24.e13.
- Janssen H, Kahles F, Liu D, Downey J, Koekkoek LL, Roudko V, et al. Monocytes re-enter the bone marrow during fasting and alter the host response to infection. Immunity. 2023;56(4):783-96.e7.
- Scott CL, Zheng F, De Baetselier P, Martens L, Saeys Y, De Prijck S, et al. Bone marrowderived monocytes give rise to self-renewing and fully differentiated Kupffer cells. Nature Communications. 2016;7(1):10321.
- 10. Buchrieser J, James W, Moore MD. Human Induced Pluripotent Stem Cell-Derived Macrophages Share Ontogeny with MYB-Independent Tissue-Resident Macrophages. Stem Cell Reports. 2017;8(2):334-45.
- 11. Patsch C, Challet-Meylan L, Thoma EC, Urich E, Heckel T, O'Sullivan JF, et al. Generation of vascular endothelial and smooth muscle cells from human pluripotent stem cells. Nat Cell Biol. 2015;17(8):994-1003.
- 12. Feher K, Kirsch J, Radbruch A, Chang HD, Kaiser T. Cell population identification using fluorescenceminus-one controls with a one-class classifying algorithm. Bioinformatics. 2014;30(23):3372-8.
- 13. Buenrostro JD, Wu B, Chang HY, Greenleaf WJ. ATAC-seq: A Method for Assaying Chromatin Accessibility Genome-Wide. Curr Protoc Mol Biol. 2015;109:21.9.1-.9.9.
- 14. Li H, Durbin R. Fast and accurate short read alignment with Burrows-Wheeler transform. Bioinformatics. 2009:25(14):1754-60.
- 15. Li H, Handsaker B, Wysoker A, Fennell T, Ruan J, Homer N, et al. The Sequence Alignment/Map format and SAMtools. Bioinformatics. 2009;25(16):2078-9.
- 16. Zhang Y, Liu T, Meyer CA, Eeckhoute J, Johnson DS, Bernstein BE, et al. Model-based analysis of ChIP-Seq (MACS). Genome Biol. 2008;9(9):R137.
- 17. Ramírez F, Ryan DP, Grüning B, Bhardwaj V, Kilpert F, Richter AS, et al. deepTools2: a next generation web server for deep-sequencing data analysis. Nucleic Acids Res. 2016;44(W1):W160-5.
- 18. Love MI, Huber W, Anders S. Moderated estimation of fold change and dispersion for RNA-seq data with DESeg2. Genome Biol. 2014;15(12):550.
- 19. Hirschfeld M, Ma Y, Weis JH, Vogel SN, Weis JJ. Cutting edge: repurification of lipopolysaccharide eliminates signaling through both human and murine toll-like receptor 2. J Immunol. 2000;165(2):618-22.

- 20. Kapellos TS, Bonaguro L, Gemünd I, Reusch N, Saglam A, Hinkley ER, et al. Human Monocyte Subsets and Phenotypes in Major Chronic Inflammatory Diseases. Front Immunol. 2019;10:2035.
- 21. Patel AA, Zhang Y, Fullerton JN, Boelen L, Rongvaux A, Maini AA, et al. The fate and lifespan of human monocyte subsets in steady state and systemic inflammation. J Exp Med. 2017;214(7):1913-23.
- 22. Ong SM, Hadadi E, Dang TM, Yeap WH, Tan CT, Ng TP, et al. The pro-inflammatory phenotype of the human non-classical monocyte subset is attributed to senescence. Cell Death Dis. 2018;9(3):266.
- 23. Ushach I, Zlotnik A. Biological role of granulocyte macrophage colony-stimulating factor (GM-CSF) and macrophage colony-stimulating factor (M-CSF) on cells of the myeloid lineage. J Leukoc Biol. 2016;100(3):481-9.
- 24. Cao X, Yakala GK, van den Hil FE, Cochrane A, Mummery CL, Orlova VV. Differentiation and Functional Comparison of Monocytes and Macrophages from hiPSCs with Peripheral Blood Derivatives. Stem Cell Reports. 2019;12(6):1282-97.
- 25. Beekhuis-Hoekstra SD, Watanabe K, Werme J, de Leeuw CA, Paliukhovich I, Li KW, et al. Systematic assessment of variability in the proteome of iPSC derivatives. Stem Cell Res. 2021;56:102512.
- 26. Tanaka T, Shiba T, Honda Y, Izawa K, Yasumi T, Saito MK, et al. Induced Pluripotent Stem Cell-Derived Monocytes/Macrophages in Autoinflammatory Diseases. Frontiers in Immunology. 2022;13.
- 27. Helft J, Böttcher J, Chakravarty P, Zelenay S, Huotari J, Schraml BU, et al. GM-CSF Mouse Bone Marrow Cultures Comprise a Heterogeneous Population of CD11c(+)MHCII(+) Macrophages and Dendritic Cells. Immunity. 2015;42(6):1197-211.
- 28. Nielsen MC, Andersen MN, Møller HJ. Monocyte isolation techniques significantly impact the phenotype of both isolated monocytes and derived macrophages in vitro. Immunology. 2020;159(1):63-74.
- 29. Ye L, Wang J, Beyer Al, Tegue F, Cradick TJ, Qi Z, et al. Seamless modification of wild-type induced pluripotent stem cells to the natural CCR5Δ32 mutation confers resistance to HIV infection. Proc Natl Acad Sci U S A. 2014;111(26):9591-6.
- 30. Zhou K, Han J, Wang Y, Xu Y, Zhang Y, Zhu C. The therapeutic potential of bone marrow-derived macrophages in neurological diseases. CNS Neuroscience & Therapeutics. 2022;28(12):1942-52.
- 31. Askenase MH, Han SJ, Byrd AL, Morais da Fonseca D, Bouladoux N, Wilhelm C, et al. Bone-Marrow-Resident NK Cells Prime Monocytes for Regulatory Function during Infection. Immunity. 2015;42(6):1130-42.
- 32. Zhou K, Han J, Wang Y, Xu Y, Zhang Y, Zhu C. The therapeutic potential of bone marrow-derived macrophages in neurological diseases. CNS Neurosci Ther. 2022;28(12):1942-52.
- 33. Mulder K, Patel AA, Kong WT, Piot C, Halitzki E, Dunsmore G, et al. Cross-tissue singlecell landscape of human monocytes and macrophages in health and disease. Immunity. 2021;54(8):1883-900.e5.
- 34. Austermann J, Roth J, Barczyk-Kahlert K. The Good and the Bad: Monocytes' and Macrophages' Diverse Functions in Inflammation. Cells. 2022;11(12).
- 35. Gumber D, Wang LD. Improving CAR-T immunotherapy: Overcoming the challenges of T cell exhaustion. EBioMedicine. 2022;77:103941.
- 36. Gao Z, Feng Y, Xu J, Liang J. T-cell exhaustion in immune-mediated inflammatory diseases: New implications for immunotherapy. Front Immunol. 2022;13:977394.

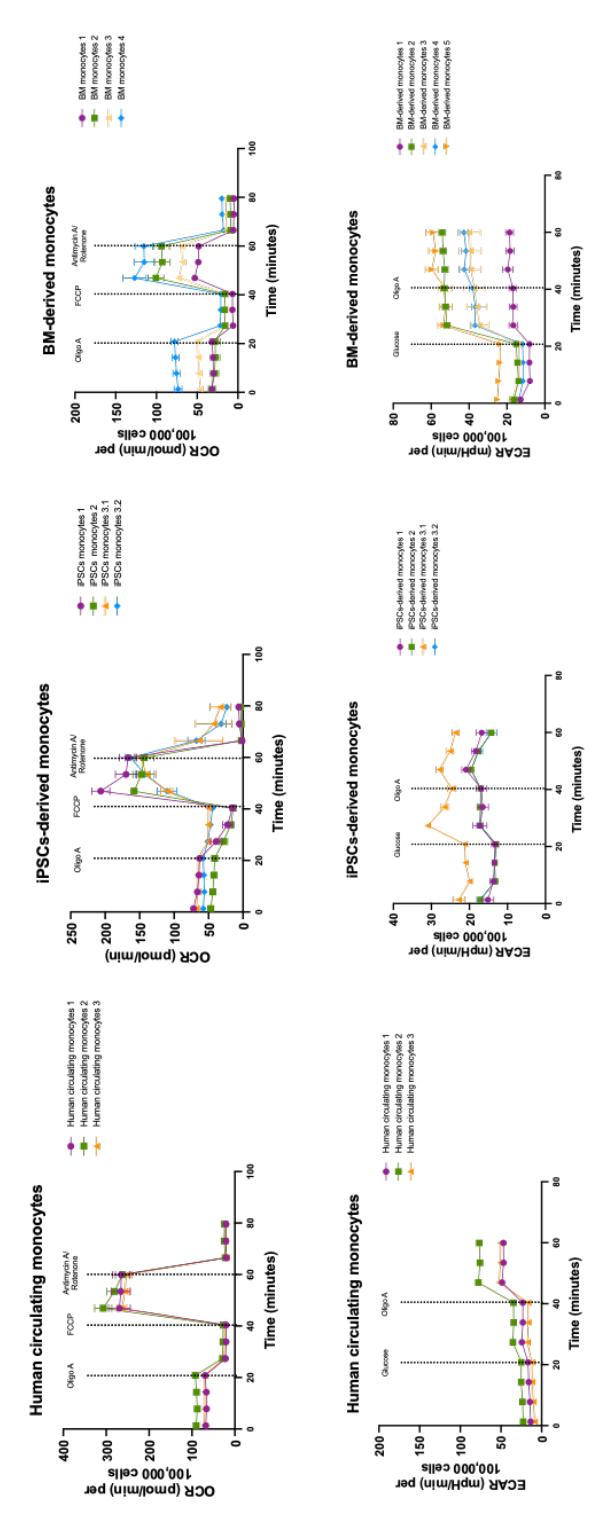
Supplementary Material



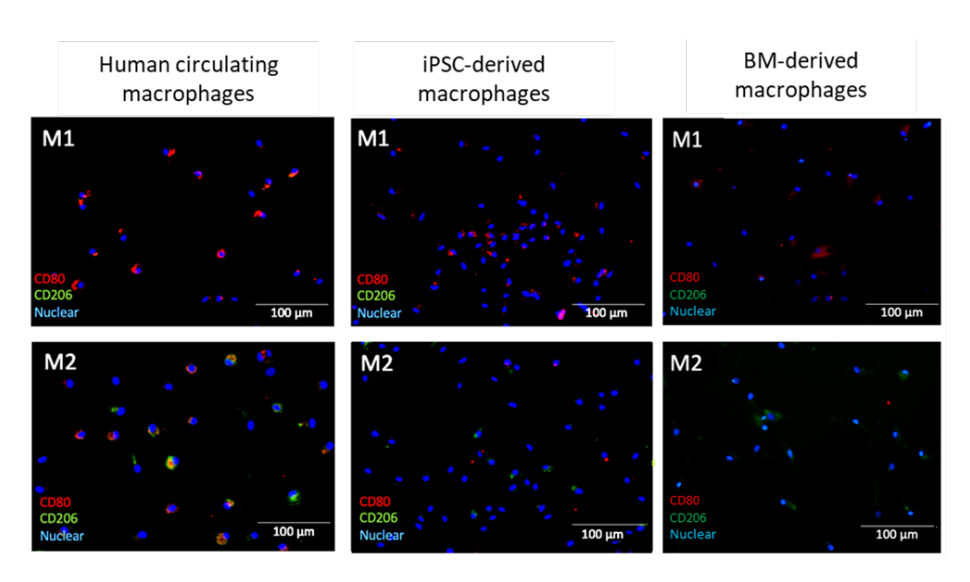
Supplementary Figure S1: Gating strategy of monocytes. In short, monocytes were selected based on CD45+ and forward scatter properties; subsequently, monocyte subsets were selected using the CD14/CD16 plot as percentage (%) of gated (HLA-DR/CD16). Monocyte subsets were identified according to current recommendations (Weber C, Schober A, Zernecke A. Chemokines: key regulators of mononuclear cell recruitment in atherosclerotic vascular disease. Arterioscler Thromb Vasc Biol. 2004 Nov;24(11):1997-2008. doi: 10.1161/01.ATV.0000142812.03840.6f. Epub 2004 Aug 19. PMID: 15319268). A) Gating strategy for human circulating monocytes. B) Gating strategy for iPSC-derived monocytes. C) Gating strategy for BM-derived monocytes.



Supplementary Figure S2: Individual dot plots of monocyte sources. Flow cytometry data of classical, intermediate, and non-classical monocytes of all cell sources and donors. Left column is n=3 for human circulating monocytes, middle column is n=3 for iPSC-derived monocytes, and right column is n=3 for bone marrow-derived monocytes.



Supplementary Figure 53: Individual Seahorse data for all donors per monocyte source. Mitochondrial respiration was measured by oxygen consumption rate (OCR) using a Cell Mito Stress Test Kit and glycolysis/extracellular acidification rate (ECAR) was measured using a Glyco Stress Test Kit.



Supplementary Figure S4: Supplementary Figure S4. Macrophages were stained to identify the presence of M1 (CD80) and M2 (CD206) macrophage surface markers (CD80 in red, CD206 in green, and Hoechst nuclear labeling in blue).

Supplementary Table S1: Flow cytometry panel used to identify monocytes and monocyte subsets from the different monocyte sources.

	Marker Fluorochrome Clone		Manufacturer	Cat #	RRID#	Dilution	
	CD16	FITC	3g8	Biolegend	302006	AB_314206	1:50
	HLA-DR	PE	immu-357	Beckman Coulter	IM1639	AB_131284	1:10
	CD10	PC5.5	HI10	Biolegend	312215	AB_ 10643591	1:10
	CD14	PC7	61D3	LifeTechnologies	25-0149-42	AB_1582276	1:50
	CD45	BV510	HI30	Biolegend	304036	AB_2561940	1:50
	CD66b	APC-700	G10F5	Biolegend	305114	AB_2566038	1:10
	CD15	APC-Cy7	W6D3	Biolegend	323047	AB_2750189	1:10

Abbreviations: Cluster of differentiation (CD), fluorescein isothiocyanate (FITC), phycoerythrin (PE), allophycocyanin (APC).



Chapter 6

Altered neutrophil phenotype and function in patients with calcific aortic valve disease

Wieteke Broeders*, Daniela Flores-Gomez*, Nils Rother, Niels van Royen, Erwin S. Zegers, Mihai G. Netea, Leo A. B. Joosten, Niels P. Riksen, Siroon Bekkering†, Saloua El Messaoudi†.

*Shared First Author
†Shared Senior Authors

In preparation

Abstract

Calcific aortic valve disease (CAVD) is characterized by valvular inflammation, fibrosis, and calcification, leading to valve thickening and subsequent outflow obstruction (aortic valve stenosis (AVS)). The exact underlying pathophysiology is not yet fully understood, but CAVD resembles atherosclerosis in pathology and shared risk factors. Neutrophils play an important role in cardiovascular inflammation and the possible contribution of neutrophils to CAVD pathogenesis recently gained attention. This study aimed to investigate in detail neutrophil phenotype and function in patients with CAVD.

In this exploratory cross-sectional study, blood was obtained from twelve patients with severe AVS and twelve age- and sex matched healthy controls. Whole blood composition was assessed, and neutrophils were characterized by flow cytometry. Granule protein secretion, reactive oxygen species (ROS) production and NADPH-oxidase (NOX)-dependent and -independent neutrophil extracellular trap (NET) formation were measured after *ex vivo* stimulation.

Patients with CAVD showed a trend towards a higher leukocyte count (p=0.054) compared to healthy controls, but there were no differences in absolute neutrophil numbers (p=0.898). Patients had a higher percentage of HLA-DR+ mature neutrophils (p=0.0148). Both unstimulated and zymosan-stimulated neutrophils of patients showed more ROS production (p=0.004 and p=0.003, respectively), but they displayed less spontaneous NET formation (p=0.034). Plasma concentrations of neutrophil granule protein S100A8/A9 were lower in patients compared to controls (p=0.008).

Neutrophils of patients with severe AVS have an altered phenotype compared to healthy controls and might contribute to CAVD pathophysiology. Validation of these data and additional in-depth studies are needed for better insights into the underlying mechanisms and for the development of new treatment targets.

Kevwords

Neutrophil, calcific aortic valve disease, cardiovascular inflammation

Introduction

Calcific aortic valve disease (CAVD) is a progressive, multifactorial disease, that is characterized by inflammation and fibrocalcific remodeling of the aortic valve (1, 2). This process leads to valve leaflet thickening and cardiac outflow obstruction, which is called aortic valve stenosis (AVS), and this can eventually result in heart failure, syncope, angina and sudden cardiac death (1). AVS has a low prevalence in patients younger than 60 years, but it increases exponentially to one in eight patients older than 75 years of age (3). Currently, there is no pharmacological treatment strategy available that can prevent or limit CAVD, and the only treatment option is surgical or percutaneous replacement of the aortic valve in patients with a symptomatic severe AVS.

The precise underlying pathophysiological process of CAVD remains incompletely understood, yet it resembles atherosclerotic cardiovascular disease (ASCVD) in shared risk factors like hypertension, dyslipidemia and diabetes mellitus (4, 5), as well as in pathology (6, 7). It is increasingly recognized that CAVD, like ASCVD, is a chronic inflammatory disease in which innate immune cells, including monocytederived macrophages, play an important role (6, 8). Neutrophils also play a crucial part in cardiovascular inflammation (9), and possibly also in the development of CAVD (6, 10).

Neutrophils are the most abundant leukocyte type in peripheral blood and they are important in the first line defense against invading micro-organisms (11). Upon activation by exogenous or endogenous stimuli, neutrophils are activated, which results in the production of reactive oxygen species (ROS), formation neutrophil extracellular traps (NETs), and secretion of granule proteins (9), processes which contribute to induction of inflammation. Recent studies have investigated a few neutrophil characteristics in the context of CAVD. An increased neutrophilto-lymphocyte ratio is associated with the presence, severity and prognosis of CAVD (12, 13). Emerging evidences indicates that ROS play a causal role in the pathophysiology of CAVD (14-16). Explanted valves of patients with severe AVS without documented significant ASCVD have a higher amount of NETs compared to healthy valves (17). Moreover, patients with severe AVS have elevated plasma concentrations of citrullinated H3 (CitH3), a biomarker for NET formation, compared to controls, and the amount of plasma concentration and valvular CitH3 was associated with disease severity (17). The concentration and activity of neutrophil elastase, a serine protease secreted by neutrophils upon stimulation which promotes inflammation and valvular calcification, is significantly higher in patients with CAVD than in controls (5).

Based on these preliminary data, we hypothesized that neutrophils of patients with CAVD have a pro-inflammatory phenotype and contribute to the progression of CAVD. Therefore, in an exploratory study, we assessed in detail neutrophil characteristics and function in patients with severe CAVD and healthy controls.

Methods

Study design

We performed a cross-sectional study at the Radboud University Medical Centre and the Canisius Wilhelmina hospital in Nijmegen, the Netherlands, to investigate the role of Myeloid Cells in Aortic Valve Stenosis (MIRACLE) (ClinicalTrials.gov Identifier: NCT04717219). Circulating neutrophils were examined in a subgroup of the participants in this study, which is presented in this manuscript. Due to its explorative nature, no formal sample size calculation was performed for these analyses. The study protocol (NL72973.091.20) was approved by the Medical Ethics Committee Region Arnhem-Nijmegen. Written informed consent was given by all participants. All the experiments were conducted in line with the Declaration of Helsinki.

Population

Patients above 18 years of age with AVS (as defined by transthoracic echocardiography according to the 2017 ESC-EACTS guidelines for the management of valvular heart disease) (18) were screened for eligibility at the Department of Cardiology or Cardiothoracic Surgery of Radboud university medical center or Canisius Wilhelmina Hospital. Healthy control subjects were recruited by local advertisements and came to the hospital for screening and a transthoracic cardiac ultrasound to rule out AVS. Mild aortic valve sclerosis without stenosis was allowed.

Exclusion criteria were a recent acute ischemic cardiac event (<3 months before inclusion), active (auto-)inflammatory or auto-immune disease, the use of anti-inflammatory drugs, recent vaccination or infection (< 1 month before inclusion), history of endocarditis, history of radiation therapy of the chest, active malignancy (except for local basal cell carcinoma of the skin or local squamous cell skin carcinoma) and a history of bone marrow transplantation.

Sample collection

Medical history, cardiovascular risk factors and medication use were obtained from the participants. Echocardiography and coronary angiography (CAG) reports were collected. A physical examination was performed, and weight, height and blood pressure were assessed.

Blood was drawn through venous puncture into EDTA vacutainers (Becton Dickinson, Franklin Lakes, NJ, USA). Glucose, glycated hemoglobin (HbA1c), creatinine, urate, triglycerides, high-density lipoprotein (HDL) cholesterol and total cholesterol were measured using standardized methods in the hospital laboratory. Low-density lipoprotein (LDL) cholesterol was calculated using the Friedewald formula. The glomerular filtration rate was determined with the Chronic Kidney Disease Epidemiology Collaboration (CKD-EPI) equation.

Whole blood composition and circulating plasma markers

The composition of the whole blood was assessed using the Sysmex XN-450 automated hematology analyzer (Sysmex, Kobe, Japan). The blood vacutainers were centrifuged for 10 minutes at 2744 g at room temperature (RT). Plasma was removed and stored immediately at -80°C until further analysis.

High sensitivity C-reactive protein (hsCRP) and high sensitivity interleukin 6 (hs IL-6) were measured in plasma using a commercially available enzyme linked immune assay (ELISA) kit (R&D systems, Minneapolis, USA, cat# DY1707 and HS600C, respectively). Plasma lipoprotein(a) (Lp(a)) was measured using an in-house developed ELISA (supplemental materials).

Flow cytometry

Circulating neutrophils were phenotyped with flow cytometry using mouse monoclonal antibodies targeting cluster of differentiation (CD) 16, HLA-DR, CD62L, CD49d, CD10, CD66b, CD15, CD123, CD45, CD365, CD11b and a lineage cocktail containing antibodies targeting CD3, CD14, CD19, CD20 and CD56 (Table S1). The preparation of the samples is described in the supplemental material. Cell populations and neutrophil activation markers were measured on a CytoFlex cytometer (Beckman Coulter, Brea, USA; RRID; SCR 017217), FlowJo software (Beckton Dickinson, version 10.8.0) was used to analyze the data with a manual gating strategy (Figure S1). A VersaComp Antibody Capture bead kit (Beckman Coulter) was used to perform a compensation every two weeks and a quality control to correct for laser setting variations was performed daily. An unstained sample was measured for all samples to check for autofluorescence.

Reagents

Cells were cultured in Roswell Park Memorial institute (RPMI, Gibco) 1640 Dutch modified culture medium without phenol red supplemented with 50 ug/ml gentamycin (Centrafarm), 1 mM pyruvate (Invitrogen) and 2 mM glutamine (Invitrogen). Toll-like receptor (TLR) agonist Pam3Cys (P3C) for TLR2 (EMC microcollections, L2000). Other reagents included Nigericin (Invivogen, tIrl-nig), phorbol 12-myristate 13-acetate (PMA, Sigma), Micrococcal Nuclease (MNase, Worthington Biochemical Corporation, LS004797) and Thrombin Receptor Activator Peptide 6 (Trap6, Sigma).

Neutrophil isolation

Neutrophils were isolated by first removing the peripheral blood mononuclear cell (PBMC) fraction by Ficoll-Paque PLUS (GE Healthcare Biosciences) density-gradient centrifugation. After separation, plasma was collected and set aside for platelet isolation. The PBMC fraction was removed by aspiration to continue with the neutrophil isolation by hypotonic lysis. In short, leftover cells (peripheral polymorphonuclear neutrophils and erythrocytes) were incubated twice (15 and 10 minutes respectively) with hypotonic lysis buffer (155 mM NH4Cl [Merck], 10 mM KHCO₃ [Sigma]) to remove the erythrocytes and other cells washing with cold phosphate buffered saline (PBS, Gibco) in between the lysis steps (348 g, 10 minutes, 4°C). Then, the neutrophils were washed two additional times with cold PBS to remove the remaining lysed erythrocytes and were resuspended in RPMI. Number and purity were determined by counting in the Sysmex.

Platelet isolation

The plasma supernatant collected after Ficoll-Paque density-gradient was diluted in platelet buffer (PBS + 0.1% human pooled serum + 1mM UltraPure EDTA [0.5 M, pH 8, Life Technologies]) and centrifuged at 190 G, 15 minutes at RT to obtain platelet rich plasma (PRP). To isolate the platelets, PRP was centrifuged for 5 minutes at 2500 G, 4°C. Platelets were resuspended in RPMI, counted in the Sysmex and diluted to a concentration of 200 million per ml.

Neutrophil stimulation assay

Neutrophils were diluted to a concentration of 5 million cells per ml. 500,000 cells were then seeded in duplo in a 96-well flat bottom plate (Sarstedt) and were incubated with culture medium or 0.014% ethanol (Merck) only as negative controls, 1 ug/ml LPS, 10 ug/ml P3C, 1 uM Nigericin and 50 nM PMA for 4 hours at 37°C, 5% CO₂. After incubation, the plate was centrifuged at 348 g for 8 minutes at RT, and 180 ul of cell culture supernatant was collected. Additionally, 100 ul of

0.5% Triton X (Sigma) were added to the well for intracellular measurements. All the material was stored at -80°C until further analysis.

NOX-dependent neutrophil extracellular traps (NET) formation assay

Neutrophils were diluted to a concentration of 1 million cells per ml. 100,000 cells were seeded in quadruple in a flat bottom plate and attached for 20 minutes at 37°C, 5% CO₂. After attachment, medium was removed and cells were stimulated with cell culture medium and ethanol as negative control, 1 uM Nigericin and 50 nM PMA and incubated for 3 hours at 37°C, 5% CO₃ to induce NOX-dependent NETosis. After 3 hours, cells were washed 2 times with warm PBS, after which NETs were digested with 5 U/ml of MNase for 20 minutes at 37°C, 5% CO₂, followed by deactivation of the enzyme by vortexing and pooling of quadruples in duplos. Supernatants were collected by first centrifuging the samples for 5 minutes at 1000 g RT and stored at -80°C until further analysis.

NOX-independent NETs formation assay

100 million platelets were incubated with cell culture medium only or stimulated with 156 uM Trap6, which activates protease activated receptor 1 and induces aggregates, for 30 min at 37°C, 5% CO₃. After incubation, platelets were diluted 1:4 in RPMI. In the meantime, neutrophils were diluted to a concentration of 1 million cells per ml. 100,000 cells were seeded in quadruple in a flat bottom plate and attached for 20 min at 37°C, 5% CO₂. After attachment, cells were incubated with RPMI cell culture medium as negative control, 1:4 diluted unstimulated or Trap6 stimulated platelets for 1 hour at 37°C, 5% CO₂ to induce NOX-independent NETosis. After incubation, NETs were digested with MNase and supernatant was collected and stored as described in the NOX-dependent assay above.

ROS production in neutrophils

Reactive oxygen species (ROS) production by neutrophils was measured with a luminol-based luminescence assay, which measures both intra- and extracellular ROS. Neutrophils were diluted to a concentration of 1 million cells per ml. 200,000 cells were seeded in quadruplicate in a white flat bottom plate (Corning) and were stimulated with cell culture medium only as negative control, 3.6 mg/ml Zymosan or 50 nM PMA. Relative integral luminesce units per second (RLU/s) were measured in the BioTek Synergy HT multi-reader during one hour in intervals of 142 seconds.

NET formation measurement with Sytox Orange

The DNA content in the NETs formation assay supernatants (NOX-dependent and NOX-independent formation assay) was quantified by adding 5 mM Sytox Orange Nucleic Acid Stain (Life Technologies) solution to a pooled and undiluted sample. Fluorescence was measured with excitation and emission of 530/560 nm respectively in the BioTek Synergy HT multi-reader. All the measurements were done in singular.

NET formation measurement with ELISA

NET quantification in plasma (NOX-dependent and NOX-independent NETs formation assay) was done as previously described (19). In short, plates were coated with anti-DNA antibody (#36) or anti-histone antibody (KM2) to detect N-terminal histone tails in NOX-dependent and NOX-independent NETs. Plates were then blocked with 2% fish gelatin (Sigma). Plasma was added and incubated with an anti-MPO IgG1 secondary antibody (BioLegend, 667802, dilution 1:2000). Horseradish peroxidase (HRP) conjugated with streptavidin (R&D) was added followed by substrate solution to catalyze the colored reaction. ELISA was read at 450 nm in Biotek 800TS microplate reader.

Granule proteins measurement

Human neutrophil elastase (ELA2, DY9167) was measured in previously collected plasma. Human myeloperoxidase (MPO, DY3174), human lipocalin-2 (NGAL, DY1757), and human S100A8/S100A9 heterodimer (DY8226) were measured in previously collected plasma as well as cell culture supernatants after 4 hours stimulation. All granule proteins were measured according to the manufacturer's instructions (BioTechne R&D Systems). The ELISA was read at 450 nm in a Biotek 800TS microplate reader.

Statistical analysis

Continuous baseline characteristics are reported as mean ± standard deviation (SD) for normally distributed variables or as median with interquartile range (Q1-Q3) for not normally distributed variables and are compared between patients with CAVD and healthy controls with the independent samples T-test (normal distribution) or Mann-Whitney U test (non-normal distribution). The Shapiro-Wilk test was used to test for normality of the baseline characteristics. The categorical variables are presented as numbers with the percentage and are compared using the Chisquare test or Fisher's exact test. Due to the small sample size and since most of the inflammatory parameters have a non-Gaussian distribution, the Mann-Whitney U test was used to compare the *ex vivo* data. The data was visually inspected and in case of potential outliers, the Robust regression and outlier removal (ROUT) test was performed. No imputation was performed in case of missing data. A two-sided p-value below 0.05 was considered to be statistically significant. The specific details per statistical comparison are mentioned in the Figure legends. The analyses were performed using GraphPad prism version 10.0.1 and SPSS version 27.

Results

Patient characteristics

Twelve patients with severe AVS without a history of atherosclerotic events and 12 age- and sex-matched healthy controls were included in the analyses. Their baseline characteristics are listed in Table 1. There were no statistically significant differences in BMI and blood pressure. All participants had a tricuspid aortic valve. In nine (75%) of the patients with severe AVS, a recent coronary angiogram (CAG) had recently been performed. None of these patients had obstructive coronary artery disease. The patients with CAVD used more medication, but the difference was only statistically significant for the use of acetylsalicylic acid (p=0.037). The concentrations of total cholesterol and LDL cholesterol were higher in the healthy controls (p=0.013 and p=0.011, respectively).

Table 1: Participant characteristics

	Healthy controls (N=12)	Patients with CAVD (N=12)	p-value
Demographics			
Age (years)	74.4 ± 4.9	75.5 ± 5.1	0.604
Sex, male (%)	7 (58)	7 (58)	-
Clinical parameters			
BMI (kg/m²)	23.1 [21.5-29.0]	28.4 [21.8-31.8]	0.319
Systolic blood pressure (mmHg)#	144 ± 10	152 ± 27	0.376
Diastolic blood pressure (mmHg)#	80 ± 10	76 ± 10	0.232
Medical history			
Angina (%)	0 (0)	2 (16.7)	0.478
Peripheral artery disease (%)	0 (0)	0 (0)	-
Heart failure (%)			<0.001
No heart failure	12 (100)	2 (16.7)	
NYHA II	0 (0)	8 (66.7)	
NHYA III	0 (0)	2 (16.7)	
Atrial fibrillation (%)	0 (0)	3 (25)	0.217
Pacemaker (%)	0 (0)	1 (8.3)	1.000
Diabetes mellitus type II	0 (0)	3 (25)	0.217
Hypertension (%)	4 (33)	6 (50)	0.680
Hyperlipidaemia (%)	1 (8)	5 (42)	0.155
Smoking (%)			0.667
Never smoked	3 (75)	4 (33)	

Table 1: Continued

	Healthy controls (N=12)	Patients with CAVD (N=12)	p-value
Stopped smoking	9 (75)	7 (58)	
Currently smoking	0 (0)	1 (8)	
Packyears (years)†	15 [12-27]	15 [4-38]	0.689
Medication use			
Lipid lowering therapy			
Statins (%)	1 (8)	5 (42)	0.155
Ezetimib (%)	0 (0)	1 (8)	1.000
Antiplatelet / anticoagulant			
Acetylsalicylic acid (%)	0 (0)	5 (42)	0.037
DOAC (%)	0 (0)	3 (25)	0.217
Diuretics (%)	1 (8)	5 (42)	0.155
Beta blocker (%)	2 (17)	3 (25)	1.000
Calcium channel blocker (%)	1 (8)	2 (17)	1.000
RAAS inhibitor (%)	1 (8)	4 (33)	0.317
Antidiabetic drugs			
Metformin (%)	0 (0)	3 (25)	0.217
Sulfonylurea derivates (%)	0 (0)	1 (8)	1.000
GLP1 agonist (%)	0 (0)	1 (8)	1.000
Blood measurements			
Total cholesterol (mmol/L)	5.38 ± 0.85	4.41 ± 0.929	0.013
LDL cholesterol (mmol/L)	3.21 ± 0.90	2.27 ± 0.76	0.011
HDL cholesterol (mmol/L)	1.63 ± 0.38	1.52 ± 0.38	0.464
Triglycerides (mmol/L)	1.19 [0.81-1.48]	1.16 [0.71-1,.9]	0.932
Lp(a) (mg/L)	110 [33-268]	155 [40-231]	0.514
Creatinine (µmol/L)	80 ± 19	75 ± 16	0.539
GFR (CKD-EPI, ml/min/1.73m2)	84 [62-87]	80 [67-89]	0.671
Uric acid (mmol/L)	0.32 ± 0.07	$0.33 \pm 0,09$	0.557
Glucose (mmol/L)	5.6 [5.3-5.9]	5.9 [4.9-7.6]	0.630
HbA1c (mmol/mol)	37 [36-40]	40 [38-47]	0.128
Imaging			
Echocardiography		N.A.	
AVA (cm²)	0.76 ± 0.23		-
Mean gradient (mmHg)	50 ± 14		-
Maximum aortic velocity (m/s)	4.55 ± 0.60		-
Left ventricular function (%)*	56 [50-60]		-

Table 1: Continued

	Healthy controls (N=12)	Patients with CAVD (N=12)	p-value
Coronary angiography		N.A.	
CAG present (%)	9 (75)		-
No abnormalities / wall irregularities (<30%) (%)	6 (50)		-
30-49% stenosis (%)	2 (16.7)		-
50-69% stenosis (%)	1 (8.3)		-

Data is presented as mean ± standard deviation, median with interquartile range [Q1-Q3] or as number with the percentage and is compared using the appropriate statistical test.

Data is missing for one healthy control, † data is missing for two patients with CAVD, * data is missing for 1 CAVD patient. (AVA) aortic valve area, (BMI) Body mass index, (CAG) coronary angiography (CAVD) Calcific aortic valve disease, (CKD-EPI) chronic kidney disease epidemiology collaboration, (DOAC) Direct oral anticoagulant, (GLP) Glucagon-like peptide, (HbA1c) Glycated haemoglobin, (HDL) highdensity lipoprotein, (LDL) low-density lipoprotein, Lp(a) lipoprotein (a), (N.A.) Not applicable, (NYHA) New York Heart Association, (RAAS) Renin-angiotensin-aldosterone system.

Whole blood composition and circulating inflammatory markers

Whole blood composition was assessed, and the results are shown in Table 2. Patients showed a trend towards a higher absolute leukocyte count as compared to healthy controls (p=0.054). There was no difference in the absolute number of neutrophils or monocytes, but patients had a higher number of lymphocytes (p=0.014). This resulted into a lower percentage of neutrophils (p=0.002) for the patients compared to the healthy controls.

To further study systemic inflammation, circulating hslL-6 and hsCRP concentrations were measured. No differences were seen in circulating plasma hsIL-6 (p=0.932) and hsCRP (p=0.410) concentrations between patients with CAVD and healthy controls (Table 2).

Patients with CAVD have more HLA-DR+ mature neutrophils

Neutrophils were subsequently phenotyped using flow cytometry (Figure 1, Table S2). Firstly, the maturation status was determined. There were no differences in the percentage of immature (CD10-) and mature (CD10+) neutrophils between patients with CAVD and healthy controls (p=0.182 and p=0.828, respectively) and the expression of CD49d, an integrin expressed by immature neutrophils (20), was similar (p=0.745, Table S2). The presence and MFI of multiple activation markers was then assessed on both mature and immature neutrophils. There was a higher percentage of HLA-DR+ mature neutrophils in patients with CAVD (p=0.015), although the HLA-

DR MFI did not differ (p= 0.319) (Figure 1A). The percentage of HLA-DR+ immature neutrophils was also higher in patients than in healthy controls, yet the difference was not statistically significant (p=0.053, Figure 1B). Furthermore, the patients had less CD62L+ immature neutrophils (p=0.002), but with a similar MFI compared to the healthy controls (p=0.410, Figure 1C). There were no differences in the expression of the activation marker CD62L on mature neutrophils and of CD16, CD66b, CD15, CD11b and CD35+ on both mature and immature neutrophils (Table S2).

Table 2: Whole blood composition and circulating inflammatory parameters

	Healthy controls N = 12	Patients with CAVD N = 12	P-value
Leukocytes (10³/uL)	5.1 [4.8-6.0]	5.9 [5.3-7.0]	0.054
Hemoglobin (mmol/L)	8.9 [8.1-9.3]	8.5 [8.1-9.9]	0.944
Platelets (10³/uL)	231 [194-264]	189 [174-245]	0.236
Neutrophils (10³/uL)	3.2 [2.8-3.8]	3.2 [2.6-4.1]	0.898
Lymphocytes (10³/uL)	1.3 [1.2-1.6]	1.7 [1.6-2.6]	0.014
Monocytes (10³/uL)	0.5 [0.4-0.5]	0.5 [0.4-0.6]	0.086
Eosinophils (10³/uL)	0.1 [0.1-0.1]	0.2 [0.1-0.3]	0.013
Basophils (10³/uL)	0.03 [0.0-0.04]	0.02 [0.02-0.03]	>0.999
Neutrophils % of leukocytes)	61.7 [59.9-68.0]	50.6 [49.2 -58.1]	0.002
Lymphocytes (% of leukocytes)	26.5 [22.6-28.2]	32.2 [25.7-39.0]	0.092
Monocytes (% of leukocytes)	8.7 [7.6-10.2]	8.8 [7.8-10.7]	0.744
Eosinophils (% of leukocytes)	1.9 [1.5-2.7]	3.6 [1.6-4.9]	0.043
Basophils (% of leukocytes)	0.5 [0.3-0.6]	0.4 [0.3-0.4]	0.370
hsCRP (mg/L)	1.2 [0.7-6.9]	1.5 [0.9-2.1]	0.932
hs IL-6 (mg/L)	1.5 [0.9-3.1]	2.4 [1.3-4.0]	0.410

Neutrophils can be divided into subsets based on their expression of CD16 and CD62L (21, 22). The neutrophils of patients with CAVD and healthy controls showed a similar subset distribution (Figure 1D).

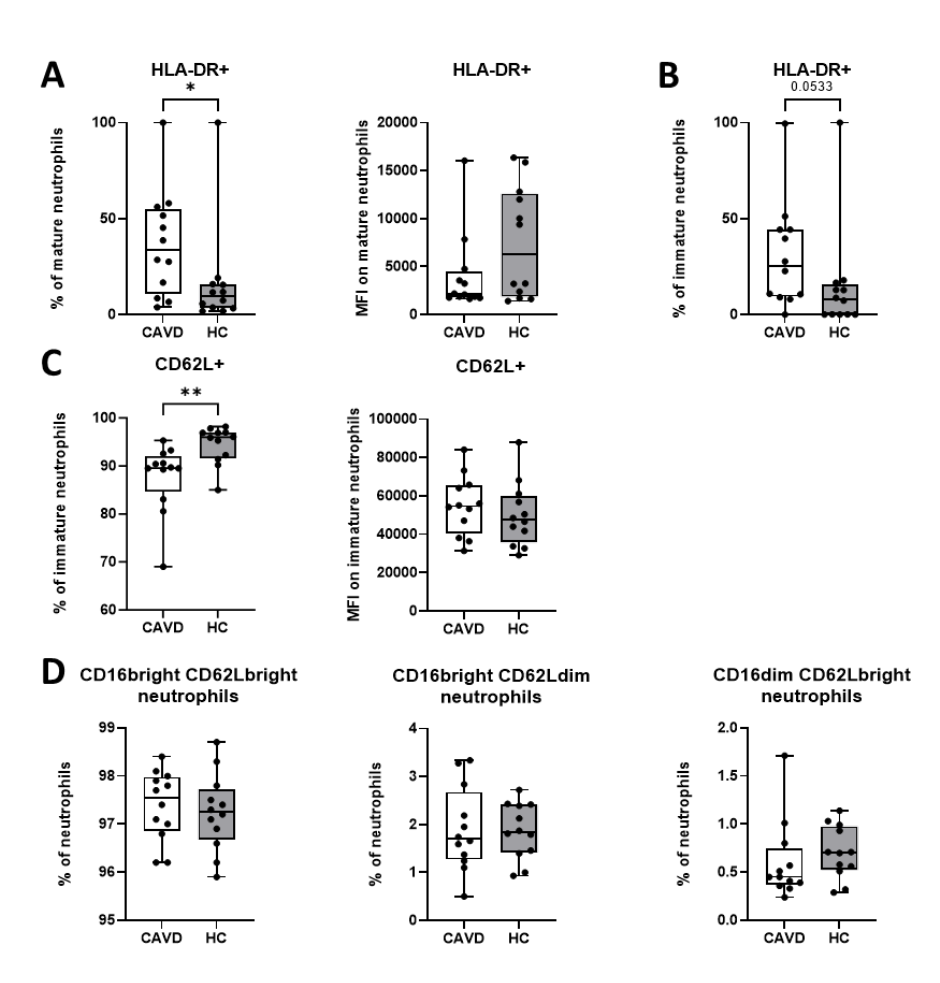


Figure 1: Mature neutrophils from patients with CAVD express more HLA-DR. Neutrophils were phenotyped using flow cytometry. (A) Percentage of HLA-DR positive mature neutrophils and the median fluorescence intensity (MFI) of HLA-DR on these mature neutrophils. (B) Percentage of HLA-DR positive immature neutrophils. (C) Percentage of CD62L positive immature neutrophils and the MFI of CD62L on these immature neutrophils. (D) Neutrophil subsets, divided into CD16brightCD62Lbright, CD16brightCD62Ldim and CD16dimCD62Lbright neutrophils. Data is presented with boxplots and is compared with the Mann-Whitney U test; *p<0.05, **p<0.01; n=12 healthy controls and n=12 patients with CAVD. (CAVD) Calcific aortic valve disease, (HC) healthy control.

Neutrophils from patients with CAVD produce more ROS

To measure intra- and extracellular ROS, neutrophils were exposed to RPMI (negative control), zymosan and PMA, and ROS production was subsequently measured with a luminescence-based assay. Figure 2A shows the ROS production over time in intervals of one hour. We then calculated the mean area under the curve as indication of the total ROS production measured over time (Figure 2B). Neutrophils from patients produced more ROS than controls in all three conditions, however this was only statistically significant for unstimulated neutrophils (p=0.004) and after restimulation with zymosan (p=0.003).

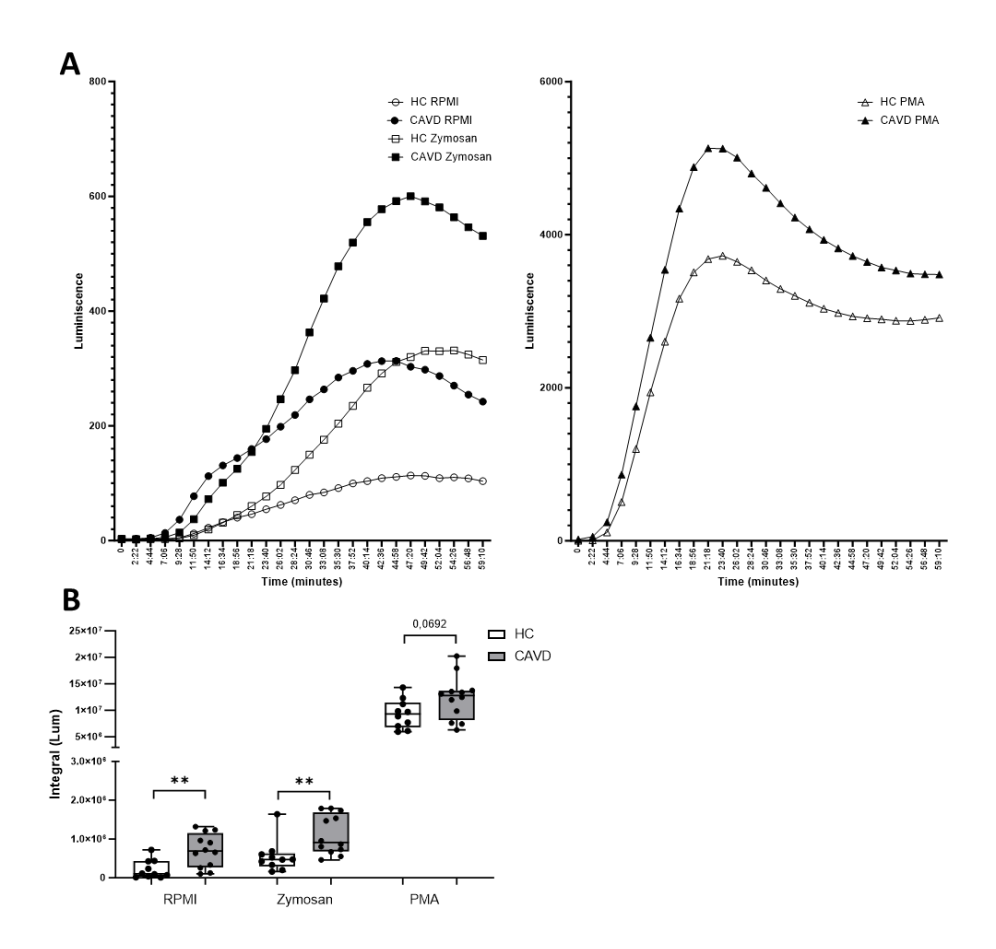


Figure 2: Neutrophils of patients with CAVD produce more ROS. Neutrophils from patients with CAVD and healthy controls were exposure for 1 hour to RPMI (negative control), zymosan and PMA and total reactive oxygen species (ROS) production was measured. (A) ROS production measured over time in intervals of 142 seconds for 1 hour. (B) Integral luminescence indicating total ROS production after 1 hour of stimulation of neutrophils from patients with CAVD and controls with RPMI (negative control), zymosan and PMA. Data is presented with boxplots and is compared with the Mann-Whitney U test; **p<0.01; n=10 for controls and n=12 for patients with CAVD; outliers removed using ROUT method (see materials and methods). (CAVD) Calcific aortic valve disease, (HC) healthy control.

Less neutrophil extracellular trap formation by patients with CAVD

To evaluate NET formation in patients with CAVD and healthy controls, we assessed both circulating levels of NETs as well as induced NOX-dependent and NOX-independent NET formation in stimulated neutrophils.

We quantified N-terminal histone tails (#36) exclusive to NOX-dependent NET formation and N-terminal histone tails exclusive of NOX-independent NET formation (KM2) in plasma. A trend to less NOX-dependent circulating NETs was observed in patients (p=0.066, Figure 3A), but there was no difference in the amount of circulating NOX-independent NETs (p=0.9774, Figure 3B).

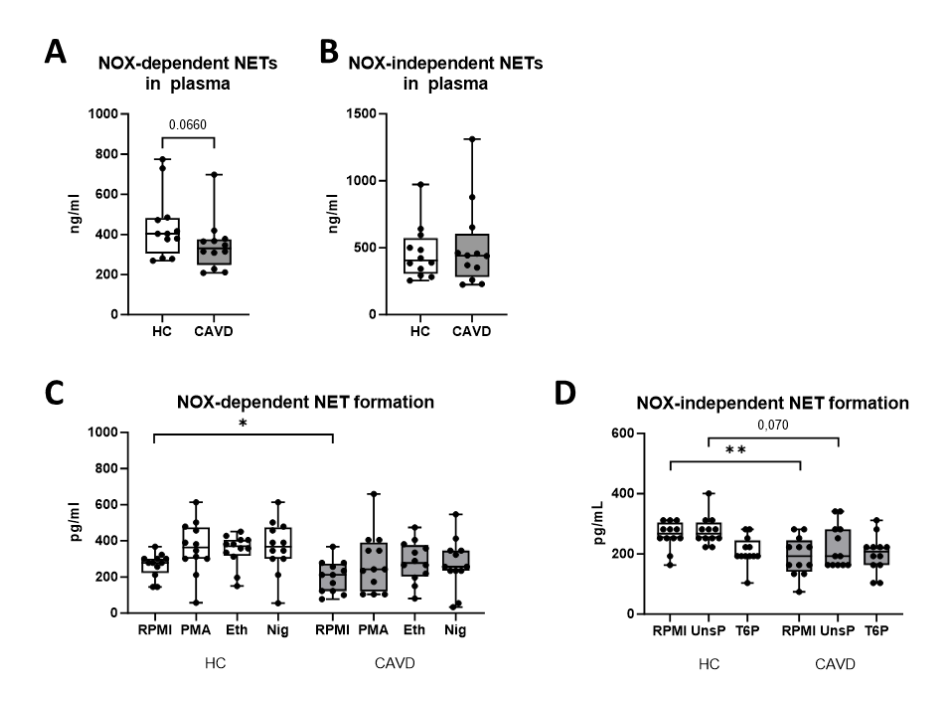


Figure 3: NADPH-oxidase-dependent and NOX-independent neutrophil extracellular trap formation after stimulation of neutrophils from patients with CAVD and healthy controls. Circulatory (A) NADPHoxidase (NOX) -dependent and (B) NOX-independent neutrophil extracellular traps (NETs) were quantified with ELISAs using anti-DNA antibodies (#36) or anti-histone antibodies (KM2), respectively. Neutrophils isolated from patients with CAVD and controls were stimulated for 3 hours with nigericin and PMA (RPMI and ethanol as negative controls) to induce NOX-dependent NET formation and for 1 hour with unstimulated and Trap6 stimulated autologous platelets for induce NOX-independent NET formation. (C) Total DNA from NETs produced by NOX-dependent and (D) independent NET formation measured in cell culture supernatants with Sytox Orange. Data is presented with boxplots and is compared with the Mann-Whitney U test; *p<0.05, **p<0.01; n=12 healthy controls and n=12 patients with CAVD. (CAVD) Calcific aortic valve disease, (HC) healthy control.

Purified neutrophils were stimulated for 3 hours with nigericin and PMA (RPMI and ethanol as negative controls) to induce NOX-dependent NET formation. Unstimulated neutrophils (RPMI control) of patients showed less spontaneous NOXdependent NET formation compared to controls (p=0.034, Figure 3C). Furthermore, both neutrophils from patients and controls produce significantly more total NETs after exposure to ethanol compared to RPMI (p=0.002; p<0.001) but not to nigericin compared to ethanol (p=0.776; p=0.470). This is also true for stimulation with PMA in controls (p=0.014) (Figure 3C).

Isolated neutrophils were stimulated for 1 hour with unstimulated and Trap6 stimulated autologous platelets for induce NOX-independent NET formation. Unstimulated neutrophils (RPMI control) of patients also showed less NOX-independent NET formation compared to controls (p=0.006, Figure 3D). The same can also be observed after exposure to unstimulated platelets, however this effect was not significant (p=0.070). In addition, stimulated platelets significantly reduce total NET formation in controls but not in patients (p=0.006).

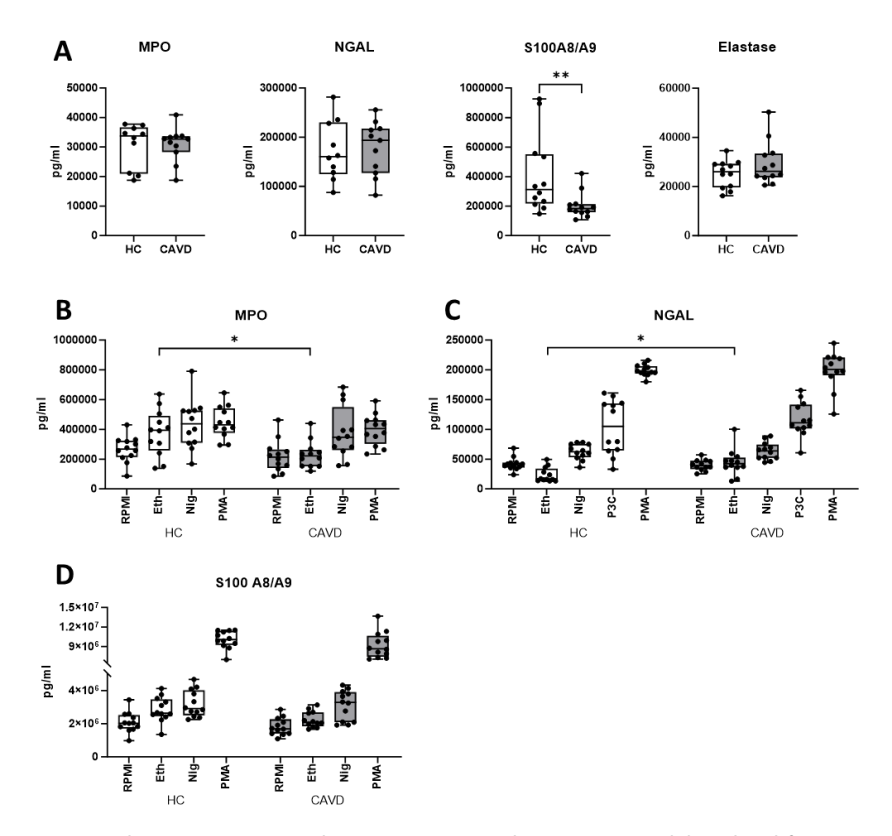


Figure 4: Circulating S100 A8/A9 is lower in patients with CAVD. Neutrophils isolated from patients with CAVD and controls were exposed for 4 hours to LPS, Pam3Cys (P3C), Nigericin (Nig) and PMA (RPMI and ethanol (Eth) as negative controls) and granule proteins were measured in circulation (plasma) and cell culture supernatants. (A) The circulatory granule proteins MPO, NGAL, S100 A8/A9 and elastase present in plasma of healthy controls and patients with CAVD. (B) MPO, (C) NGAL and (D) S100 A8/A9 secretion after stimulation. Data is presented with boxplots and is compared with the Mann-Whitney U test; *p<0.05, **p<0.01; n=12 healthy controls and n=12 patients with CAVD. (CAVD) Calcific aortic valve disease, (HC) healthy control.

Circulating \$100A8/A9 granule protein concentration is lower in patients with CAVD

To study neutrophil granule proteins, we measured MPO, NGAL, S100A8/A9 and elastase in plasma and MPO, NGAL and \$100A8/A9 in cell culture supernatants after stimulation with LPS, P3C, Nigericin and PMA (RPMI and ethanol as negative controls) for 4 hours., Circulating S100 A8/A9 was significantly lower in patients than in controls (p=0.008); there were no differences in the other circulating granule proteins (Figure 4A).

Upon stimulation with P3C, PMA and Nigericin, neutrophils from patients and controls produced similar amounts of the granule proteins MPO (Figure 4B), NGAL (Figure 4C) and \$100A8/A9 (Figure 4D). Interestingly, after exposing the cells to ethanol as control for nigericin (which is dissolved in ethanol), neutrophils of healthy controls released significantly more MPO and \$100A8/A9 compared to medium only and neutrophils of patients released more \$100A8/A9 (Figure 4B and 4D).

Discussion

CAVD is a chronic inflammatory disease leading to fibrocalcific remodeling of the aortic valve with currently no pharmacological treatment options (2). In search of better understanding of the underlying pathophysiology and to open up new treatment avenues, we hypothesized that neutrophils contribute to the development of AVS, and that neutrophils of patients with CAVD have a stronger pro-inflammatory phenotype. The current exploratory study revealed an altered neutrophil phenotype in patients with severe AVS compared to healthy controls. The neutrophils of patients with CAVD demonstrated a higher HLA-DR expression and produced more ROS, while they exhibited less NET formation. To the best of our knowledge, no previous study has investigated circulating neutrophil function in patients with CAVD.

Neutrophils have a short half-life (11), but despite their brief lifespan, they play a role in chronic inflammatory diseases, such as atherosclerosis, rheumatoid arthritis, systemic lupus erythematosus and periodontitis (9, 23, 24). This is believed to be facilitated by prolonged alterations in neutrophil phenotype due to reprogramming of their progenitor cells. Innate immune cells can adopt a sustained immune memory phenotype, triggered by exogenous or endogenous stimuli, resulting in an increased reaction upon secondary stimulation, a process called trained immunity (25). Previous research has shown that trained immunity can also arise in neutrophils. For example, Bacillus Calmette-Guérin vaccination induces longlasting enhanced cellular functions in neutrophils (26), which are retained due to epigenetic reprogramming of hematopoietic stem and progenitor cells in the bone marrow (27,28). Additionally, in patients with atherosclerosis, there is myeloid skewing in bone marrow granulocyte- and myeloid progenitors and hematopoietic stem cells with enrichment of genes involved in neutrophil activation pathways (27, 29). In atherosclerosis-prone mice, alternating high-fat diet accelerates atherosclerosis by inducing prolonged activation of circulating neutrophils via reprogramming of Granulocyte-Macrophage Progenitor cells (30).

As CAVD is a chronic inflammatory condition that shows many similarities with atherosclerosis, it is interesting to look for inflammatory changes in neutrophil function in patients with CAVD.

The present study revealed significant differences in neutrophil phenotype between patients with CAVD and age- and sex-matched healthy control subjects. Patients with CAVD have more circulating HLA-DR+ neutrophils. HLA-DR is usually not expressed by circulating neutrophils of healthy individuals, or only to a limited extent (31). However, HLA-DR+ neutrophils can appear in specific inflammatory environments linked to high cytokine levels, such as certain auto-immune diseases or infections, including granulomatosis with polyangiitis (32), rheumatoid arthritis (33) and cutaneous leishmaniasis infections (31, 34). Moreover, neutrophils also express HLA-DR after treatment with interferon-y or granulocyte/macrophage colony-stimulating factor exposure (35, 36). HLA-DR+ neutrophils have antigen-presenting capacities to memory CD4+ T-lymphocytes and might have a role in regulating antigenspecific T-lymphocyte responses (37). Interestingly, an increased number of antigenpresenting cell-like (APC-like) HLA-DR+ neutrophils has recently been reported in hyperlipidemic patients and atherosclerotic mice (38). Furthermore, in the study by Zhao et al., PMA-activated neutrophils from healthy controls were able to differentiate into APC-like HLA-DR+ neutrophils upon oxidized LDL stimulation (38), which is also suggested to contribute to the pathogenesis of CAVD (39). This APClike neutrophil phenotype could also be involved in CAVD progression. In addition to HLA-DR, we quantified the expression of CD16 and CD62L. Circulating neutrophils have a high expression of both CD16 and CD62L in homeostasis (CD16bright/ CD62Lbright) (21). However, during acute inflammation, more immature CD16low banded neutrophils (CD16dimCD62Lbright) are released into the circulation, which have stronger anti-bacterial effects. Hypersegmented CD16brightCD62Ldim are also found after inflammatory stimuli and exhibit suppression of T-lymphocyte proliferation and poor bacterial killing (22). There was no difference in CD16 and CD62L expression in the patients compared to the control subjects.

There is emerging evidence that ROS play a causal role in the development of CAVD (14-16). ROS promote the inflammatory valvular environment and stimulate myofibroblastic and osteoblastic differentiation of valvular interstitial cells (40). Oxidative stress is not only increased in calcified valves (41, 42), but is already present in higher amounts in sclerotic aortic valves (15). In our study, neutrophils of patients with severe AVS showed higher spontaneous and stimulated ROS production compared to healthy controls. Neutrophil ROS production is often higher in chronic inflammatory diseases (43, 44). Interestingly, both unstimulated and stimulated neutrophils from patients with peripheral artery disease due to atherosclerosis produce significantly more ROS than neutrophils from healthy controls as well (44). Circulating neutrophils might provide a source for ROS in the context of CAVD and thereby contribute to the development and progression of the disease.

Experimental and clinical research have linked NETs to multiple cardiovascular conditions (45). In atherosclerosis, NETs activate leukocytes, endothelial cells and platelets and can present various neutrophil granule proteins, contributing to the inflammatory milieu and plague instability (45, 46). However, their role in CAVD remains unclear. In the current study, neutrophils of patients with CAVD showed less spontaneous NET formation via both NOX-dependent and NOX-independent NET formation pathways compared to healthy controls and there were less NETs found in the plasma of the patients. The neutrophils showed similar NET formation upon stimulation, indicating that their ability to form NETs was not impaired. Interestingly, there was a previous study that demonstrated a higher amount of NETs in plasma and in the calcified valves of patients with CAVD compared to controls (17). We did not measure valvular NETs and used a different method to measure NETs in the plasma. Since the patients showed a higher spontaneous ROS production, we expected higher level of NETs in the patients with CAVD, as NET formation can be dependent on ROS (47). There are many other processes involved in NET formation (48), which might be affected in the patients with CAVD. Besides, an uncoupling of ROS production and NET formation is also seen in neutrophils with a trained immunity phenotype, as these neutrophils produce more ROS without changes in NET formation upon stimulation (26). These results together indicate that there might be immune reprogramming in neutrophils of patients with CAVD.

Neutrophils produce certain granule proteins upon stimulation, that can promote inflammation and are able to degrade extracellular matrix (46). We demonstrated a lower concentration of the protein \$100A8/A9 in the plasma of patients with CAVD. There were no differences between the patients and healthy controls in neutrophil granule protein secretion upon stimulation. S100A8/A9 is a danger-associated molecular pattern that is secreted by multiple cells, including neutrophils, during situations of stress, such as infection and trauma, and plays an important role in regulating the inflammatory response by inducing the production of cytokines and stimulating the recruitment of leukocytes (49, 50). Although the S100A8/A9 concentration was lower in the plasma of patients with CAVD, the amount in the aortic valves was not measured. Since S100A8/A9 is produced by several cell types, and production of S100A8/A9 upon stimulation was similar, the lower plasma concentrations of S100A8/A9 could as well be due to lower activation of other cells (50).

Strengths of this study include the extensive assessment of neutrophil phenotype and function, which has not been performed in patients with CAVD before, and the amount of clinical data known about the participants. This study also has some limitations. First, no phagocytosis assay was performed and since phagocytosis is an important function of neutrophils, this would have provided additional information about their function. Furthermore, the study has a small sample size, and it is a cross-sectional study without longitudinal samples and therefore conclusions about causality cannot be drawn. Moreover, only patients with severe CAVD were included and therefore nothing can be concluded about neutrophil function and phenotype in earlier disease stages. It would be interesting to further study neutrophil function throughout the disease progression. Lastly, the patients differed from the healthy controls in terms of medical history and medication use. This might have affected the results, although these differences are inherent characteristic of patients with cardiovascular disease. Importantly, a sensitivity analysis excluding participants using statins showed the same altered neutrophil phenotype in patients compared to healthy controls (data not shown).

In conclusion, this study demonstrates that patients with severe CAVD have an altered neutrophil phenotype compared to healthy controls. These results might indicate possible immune reprogramming of neutrophils in CAVD and suggest a role for neutrophils in CAVD. Further elucidation and validation in larger and prospective cohorts are necessary for a better understanding of the underlying mechanisms and for the development of new therapies, making neutrophils an interesting target for future CAVD studies.

Sources of funding

This study was financially supported by a research grant from Radboud University Medical Center to NPR and NvR. SB is supported by the Dutch Heart Foundation in the Hague (Dekker grant 2018-T028).

Disclosures

MGN and LABJ are scientific founders of TTxD, Lemba TX and Salvina TX. MGN is scientific founder of Biotrip.

Author contributions

Conceptualization; WB, NPR, NvR, SB, SEM, Data curation; WB, DFG, Formal analysis; WB, DFG. Investigation; WB, DFG, Methodology; NPR, SB, DFG, Project administration; WB, Supervision; NPR, SB, SEM, Visualization; Writing - original draft; WB, DFG, Writing - review & editing; NR, NPR, ESZ, MGN, LABJ, NvR, SB, SEM.

Data availability

The data is available upon reasonable request to the corresponding author.

Declaration of Competing Interest

The authors declare no competing interest.

Acknowledgements

We would like to thank Iris Oving, who contributed to the inclusion of patients in the Canisius Wilhelmina Hospital. The graphical abstract was created with BioRender.com

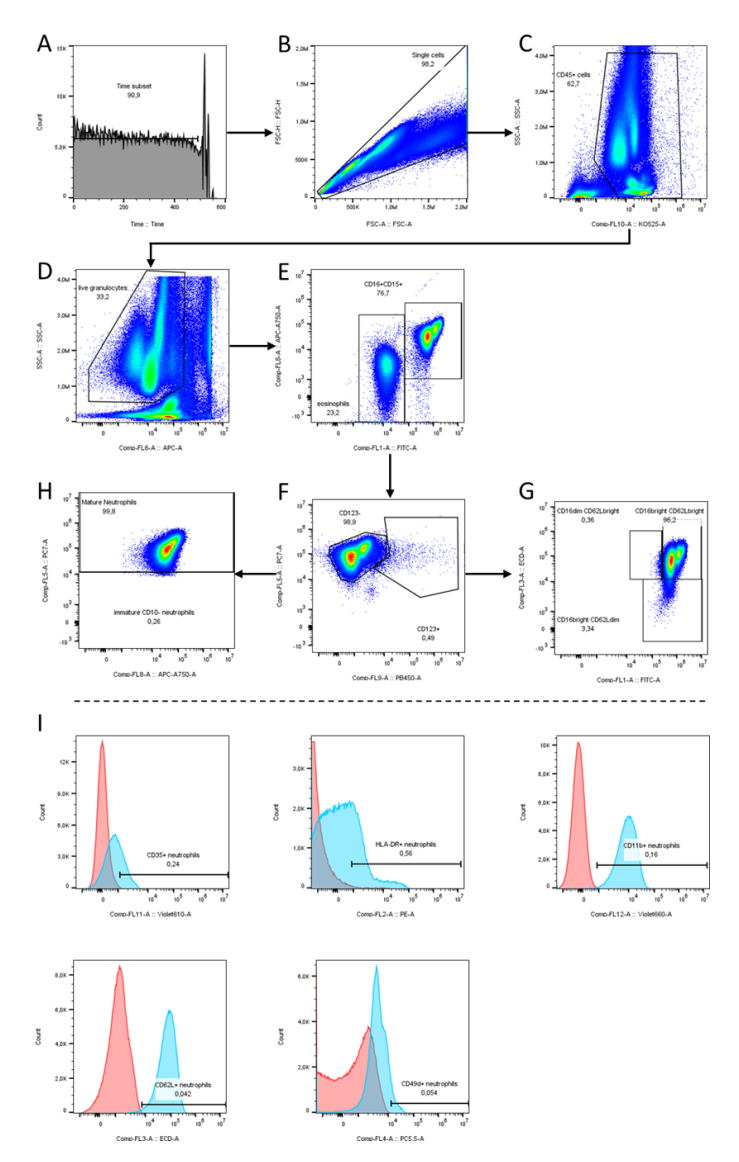
References

- Cho KI, Sakuma I, Sohn IS, Jo SH, Koh KK. Inflammatory and metabolic mechanisms underlying the calcific aortic valve disease. Atherosclerosis. 2018:277:60-5.
- Moncla LM, Briend M, Bossé Y, Mathieu P. Calcific aortic valve disease: mechanisms, prevention 2. and treatment. Nat Rev Cardiol. 2023;20(8):546-59.
- Osnabrugge RLJ, Mylotte D, Head SJ, Van Mieghem NM, Nkomo VT, LeReun CM, et al. Aortic Stenosis in the Elderly: Disease Prevalence and Number of Candidates for Transcatheter Aortic Valve Replacement: A Meta-Analysis and Modeling Study. Journal of the American College of Cardiology. 2013;62(11):1002-12.
- Yan AT, Koh M, Chan KK, Guo H, Alter DA, Austin PC, et al. Association Between Cardiovascular Risk Factors and Aortic Stenosis: The CANHEART Aortic Stenosis Study. J Am Coll Cardiol. 2017;69(12):1523-32.
- Liu Q, Yu Y, Xi R, Li J, Lai R, Wang T, et al. Association Between Lipoprotein(a) and Calcific Aortic Valve Disease: A Systematic Review and Meta-Analysis. Front Cardiovasc Med. 2022;9:877140.
- Broeders W, Bekkering S, El Messaoudi S, Joosten LAB, van Royen N, Riksen NP. Innate immune cells in the pathophysiology of calcific aortic valve disease: lessons to be learned from atherosclerotic cardiovascular disease? Basic Res Cardiol. 2022;117(1):28.
- New SE, Aikawa E. Molecular imaging insights into early inflammatory stages of arterial and aortic valve calcification. Circ Res. 2011;108(11):1381-91.
- Abdul-Rahman T, Lizano-Jubert I, Garg N, Talukder S, Lopez PP, Awuah WA, et al. The common pathobiology between coronary artery disease and calcific aortic stenosis: Evidence and clinical implications. Prog Cardiovasc Dis. 2023;79:89-99.
- Silvestre-Roig C, Braster Q, Ortega-Gomez A, Soehnlein O. Neutrophils as regulators of cardiovascular inflammation. Nat Rev Cardiol. 2020;17(6):327-40.
- 10. Li S, Xu L, Liu B. The Neglected Role of Neutrophils in the Severity of Aortic Valve Stenosis. J Cardiovasc Pharmacol. 2019;74(5):367-8.
- 11. Amulic B, Cazalet C, Hayes GL, Metzler KD, Zychlinsky A. Neutrophil function: from mechanisms to disease. Annu Rev Immunol. 2012;30:459-89.
- 12. Song J, Zheng Q, Ma X, Zhang Q, Xu Z, Zou C, et al. Predictive Roles of Neutrophil-to-Lymphocyte Ratio and C-Reactive Protein in Patients with Calcific Aortic Valve Disease. Int Heart J. 2019;60(2):345-51.
- 13. Cho KI, Cho SH, Her AY, Singh GB, Shin ES. Prognostic Utility of Neutrophil-to-Lymphocyte Ratio on Adverse Clinical Outcomes in Patients with Severe Calcific Aortic Stenosis. PLoS One. 2016;11(8):e0161530.
- 14. Liberman M, Bassi E, Martinatti MK, Lario FC, Wosniak J, Jr., Pomerantzeff PM, et al. Oxidant generation predominates around calcifying foci and enhances progression of aortic valve calcification. Arterioscler Thromb Vasc Biol. 2008;28(3):463-70.
- 15. Branchetti E, Sainger R, Poggio P, Grau JB, Patterson-Fortin J, Bavaria JE, et al. Antioxidant enzymes reduce DNA damage and early activation of valvular interstitial cells in aortic valve sclerosis. Arterioscler Thromb Vasc Biol. 2013;33(2):e66-74.
- 16. Liu H, Wang L, Pan Y, Wang X, Ding Y, Zhou C, et al. Celastrol Alleviates Aortic Valve Calcification Via Inhibition of NADPH Oxidase 2 in Valvular Interstitial Cells. JACC Basic Transl Sci. 2020;5(1):35-49.
- 17. Kopytek M, Kolasa-Trela R, Ząbczyk M, Undas A, Natorska J. NETosis is associated with the severity of aortic stenosis: Links with inflammation. Int J Cardiol. 2019:286:121-6.

- Baumgartner H. Falk V. Bax JJ. De Bonis M. Hamm C. Holm PJ, et al. 2017 ESC/EACTS Guidelines for the Management of Valvular Heart Disease. Rev Esp Cardiol (Engl Ed). 2018;71(2):110.
- 19. Pieterse E, Rother N, Yanginlar C, Gerretsen J, Boeltz S, Munoz LE, et al. Cleaved N-terminal histone tails distinguish between NADPH oxidase (NOX)-dependent and NOX-independent pathways of neutrophil extracellular trap formation. Ann Rheum Dis. 2018;77(12):1790-8.
- 20. Lund-Johansen F, Terstappen LWMM. Differential surface expression of cell adhesion molecules during granulocyte maturation. Journal of Leukocyte Biology. 1993;54(1):47-55.
- 21. Pillay J, Ramakers BP, Kamp VM, Loi AL, Lam SW, Hietbrink F, et al. Functional heterogeneity and differential priming of circulating neutrophils in human experimental endotoxemia. J Leukoc Biol. 2010;88(1):211-20.
- 22. Leliefeld PHC, Pillay J, Vrisekoop N, Heeres M, Tak T, Kox M, et al. Differential antibacterial control by neutrophil subsets. Blood Adv. 2018;2(11):1344-55.
- 23. Hajishengallis G, Chavakis T, Hajishengallis E, Lambris JD. Neutrophil homeostasis and inflammation: novel paradigms from studying periodontitis. J Leukoc Biol. 2015;98(4):539-48.
- 24. Bissenova S, Ellis D, Mathieu C, Gysemans C. Neutrophils in autoimmunity: when the hero becomes the villain. Clin Exp Immunol. 2022;210(2):128-40.
- 25. Bekkering S, Domínguez-Andrés J, Joosten LAB, Riksen NP, Netea MG. Trained Immunity: Reprogramming Innate Immunity in Health and Disease. Annu Rev Immunol. 2021;39:667-93.
- 26. Moorlag S, Rodriguez-Rosales YA, Gillard J, Fanucchi S, Theunissen K, Novakovic B, et al. BCG Vaccination Induces Long-Term Functional Reprogramming of Human Neutrophils. Cell Rep. 2020:33(7):108387.
- 27. Kalafati L, Hatzioannou A, Hajishengallis G, Chavakis T. The role of neutrophils in trained immunity. Immunol Rev. 2023;314(1):142-57.
- 28. Cirovic B, de Bree LCJ, Groh L, Blok BA, Chan J, van der Velden W, et al. BCG Vaccination in Humans Elicits Trained Immunity via the Hematopoietic Progenitor Compartment. Cell Host Microbe. 2020;28(2):322-34.e5.
- 29. Noz MP, Bekkering S, Groh L, Nielen TM, Lamfers EJ, Schlitzer A, et al. Reprogramming of bone marrow myeloid progenitor cells in patients with severe coronary artery disease. Elife. 2020;9.
- 30. Lavillegrand JR, Al-Rifai R, Thietart S, Guyon T, Vandestienne M, Cohen R, et al. Alternating highfat diet enhances atherosclerosis by neutrophil reprogramming. Nature. 2024;634(8033):447-56.
- 31. Davis RE, Sharma S, Conceição J, Carneiro P, Novais F, Scott P, et al. Phenotypic and functional characteristics of HLA-DR(+) neutrophils in Brazilians with cutaneous leishmaniasis. J Leukoc Biol. 2017;101(3):739-49.
- 32. Iking-Konert C, Vogt S, Radsak M, Wagner C, Hänsch GM, Andrassy K. Polymorphonuclear neutrophils in Wegener's granulomatosis acquire characteristics of antigen presenting cells. Kidney Int. 2001;60(6):2247-62.
- 33. Cross A, Bucknall RC, Cassatella MA, Edwards SW, Moots RJ. Synovial fluid neutrophils transcribe and express class II major histocompatibility complex molecules in rheumatoid arthritis. Arthritis Rheum. 2003;48(10):2796-806.
- 34. Sharma S, Davis RE, Srivastva S, Nylén S, Sundar S, Wilson ME. A Subset of Neutrophils Expressing Markers of Antigen-Presenting Cells in Human Visceral Leishmaniasis. J Infect Dis. 2016;214(10):1531-8.

- 35. Gosselin EJ, Wardwell K, Rigby WF, Guyre PM. Induction of MHC class II on human polymorphonuclear neutrophils by granulocyte/macrophage colony-stimulating factor, IFN-gamma, and IL-3. J Immunol. 1993;151(3):1482-90.
- Mudzinski SP, Christian TP, Guo TL, Cirenza E, Hazlett KR, Gosselin EJ. Expression of HLA-DR (major histocompatibility complex class II) on neutrophils from patients treated with granulocytemacrophage colony-stimulating factor for mobilization of stem cells. Blood. 1995;86(6):2452-3.
- 37. Vono M, Lin A, Norrby-Teglund A, Koup RA, Liang F, Loré K. Neutrophils acquire the capacity for antigen presentation to memory CD4(+) T cells *in vitro* and *ex vivo*. Blood. 2017;129(14):1991-2001.
- 38. Zhao T, Jiang Q, Li W, Wang Y, Zou Y, Chai X, et al. Antigen-Presenting Cell-Like Neutrophils Foster T Cell Response in Hyperlipidemic Patients and Atherosclerotic Mice. Front Immunol. 2022;13:851713.
- 39. Nsaibia MJ, Devendran A, Goubaa E, Bouitbir J, Capoulade R, Bouchareb R. Implication of Lipids in Calcified Aortic Valve Pathogenesis: Why Did Statins Fail? J Clin Med. 2022;11(12).
- 40. Greenberg HZE, Zhao G, Shah AM, Zhang M. Role of oxidative stress in calcific aortic valve disease and its therapeutic implications. Cardiovasc Res. 2022;118(6):1433-51.
- Miller JD, Chu Y, Brooks RM, Richenbacher WE, Peña-Silva R, Heistad DD. Dysregulation of antioxidant mechanisms contributes to increased oxidative stress in calcific aortic valvular stenosis in humans. J Am Coll Cardiol. 2008;52(10):843-50.
- 42. Weiss RM, Ohashi M, Miller JD, Young SG, Heistad DD. Calcific aortic valve stenosis in old hypercholesterolemic mice. Circulation. 2006;114(19):2065-9.
- 43. Kundu S, Ghosh P, Datta S, Ghosh A, Chattopadhyay S, Chatterjee M. Oxidative stress as a potential biomarker for determining disease activity in patients with rheumatoid arthritis. Free Radic Res. 2012;46(12):1482-9.
- 44. Kraft JD, Blomgran R, Bergström I, Soták M, Clark M, Rani A, et al. Lipoxins modulate neutrophil oxidative burst, integrin expression and lymphatic transmigration differentially in human health and atherosclerosis. Faseb j. 2022;36(3):e22173.
- 45. Döring Y, Libby P, Soehnlein O. Neutrophil Extracellular Traps Participate in Cardiovascular Diseases: Recent Experimental and Clinical Insights. Circ Res. 2020;126(9):1228-41.
- 46. Sreejit G, Johnson J, Jaggers RM, Dahdah A, Murphy AJ, Hanssen NMJ, et al. Neutrophils in cardiovascular disease: warmongers, peacemakers, or both? Cardiovasc Res. 2022;118(12):2596-609.
- 47. Azzouz D, Khan MA, Palaniyar N. ROS induces NETosis by oxidizing DNA and initiating DNA repair. Cell Death Discovery. 2021;7(1):113.
- 48. Thiam HR, Wong SL, Wagner DD, Waterman CM. Cellular Mechanisms of NETosis. Annu Rev Cell Dev Biol. 2020;36:191-218.
- 49. Wang S, Song R, Wang Z, Jing Z, Wang S, Ma J. S100A8/A9 in Inflammation. Front Immunol. 2018;9:1298.
- 50. Averill MM, Kerkhoff C, Bornfeldt KE. S100A8 and S100A9 in cardiovascular biology and disease. Arterioscler Thromb Vasc Biol. 2012;32(2):223-9.

Supplementary material



Supplementary figure 1: Flow cytometry gating strategy. After removing doublets and debris (A and B), live granulocytes were selected from CD45+ cells (C and D). Thereafter, eosinophils (CD16-, E) and basophils (CD123+, F) were removed and the presence and median fluorescence intensity (MFI) of the maturation marker CD49d was assessed on all neutrophils. Then, the neutrophils were divided into subsets based on their expression of CD16 and CD62L (G). Lastly, the neutrophils were divided into CD10+ mature and CD10- immature neutrophils (H) and the expression and MFI of HLA-DR, CD35, CD11b and CD62L (neutrophil activation markers) were analyzed on both mature and immature neutrophils. The fluorescence-minus-one (FMO) method50 was used to set the gates for the maturation and activation markers (I).

Supplemental Table 1: Antibodies for flow cytometry

Reagent	Company	Identifyer
Antibodies		
Anti-human CD16, FITC, clone 3G8	Biolegend	Cat# 302006 RRID AB_314206
Anti-human HLA-DR, PE, clone Immu-357	Beckman Coulter	Cat# IM1639U RRID AB_2876782
Anti-human CD62L, PEDazzle594, clone DREG-56	Biolegend	Cat# 304842 RRID AB_2565874
Anti-human CD49d, PECy5.5, 9F10	Biolegend	Cat# 304312 RRID AB_10641699
Anti-human CD10, PC7, clone HI10a	Biolegend	Cat# 312213 RRID AB_2146549
Anti-human lineage cocktail (CD3, CD14, CD19, CD20, CD56), APC, clones: UCHT1; HCD14; HIB19; 2H7; HCD56	Biolegend	Cat# 348703 RRID: AB_3076251
Anti-human CD66b, APC-700, clone G10F5	Biolegend	Cat# 305114 RRID AB_2566038
Anti-human CD15, APC-Cy7, clone W3D3	Biolegend	Cat# 323047 RRID AB_2750189
Anti-human CD123, BV421, clone 6H6	Biolegend	Cat# 306018 RRID AB_10962571
Anti-human CD45, BV510, clone HI30	Biolegend	Cat# 304036 RRID AB_2561940
Anti-human CD35, BV650, clone E11	Becton Dickinson	Cat# 744277 RRID AB_2742115
Anti-human CD11b, BV785, clone ICRF44	Biolegend	Cat# 301346 RRID AB_2563794
Helix NP™ NIR	Biolegend	Cat# 425301

Supplemental Table 2. Flow cytometry analyses

	Healthy controls N=12	Patients with CAVD N=12	P-value
	0.7 [0.6-2.2]	0.8 [0.6-1.1]	0.745
CD49d+ neu (x10³, MFI)	25.3 [20.4-34.1]	26.4 [17.9-37.1]	0.876
Mature neu (% of neu)	99.8 [99.7-99.8]	99.7 [99.7-99.8]	0.828
CD16+ mature neu (x10³, MFI)	686.0 [546.8-767.0]	647.5 [626.3-704.0]	0.600
CD66b+ mature neu (x10³, MFI)	18.6 [12.4-20.7]	18.2 [12.8-19.1]	0.514
CD15+ mature neu (x10 ³ , MFI)	33.0 [27.9-39.3]	36.8 [29.1-43.6]	0.630
CD11b+ mature neu (% gated)	100 [100-100]	100 [100-100]	>0.999
CD11b+ mature neu (x10 ³ , MFI)	26.6 [14.8-28.1]	19.0 [16.7-25.5]	0.443
CD35+ mature neu (% gated)	100.0 [99.9-100.0]	100 [99.8-100.0]	0.749
CD35+ mature neu (x10³, MFI)	22.1 [15.7-29.6]	21.1 [12.1-24.8]	0.298
CD62L+ mature neu (% gated)	99.6 [98.5-99.7]	99.1 [98.8-99.6]	0.384
CD62L+ mature neu (x10³, MFI)	60.7 [54.6-79.8]	65.3 [56.9-74.3]	0.855
HLA-DR+ mature neu (% gated)	9.5 [3.4-15.8]	33.6 [10.6-55.0]	0.015
HLA-DR+ mature neu (MFI)	6316 [1882-12604]	2138 [1804-4456]	0.319
Immature neu (% of neu)	0.2 [0.2-0.3]	0.3 [0.2-0.3]	0.182
CD16+ immature neu (x10³, MFI)	229.5 [183.9-308.7]	308.0 [202.0-453.0]	0.224
CD66b+ immature neu (x10³, MFI)	13.8 [9.2-17.3]	11.3 [7.6-13.5]	0.164
CD15+ immature neu (x10 ³ , MFI)	30.2 [24.5-40.3]	27.9 [24.9-34.4]	0.401
CD11b+ immature neu (% gated)	100.0 [99.5-100.0]	100.0 [99.5-100.0]	>0.999
CD11b+ immature neu (x10³, MFI)	12.3 [7.1-14.7]	9.2 [6.5-11.9]	0.347
CD35+ immature neu (% gated)	98.4 [97.8-99.0]	98.1 [96.2-98.9]	0.468
CD35+ immature neu (MFI)	8.2 [6.3-11.4]	8.5 [6.0-9.8]	0.810
CD62L+ immature neu (% gated)	96 [91.6-97.0]	89.6 [84.7-92.1]	0.002
CD62L+ immature neu (MFI)	47.6 [35.8-60.0]	54.7 [40.4-65.5]	0.410
HLA-DR+ immature neu (% gated)	8.0 [0.02-15.7]	25.2 [9.4-44.3]	0.053
Neutrophil subsets			
CD16 ^{bright} CD62L ^{bright} (% of neu)	97.3 [96.7-97.7]	97.6 [96.9-98.0]	0.599
CD16 ^{bright} CD62L ^{dim} (% of neu)	1.8 [1.4-2.4]	1.7 [1.3-2.7]	0.887
CD16 ^{dim} CD62L ^{bright} (% of neu)	0.7 [0.5-1.0]	0.5 [0.4-0.7]	0.183

Flow cytometry data are presented as median with interquartile range [Q1-Q3] and is assessed using the Mann-Whitney U test. (neu) neutrophils.

Supplemental methods

Supplemental method 1. Lipoprotein (a) ELISA

Plates were coated with rabbit anti-human lipoprotein (a) (Lp(a)) IgG antibodies (5 μg/mL) overnight at RT, washed 5 times with wash buffer (PBS with 0.05% Tween-20 (Merck, Darmstadt, Germany). Blocking was performed with 1% BSA in PBS for one hour at RT. Samples were incubated for two hours on a shaker at 400rpm at RT. Then, the plates were washed and biotinylated rabbit anti-human Lp(a) IgG detection antibody (0.2 ng/mL) was added for one hour at RT on the shaker. Subsequently, Streptavidin-HRP was added for 45 minutes after washing the plates. The plates were then washed again, after which they were incubated for 20 minutes with substrate buffer. Finally, stop-solution was added, and the plate was read on the ELISA plate reader at 450 nm.

Supplemental method 2. Flow cytometry

One mL of EDTA blood was added to 10 mL lysis buffer (BD Pharm Lyse Lysing buffer, BD, Franklin Lakes, USA) for a maximum of 15 minutes in the dark at RT to lyse the erythrocytes. The cells were washed with 1% BSA in PBS with 2 mM EDTA (PBA-E) and resuspended in 100 uL PBA-E. This cell suspension was then incubated with 10 uL Human TruStain FcX (Biolegend, San Diego, CA, USA) to block unwanted FcR-involved unspecific staining for 10 minutes. Subsequently, 50 uL of the cell suspension was added to an antibody mix containing brilliant stain buffer (Becton Dickinson, Franklin Lakes, NJ, USA), The cells were stained for 30 minutes at RT in the dark and afterwards washed and resuspended in PBA-E. Subsequently, the cells were incubated for 15 minutes in the dark at RT with the live/dead staining Helix NPTM NIR (Biolegend).



Chapter 7

Summary

Cardiovascular disease (CVD) is one of the leading causes of morbidity and mortality worldwide, exacerbated in recent days by sedentary lifestyle and poor diet. Yearly, nearly 18 million people die as consequence of CVD, with atherosclerosis – a low-grade inflammatory disorder of the arterial wall – as cause of most of them. Atherosclerosis can cause myocardial infarction, stroke and peripheral arterial disease, depending on the location of the plaques. Calcific aortic valve disease (CAVD) is another CVD that causes the progressive narrowing of the valve, leading to severe outcomes if untreated. Both atherosclerotic CVD (ASCVD) and CAVD share pathophysiological characteristics, including involvement of chronic inflammation.

Several risk factors such as aging, high blood pressure, smoking, obesity, and diabetes contribute to the development of ASCVD and CAVD. The pathogenesis of ASCVD is complex; while a key mechanism contributing to the plaque formation is lipid accumulation in the arterial walls, innate immune cells also play a pivotal role. Endothelial cell activation leads to increased expression of adhesion molecules and chemokines such as MCP-1, attracting monocytes to the lesion site. These monocytes then migrate to the intima, differentiate into macrophages and take up modified lipoproteins, subsequently becoming foam cells. Then, they form a necrotic core, which can erode or rupture ultimately causing arterial occlusion which triggers a cardiovascular event.

With a better understanding of the role of inflammation in ASCVD pathophysiology, trained immunity was proposed as an important mechanism. In recent years, it was established that cells from the innate immune system can also develop memory. This has been termed trained immunity and results in a heightened response of innate immune cells long after the initial trigger is gone. Traditionally, immune memory was thought to be exclusive to adaptive immunity. However, trained immunity enables innate immune cells such as monocytes and neutrophils to develop innate immune memory after exposure to certain stimuli, maintaining a long-term pro-inflammatory phenotype. Initially observed in response to infections, trained immunity can also be triggered by endogenous factors associated with CVD, such as oxidized LDL and high glucose levels. This memory-like response is due to metabolic and epigenetic changes, both in mature circulating innate immune cells as well as their progenitors in the bone marrow, allowing the inflammatory response to persist.

Traditional CVD treatments focus primarily on managing risk factors, such as lowering blood pressure and reducing LDL cholesterol though medication like statins. However, with the new role of inflammation in atherogenesis, several

clinical studies recently showed that anti-inflammatory treatments reduce the risk of ASCVD. In contrast, for CAVD there is currently no effective pharmacological treatment and once the symptoms become severe, patients often require surgical or endovascular valve replacement. Despite current therapies, residual ASCVD risk remains high and research into the inflammatory landscape underlying both ASCVD and CAVD is essential to identify more selective treatment targets.

In this thesis, I explored the role of monocyte reprogramming in the pathophysiology of ASCVD with a main focus on innate immune memory. Firstly, in **Chapter 2** I provided an overview on the triggers and mechanisms of trained immunity in ASCVD. Then, in **Chapter 3**, we explored how leptin, a hormone linked to obesity-related complications, influenced monocyte function and inflammation. We found that in vitro, leptin induced trained immunity in human primary monocytes. Additionally, in an in vivo study involving 302 obese individuals (BMI >27 kg/m², aged 55–81), circulating leptin levels were positively associated with inflammatory markers IL-1 β and IL-6, with this effect being more pronounced in men. Furthermore, genetic variations in the form of single nucleotide polymorphisms (SNP) in the leptin gene influenced IL-6 levels in men, suggesting a direct role for leptin in driving inflammation.

Some murine models show that trained immunity can accelerate atherosclerosis progression under conditions like high-fat diet, hyperglycemia and post-myocardial infarction, primarily through IL-1 β signaling in the bone marrow. To investigate in more detail the long-term effects of IL-1 β on human HSPC phenotype, I subsequently performed the studies described in **Chapter 4**. We exposed isolated human HSCs for 4-hours to IL-1 β . Then, HSCs were expanded and differentiated into monocytes for about 3 weeks after which we measured key immunological parameters to determine the induction of trained immunity. IL-1 β -treated HSCs generated more granulocyte-macrophage colony-forming units. In addition, monocytes derived from IL-1 β -treated cells showed enhanced production of TNF and IL-1 β upon restimulation with LPS and Pam3Cys, along with increased metabolic activity, similar to primary trained monocytes. Transcriptomic analysis revealed upregulation of key inflammatory and atherogenic pathways. These findings demonstrated that brief exposure to IL-1 β induces a trained immunity phenotype in human HSCs in vitro.

In this thesis I studied trained immunity in human circulating monocytes in chapter 3 and HSC-derived monocytes in Chapter 4. Hence, it was important to compare their phenotypes in order to be able to compare the results of the different

models. In **Chapter 5**, we systematically compared human circulating monocytes and macrophages with those derived from induced pluripotent stem cells (iPSCs) and HSCs to assess their suitability for in vitro disease modeling. Human circulating monocytes have a higher percentage of classical monocytes compared to iPSC-and BM- derived monocytes. All types produce cytokine (IL-6, TNF and IL-1ra) upon stimulation with TLR ligands, with minor differences. Circulating and BM-derived monocytes exhibit higher glycolytic capacity compared to iPSC-derived monocytes. Epigenetic and transcriptomic analyses suggest that BM- and iPSC-derived monocytes are more differentiated along the monocyte-to-macrophage lineage than circulating monocytes. This aligns with a higher phagocytic capacity in these cells compared to the primary monocytes. We highlighted that while iPSCs- and BM-derived monocytes/macrophages are viable alternatives for research, however they had distinct functional characteristics compared to circulating monocytes.

As previously mentioned, neutrophils also contribute to vascular inflammation in ASCVD. These cells can respond to inflammation by forming neutrophil extracellular traps (NETs) and releasing reactive oxygen species (ROS), further damaging the vascular integrity and enhancing the recruitment of monocytes. NETs can also modulate macrophage behavior and destabilize plagues, increasing the risk of a cardiovascular event. Elevated counts of circulating granulocytes are linked with higher ASCVD incidence, indicating a causal relationship. For CAVD, the pathophysiological role of neutrophils is less well established. Therefore, in Chapter 6, we investigated the neutrophil phenotype and function in patients with severe CAVD compared to healthy controls. In an exploratory cross-sectional study, which included 12 patients with severe CAVD and 12 age and sex matched healthy controls, we observed higher leukocyte count in CAVD patients compared to controls but no differences in absolute number of neutrophils. CAVD patients had a higher percentage of HLA-DR+ mature neutrophils. Neutrophils from patients also produced more ROS both at baseline and after zymosan stimulation but exhibited reduces spontaneous NET formation. Even though with the present results we suggested that neutrophils in severe CAVD have an altered phenotype and functional profile, potentially contributing to the disease progression, further studies in larger cohorts are needed.



Chapter 8

General Discussion

Cardiovascular diseases (CVDs) are among the most prevalent chronic diseases and are the leading cause of death worldwide. This is projected to further increase in the next decades mainly due to aging of the overall population and an increased prevalence of obesity (1). Atherosclerosis is the main underlying cause of CVD, and it is now known that its pathophysiology involves chronic low-grade inflammation (2). Calcific aortic valve disease (CAVD) is another CVD that shares common risk factors and pathophysiology with atherosclerotic cardiovascular disease (ASCVD) (3). For ASCVD, despite the optimal treatment of classical risk factors, such as dyslipidemia and hypertension, there is still a large residual risk in many patients. For CAVD, there is no pharmacological treatment available to halt the disease progression leaving surgical or endovascular valve replacement as the only treatment option (3, 4). There is accumulating evidence that for both diseases, inflammation plays an important role. Indeed, for ASCVD, recent trials have shown that broad anti-inflammatory drugs, including colchicine, and canakinumab, effectively reduce the incidence of cardiovascular events in high-risk patients (5-7). However, these anti-inflammatory treatment options come at a cost of infectious complications. Our vision is that unraveling the role of innate immune cells in the pathophysiology of these diseases will lead to the discovery of novel more specific pharmacological targets that can be used to prevent or treat ASCVD and CAVD.

In this thesis I focused on how innate immune reprogramming might contribute to the development and progression of CVD. In the first chapters I focused on trained immunity in the context of ASCVD. We made use of a well-established *in vitro* trained immunity protocol to investigate whether endogenous pro-inflammatory adipokines such as leptin can induce trained immunity in monocytes. Additionally, I explored how trained immunity can also occur in the bone marrow niche by briefly exposing human primary bone marrow-derived hematopoietic stem cells (HSCs) to IL-1 β to induce trained immunity. Also, I investigated the similarities and differences of human circulating, bone marrow-derived and iPSC-derived monocytes since all these models are used *in vitro* to study immune reprogramming. Lastly, I explored the function and phenotype of another innate immune cell, the neutrophil granulocyte, in patients with severe CAVD.

Trained immunity: a key immunological mechanism contributing to CVD?

In this thesis, we explored the concept of trained immunity in obesity and CVD. In **Chapter 2**, I gave an overall review of trained immunity and how it can contribute to ASCVD. During the past several years, trained immunity was established as an underlying mechanism to the low-grade chronic inflammation that is characteristic

of atherosclerosis. This is triggered by endogenous atherogenic factors such as lipoproteins, high glucose levels, or adrenal hormones causing epigenetic and metabolic reprogramming of the cells (8). Trained immunity has mainly been studied in circulating monocytes, however it can also affect other circulating innate immune cells such as neutrophils and NK cells (9). This is known as peripheral trained immunity. In addition, trained immunity can happen in the bone marrow niche causing immune reprograming of myeloid progenitors, known as central trained immunity (8, 10).

Central trained immunity has been reported in humans and in mice. In humans, despite the short half-life of monocytes, a trained immunity phenotype persists in circulating monocytes up to 3 months and even one year after receiving BCG vaccination (11). In the context of ASCVD, bone marrow-derived HSCs showed functional and transcriptomic reprogramming in patients with coronary artery disease (12). Mice studies showed that brief exposure to BCG and β -glucan cause epigenetic and metabolic changes in HSCs and increased hyper-responsiveness, mediated by IL-1ß signaling in the bone marrow (11, 13). Also, in atherosclerosisprone mice, a 4-week exposure to Western Type Diet induced trained immunity in myeloid progenitor cells mediated by NLRP3 inflammasome activation and IL-1β signaling (14). Recent studies have unequivocally demonstrated that trained immunity can indeed accelerate experimental atherosclerosis. Dong et al. showed that after a myocardial infarction, monocytes developed a hyperresponsive trained immunity phenotype due to the activation of the histone methyltransferase enzyme KMT5A accelerating the subsequent progression of atherosclerosis in mice (15). Similarly, it was recently reported that innate immune memory mechanisms contribute to important comorbidities in remote organs after infarction (e.g. cardiac dysfunction following a stroke) (16). Also, brief exposure to high fat diet (17) and to hyperglycemia (18) accelerated atherosclerosis in mice due to the reprogramming of myeloid progenitors in the bone marrow. Interestingly, IL-1ß was a common mediator of trained immunity in most of the aforementioned studies, highlighting its importance in the bone marrow niche in the context of CVD and innate immune reprogramming. These findings underscore the importance of further investigating the mechanisms of trained immunity; and more importantly, translate these findings to humans and to uncover ways to modulate these mechanisms.

In Chapter 3, we studied the role of leptin in trained immunity. Leptin is a proinflammatory adipokine that is known to contribute to low-grade chronic inflammation in obesity. Many individuals with obesity develop a state of insulin resistance, dyslipidemia, and hypertension, which is called metabolic syndrome, and which strongly predisposes to ASCVD. To investigate the mechanisms underlying the development of these metabolic and cardiovascular complications, our research group recruited a cohort of 302 individuals with a BMI >27 kg/m² (19). Approximately half of these individuals appeared to fulfill the criteria of the metabolic syndrome, and also half of them had presence of atherosclerotic plagues in the carotid arteries (19). Using this cohort, our research group recently reported that in obese and overweight men with metabolic syndrome, leptin and IL-6 circulating concentrations were higher compared to men without metabolic syndrome, independent of their BMI. In addition, PBMC cytokine production capacity was higher in men with metabolic syndrome (19). Based on these data, I hypothesized that leptin could induce innate immune reprogramming and thereby contribute to the metabolic and cardiovascular complications of obesity. Indeed, we could confirm that leptin induced trained immunity by increasing the production of TNF and IL-1ß and augmented foam cell formation in vitro. We also reported that, in vivo, there was a strong positive association between circulating leptin and circulating IL-6 and IL-1β concentrations, but only in men. At the gene level, we identified 4 SNPs in the LEP gene that have an effect on circulating IL-6 concentrations, only in men, strongly suggesting a causal effect of leptin on IL-6. It's important to emphasize that these conclusions need to be interpreted with caution, since the P-values did not reach the threshold for genome wide significance (20). Also, these causal associations do not inform about the underlying mechanisms of the association, which could relate to leptin-induced trained immunity, or direct effects of leptin on circulating or tissue resident immune or non-immune cells producing IL-6. Here I focused on the effect of leptin on circulating monocytes, however, it is known that leptin also affects other innate and adaptive immune cells. Leptin is an adipokine that regulates appetite, but whenever the leptin concentration increases above the normal leptin levels (0.5-15.2 ng/ml in females and 0.5-12.5 ng/ml in males), it can have effects on the immune system. Leptin deficiency can lead to impairment in T cell differentiation and function in mice and humans in vivo (21, 22). On the other hand, excessive leptin concentrations can promote pro-inflammatory phenotype in human mast cells in vitro and in vivo in mice models, immune senescence in human B cells in vitro (23), dendritic cell maturation and function in vivo in mice (21), higher neutrophil infiltration in murine models in vivo and murine cells in vitro (22, 24) and changes in the inflammatory properties and signaling of NK cells in humans in vivo and in vitro in human primary cells and NK cell lines (21, 22). It is important to investigate these effects in the context of ASCVD in more detail in future studies.

Leptin triggers immune effects by binding to the leptin receptor, which is expressed on the surface of a range of immune cells. Leptin signaling has been widely studied and the signaling pathways in immune cells have been identified. JAK2 and PI3K pathways are key pathways in immune regulation of macrophages and neutrophils. After binding, leptin activates JAK2/PI3K further activating mTOR inducing cell activation (21). Even though we did not explore the underlying pathways of leptininduced trained immunity in **Chapter 3**, we hypothesize that this signaling cascade of mTOR activation is probably involved. This is based on other work showing an important contribution of mTOR activation in trained immunity development induced by other trained immunity triggers, including β -glucan (25) and oxLDL (26), but this needs further investigation.

IL-1β - A key player in trained immunity

The IL-1 family of cytokines, particularly IL-1\(\beta\), is one of the key drivers of systemic inflammation. IL-1\beta is secreted by immune cells after enzymatic cleavage of pro-IL-1\beta by caspase-1. Caspase-1 is activated by recruitment to a multi-protein complex termed the NLRP3 inflammasome (27).

The pro-atherosclerotic effects of IL-1 β have been well established in human studies (28). Various randomized controlled clinical trials were conducted using pharmacological inhibitors such as canakinumab (monoclonal IL-1ß antibody) and anakinra (recombinant IL-1 receptor antagonist) (29). Additionally, colchicine was also used because of its anti-inflammatory role by inhibiting NLRP3 inflammasome activity (30). The LoDoCo-2, COLCOT, and CANTOS trials showed that colchicine and canakinumab effectively lowered CVD events in high-risk patients (5-7). These studies strongly confirmed the importance of IL-1ß in the pathophysiology of ASCVD and how targeting IL-1β can improve clinical outcomes.

Parallel to these clinical cardiovascular studies, experimental immunological studies revealed an important role for IL-1β in trained immunity. In mice, the development of trained immunity following administration of BCG, or β-glucan involved IL-1β signaling in the bone marrow niche (11, 13). In addition, functional and epigenetic reprogramming of HSCs in Ldlr -/- mice fed a western-type diet for a short time was critically dependent on activation of the NLRP3 inflammasome (14). More recently, it was shown that intermittent high fat diet-induced trained immunity could aggravate atherosclerosis progression, and that this was mediated by IL-1β dependent reprogramming of granulocyte-macrophage progenitor cells in the bone marrow (17).

Whether IL-1ß could also induce trained immunity in humans HSCs had not been previously explored. Therefore, in Chapter 4, I investigated for the first time the effects of brief IL-1\beta exposure on human primary HSCs. Specifically, I aimed to investigate if IL-1ß could induce trained immunity in human HSCs in vitro and assessed in detail the phenotypical, functional and transcriptomic parameters of trained HSC-derived monocytes and macrophages. After brief exposure of HSCs to IL-1\u00ed there was more granulocyte-macrophage colony formation. Also, the IL-1β-exposed HSC-derived differentiated macrophages showed more TNF and IL-1β cytokine production capacity, which was associated with augmented glycolysis and oxidative phosphorylation.

The findings in **Chapter 4** are important because they show for the first time in human primary bone marrow-derived progenitor cells that a brief exposure to IL-1β was sufficient to induce persistent pro-inflammatory effects in the monocyte/ macrophage offspring. From a clinical point of view, this scenario opens the possibility to refine anti-inflammatory treatment options. In this paradigm, discrete clinical situations in which IL-1B concentrations in bone marrow are increased and could induce long-term pro-inflammatory reprogramming, e.g. myocardial infarction, stroke, or during acute infections, could be the optimal time windows to briefly administer anti-IL-1 treatment to prevent these long-term consequences. Implementation of this new strategy first requires to identify clinical scenarios in which bone marrow IL-1β indeed induces these long-term immunological effects. Several experimental studies showed that after acute myocardial infarction, bone marrow concentrations of IL-1\(\beta\) increase. Soon after myocardial infarction, there was an increase in circulating IL-1β, and in mouse experimental models this subsequently led to activation and proliferation of HSCs (31). In addition to IL-1β being released in the circulation to reach the bone marrow niche, recent murine studies also revealed that an acute myocardial infarction led to priming of circulating neutrophils that subsequently secreted more IL-1\(\beta\) in the bone marrow niche to stimulate granulopoiesis (32). In mice, after myocardial infarction, plasma IL-1β peaked at 24 hours and was almost normal after 72 hours; in the bone marrow, it is still higher after 72 hours (31).

Models of trained immunity

The first model that was developed to investigate peripheral trained immunity consists of the exposure for 24 hours of human primary monocytes to a training stimulus, followed by 6 days of resting period. Finally, the monocyte-derived macrophages are restimulated with another inflammatory stimulus, typically LPS and Pam3Cys (TLR4/ and 2 agonists, respectively) for 24 hours, to measure cytokine production (33). This protocol was used in Chapter 2. In spite of the murine and human studies describing trained immunity mechanisms in bone marrow progenitors in vivo (11-14), there was no model available to study central trained immunity in human HSCs. Therefore, I set out to develop such an in vitro model of central trained immunity, which I described in detail in Chapter 4. In summary, we exposed human BM-derived HSCs to IL-1\beta for 4 hours, followed by subsequent expansion of HSCs for 10 days and differentiation into monocytes for 7 days. After the differentiation period, human BM-derived trained monocytes were restimulated for 24 hours with LPS and Pam3Cvs. This was followed by functional and transcriptomic characterization. Although this model allowed us to investigate how temporary stimulation of HSCs affects proliferation rate and the phenotype of the mature offspring cells, it is important to realize that it has several limitations, e.g. relating to the absence of bone marrow niche cells. These limitations are discussed in more detail in the Limitations section at the end of this chapter.

In addition to primary human monocytes, and HSC-derived monocytes, in the last years induced pluripotent stem cells (iPSC) were used as an alternative source to obtain monocytes and macrophage in the laboratory setting. These iPSCs are first dedifferentiated from a human somatic cell and can be re-differentiated into a number of different cell types including monocytes and monocyte-derived macrophages (MDM) (34). Additionally, iPSCs-derived monocytes are of great interest due to their plasticity for disease modeling, since one iPSC can be derived from cells from different tissues or from cells that carry certain genetic mutations that predispose to disease (34, 35).

To allow comparison of experimental studies using different origins of human monocytes, in Chapter 5, we studied the similarities and differences between primary human circulating monocytes, HSC-derived monocytes, and iPSC-derived monocytes. We observed that functionally, all the monocytes and macrophages produced cytokines upon restimulation with LPS and were all metabolically active; however, they had differences in CD14/CD16 expression. While human circulating monocytes consisted mainly of classical monocytes, the other two monocyte pools in our study consisted of more intermediate monocytes. Additionally, at a transcriptional level the iPSC- and BM-derived monocytes resembled more human primary MDM, than circulating monocytes. Given these differences, our results underlined the importance of choosing the adequate differentiation protocol as well as the adequate source of monocyte according to the research question and the main readouts.

Innate immune reprogramming in CAVD

Compared to ASCVD, knowledge on how innate immune cells contribute to the pathophysiology of CAVD is far less developed. Some studies now start to indicate that monocytes/macrophages and neutrophils are involved (3). To investigate this in detail, my colleague Wieteke Broeders started a prospective case-control study in 2020 in which she studied monocyte reprogramming in patients with mild and severe CAVD compared to healthy controls (the 'MIRACLE' study).

Driven by the suggestions that neutrophils are also involved in CAVD and by our previous observations that trained immunity mechanisms can also augment the inflammatory function of neutrophils (36), I performed an exploratory crosssectional sub study in the MIRACLE cohort to investigate in detail the phenotype and function of neutrophils in patients with severe CAVD compared to healthy controls as described in Chapter 6. Our results revealed that patients had an altered neutrophil phenotype compared to controls, reflected in increased HLA-DR expression, higher ROS production and less NET formation. It was previously reported that neutrophils that express HLA-DR are associated with high circulating cytokine levels and infections (37-39). However, these neutrophils were also positive for CD80, CD86 and CD40, markers that were not measured in out neutrophil panel (37). HLA-DR+ neutrophils showed antigen-presentinglike properties as seen in mice with atherosclerosis (in vivo) and can be induced upon stimulation with oxLDL (in vitro) (40). Nonetheless we hypothesized that, similarly to ASCVD, neutrophils may play a role in promoting aortic valve disease progression. Oxidative stress is known to be a key factor in atherosclerosis as ROS can oxidize lipids and cause endothelial inflammation and dysfunction, which could promote atherosclerosis. Furthermore, ROS enhances the production of IL-1β, a pro-inflammatory cytokine pivotal in ASCVD pathogenesis, via NLRP3 inflammasome (41). In the context of CAVD, elevated ROS levels were detected in calcified and sclerotic valves, with growing evidence suggesting that it plays a critical role in different stages of CAVD (42-44). In our results in Chapter 6, we observed that neutrophils from CAVD patients exhibited increased ROS production compared to healthy controls upon stimulation with PMA. Although ROS levels were not directly measured in valve tissue, we hypothesize that the increased ROS production we observed in CAVD patients likely originated from circulating neutrophils, which may contribute to the progression and severity of CAVD.

Similarly, NETs have been identified at the sites of atherosclerotic lesions in both humans and mice although its exact role in the pathogenesis of ASCVD is still being investigated (45). In ASCVD, neutrophils can contribute to plaque instability by

releasing NETs and granule proteins within the plague microenvironment. These NETs activate immune and endothelial cells, exacerbating local inflammation (46). As described for our study in **Chapter 6**, we observed lower presence of NETs in plasma of CAVD patients compared to healthy controls, despite previous studies reporting elevated NETs in both plasma and calcified valves of CAVD patients (47). Moreover, we assessed both NOX-dependent and independent NET formation upon neutrophil stimulation from CAVD patients and healthy controls. Consistent with the lower amounts of NETs in the plasma, neutrophils from patients released fewer NETs than those from healthy controls. However, upon stimulation, both patients and healthy controls showed enhanced NET formation relative to baseline, indicating that neutrophil NET production capacity remained intact. Although ROS can drive NET formation (48), we observed increased ROS but decreased NET formation in CAVD patients. Even though this uncoupling may be attributed to other factors, this was previously observed in neutrophils following BCG training (36), suggesting a possible role of trained immunity in CAVD as well.

While our study highlighted the potential involvement of neutrophils in the pathophysiology of CAVD, further research is needed to understand the underlying mechanisms. It would be beneficial to include a larger cohort to improve our understanding of neutrophil dynamics in CAVD and explore the contribution of trained immunity. Such insights will allow us to develop novel therapies targeting neutrophil-related pathways or functions, potentially offering new approaches to managing CAVD progression and/or severity.

Limitations

In the separate chapters, I have discussed the specific limitations for each study. In this paragraph, I will summarize the most important overall limitations of our approach and models.

This thesis presents the results of *in vitro* as well as *in vivo* studies. Some of the *in* vivo findings enclosed in Chapter 3 and Chapter 6 described innate immune cells hyperresponsiveness or altered innate immune function; however, in these studies, we did not assess underlying mechanisms that are responsible for this. In the aforementioned chapters, we hypothesized that trained immunity could be largely responsible for these changes, but additional studies are required to confirm this. These studies should be aimed to investigate the metabolic and epigenetic characteristics that are known to mediate trained immunity. Another limitation of the cohort studies (in subjects with obesity/overweight and patients with CAVD) is that the cross-sectional nature of these studies prevents conclusions on causality. For example, we cannot exclude that the hemodynamic changes induced by the aortic valve stenosis have effects on circulating neutrophils. To assess causality, prospective follow up of the patients and assessment of CAVD progression is needed. An alternative approach to assess causality is to use genetic data. For example, in **Chapter 3**, we described how SNPs in the *LEP* gene affected circulating IL-6 concentration. This finding increases the likelihood that leptin signaling causally affects IL-6 biology, but this does not inform about the underlying mechanisms.

The *in vitro* models with isolated monocytes and HSCs also have limitations. Even though we made the design to mimic as close as possible the physiological conditions, these models do not capture the micro-environment of the monocytes/ HSCs in vivo. Specifically for the HSCs it is important to realize that in the bone marrow these cells are located in specialized niches surrounded by many other cells types, such as endothelial cells, adipocytes, and other mesenchymal cells that also regulate the nutritional exposure and the function of the HSCs (49). Another important limitation of these in vitro studies using primary human cells is that we often do not have detailed demographic and clinical information from the donors. Even though they are all described as "healthy", we cannot exclude variation induced by previous or present medical conditions, medication use, etc. In this regard, it is also of importance to discuss the known interindividual variation in the development of trained immunity. Moorlag, et. al., recently investigated the strengths of the in vivo trained immunity response in 323 individuals by BCG vaccination (50). They showed considerable interindividual heterogeneity in the susceptibility to mount a trained immunity response, with approximately 25% of individuals being non-responders in terms of augmentation of cytokine production capacity. This variability is determined to a large extent by the chromatin accessibility of certain genes in the cells before exposure to the training stimulus. This intrinsic interindividual variability in trained immunity susceptibility probably contributed to the variation in trained immunity by leptin (Chapter 2) and IL-1B (Chapter 4) that we also observed in our studies.

In all the chapters we aimed to use male and female donors/participants, however it was not possible to have a balanced sex distribution. It is of great importance to replicate our findings in a cohort with the same number of males and females to better understand sex-specific effects. This importance is emphasized by the previously published strong sex-dependent differences in the regulation of inflammation in our cohort of 300 individuals with overweight and obesity (19).

A final limitation concerns the sample size of the samples used in the various chapters. In some in vitro studies, the number of cell donors and the group sizes were very limited for some complex and labor-intensive functional assays, such as phagocytosis assays and interaction of BM-derived monocytes with iPSC-derived endothelial cells (IBIDI) in Chapter 4. In Chapter 6, we included only 12 CAVD patients and 12 matched healthy controls to perform the deep immunophenotyping of the neutrophil cell population. Given the sample size, it is important to validate the most important findings in separate studies. Therefore, some of the results in this thesis are merely hypothesis generating and require extra experiments or larger number of participants.

Conclusions and future perspectives

The studies presented in this thesis give insight into how innate immune reprogramming might contribute to the development of CVD. In Chapter 3, we showed that high concentrations of leptin, a pro-inflammatory adipokine, induced trained immunity in vitro and we showed a sex-dependent association in a cohort of overweight and obese individuals between circulating leptin and IL-6, only in men. These findings provide an exciting novel immunological mechanism that could contribute to the metabolic and cardiovascular consequences of obesity. In addition, the mechanism that leptin can trigger long-lasting pro-inflammatory effects in monocytes/macrophages could contribute to the concept of 'obesogenic memory'. This describes the finding that in obese mice, despite weight loss, adipose tissue macrophages, and also HSCs retain a hyperinflammatory phenotype (51, 52). It would be interesting to investigate in future studies the role of leptin signaling in these persistent effects of obesity.

In Chapter 4 we described that trained immunity can also occur in human BMderived HSCs in vitro by exposing them briefly to IL-1β, which results in increased cytokine production, higher cell metabolism and atherogenic phenotype in their monocytes offspring. As described before in this Discussion chapter, the IL-1 pathway and more specifically, IL-1\u03b3, is of great relevance in ASCVD pathophysiology. The clinical studies performed to date have focused on targeting IL-1β in patients suffering from CVD (CANTOS). However, our findings suggest that IL-1β affects HSCs in the bone marrow and might open the door to new studies focusing on molecular targets in the bone marrow niche as a preventive therapeutic option. In addition, as described above, our findings of long-lasting effects of IL-1\beta on HSCs open the possibility to develop short-term anti-IL-1 strategies in situations of increased IL-1β signaling, with long-term beneficial effects.

Although we used monocytes in both studies, in **Chapter 5** we observed that BM-derived monocytes have a more macrophage-like transcriptomic profile, potentially caused by the differentiation protocol. These results emphasize that it is very relevant to take into account the specific source of the monocytes and macrophages in future *in vitro* studies.

In **Chapter 6**, we switched our focus from monocytes to understand how neutrophil phenotype is altered in patients with CAVD compared to healthy controls. We showed higher percentage of HLA-DR+ neutrophils in patients compared to controls. Upon stimulation, neutrophils from patients displayed more ROS production, nonetheless they showed less NET formation. While we successfully described an altered neutrophil phenotype in patients with CAVD, we did not investigate any underlying mechanisms. Therefore, I consider a follow-up study is necessary to understand if and how this altered neutrophil phenotype contributes to CAVD. This follow-up study needs to count with a bigger population, as well as additional functional assays and RNA sequencing, to determine if the functional changes match with any transcriptomic alterations.

References

- 1 Timmis A, Townsend N, Gale CP, Torbica A, Lettino M, Petersen SE, et al. European Society of Cardiology: Cardiovascular Disease Statistics 2019. Eur Heart J. 2020;41(1):12-85.
- 2. Libby P. The changing landscape of atherosclerosis. Nature. 2021;592(7855):524-33.
- 3. Broeders W, Bekkering S, El Messaoudi S, Joosten LAB, van Royen N, Riksen NP. Innate immune cells in the pathophysiology of calcific aortic valve disease: lessons to be learned from atherosclerotic cardiovascular disease? Basic Res Cardiol. 2022;117(1):28.
- Donato M, Ferri N, Lupo MG, Faggin E, Rattazzi M. Current Evidence and Future Perspectives on 4. Pharmacological Treatment of Calcific Aortic Valve Stenosis. Int J Mol Sci. 2020;21(21).
- Nidorf SM, Fiolet ATL, Mosterd A, Eikelboom JW, Schut A, Opstal TSJ, et al. Colchicine in Patients 5. with Chronic Coronary Disease. N Engl J Med. 2020;383(19):1838-47.
- 6. Tardif JC, Kouz S, Waters DD, Bertrand OF, Diaz R, Maggioni AP, et al. Efficacy and Safety of Low-Dose Colchicine after Myocardial Infarction. N Engl J Med. 2019;381(26):2497-505.
- Ridker PM, Everett BM, Thuren T, MacFadyen JG, Chang WH, Ballantyne C, et al. Antiinflammatory 7. Therapy with Canakinumab for Atherosclerotic Disease. N Engl J Med. 2017;377(12):1119-31.
- Riksen NP, Bekkering S, Mulder WJM, Netea MG. Trained immunity in atherosclerotic 8. cardiovascular disease. Nat Rev Cardiol. 2023;20(12):799-811.
- Acevedo OA, Berrios RV, Rodríguez-Guilarte L, Lillo-Dapremont B, Kalergis AM. Molecular and Cellular Mechanisms Modulating Trained Immunity by Various Cell Types in Response to Pathogen Encounter. Front Immunol. 2021;12:745332.
- 10. Vuscan P, Kischkel B, Joosten LAB, Netea MG. Trained immunity: General and emerging concepts. Immunol Rev. 2024;323(1):164-85.
- 11. Cirovic B, de Bree LCJ, Groh L, Blok BA, Chan J, van der Velden W, et al. BCG Vaccination in Humans Elicits Trained Immunity via the Hematopoietic Progenitor Compartment. Cell Host Microbe. 2020;28(2):322-34.e5.
- 12. Noz MP, Bekkering S, Groh L, Nielen TMJ, Lamfers EJP, Schlitzer A, et al. Reprogramming of bone marrow myeloid progenitor cells in patients with severe coronary artery disease. eLife. 2020;9:e60939.
- 13. Mitroulis I, Ruppova K, Wang B, Chen LS, Grzybek M, Grinenko T, et al. Modulation of Myelopoiesis Progenitors Is an Integral Component of Trained Immunity. Cell. 2018;172(1-2):147-61.e12.
- 14. Christ A, Günther P, Lauterbach MAR, Duewell P, Biswas D, Pelka K, et al. Western Diet Triggers NLRP3-Dependent Innate Immune Reprogramming. Cell. 2018;172(1-2):162-75.e14.
- 15. Dong Z, Hou L, Luo W, Pan LH, Li X, Tan HP, et al. Myocardial infarction drives trained immunity of monocytes, accelerating atherosclerosis. Eur Heart J. 2024;45(9):669-84.
- 16. Simats A, Zhang S, Messerer D, Chong F, Beşkardeş S, Chivukula AS, et al. Innate immune memory after brain injury drives inflammatory cardiac dysfunction. Cell. 2024.
- 17. Lavillegrand J-R, Al-Rifai R, Thietart S, Guyon T, Vandestienne M, Cohen R, et al. Alternating highfat diet enhances atherosclerosis by neutrophil reprogramming. Nature. 2024.
- 18. Edgar L, Akbar N, Braithwaite AT, Krausgruber T, Gallart-Ayala H, Bailey J, et al. Hyperglycemia Induces Trained Immunity in Macrophages and Their Precursors and Promotes Atherosclerosis. Circulation. 2021;144(12):961-82.
- 19. Ter Horst R, van den Munckhof ICL, Schraa K, Aguirre-Gamboa R, Jaeger M, Smeekens SP, et al. Sex-Specific Regulation of Inflammation and Metabolic Syndrome in Obesity. Arterioscler Thromb Vasc Biol. 2020;40(7):1787-800.

- 20. Chen Z, Boehnke M, Wen X, Mukherjee B. Revisiting the genome-wide significance threshold for common variant GWAS. G3 (Bethesda). 2021;11(2).
- 21. Naylor C, Petri WA, Jr. Leptin Regulation of Immune Responses. Trends Mol Med. 2016;22(2):88-98.
- 22. Fernández-Riejos P, Najib S, Santos-Alvarez J, Martín-Romero C, Pérez-Pérez A, González-Yanes C, et al. Role of leptin in the activation of immune cells. Mediators Inflamm. 2010:2010:568343.
- 23. Frasca D, Diaz A, Romero M, Blomberg BB. Leptin induces immunosenescence in human B cells. Cell Immunol. 2020;348:103994.
- 24. Souza-Almeida G, D'Avila H, Almeida PE, Luna-Gomes T, Liechocki S, Walzog B, et al. Leptin Mediates In vivo Neutrophil Migration: Involvement of Tumor Necrosis Factor-Alpha and CXCL1. Front Immunol. 2018:9:111.
- 25. Cheng SC, Quintin J, Cramer RA, Shepardson KM, Saeed S, Kumar V, et al. mTOR- and HIF-1α-mediated aerobic glycolysis as metabolic basis for trained immunity. Science. 2014;345(6204):1250684.
- 26. van Leent MMT, Beldman TJ, Toner YC, Lameijer MA, Rother N, Bekkering S, et al. Prosaposin mediates inflammation in atherosclerosis. Sci Transl Med. 2021;13(584).
- 27. Lopez-Castejon G, Brough D. Understanding the mechanism of IL-1ß secretion. Cytokine Growth Factor Rev. 2011;22(4):189-95.
- 28. van der Vaart JI, van Eenige R, Rensen PCN, Kooijman S. Atherosclerosis: an overview of mouse models and a detailed methodology to quantify lesions in the aortic root. Vasc Biol. 2024;6(1).
- 29. Abbate A, Toldo S, Marchetti C, Kron J, Van Tassell BW, Dinarello CA. Interleukin-1 and the Inflammasome as Therapeutic Targets in Cardiovascular Disease. Circ Res. 2020;126(9):1260-80.
- 30. Liao Y, Liu K, Zhu L. Emerging Roles of Inflammasomes in Cardiovascular Diseases. Front Immunol. 2022;13:834289.
- 31. Sager HB, Heidt T, Hulsmans M, Dutta P, Courties G, Sebas M, et al. Targeting Interleukin-1ß Reduces Leukocyte Production After Acute Myocardial Infarction. Circulation. 2015;132(20):1880-90.
- 32. Sreejit G, Nooti SK, Jaggers RM, Athmanathan B, Ho Park K, Al-Sharea A, et al. Retention of the NLRP3 Inflammasome-Primed Neutrophils in the Bone Marrow Is Essential for Myocardial Infarction-Induced Granulopoiesis. Circulation. 2022;145(1):31-44.
- 33. Domínguez-Andrés J, Arts RJW, Bekkering S, Bahrar H, Blok BA, de Bree LCJ, et al. *In vitro* induction of trained immunity in adherent human monocytes. STAR Protoc. 2021;2(1):100365.
- 34. Cerneckis J, Cai H, Shi Y. Induced pluripotent stem cells (iPSCs): molecular mechanisms of induction and applications. Signal Transduction and Targeted Therapy. 2024;9(1):112.
- 35. Poulis N, Martin M, Hoerstrup SP, Emmert MY, Fioretta ES. Development of an iPSC-derived tissueresident macrophage-based platform for the in vitro immunocompatibility assessment of human tissue engineered matrices. Scientific Reports. 2024;14(1):12171.
- 36. Moorlag S, Rodriguez-Rosales YA, Gillard J, Fanucchi S, Theunissen K, Novakovic B, et al. BCG Vaccination Induces Long-Term Functional Reprogramming of Human Neutrophils. Cell Rep. 2020;33(7):108387.
- 37. Davis RE, Sharma S, Conceição J, Carneiro P, Novais F, Scott P, et al. Phenotypic and functional characteristics of HLA-DR(+) neutrophils in Brazilians with cutaneous leishmaniasis. J Leukoc Biol. 2017;101(3):739-49.
- 38. Polak D, Bohle B. Neutrophils-typical atypical antigen presenting cells? Immunology Letters. 2022;247:52-8.
- 39. Wu Y, Ma J, Yang X, Nan F, Zhang T, Ji S, et al. Neutrophil profiling illuminates anti-tumor antigenpresenting potency. Cell. 2024;187(6):1422-39.e24.

- 40. Zhao T, Jiang Q, Li W, Wang Y, Zou Y, Chai X, et al. Antigen-Presenting Cell-Like Neutrophils Foster T Cell Response in Hyperlipidemic Patients and Atherosclerotic Mice. Front Immunol. 2022:13:851713.
- 41. Batty M, Bennett MR, Yu E. The Role of Oxidative Stress in Atherosclerosis. Cells. 2022;11(23).
- 42. Greenberg HZE, Zhao G, Shah AM, Zhang M, Role of oxidative stress in calcific aortic valve disease and its therapeutic implications. Cardiovasc Res. 2022;118(6):1433-51.
- 43. Miller JD, Chu Y, Brooks RM, Richenbacher WE, Peña-Silva R, Heistad DD. Dysregulation of antioxidant mechanisms contributes to increased oxidative stress in calcific aortic valvular stenosis in humans. J Am Coll Cardiol. 2008;52(10):843-50.
- 44. Branchetti E, Sainger R, Poggio P, Grau JB, Patterson-Fortin J, Bavaria JE, et al. Antioxidant enzymes reduce DNA damage and early activation of valvular interstitial cells in aortic valve sclerosis. Arterioscler Thromb Vasc Biol. 2013;33(2):e66-74.
- 45. Mostafa MN, Osama M. The implications of neutrophil extracellular traps in the pathophysiology of atherosclerosis and atherothrombosis. Exp Biol Med (Maywood). 2020;245(15):1376-84.
- 46. Döring Y, Libby P, Soehnlein O. Neutrophil Extracellular Traps Participate in Cardiovascular Diseases: Recent Experimental and Clinical Insights. Circ Res. 2020;126(9):1228-41.
- 47. Kopytek M, Kolasa-Trela R, Ząbczyk M, Undas A, Natorska J. NETosis is associated with the severity of aortic stenosis: Links with inflammation. Int J Cardiol. 2019;286:121-6.
- 48. Kirchner T, Möller S, Klinger M, Solbach W, Laskay T, Behnen M. The impact of various reactive oxygen species on the formation of neutrophil extracellular traps. Mediators Inflamm. 2012;2012:849136.
- 49. Xiao Y, McGuinness CS, Doherty-Boyd WS, Salmeron-Sanchez M, Donnelly H, Dalby MJ. Current insights into the bone marrow niche: From biology in vivo to bioengineering ex vivo. Biomaterials. 2022;286:121568.
- 50. Moorlag S, Folkman L, Ter Horst R, Krausgruber T, Barreca D, Schuster LC, et al. Multi-omics analysis of innate and adaptive responses to BCG vaccination reveals epigenetic cell states that predict trained immunity. Immunity. 2024;57(1):171-87.e14.
- 51. Schmitz J, Evers N, Awazawa M, Nicholls HT, Brönneke HS, Dietrich A, et al. Obesogenic memory can confer long-term increases in adipose tissue but not liver inflammation and insulin resistance after weight loss. Mol Metab. 2016;5(5):328-39.
- 52. Hata M, Andriessen EMMA, Hata M, Diaz-Marin R, Fournier F, Crespo-Garcia S, et al. Past history of obesity triggers persistent epigenetic changes in innate immunity and exacerbates neuroinflammation. Science. 2023;379(6627):45-62.



Chapter 9

Nederlandse samenvatting

Hart- en vaatziekten (HVZ) zijn een van de belangrijkste oorzaken van morbiditeit en mortaliteit wereldwijd, en door een zittende levensstijl en een ongezonder dieet wordt dit alleen maar erger. Jaarlijks sterven bijna 18 miljoen mensen als gevolg van HVZ, met atherosclerose - een laaggradige ontstekingsziekte van de slagaderwand - als belangrijkste onderliggende oorzaak van de HVZ. Atherosclerose kan een hartinfarct, beroerte en perifeer arterieel vaatlijden veroorzaken, afhankelijk van de locatie van de plaques. Een andere veel voorkomende hartaandoening is aortaklepstenose. Dit behelst een progressieve vernauwing van de aortaklep, wat ernstige gevolgen heeft als het niet wordt behandeld. Atherosclerotische cardiovasculaire ziekte (afgekort in dit proefschrift als ASCVD, Atherosclerotic Cardiovascular Disease) als aortaklepstenose delen pathologische kenmerken, waaronder chronische ontsteking.

Verschillende risicofactoren zoals veroudering, hoge bloeddruk, roken, obesitas en diabetes dragen bij aan de ontwikkeling van ASCVD en aortaklepstenose. De pathogenese van ASCVD is complex; een belangrijk mechanisme dat bijdraagt aan plaquevorming is de ophoping van vetten in de slagaderwanden, maar cellen van het aangeboren afweersysteem spelen een cruciale rol. Activatie van endotheelcellen (de binnenbekleding van de vaatwand) leidt tot verhoogde expressie van adhesiemoleculen waardoor monocyten naar de laesieplaats worden aangetrokken. Deze monocyten migreren vervolgens de vaatwand in, differentiëren daar tot macrofagen en nemen de lipiden op, waardoor ze 'schuimcellen' worden. De ophoping van deze schuimcellen leidt tot de vorming van een necrotische kern, die kan eroderen of scheuren, wat uiteindelijk kan leiden tot arteriële occlusie, waardoor een infarct ontstaat.

De afgelopen jaren werd een nieuw immunologisch mechanisme ontdekt dat mogelijk een rol speelt in het ontstaan van ASCVD, genaamd getrainde immuniteit (in het Engels trained immunity). In de afgelopen jaren werd beschreven dat cellen van het aangeboren immuunsysteem ook een geheugen kunnen ontwikkelen. Dit wordt getrainde immuniteit genoemd en kan worden uitgelegd als een verhoogde reactiviteit van aangeboren immuuncellen, lang nadat de initiële stimulus voor de immuuncellen is verdwenen. Getrainde immuniteit stelt cellen van het aangeboren immuunsysteem, zoals monocyten en neutrofielen, dus in staat om een geheugen te ontwikkelen na blootstelling aan bepaalde stimuli, waardoor ze langdurig een actievere functie hebben. Getrainde immuniteit, wat aanvankelijk werd ontdekt als reactie op infecties, kan ook worden getriggerd door lichaamseigen factoren die verband houden met HVZ, zoals geoxideerde lipiden en hoge glucosespiegels. Deze geheugenachtige respons is te wijten aan metabole

9

en epigenetische veranderingen in de immuuncellen, zowel in 'volwassen' circulerende immuuncellen als in hun voorlopers in het beenmerg, waardoor de ontstekingsreactie kan aanhouden.

Tot op heden worden bestaat de behandeling van patiënten met HVZ vooral op het behandelen van risicofactoren, zoals het verlagen van de bloeddruk en het verlagen van LDL-cholesterol door medicijnen. De laatste jaren hebben verschillende klinische studies aangetoond dat ook ontstekingsremmende behandelingen het risico op ASCVD verminderen. Voor aortaklepstenose is helaas nog geen enkele effectieve medicamenteuze behandeling voorhanden. Daarom is de enige behandeling chirurgische of endovasculaire klepvervanging, als de symptomen van de aortaklepstenose ernstig zijn geworden. Ondanks de huidige therapieën blijft in veel patiënten het risico op ASCVD hoog en is onderzoek naar de specifiek rol van ontsteking en het afweersysteem dat ten grondslag ligt aan zowel ASCVD als aortaklepstnose essentieel om betere behandelingsdoelen te identificeren.

In dit proefschrift heb ik de rol van monocyten in de pathofysiologie van ASCVD onderzocht, met een focus op getrainde immuniteit. Ten eerste heb ik in **Hoofdstuk 2** een overzicht gegeven van de triggers en mechanismen van getrainde immuniteit bij ASCVD. Vervolgens hebben we in Hoofdstuk 3 onderzocht hoe leptine, een hormoon dat verband houdt met obesitasgerelateerde complicaties, de monocytenfunctie en ontsteking beïnvloedt. We ontdekten dat leptine in vitro getrainde immuniteit induceerde in monocyten van gezonde vrijwilligers. Bovendien waren circulerende leptinespiegels in een cohort van 302 mensen met overgewicht of obesitas (BMI > 27 kg/m², leeftijd 55-81) positief geassocieerd met ontstekingsmarkers IL-1β en IL-6, waarbij dit effect uitgesprokener was bij mannen. Daarnaast beïnvloedden genetische variaties in de vorm van kleine variaties in de DNA code (in het Engels Single Nucleotide Polymorphism, SNP) in het leptinegen de IL-6-spiegels bij mannen, wat suggereert dat leptine een directe rol speelt bij het aansturen van ontstekingen.

Sommige muizenmodellen laten zien dat getrainde immuniteit de progressie van atherosclerose kan versnellen onder omstandigheden zoals een vetrijk dieet, hoge bloedsuikerspiegels, en na een hartinfarct, voornamelijk via IL-1β-signalering in het beenmerg. Om de langetermijneffecten van IL-1 β op voorlopercellen van witte bloedcellen uit het beenmerg van mensen gedetailleerder te onderzoeken, heb ik de studies uitgevoerd die in Hoofdstuk 4 worden beschreven. We stelden stamcellen die geïsoleerd waren uit het beenmerg van vrijwilligers 4 uur lang bloot aan IL-1β. Vervolgens werden deze stamcellen vermeerderd en gedifferentieerd tot monocyten gedurende ongeveer 3 weken, waarna we belangrijke immunologische parameters maten om de inductie van getrainde immuniteit te bepalen. Met IL-1 β behandelde stamcellen genereerden meer granulocyt-macrofaag kolonievormende eenheden; met andere woorden: deze cellen deelden sneller. Bovendien vertoonden monocyten afkomstig van met IL-1 β behandelde cellen een verhoogde productie van TNF en IL-1 β na herstimulatie met LPS en Pam3Cys, samen met een verhoogde metabole activiteit, vergelijkbaar met getrainde monocyten uit het bloed. Analyse van het RNA onthulde verhoging van belangrijke ontstekings- en atherogene netwerken. Deze bevindingen tonen aan dat korte blootstelling aan IL-1 β getrainde immuniteit induceert in humane stamcellen in vitro.

In dit proefschrift heb ik getrainde immuniteit bestudeerd in menselijke circulerende monocyten in hoofdstuk 3 en stamcel-afgeleide monocyten in hoofdstuk 4. Daarom was het belangrijk om deze verschillende cellen systematisch te vergelijken om de resultaten van de verschillende modellen te kunnen begrijpen. In Hoofdstuk 5 hebben we systematisch humane circulerende monocyten en macrofagen vergeleken met die afkomstig van geïnduceerde pluripotente stamcellen (iPSCs) en humane stamcellen. Humane circulerende monocyten hebben een hoger percentage klassieke monocyten vergeleken met monocyten die voortkomen uit iPSCs en stamcel. Alle soorten monocyten produceren cytokines (IL-6, TNF en IL-1ra) na stimulatie met TLR-liganden, met kleine verschillen. Circulerende en stamcelafgeleide monocyten vertonen een hogere glycolytische capaciteit vergeleken met iPSC-afgeleide monocyten. Epigenetische en transcriptoomanalyses suggereren dat monocyten die voortkomen uit stamcellen en uit iPSCs meer gedifferentieerd zijn richting macrofaag dan circulerende monocyten. Dit komt overeen met een hogere fagocytosecapaciteit van deze cellen vergeleken met de primaire monocyten. We benadrukken dat hoewel iPSC- en stamcel-afgeleide monocyten/ macrofagen goede alternatieven zijn voor onderzoek, ze echter verschillende functionele kenmerken hebben vergeleken met circulerende monocyten.

Zoals eerder vermeld, dragen neutrofielen ook bij aan de chronische ontsteking van de slagaders die ASCVD geeft. Deze cellen kunnen reageren op ontstekingen doordat ze een soort "vallen" kunnenmaken van DNA (in het Engels *Neutrophil Extracellular Traps*, NETs) en reactieve zuurstofsoorten (in het Engels *Reactive Oxygen Species*, ROS) uit te spuwen, waardoor de vaatwand verder wordt beschadigd en de rekrutering van monocyten wordt versneld. NETs kunnen ook het gedrag van macrofagen veranderen en plaques destabiliseren, waardoor het risico op een cardiovasculair event toeneemt. Verhoogde aantallen circulerende neutrofielen zijn geassocieerd met het meer voorkomen van ASCVD. Alhoewel

ontsteking voor beide ziekten belangrijk is, is voor aortaklepstenose de rol van neutrofielen nog veel minder goed vastgesteld. Daarom hebben we in **Hoofdstuk 6** het neutrofielenfenotype en de functie onderzocht bij patiënten met ernstige aortaklepstenose in vergelijking met gezonde controles. In een exploratief cross-sectioneel onderzoek, dat 12 patiënten met ernstige aortaklepstenose en 12 gezonde controles met dezelfde leeftijd en geslacht omvatte, zagen we een hoger aantal leukocyten bij de patiënten in vergelijking met controles, maar geen verschillen in het absolute aantal neutrofielen. Patiënten met aortaklepstenose hadden een hoger percentage neutrofielen met het molecuul HLA-DR aan de buitenkant. Neutrofielen van patiënten produceerden ook meer ROS, zowel bij aanvang als na stimulatie, maar vertoonden een verminderde spontane NETvorming. Hoewel we met de huidige resultaten suggereerden dat neutrofielen bij ernstige aortaklepstenose een veranderd fenotype en functioneel profiel hebben, wat mogelijk bijdraagt aan de progressie van de ziekte, zijn verdere studies in grotere cohorten nodig om de rol echt te begrijpen.



Chapter 10

Resumen

Las enfermedades cardiovasculares (ECV) son una de las principales causas de morbilidad y mortalidad a nivel global, y este número de casos va en aumento debido al estilo de vida sedentario y una dieta poco saludable. Alrededor de 18 millones de personas mueren cada año a causa de enfermedades cardiovasculares, siendo la aterosclerosis (una enfermedad inflamatoria de bajo grado en la pared arterial) la principal causa subyacente. La aterosclerosis, según la ubicación de las placas, puede provocar infarto de miocardio, accidente cerebrovascular y enfermedad arterial periférica. Otra afección cardiaca es la estenosis aórtica, en la cual ocurre un estrechamiento progresivo de la válvula aórtica, sin tratamiento y puede comprometer la vida de quien la padece. La enfermedad cardiovascular aterosclerótica (ECVA) y la estenosis aórtica comparten características patológicas, incluida la inflamación crónica.

Diversos factores de riesgo, como el envejecimiento, la presión arterial alta, el tabaquismo, la obesidad y la diabetes, contribuyen al desarrollo de ECVA y estenosis aórtica. En la patogénesis de la ECVA, la acumulación de lípidos en las paredes arteriales contribuye a la formación de placa al igual que las funciones efectoras de las células inmunes innatas. Por otro lado, La activación de las células endoteliales conduce a una mayor expresión de moléculas de adhesión y quimiocinas como la proteína quimiotáctica de monocitos (MCP-1 por sus siglas en inglés), que atrae monocitos al sitio de la lesión. Estos monocitos migran a la íntima, se diferencian en macrófagos y absorben lipoproteínas modificadas, convirtiéndose posteriormente en células espumosas. Luego, forman un núcleo necrótico, que puede erosionarse o romperse provocando una oclusión arterial que puede desencadenar un evento cardiovascular.

Con una mejor comprensión del papel de la inflamación en la fisiopatología de la ECVA, se propuso la inmunidad entrenada (trained immunity por su término en inglés) como un mecanismo importante. La inmunidad entrenada es un tipo de memoria inmunológica que ocurre en el sistema inmunológico innato. A diferencia de la inmunidad adaptativa, que usa células especializadas como los linfocitos (capaces de generar memoria a largo plazo a través de antígenos y anticuerpos), la inmunidad entrenada ocurre en células como los neutrófilos y monocitos. Estas células, después de haber estado expuestas a ciertos patógenos o estímulos, cambian su metabolismo y respuesta inflamatoria, lo que les permite reaccionar más rápido y fuerte ante futuras infecciones o estímulos, incluso si son causadas por algo completamente diferente. Aunque inicialmente fue observada como respuesta a infecciones, la inmunidad entrenada también puede desencadenarse por otros factores endógenos asociados a ECV, como la lipoproteína de baja

densidad oxidada (oxLDL por sus siglas en inglés) y los niveles elevados de glucosa. Esta respuesta se debe a cambios metabólicos y epigenéticos, tanto en las células inmunes innatas 'adultas' como en sus progenitores en la médula ósea, lo que permite que esta respuesta inflamatoria persista.

Hasta hoy en día, el tratamiento para los pacientes con ECV se enfoca principalmente en controlar los factores de riesgo, como la reducción de la presión arterial y el colesterol LDL con uso de medicamentos. En los últimos años, diversos estudios clínicos han mostrado que algunas terapias antiinflamatorias también reducen el riesgo de ECVA. Desafortunadamente, aún no existe ningún tratamiento farmacológico eficaz para la estenosis de la válvula aórtica siendo el reemplazo el remplazo endovascular o quirúrgico de la válvula el único tratamiento si los síntomas se han vuelto graves. A pesar de las terapias actuales, el riesgo de ECVA continúa siendo alto en muchos pacientes y la investigación sobre el papel especifico de la inflamación y el sistema inmune subyacentes tanto a la ECVA como a la estenosis de la válvula aórtica es esencial para identificar mejores blancos de tratamiento.

En esta tesis investiqué el papel de los monocitos en la fisiopatología de la ECVA, con un enfoque en la inmunidad entrenada. En primer lugar, en el Capítulo 2, describí de manera general los desencadenantes y mecanismos de la inmunidad entrenada en la ECVA. Después, en el Capítulo 3, estudié cómo la leptina, una hormona vinculada a las complicaciones relacionadas con la obesidad, influye en la función de los monocitos y la modulación de inflamación. Descubrimos que la leptina inducía inmunidad entrenada en monocitos de donadores voluntarios sanos in vitro. Además, en una cohorte de 302 individuos con sobrepeso u obesidad, (IMC >27 kg/m², edad 55-81), los niveles en circulación de leptina tenían una asociación positiva con algunos marcadores inflamatorios como IL-1β e IL-6, siendo este efecto más pronunciado en hombres. Además, variaciones en forma de polimorfismos de nucleótido único (SNP por sus siglas en inglés) en el gen de leptina influyeron en los niveles de IL-6 en hombres, lo que sugiere que la leptina juega un papel directo en la inflamación.

Algunos modelos de ratón muestran que la inmunidad entrenada puede acelerar la progresión de aterosclerosis en condiciones como una dieta rica en grasas saturadas, niveles elevados de glucosa en sangre y después de haber sufrido un infarto al miocardio; esto principalmente a través de la señalización de IL-1β en la médula ósea. Para investigar más a detalle los efectos a largo plazo de IL-1β sobre las células progenitoras precursoras de los glóbulos blancos derivados de la médula ósea, realicé el estudio descrito en el Capítulo 4.

Expusimos células madre (CD34+) aisladas de la médula ósea de personas voluntarias a IL-1β por 4 horas. Posteriormente, estas células madre se expandieron y diferenciaron en monocitos durante aproximadamente 3 semanas, después de las cuales medimos parámetros inmunológicos clave para determinar la inducción de inmunidad entrenada. Las células madre que fueron expuestas a IL-1β generaron mas unidades formadoras de colonias de granulocitos y macrófagos; en otras palabras, estas células se dividieron más rápido. Además, los monocitos derivados de las células expuestas a IL-1β mostraron una mayor producción de TNF e IL-1β, después de la re-estimulación con lipopolisacáridos (LPS) y Pam3Cys. Asimismo, estas células presentaron una mayor actividad metabólica, similar a los monocitos entrenados en sangre. El análisis de ARN reveló una regulación positiva de ciertas vías de señalización en inflamación y aterogénesis. Estos hallazgos demuestran que la exposición a corto plazo a IL-1β induce inmunidad entrenada en células madre humanas in vitro

En esta tesis, estudié la inmunidad entrenada en monocitos en circulación en humanos en el capítulo 3 y en monocitos derivados de células madre en el capítulo 4. Por lo tanto, era importante comparar sistemáticamente estas diferentes células para comprender los resultados de los diferentes modelos. En el Capítulo 5, comparamos sistemáticamente los monocitos y macrófagos en circulación en humanos con monocitos derivados de células madre pluripotente inducida (iPSC por sus siglas en inglés) y células madre derivadas de médula ósea en humanos. Los monocitos en circulación en humanos tienen un mayor porcentaje de monocitos clásicos en comparación con los monocitos derivados de iPSC y células madre de la médula ósea. Todos los tipos de monocitos producen citocinas (IL-6, TNF e IL-1ra) en respuesta a la estimulación con ligandos TLR. Los monocitos en circulación y aquellos derivados de células madre exhiben una mayor capacidad glucolítica en comparación con monocitos derivados de iPSC. Los análisis de epigenética y transcriptómica sugieren que los monocitos derivados de células madre de medula ósea y pluripotente están más diferenciados hacia macrófagos que los monocitos derivados de circulación. Esto es consistente con una mayor capacidad fagocítica de estas células en comparación con los monocitos derivados de circulación. Cabe destacar que si bien los monocitos/ macrófagos derivados de iPSC de células madre de médula ósea son buenas alternativas para su uso en investigación, tienen características funcionales diferentes en comparación con los monocitos derivados de circulación.

Como se mencionó anteriormente, los neutrófilos también contribuyen a la inflamación crónica de las arterias que produce la ECVA. Estas células pueden responder a la inflamación creando trampas extracelulares de neutrófilos (Neutrophil

Extracellular Traps, NETs) y secretando especies reactivas de oxígeno (Reactive Oxigen Species, ROS), dañando aún más la pared arterial y acelerando el reclutamiento de monocitos. Las NETs también pueden alterar el comportamiento de los macrófagos y desestabilizar las placas, aumentando el riesgo de un evento cardiovascular. El aumento del número de neutrófilos en circulación se asocia con una mayor incidencia de ECVA. Aunque la inflamación es importante para ambas enfermedades, el papel de los neutrófilos en la estenosis de la válvula aórtica ha sido mucho menos estudiado. Por lo tanto, en el Capítulo 6 investigamos el fenotipo y la función de los neutrófilos en 12 pacientes con estenosis aórtica grave en comparación con 12 controles sanos pareados por sexo y edad. Observamos un mayor número de leucocitos en los pacientes en comparación con los controles, pero no hubo diferencias en los números absolutos de neutrófilos. Los pacientes con estenosis de la válvula aórtica tenían un mayor porcentaje de neutrófilos positivos para el receptor de superficie celular HLA-DR. Los neutrófilos en pacientes también secretaron mayores niveles de ROS, tanto al inicio como después de la estimulación, pero mostraron una formación espontánea reducida de NETs. Aunque los resultados actuales sugieren que los neutrófilos tienen un fenotipo y un perfil funcional alterados en la estenosis aórtica grave, lo que posiblemente contribuya a la progresión de la enfermedad, se necesitan más estudios en cohortes más grandes para comprender verdaderamente su papel.



Appendices

Data Management
Portfolio
List of publications
Acknowledgements
Curriculum Vitae
About the Author

Research Data Management

Ethics and privacy

This thesis in mainly based on research with human participants, and all the experiments were performed according to the principles in the declaration of Helsinki. Clinical studies were performed according to good clinical practice quidelines (ICH-GCP) and were subject to the Medical Research Involving Human Subjects Act (WMO). All participants provided informed written consent.

The 300OB cohort used in Chapter 3 was approved by the Ethical Committee of Radboud University (Nr. 46846.091.13).

In Chapter 4 and 5, the use of the bone marrow aspiration material was approved by the Medical Ethics Review Committee 'METC Oost-Nederland' (Ethical Approval CMO Arnhem-Nijmegen, 2013/064).

The iPSCs used in Chapter 5 were registered in the online registry for human iPSC lines in the European Bank for induced pluripotent Stem Cells (EBiSC).

The work described in Chapter 6 was derived from the MIRACLE study (ClinicalTrials. gov Identifier: NCT04717219) and the study protocol was approved by the Medical Ethics Committee (NL72973.091.20).

To protect the privacy of the participants, pseudo anonymization was used and data was stored in a secure way in folders with restricted access.

Data collection and storage

All the data presented in this thesis is stored according to the FAIR (Findability, Accessibility, Interoperability and Reusability) principles.

Data presented in Chapter 3, 4 and 5 was obtained largely through laboratory experiments involving anonymous primary human material. These data are stored on the secured department server, which is only accessible by project members working at Radboudumc.

In Chapter 3, we re-used pseudonymized data from the 300OB study which was previously collected at our department and stored on the secured department server, which is only accessible by project members working at Radboudumc.

The clinical data presented in Chapter 6 was collected in electronic Case Report Forms (eCRF) in Castor EDC. The data was stored in Castor EDC and on the secured department server (for the laboratory data), which is only accessible by project members working at Radboudumc

Additionally, details on protocols were annotated in physical lab journals, which are kept under lock in the department.

Availability of data

Chapters 2, 3 and 4 are published in open access journals.

The data presented in Chapter 3 concerned the 300OB cohort, that was part of the Human Functional Genomics Project. Anonymized data and materials have been made publicly available at the Human Functional Genomics Project (HFGP) website and can be accessed at https://hfgp.bbmri.nl/ and via https://data.mendeley.com/ datasets/4tb8spry4b/1.

For Chapter 4 and 5, all newly generated sequencing results are deposited in public databases, as described below. The RNA sequencing data reported in Chapter 4 can be found in the NCBI Gene Expression Omnibus (GEO) database with accession number GSE253764. The ATAC and RNA sequencing data reported in Chapter 5 can be found in the GEO database under accession numbers GSE261697 and GSE261696 respectively.

The data presented in Chapter 6 are part of the ongoing MIRACLE study, and data will be made publicly available after publication of all other research papers that are part of this project.

PhD Portfolio of Daniela Flores Gomez

 Department:
 Internal Medicine

 PhD period:
 15/08/2019 - 15/08/2023

PhD Supervisor(s): Prof. N.P. Riksen and Prof. M. G. Netea

PhD Co-supervisor(s): Dr. Siroon Bekkering

Training activities			
Courses			
• Literature Review for your PhD: how to search and where to publish (2019)	6.00		
Introduction to R (2019)	8.00		
Radboudumc - Introduction day (2020)	6.00		
RIMLS - Introduction course "In the lead of my PhD" (2020)	15.00		
R programming for data science (2020)	20.00		
RU - Projectmanagement for PhD candidates (2020)	52.00		
Statistics for PhD candidates using SPSS (2020)	60.00		
Radboudumc - Scientific integrity (2021)	20.00		
How to write a medical scientific paper (2022)	4.50		
IMM - The Art of Presenting Science (2022)	33.00		
RU - Effective Writing Strategies (2022)	75.00		
What is the next step in my career (2022)	16.00		
Meet the Expert - LinkedIn Workshop (2022)	2.00		
Flow cytometry masterclass (2022)	1.00		
Visualizations in R: from basics to advanced (2022)	2.00		
What is the next step in my career (2023)	20.00		
Flow cytometry masterclass (2023)	1.00		
RU - The Art of Finishing Up (2023)	10.00		
How to prepare for your PhD Defense (2023)	4.00		
Meet the Expert: Peer Review and Rebuttal Writing (2023)	4.00		
Seminars			
Immunometnet Seminars (2021)	20.00		
Cardiovascular Research Discoveries (2021)	10.00		
5th DCVA Translational Cardiovascular Meeting (2021)	8.00		
Nanotherapeutics masterclass (2022)	2.00		
Young @ Heart Fall event 2022 (2022)	8.00		
Radboud Research Rounds (2023)	15.00		
Conferences			
4th International Conference on Innate Immune Memory (participation) (2019)	28.00		
EAS Congress 2020 (participation) (2020)	24.00		
RIMLS PhD Retreat 2020 (poster presentation) (2020)	7.00		
EAS Congress 2021 (participation) (2021)	24.00		
RIMLS PhD retreat 2021 (poster presentation) (2021)	16.00		
SSAR meeting 2022 (poster presentation) (2022)	30.00		
Dutch Atherosclerosis Society Meeting 2022 (participation) (2022)	8.00		
RIMLS PhD retreat 2022 (oral presentation) (2022)	20.00		
International Trained Immunity Consortium Meeting 2022 (poster presentation) (2022)	25.00		
5th International Conferences on Innate Immune Memory (poster presentation) (2023)	30.00		
Dutch Atherosclerosis Society Meeting 2023 (oral presentation) (2023)	16.00		
6th International Symposium on Trained Immunity (participation) (2024)	28.00		

Total		919.00
•	Supervision first year master Biomedical Sciences (6 months) (2022)	80.00
Su •	pervision of internships / other Supervision visiting PhD student (2 months) (2021)	50.00
	aching activities	
•	Vascular Research Meeting (2023)	15.00
	Department Weekly Research Meeting (2023)	40.00
	MIMETAS: Grow, learn, discover (2023)	4.00
	ERA CVD Consortium Meeting (2022)	4.00
	ERA CVD Consortium Meeting (2021)	4.00
	IGEM Giant Jamboree (2020)	20.00
	Vasculometabolic meeting (2020)	15.00
	ERA CVD consortium meeting (2020)	4.00
	In Control II Consortium Meeting (2019)	4.50
)t	her	4.5

List of publications

- 1. Piluso S, **Flores Gomez D**, Dokter I, Moreira Texeira L, Li Y, Leijten J, van Weeren R, Vermonden T, Karperien M, Malda J. Rapid and cytocompatible cell-laden silk hydrogel formation *via* riboflavin-mediated crosslinking. J Mater Chem B. 2020 Oct 28;8(41):9566-9575. doi: 10.1039/d0tb01731k. PMID: 33001117.
- Flores-Gomez D, Bekkering S, Netea MG, Riksen NP. Trained Immunity in Atherosclerotic Cardiovascular Disease. Arterioscler Thromb Vasc Biol. 2021 Jan;41(1):62-69. doi: 10.1161/ATVBAHA.120.314216. Epub 2020 Nov 5. PMID: 33147995.
- Domínguez-Andrés J, Arts RJW, Bekkering S, Bahrar H, Blok BA, de Bree LCJ, Bruno M, Bulut Ö, Debisarun PA, Dijkstra H, Cristina Dos Santos J, Ferreira AV, Flores-Gomez D, Groh LA, Grondman I, Helder L, Jacobs C, Jacobs L, Jansen T, Kilic G, Klück V, Koeken VACM, Lemmers H, Moorlag SJCFM, Mourits VP, van Puffelen JH, Rabold K, Röring RJ, Rosati D, Tercan H, van Tuijl J, Quintin J, van Crevel R, Riksen NP, Joosten LAB, Netea MG. *In vitro* induction of trained immunity in adherent human monocytes. STAR Protoc. 2021 Feb 24;2(1):100365. doi: 10.1016/j.xpro.2021.100365. PMID: 33718890; PMCID: PMC7921712.
- 4. **Flores Gomez D**, Bekkering S, Ter Horst R, Cossins B, van den Munckhof ICL, Rutten JHW, Joosten LAB, Netea MG, Riksen NP. The effect of leptin on trained innate immunity and on systemic inflammation in subjects with obesity. J Leukoc Biol. 2024 Jan 19;115(2):374-384. doi: 10.1093/jleuko/qiad118. PMID: 37776323.
- 5. **Flores-Gomez D**, Hobo W, van Ens D, Kessler EL, Novakovic B, Schaap NPM, Rijnen WHC, Joosten LAB, Netea MG, Riksen NP, Bekkering S. Interleukin-1β induces trained innate immunity in human hematopoietic progenitor cells in vitro. Stem Cell Reports. 2024 Dec 10;19(12):1651-1664. doi: 10.1016/j. stemcr.2024.09.004. Epub 2024 Nov 7. PMID: 39515317.

Acknowledgements

They say it takes a village to raise a child - well, it definitely takes an army of brilliant, patient, loving and mostly coffee-fueled individuals to complete a PhD.

First and foremost, I would like to sincerely thank all the bone marrow and blood donors that made my research and the contents of this book possible. To my advisors, colleagues, friends and family - thank you for enduring with me, the happy and not so happy moments and for reminding me that science is beautiful but so is life beyond the lab. This journey has been long and challenging and I wouldn't have made it without you all.

Dear Prof. Riksen, dear **Niels**, these past years haven been a whirlwind of learning, experimenting and every now and then wondering why science can be so stubborn. But through it all, your support, patience and guidance made this journey so much easier. From day one, you trusted me to grow as an independent researcher, giving me the freedom to figure things out while always being there when I needed to be pushed in the right direction. I am especially grateful for your leadership during the pandemic, when everything felt uncertain. You not only kept us motivated and focused but also genuinely cared about our well-being. It made all the difference to be part of a team where we felt supported, both professionally and personally. And of course, a huge thank you for all your constructive criticism and feedback. Your insights have helped me grow so much and I am incredibly grateful to have you as a mentor.

Dear Prof. Netea, dear Mihai, I have always been in awe of your ability to turn a simple meeting – with nothing more than a pen and a paper – into an entire PhD project in one sitting and to see your scientific mind at work! Your ability to see the bigger picture, connect the dots and generate ideas has been nothing but inspiring. Thank you for always keeping us motivated, for all your enthusiasm and for reminding us that the work we were doing was 'fantastic'. As the same time, you never hesitated to push us to improve, offering feedback and encouraging us to refine our experiments and interpretations.

Dear Dr. Bekkering, dear **Siroon**, what a ride it's been! I still remember receiving that email from you all the way from the other side of the world, letting me know you would be my daily supervisor. And let me tell you, I could not have asked for a better one! From day one, you were there with your guidance, support and reassuring presence that made even the most chaotic PhD moments feel a little less overwhelming. There were of course, frustrating times, failed experiments and an occasional broken finger, but no matter what, you were always on top of it, ready with a plan, a solution and so much-needed perspective to keep me going. You have been, and continue to be, a role model for me in so many ways. You didn't just teach me how to be a good researcher – you taught me how to take care of myself outside of the lab, how to know when to push a little harder but also when to stop and take a breather. You showed me that having a good work-life balance isn't just a nice idea; it is essential for staying sane in this wild world of research. So, thank you for everything! For your patience, your wisdom and for making this journey one that I will always look back on with gratitude (and maybe a little nostalgia).

Dear Prof. Joosten, dear Leo, thank you for always being there to help troubleshoot experiments. Your insights were invaluable, not just in fixing issues but in teaching me how to think critically and approach challenges creatively.

Dear Dr. Kessler, dear Elise, thank you for introducing me to the wonderful world of iPSCs! I am really grateful that us working together started with nothing more than a funny-looking flow cytometry plot... Who knew curiosity (and a bit of confusion) could lead to such great collaborative work. You have truly inspired me in so many ways: teaching me to be more creative, assertive and definitely more efficient! I am also thankful for the time I spent in your lab in Utrecht. Those IBIDI experiments were the cherry on top of an already good experience. And our writing sessions? Who would have thought that drafting the first version of a paper in one sitting was possible with the right company and of course the right snacks 😉. Even though our paths have diverged (1072 km to be exact), you continue to be a role model for me. Next time you're in the Netherlands, how about lunch?

Dear Lucienne and Susanna, working with both of you during my internships was such a great experience! I still remember stepping into the lab, knowing next to nothing about cell culture, and how much I learned thanks to your patience and guidance. You made the learning process fun and engaging, and I can't thank you enough for all your support. I'm really grateful for everything you taught me

Some of the work presented in this thesis would not have been possible without the help from our collaborators. Dear **Dr. Willemijn Hobo** and **Diede van Ens**, I still remember the moment I found I would be working with bone marrow, I was absolutely terrified! But you, along all your wonderful colleagues from Hematology, made the experiences so much easier. Your patience and willingness to teach me the techniques (and answer our endless questions) made all the difference. I can't thank you enough for your support! Dear Boris, thank you for all your help with the data analysis (and for meeting with us in spite of the time difference). To our colleagues from Nephrology and Cardiology, Dr. Nils Rother, Dr. Niels van Royen and Dr. Saloua El Messaoudi, thank you for the help with the MIRACLE neutrophil study. To all the people in Experimental Cardiology at UMC Utrecht, especially to Dr. Joost Sluijter, Dr. Saskia de Jager and to Daniek Kapteyn, thank you for your help with experiments involving iPSC cells and for receiving me in your lab. I feel incredibly lucky to have worked with such a fantastic group of collaborators, thank vou all!

To all my colleagues in AIG, present and past, thank you for all the help, the trips, the retreats and all the fun – but most importantly for all the delicious cakes at the baking competition!

Ajie, Aline, Alisa, Anaisa, Anna, Arslan, Bram, Brenda, Büşra, Cas, Chon-Kit, Clementine, Collins, Corlinda, David, Dennis, Diletta, Dogukan, Elisabeth, Eli, Esther, Ezio, Fadel, Flavia, Freek, Georgiana, Gizem, Godfrey, Inge G, Inge M, Intan, Isis, Jan-Quinten, Janneke, Jasmiin, Jelle, Jelmer, Jeroen, Jessica, Job, Jorge, Julia B, Julia H, Katrin, Konstantin, Laura, Leonie, Lieke, Linda, Lisa K, Lisa T, Lorenzo, Lotte, Maartje, Margo, Marijn, Mariolina, Marlies, Martin, Medeea, Michelle, Mümin, Nadira, Nick, Nico, Niklas, Noriko, Orsi, Peng, Prashant, Priya, Rianne, Rob A, Rob H, Rosalie, Ruigi, Sanne, Simone, Suzanne, Tania, Thanasis, Thijs, Todia, Tom, Valerie, Vera, Vicky, Victoria, Viola, Yohana, Yuri, Yutaka, Zara

Ilayda, thanks for being a great office mate! For all the chats, especially the muchneeded debriefs after ridiculously long lab days. From science struggles to life's random topics, our conversations made the PhD journey so much more enjoyable. Özlem, my favorite concert buddy! Thank you for not only sharing great music experiences with me but also for simply being there. I'm so glad we got to know each other better, and I truly appreciate your friendship (and impeccable music taste, of course). Pepiin, who knew bone marrow days could actually be fun? Thanks for making them much more entertaining and for being such a good labmate. Wishing you all the best with the rest of your PhD. May all your experiments be successful and your data always make sense.

Marisol, qué bonito fue compartir el laboratorio contigo. Gracias por todas las pláticas, la comida y sobre todo, por contagiarme siempre tu alegría. Sofi, qué alegría haberte conocido. Gracias por acompañarme a Fiesta Macumba y por introducirme al mundo del mate, definitivamente una experiencia que no olvidaré. Querida Adriana, qué increíble haber coincidido contigo, no solo en este lado del mundo, sino en el mismo laboratorio. Gracias por todas nuestras conversaciones y por esas veces en las que, después de un día pesado, sabía que podía tocar tu puerta y encontrar un espacio seguro. Siempre fuiste ese pedacito de calma en medio del caos, y eso significó muchísimo para mí.

Dear **Helga**, **Heidi** and **Liesbeth**, thank you for all the help during all of these years! You are essential part in the lab and were as well during my PhD. I still don't speak good Dutch, but next time we grab a coffee, I promise I will do my best (just be ready for some creative grammar) $\stackrel{\smile}{\Leftrightarrow}$. Dear **Cor**[†], thank you for the great BBQs and for helping me getting acquainted in the lab. You are truly missed. Dear **Andy**, chico! Wednesday mornings wouldn't have been the same without you, hands down the best DJ/scientist combo ever! Thanks for all the fun, the pep talks and for making the lab feel a little less like work and a lot more like a place to enjoy.

My beloved **Athero Groupies**: I honestly couldn't have picked a better group to be part of. You made my PhD experience unforgettable. Thank you for everything: the help, the conferences, the trips, the endless discussions, and most importantly, the shared meals!

Dear Alice, first of all, it was such a pleasure to supervise you in the early days of your PhD. Even then, I knew you were going to be an amazing researcher. I've truly cherished our talks, our rants (some featuring a few dramatic tears), and of course, our top-tier gossip sessions

Dear **Ben**, thank you for helping turn our crazy data analysis ideas into reality and for explaining them to me with endless patience! Also, a special shoutout for all the incredible food and baked goods. No cinnamon roll will ever taste as good as yours (seriously, can I have the recipe?).

Dear **Dorien**, thank you for making lab life so much fun! Sitting next to you in the flow cabinet was never boring, your unique personality and good vibes are contagious.

Dear Julia, thank you for sharing some of my most questionable guilty pleasures (cough, cough El Taxi). I had an absolute blast with you in the office and the lab. P.S. I promise to sneakily do your hair whenever you want!

Dear Harsh, how you doin'? Thanks for all the fun times as office buddies and for always being willing to help, despite the mountain of work you already had. You made the office a much more entertaining place, and I really appreciated it!

Dear Wieteke, working with you was such a pleasure! Those long MIRACLE days wouldn't have been the same without you. I loved our talks, whether side by side in the flow cabinet or outside the lab. I've admired how much you've grown since we first met, and I can't wait to see the results of all your hard work!

Dear Laszlo, thank you for all your help during my PhD! From mastering the art of preparing oxLDL to fine-tuning Seahorse optimizations for our BM-derived macrophages, your guidance was invaluable. It was always great to chat with you.

I would also like to thank all my colleagues at IRAS Toxicology, who have made my time as a postdoc truly gezellig.

Dear Jorke and Ray, thank you for taking this immunologist under your wing and introducing me to the fascinating world of toxicology. I truly appreciate the trust you placed in me as I embarked on this postdoc journey, as well as the flexibility and support you gave me to finish my PhD. Your leadership and guidance have made this transition an exciting and enriching experience, and I genuinely enjoy working with both of you. I'm looking forward to all the exciting projects ahead and everything we will accomplish together! Dear Juliette, you have always been such an inspiration to me. Your dedication to finding ways to contribute and create meaningful change is something I truly look up to. Thank you for your guidance, your encouragement, and for being such a fantastic role model.

Dear ETXers, Hania, Hana, Roeland, Deniz, Sander, Nikita, Justine, Jiayi, Leontine, Menno, Elise, Lars, Izzy, Laura, Laurens, Fela and Merel, thank you for all the great discussions during our lunch meetings. Who knew that lunchtime could be a mix of brilliant science, philosophical debates and the occasional ridiculous topic that had nothing to do with work? Dear ITXers, Annemijne, Esther, Ivo, Kas, Suze, Soraya and Marianne, thank you for all your input, help and willingness to share your knowledge. You've been an invaluable part of this journey, and I've learned so much from working with you. Emma, Ilia, Pepijn, Theo, Esmeralda, Lennart, Lora, Jeske, Chiel, Sara, Heetak, Anna, Kim, Gina, Priscilla, Remco and Aniek, you made the office an absolute joy to be in! Whether it was science talk, coffee breaks or much-needed distractions from never-ending work.

To my students, Ana, Irma, Sara, Floortie, Christophe, Fay and Siyao. It has been (and still is, for some of you!) such a joy being your supervisor. Each one of you has taught me something different: whether it was a fresh perspective, a new way to tackle a problem or just a reminder of how exciting science can be when seen through new eyes. I'm so grateful to have had the chance to share my love for science with you, and I hope I managed to pass on at least a little bit of my enthusiasm (and maybe some useful lab tricks too). Keep that curiosity alive, and I have no doubt you'll go on to do amazing things!

Dear **Sophie** and **Dennis**, you were one of my first friends when I arrived in the Netherlands. Thank you for all these years of friendship, for always being there and for your support during the tougher times, I'm so happy we've shared so many great moments together, and I can't wait for all the new memories we'll create in the future!

Queridas Macumberas, Celia, Jara, Ane, Flor y Pau. Qué alegría tenerlas en mi vida. Sin duda, han hecho de estos últimos años una experiencia mucho más divertida, llena de risas, baile y momentos inolvidables. Gracias por siempre estar ahí, por las noches de fiesta, las charlas interminables y por ser ese grupo con el que siempre puedo contar. No importa dónde estemos, siempre las tengo cerquita de mí.

Queridas Karina, Cindy y Lucy. Mi pedacito de México en Países Bajos. Gracias por haber sido parte de esta etapa, en las buenas, en las malas, y en esos momentos de crisis en los que solo una buena plática y comida mexicana podían salvar el día. Ustedes han sido mi mejor distracción del estrés, siempre trayendo risas, antojitos, y pura cosa bonita a mi vida. No sé qué hubiera hecho sin ustedes, pero seguro hubiera sido mucho más aburrido 😂!

A mis queridos profesores del Tec, Ana Laura, Cesar, Bere, Juan Carlos, Jackie y Aurora. Gracias por ser los primeros en despertar mi interés por la investigación y por mostrarme lo increíble que puede ser la ciencia. Siempre voy a estar agradecida por todo lo que me enseñaron. Además, gracias por todo su apoyo cuando decidí lanzarme a la aventura de estudiar en el extranjero. Sin duda, tener su confianza y motivación hizo que ese gran salto fuera un poco menos aterrador. Ustedes fueron parte fundamental de mi camino, y siempre llevaré conmigo lo que aprendí de ustedes.

Mi Leading Strand, Oli, Roger, Alex, Chio y Kiki. Desde la universidad, ustedes han sido mi sistema de soporte y no pude haber encontrado amigos más inspiradores e increíbles. De cada uno de ustedes he aprendido mucho y lo mejor de todo, hemos acumulado juntos algunos de los recuerdos más bonitos. Gracias por seguir al pie del cañón en esta etapa, a pesar de la distancia y las locuras del día a día. Saber que siempre están ahí, listos para una plática, una risa o simplemente para compartir la vida, hace que todo sea mucho más especial. No importa dónde estemos, nuestra Leading Strand sigue fuerte.

Queridísima Oli, Loli, Oliva. Gracias, gracias, gracias por siempre estar ahí. Has sido, y siques siendo, una parte fundamental de mi vida. Contigo he compartido momentos inolvidables, tanto personales como profesionales; desde alegrías hasta retos que no habrían sido lo mismo sin tu apoyo. Pero más allá de los recuerdos compartidos, lo que más valoro es todo lo que he aprendido de ti. Te admiro profundamente, no solo por la persona increíble que eres, sino también por tu trabajo y tu impacto como mujer en STEM. Tu dedicación, inteligencia y perseverancia son una inspiración constante, y ver todo lo que has logrado y lo que sigues construyendo me llena de orgullo. Es un honor compartir este camino contigo, y sé que aún nos esperan muchas más aventuras, desafíos y logros por celebrar iuntas.

Querido Mau, gracias por todos estos años de amistad y por siempre estar ahí cuando te necesito. No importa la distancia, el tiempo o lo que esté pasando, siempre has sido un apoyo incondicional y eso es algo que valoro muchísimo. Me hace muy feliz saber que formas parte de mi vida y que hemos compartido tantas etapas juntos, cada una con sus propias historias, risas y aprendizajes. Y por supuesto, esto incluye a **Eli** también, porque no hay mejor equipo que ustedes dos. Sé que aún nos quedan muchísimos momentos más por vivir, y no puedo esperar para ver qué sigue en esta aventura de la vida.

Querido Iván, cachetes. ¿Qué te puedo decir después de toda una vida de amistad? Desde siempre, has estado ahí, acompañándome en tantas experiencias que ya hasta perdí la cuenta. Agradezco muchísimo tu apoyo, tus porras incondicionales y esa manera única que tienes de ver la vida. Sin duda, te has convertido en familia. Me da muchísima alegría seguir compartiendo momentos contigo, ya sea en México o en el extranjero, y saber que, sin importar dónde estemos, siempre habrá nuevas historias por escribir juntos.

My dearest paranymphs, best partners-in-crime for this journey! You three have been such a huge part of my PhD experience, and I'm beyond grateful for all the memories, support, and laughs we've shared along the way.

Ilse, guuuuurl. Where do I even begin? Thank you for everything: for your help in the lab (including those wtf moments), for all the coffee breaks that somehow turned into therapy sessions and for the endless talks about anything and everything. And of course, for making sure people wore pink on Wednesdays But most importantly, thank you for always being there when I needed advice, for your honesty, your kindness and your way of always finding the right words. You are truly one of a kind, and I feel so lucky to have shared this experience with you.

Helin, we didn't just share one, not two, but three offices together. Every time I think back to a nice memory from my PhD, you're there, making things easier, funnier or just way more bearable. Thank you for being my go-to person for help, deep talks and of course, top-tier gossip O. You have the kindest heart and I feel so lucky to have you as a friend (even though I still can't believe civ civ exists hahaha). And even though we're no longer office buddies, I love that we're still in the same city, continuing to create more memories together.

Querido **Oscar**, Pecas. Gracias por acompañarme en esta aventura, por estar siempre ahí sin importar nada v por demostrar que el verdadero vínculo de hermanos no necesita explicaciones... Literal, porque después de tantos años todavía no puedes explicar exactamente qué hago jajajaja. Pero bueno, lo importante es que siempre has estado presente, apoyándome incluso cuando no entiendes muchas de mis locuras científicas. Me llena de orgullo verte crecer y desarrollarte, ver cómo enfrentas nuevos retos y te conviertes en la increíble persona que eres hoy. Siempre he querido ser una fuente de inspiración para ti, pero la verdad es que tú también lo eres para mí. Gracias por ser mi compañero de aventuras y por compartir conmigo este camino. Y no te preocupes, la próxima vez que nos veamos te explico de nuevo de qué se trata mi trabajo. Te quiero mucho.

I couldn't have survived this ride without you. Thank you for being the incredible, supportive, and all-around amazing people that you are!

Lieve Ineke en Rene, dank jullie wel voor het zijn van mijn familie ver van huis en voor jullie onvoorwaardelijke steun en warmte. Vanaf het eerste moment hebben jullie me met open armen ontvangen, en dat heeft ontzettend veel voor me betekend tijdens deze hele periode. Jullie aanwezigheid maakte echt het verschil, vooral op die momenten waarop de afstand tot huis even extra voelbaar was. Ik ben enorm dankbaar voor jullie enthousiasme en de oprechte interesse die jullie altijd in mijn onderzoek hebben getoond. De manier waarop jullie luisterden, vragen stelden en mijn enthousiasme deelden, gaf me niet alleen motivatie, maar herinnerde me er ook aan waarom ik zo van mijn werk hou. En buiten de wetenschap om: dank jullie wel voor alle fijne gesprekken, de gezelligheid en de momenten vol lachen en plezier. Jullie hebben me altijd een thuisgevoel gegeven, zelfs als ik ver weg was. Sebas, Kimber, Sunna en Noëlle, heel veel dank, ik ben ontzettend blij dat ik jullie heb leren kennen en nog blijer dat ik me een beetje deel van jullie familie mag voelen!

A toda mi familia en México, a mis abuelitas **Esther** y **Amalia**, todos mis tíos, primos y familia por añadidura, quienes siempre me han apoyado y estado al pendiente aun estando lejos...; Gracias!

Queridos papás, Lina y Daniel, nunca serán suficientes las palabras para agradecerles todo lo que han hecho por mí, pero aquí va un intento (y sí, se me salieron unas cuantas lágrimas escribiendo esto). Desde el día uno han estado ahí, apoyándome en cada locura, cada sueño y cada meta, sin jamás dudar de mí ni de lo que soy capaz de lograr. Tenerlos a mi lado, incluso a la distancia, ha sido mi mayor fortaleza. Porque aunque los kilómetros nos separen, siempre los siento cerquita, en cada mensaje, en cada llamada y en cada pequeño gesto con el que me recuerdan que su amor y apoyo son incondicionales. Gracias por ser mi motor, por creer en mí incluso cuando yo dudaba, por enseñarme con su ejemplo lo que significa la dedicación, el esfuerzo y el amor inquebrantable de una familia. Si hoy estoy aquí escribiendo estas palabras, es porque ustedes han estado detrás de cada paso que he dado, impulsándome sin presionar, quiándome sin imponer, dándome alas pero asegurándose de que nunca olvide mis raíces. Espero que estén tan orgullosos de mí como yo lo estoy de ustedes, porque sé que sin todo su esfuerzo y sacrificio, nada de esto sería posible. Todo lo que he logrado es, en gran parte, gracias a ustedes. Los amo con todo mi corazón. 💕

Querido **Emiliano**, eres esa pequeña lucecita, que no sabía que necesitaba pero que ahora no puedo imaginar mi vida sin. Desde el momento en que llegaste, llenaste nuestros días de amor, risas y una felicidad que no se puede medir. Gracias por traer tanta alegría a nuestras vidas, por recordarme lo que realmente importa y por hacer que incluso los días más cansados sean los más bonitos solo con una sonrisa tuya. Espero siempre ser una fuente de inspiración para ti. Y te prometo que en todo lo que hagas, ahí estaré, apoyándote sin dudarlo. Te amo, chiquis. 🦂

Dear Matthijs, thank you for your unconditional support these past years—you are an absolute rockstar (and honestly deserve an honorary PhD for surviving this journey with me). Every time I tell people that I worked in Nijmegen while still living in Utrecht, they ask me how on earth I managed that. The hard truth? I didn't do it alone, it would have been impossible without you. Thank you for all the pep talks, for patiently listening to my endless rants, for rehearsing my presentations with me (even when you had no idea what I was talking about), and for making sure I was actually eating by preparing dinners in advance after those ridiculously long days. Thank you for not minding my early wake-ups (and for somehow developing the superpower of sleeping right through them). And perhaps most impressively, thank you for occasionally cutting short your La Liga and Champions League matches because they were on too late... if that's not true love, I don't know what is! You are without a doubt one of the best things that has ever happened to me, and I feel so incredibly lucky to share moments like these with you. I'm so proud of our little family, of everything we've built together, and I can't wait for all the adventures (big and small) that are yet to come.

Love you always. \forall

Curriculum Vitae Daniela Flores Gomez

EDUCATION	
Experimental Internal Medicine - Radboudumc PhD candidate	August 2023
Master in Biomedical Sciences (Grade 7.72/10) Regenerative Medicine and Technology - Utrecht University	July 2019
Bachelor of Science Biotechnology Engineering (Grade 9.1/10) Certificate in Molecular Biology - Monterrey Institute of Technology and Higher Education (ITESM CEM, Mexico) • Awards: Winner of cultural leadership and teamwork award given from the institute. Integral Formation Excellence and Student Development Diplomas	December 2015
EXPERIENCE	G
 Postdoctoral researcher Institute for Risk Assessment Sciences- Utrecht University Characterization of a 'FBS free' in vitro adipogenesis model as a new approach methodology Developing of 2D and 3D in vitro adipogenesis models to study endocrine disrupting chemicals (EDCs) Research of the effect of EDCs in the endocrine-immune axis by a 2D and 3D in vitro co-culture model of adipocytes and macrophages 	September 2023 – Present
Experimental Internal Medicine - Radboudumc PhD candidate	August 2019 – August 2023
 Developed an in vitro model to study innate immune reprogramming of human bone marrow-derived stem cells in inflammation and atherosclerosis Characterization of human bone marrow and iPSC-derived monocytes for its use in inflammatory in vitro models Research on the effect of adipokines in trained immunity of monocyte-derived macrophages in obesity and inflammation Observational study to investigate the role of neutrophils in patients with aortic valve stenosis 	
Department of Orthopedics - Regenerative Medicine Center Utrecht Research student Translational research at the Department of Orthopedics of University Medical Center Utrecht in Jos Malda's group. Characterization of silk for its use as hydrogel in in vitro cartilage regeneration. Development of a bio-inspired synovium-on-a-chip to study metabolic triggered inflammation.	November 2018 – June 2019

Department of Orthopedics - Regenerative Medicine Center Utrecht

November 2018 – June 2019

Research student

Translational research at the Department of Orthopedics of University Medical Center Utrecht in Lucienne Vonk's group. Research of in vitro meniscus cells differentiation in different 3D cultures for cartilage regeneration therapies.

July 2013 – November 2020

iGEM Competition - ITESM CEM

Participant/Advisor/Judge

• Participated in the 2014 competition as undergraduate student and mentored the iGEM Teams from undergraduate and high school in 2015 and 2016. Judge in the competition in 2020.

Safety and Pharmacovigilance - INC Research (now Syneos Health)

April 2016 – August 2017

Safety Specialist I

• Triage, processing and reporting of non-serious and serious adverse events according to country specific guidelines, good clinical practices and standard operating procedures; participation in the generation of expedited reports to the FDA. Pharmacovigilance of marketed and spontaneous solicited D cases, devices, legal and pregnancy cases. Performed internal quality control among the accreditation process of new associates.

SKILLS AND SOFTWARE

- Languages: Spanish (native), English (TOEFL IBT 95), Dutch (A2)
- Software: SPSS (statistics), GraphPad (statistics), basic knowledge of R, Kaluza (flow cytometry), FlowJo (flow cytometry)
- · Skills: Effective communication, supervision, scientific writing, and presentation skills gained during my PhD and postdoc period.

TEACHING AND SUPERVISION

Master student supervisor - Radboudumc Daily supervisor

February 2022 – August 2022

PhD student supervisor - Radboudumc Daily supervisor

October 2021 – December 2021

EXTRACURRICULAR

November 2008 – August 2017

ITESM CEM Mexican Folklore Ballet - ITESM CEM

Dancer

- Winner of rookie of the year in 2009, nominated for best dancer in 2013 and winner of the leadership award in 2013, 2014 and 2015. Assisted to Anseong Folkloriada, South Korea in October 2012 and International Folklore Festival in Zacatecas in June 2015 representing Mexico.
- As part of the group, took part in a leadership program consisting of outstanding students who taught at the school. Evaluated with the highest score a teacher can get. Received recognition for great responsibility in the department.

Casa Hogar Nuevo Sol - State of Mexico, Mexico

January 2013 – December 2014

Volunteer

· Led culturally diverse stimulating activities to assist teachers educate students with disabilities.

CERTIFICATIONS

Certified Quality Process Analyst (CQPA by ASQ)

August 2014

About the author

Daniela Flores Gómez was born in Mexico on February 13, 1993. She grew up with her parents and younger brother, developing an early appreciation for Mexican culture. This passion led her to begin practicing Mexican folklore dance at the age of eight. Alongside her cultural interests, she was also captivated by science, which inspired her to study Biotechnology Engineering with a minor in Molecular Biology at Tecnológico de Monterrey, graduating in 2015.



During her undergraduate studies, Daniela participated in the iGEM competition in Boston, first as a student in the undergraduate category and later as an advisor for the high school team. This experience deepened her enthusiasm for research and academia, setting her on a path toward a scientific career.

In 2017, she moved to the Netherlands to pursue a Master's degree in Biomedical Sciences, specializing in Regenerative Medicine and Technology, at Utrecht University. She completed her major internship in the Department of Orthopedics at the Regenerative Medicine Center Utrecht under the supervision of Dr. Lucienne Vonk, where she investigated 3D culture models for cartilage regeneration therapies. For her minor internship, she joined Jos Malda's Biofabrication Lab at the same institution, working under the guidance of Dr. Susanna Piluso and Dr. Yang Li to develop a bio-inspired synovium-on-a-chip for studying metabolism-triggered inflammation. During this period, she became particularly interested in the immune system, which ultimately led her to do a PhD in Immunology.

In 2019, Daniela joined Radboudumc, becoming part of the lab of Niels Riksen and Mihai Netea, where she was introduced to the field of trained immunity. Her doctoral research focused on investigating central and peripheral trained immunity in obesity and cardiovascular diseases, the results of which are presented in this thesis.

Continuing her passion for immunology, stem cells, and metabolic diseases, Daniela is now a postdoctoral researcher at the Institute for Risk Assessment Sciences at Utrecht University. Under the supervision of Dr. Jorke Kamstra and Dr. Raymond Pieters, she studies the effects of endocrine-disrupting chemicals on the endocrineimmune axis.

